DOCTORAL DISSERTATION SERIES

Publication No.: 18, 662

AUTHOR: Dah-Cheng Woo, Ph. D., 1956

University of Michigan

TITLE: STUDY OF OVERLAND FLOW

University Microfilms, Ann Arbor, Michigan

STUDY OF OVERLAND FLOW

by
Dah-Cheng Woo

A dissertation submitted in partial fulfillment
of the requirements for the degree of
Doctor of Philosophy in the
University of Michigan
January, 1956

Doctoral Committee:

Professor Ernest F. Brater, Chairman
Associate Professor Jack A. Borchardt
Professor Russell A. Dodge
Associate Professor Maurice W. Senstius

Abstract

STUDY OF OVERLAND FLOW

By Dah-Cheng Woo

An understanding of the hydraulics of flow in thin sheets over the land surface during rainfall is very important in the design of surface drainage systems, in the study of soil erosion and conservation problems, and in the solution of sedimentation problems. Flow over the land surface during rainfall is unsteady both with respect to time and with respect to location, and is further complicated by the disturbance caused by the impact of the raindrops. Although a rational analysis can be made, neglecting the dynamic effect of the impact of the raindrops, the final equation can hardly represent the true water surface profile of overland flow. The disturbance caused by the falling rain is too great to be neglected, especially in the shallower depths. Any experimental studies undertaken with an inadequate rainfall applicator will produce results which are inconsistent with those found in nature. Little attention has been given to the experimental phases of this problem. Therefore, a systematic experimental study of this problem was undertaken by the writer.

A rainfall applicator was developed by means of which raindrops of the desired size could be applied at a reasonably high velocity and with a uniform intensity. Rainfall was applied to a flume 29 feet 7 inches long and 6-1/4 inches wide. Rainfall of three intensities was used, but the intensity was held constant with respect to time during each test. Three different bottom surface roughnesses were used and the slope of the flume was varied from 0 to 0.075.

Roughness coefficients were obtained for uniform steady flow conditions for each type of bottom surface. The flow dealt with in this thesis falls in the laminar range of ordinary flow (without raindrop impact).

Because the bottom surfaces used were comparatively rough and the slopes were small (from 0 to 0.075), it is believed that the effect of rainfall on overland flow can be expressed in the change of coefficient of friction. Consequently, the effective coefficients of friction, f_c', were computed from the water surface profile drawn through the experimental results, and they are compared with the coefficient of friction for corresponding uniform flow for the same surface and slope. The results show no consistent relationship since the raindrop impact disturbs and hastens the change of flow from the regular laminar to the irregular turbulent condition.

However, a method of computing the water surface profile during rainfall is developed for practical use. Since this study of overland flow was carried out under certain restricted conditions, the results of this study and the suggested methods of use are only valid under similar conditions.

The original experimental data sheets and the detailed computation sheets are not shown in this thesis; they are filed in the Civil Engineering Department of the University of Michigan. Sample data sheets and computations for each purpose are included for reference.

The author wishes to dedicate

this thesis

to his beloved parents.

ACKNOWLEDGMENTS

The author wishes to express his deepest gratitude and appreciation to Professor E. F. Brater, under whose supervision this study has been carried out. His inspiration, criticism, and advice have rendered invaluable assistance in this work, without which it would have never been completed.

The author is also indebted to other members of the doctoral committee, Professors R. A. Dodge, J. A. Borchardt, and M. W. Senstius, for their valuable suggestions and guidance; also to Mr. G. L. Geisendorfer, who lent the most generous hand in helping the experimental work, and all others who added materially.

TABLE OF CONTENTS

	Page
INTRODUCTION	1
Review of Past Literature	2
CHAPTER	
I. THEORETICAL ANALYSIS	6
The Equation of Water Surface Profile Without the Raindrop Impact Effect	6
The Approximate Equation of Water Surface Profile Without the Raindrop Impact Effect	11
II. EXPERIMENTAL WORK	13
Artificial Rainfall Applicator	13
Author's Improved Rainfall Applicator	16
The Testing Flume	18
Surface Condition	18
Measuring Devices	19
Water Surface Profile	19
The inclined-tube manometer bank	20
Discharge	20
Flume Slope	21
Rainfall Distribution	21
Testing Procedure	21
Nozzle and Rainfall Distribution	21
Waterdrop Size Measurement	22
Calibration of Volumetric Tank	22
The Test	23

CHAPTER Page

Checks and adjustments of bottom slope of the flume and the rainfall distribution 24

Adjusting flume flatness 24

Maximum error in manometer reading 25

Checking rainfall distribution 25

Part 1: roughness test 26

Part 2: rainfall test 27

Presentation of Results 28

Abandoning Surface "A" Data 28

Water Depth in Surface "C" Tests 28

The Experimental Results 29

III. ANALYSIS OF EXPERIMENTAL DATA AND DISCUSSION OF RESULTS 40

Part 1: Coefficient of Friction for Uniform Flow 40

Discussion of Results 42

Part 2: Water Surface Profiles 43

Computed Water Surface Profiles Without Raindrop Impact Effect 43

Methods of determining starting point by use of the critical depth 44

For slopes less than the critical slope for the discharge at the lower end of the flume 44

For slopes greater than the critical slope for the discharge at the lower end of the flume 45

The effect of Δx value on water surface profile 46

The Raindrop Impact Effect 47

CHAPTER Page

The effect on total momentum of the flowing water 47

The effect on the intensity of turbulence of the flowing water 48

The effect on heat energy of the flowing water 49

The effect on the pressure on the bottom surface 49

Discussion of results 50

The feasibility of equation (26) 51

The Use of Actual Rainfall and Actual Slope of Bottom Surface 52

The Simplified Approximate Equation 53

The Minimum and Zero Water Depth 54

The Wave Motion and Supercritical Flow . . . 54

An Investigation of the Kinetic Energy of Waterdrops 55

IV. PRACTICAL APPLICATIONS 57

Computing Water Surface Profiles During Rainfall 57

Friction Factors 57

The C' Curves 59

The Method 60

Water Surface Profiles During Rainfall Obtained from Experimental Graphs 62

V. SUMMARY 69

APPENDIXES 188

Appendix I. Nozzle Test and Final Design Adopted; Its Arrangement and Spray Patterns 189

Appendix II. The Consideration of Actual Change of Momentum Due to the Effect of Raindrop Impact 194

Page

Appendix III. Modifying the Derivation of Equation (15) to Include the Coefficient of Momentum 196

Appendix IV. Coefficient of Momentum, C_m, for Uniform Laminar and Turbulent Flow 198

NOMENCLATURE 203

BIBLIOGRAPHY 207

LIST OF ILLUSTRATIONS

FIGURE		Page
1.	Drop size distribution for Type-F nozzle spray	15
2.	Computed water surface profile during rainfall compared with that from experimental result (Surface "B," S_o = 0.001, light rain)	66
3.	Computed water surface profile during rainfall compared with that from experimental result (Surface "C," S_o = 0.004, heavy rain)	67
4.	Computed water surface profile during rainfall compared with that from experimental result (Surface "C," S_o = 0.075, medium rain)	68
5.	Rainfall distribution along the testing flume	92
6.	f_c vs N_R (Surface "B")	94
7.	f_c vs N_R (Surface "C")	95
8.	n vs N_R (Surface "C")	96
9.	n vs N_R (Surface "C")	97
10.	C/S_o vs S_o and C vs S_o	98
11.	Water surface profiles (Surface "B," S_o = 0)	100
12.	Water surface profiles (Surface "B," S_o = 0.001)	101
13.	Water surface profiles (Surface "B," S_o = 0.002)	102
14.	Water surface profiles (Surface "B," S_o = 0.003)	103

FIGURE Page

15. Water surface profiles (Surface "B," S_o = 0.004) 104
16. Water surface profiles (Surface "B," S_o = 0.006) 105
17. Water surface profiles (Surface "B," S_o = 0.008) 106
18. Water surface profiles (Surface "B," S_o = 0.010) 107
19. Water surface profiles (Surface "B," S_o = 0.015) 108
20. Water surface profiles (Surface "B," S_o = 0.020) 109
21. Water surface profiles (Surface "B," S_o = 0.040) 110
22. Water surface profiles (Surface "B," S_o = 0.060) 111
23. Water surface profiles (Surface "B," S_o = 0.075) 112
24. Water surface profiles (Surface "C," S_o = 0) 113
25. Water surface profiles (Surface "C," S_o = 0.001) 114
26. Water surface profiles (Surface "C," S_o = 0.002) 115
27. Water surface profiles (Surface "C," S_o = 0.003) 116
28. Water surface profiles (Surface "C," S_o = 0.004) 117
29. Water surface profiles (Surface "C," S_o = 0.006) 118
30. Water surface profiles (Surface "C," S_o = 0.008) 119
31. Water surface profiles (Surface "C," S_o = 0.010) 120

FIGURE Page

32. Water surface profiles (Surface "C," S_o = 0.015) 121
33. Water surface profiles (Surface "C," S_o = 0.020) 122
34. Water surface profiles (Surface "C," S_o = 0.040) 123
35. Water surface profiles (Surface "C," S_o = 0.060) 124
36. Water surface profiles (Surface "C," S_o = 0.075) 125
37. Water surface profiles computed from actual experimental conditions and simplified equation (27) (Surface "B," S_o = 0.002) 127
38. Water surface profiles computed from actual experimental conditions and simplified equation (27) (Surface "B," S_o = 0.020) 128
39. Water surface profiles computed from actual experimental conditions and simplified equation (27) (Surface "C," S_o = 0.002) 129
40. Water surface profiles computed from actual experimental conditions and simplified equation (27) (Surface "C," S_o = 0.020) 130
41. f_c' vs N_R (Surface "B," S_o = 0) 132
42. f_c' vs N_R (Surface "B," S_o = 0.001) 133
43. f_c' vs N_R (Surface "B," S_o = 0.002) 134
44. f_c' vs N_R (Surface "B," S_o = 0.003) 135
45. f_c' vs N_R (Surface "B," S_o = 0.004) 136
46. f_c' vs N_R (Surface "B," S_o = 0.006) 137
47. f_c' vs N_R (Surface "B," S_o = 0.008) 138
48. f_c' vs N_R (Surface "B," S_o = 0.010) 139
49. f_c' vs N_R (Surface "B," S_o = 0.015) 140
50. f_c' vs N_R (Surface "B," S_o = 0.020) 141

FIGURE Page

51. f_c' vs N_R (Surface "B," S_o = 0.040) 142
52. f_c' vs N_R (Surface "B," S_o = 0.060) 143
53. f_c' vs N_R (Surface "B," S_o = 0.075) 144
54. f_c' vs N_R (Surface "C," S_o = 0) 145
55. f_c' vs N_R (Surface "C," S_o = 0.001) 146
56. f_c' vs N_R (Surface "C," S_o = 0.002) 147
57. f_c' vs N_R (Surface "C," S_o = 0.003) 148
58. f_c' vs N_R (Surface "C," S_o = 0.004) 149
59. f_c' vs N_R (Surface "C," S_o = 0.006) 150
60. f_c' vs N_R (Surface "C," S_o = 0.008) 151
61. f_c' vs N_R (Surface "C," S_o = 0.010) 152
62. f_c' vs N_R (Surface "C," S_o = 0.015) 153
63. f_c' vs N_R (Surface "C," S_o = 0.020) 154
64. f_c' vs N_R (Surface "C," S_o = 0.040) 155
65. f_c' vs N_R (Surface "C," S_o = 0.060) 156
66. f_c' vs N_R (Surface "C," S_o = 0.075) 157
67. f_c' vs N_R (Surface "B," light rain) 159
68. f_c' vs N_R (Surface "B," medium rain) 160
69. f_c' vs N_R (Surface "B," heavy rain) 161
70. f_c' vs N_R (Surface "C," light rain) 162
71. f_c' vs N_R (Surface "C," medium rain) 163
72. f_c' vs N_R (Surface "C," heavy rain) 164
73. C'/C vs S_o and C_H'/C_L' (and C_M'/C_L') vs S_o (Surface "B") 166
74. C'/C vs S_o and C_H'/C_L' (and C_M'/C_L') vs S_o (Surface "C") 167
75. Measured water surface profiles (Surface "B," light rain) 169
76. Measured water surface profiles (Surface "B," medium rain) 170

FIGURE Page

77. Measured water surface profiles (Surface "B," heavy rain) 171

78. Measured water surface profiles (Surface "C," light rain) 172

79. Measured water surface profiles (Surface "C," medium rain) 173

80. Measured water surface profiles (Surface "C," heavy rain) 174

81. The spray patterns of nozzle 193

82. C_m vs y/k_s for uniform fully turbulent flow 202

SAMPLE DATA SHEETS

Part 1. Roughness Test 72

Part 2. Rainfall Test 74

SAMPLE COMPUTATION SHEETS

Water Surface Profile During Rainfall (Surface "B," S_o = 0.001, light rain) 64

Water Surface Profile Without Raindrop Impact Effect (Surface "B," S_o = 0.020, light rain) 77

Water Surface Profile Without Raindrop Impact Effect (Surface "B," S_o = 0.020, medium rain) 79

Hinds' Method of Locating the Critical Depth, y_c, for Slopes Greater than the Critical Slope (Surface "B," S_o = 0.020, heavy rain) 81

Water Surface Profile Without Raindrop Impact Effect (Surface "B," S_o = 0.020, heavy rain) 83

f_c' from Raindrop Impact Effect (Surface "B," S_o = 0.002, light rain) 85

Water Surface Profile Without Raindrop Impact Effect from Actual Experimental Conditions (rainfall distribution and bottom surface elevations) (Surface "B," S_o = 0.002, light rain) 87

SAMPLE COMPUTATION SHEETS--Continued

Water Surface Profile Without Raindrop Impact Effect from Simplified Equation (27) (Surface "B," S_o = 0.002, light rain) 89

DRAWING

1. General Experimental Arrangement and Plan of Testing Flume 176

2. Arrangement of Nozzles 177

PHOTOGRAPH

1. Experimental arrangement (from lower end, looking upstream; S_o = 0) 179

2. Testing flume (from upper end, looking downstream; S_o = 0.075) 179

3. Cheesecloth mattress with cotton yarn strings (looking up) 180

4. Nozzles with drains (looking down on mattress) 180

5. Close-up of nozzle and drain (above the cheesecloth mattress) 180

6. Manometer bank 181

7. Volumetric tank with portable point gage 181

8. Flume support and slope indicator 182

9. Beakers to measure rainfall distribution 182

10. Part 1 roughness test (water supply to upper end; S_o = 0) 183

11. Part 2 rainfall test (from upper end looking downstream; S_o = 0.075. Note fine spray above mattress. Raindrops can be seen impinging on water surface in flume.) 183

12. Part 2 rainfall test (Surface "C," S_o = 0, light rain) 184

PHOTOGRAPH Page

13. Part 2 rainfall test (Surface "C," S_o = 0, medium rain) 184

14. Part 2 rainfall test (Surface "C," S_o = 0, heavy rain) 185

15. Surface "C"--cemented sand surface and the water depth station 185

16. Part 2 rainfall test (Surface "C," S_o = 0.075, light rain) 186

17. Part 2 rainfall test (Surface "C," S_o = 0.075, medium rain) 186

18. Part 2 rainfall test (Surface "C," S_o = 0.075, heavy rain) 187

LIST OF TABLES

TABLE		Page
I.	Results of Roughness Tests	31
II.	Part of the Results of Rainfall Test	36
III.	Summary of Experimental Conditions	38
IV.	Comparison of Kinetic Energy of a Single Waterdrop of Natural Rain with That of Experimental Rain	56
V.	Summary of Nozzle Tests	190
VI.	Values of Coefficient of Momentum, C_m, for Fully Turbulent Flow	201

ABSTRACT

An understanding of the hydraulics of flow in thin sheets over the land surface during rainfall is very important in the design of surface drainage systems, in the study of soil erosion and conservation problems, and in the solution of sedimentation problems. Flow over the land surface during rainfall is unsteady both with respect to time and with respect to location, and is further complicated by the disturbance caused by the impact of the raindrops. Although a rational analysis can be made, neglecting the dynamic effect of the impact of the raindrops, the final equation can hardly represent the true water surface profile of overland flow. The disturbance caused by the falling rain is too great to be neglected, especially in the shallower depths. Any experimental studies undertaken with an inadequate rainfall applicator will produce results which are inconsistent with those found in nature. Little attention has been given to the experimental phases of this problem. Therefore, a systematic experimental study of this problem was undertaken by the writer.

A rainfall applicator was developed by means of which raindrops of the desired size could be applied at a reasonably high velocity and with a uniform intensity. Rainfall was applied to a flume 29 feet 7 inches long and 6-1/4 inches wide. Rainfall of three intensities was used, but the intensity was held constant with respect to time during each test. Three different bottom surface roughnesses were used and the slope of the flume was varied from 0 to 0.075. Roughness coefficients were obtained for uniform steady flow conditions for each type of bottom surface. The flow dealt with in this

thesis falls in the laminar range of ordinary flow (without raindrop impact).

Because the bottom surfaces used were comparatively rough and the slopes were small (from 0 to 0.075), it is believed that the effect of rainfall on overland flow can be expressed in the change of coefficient of friction. Consequently, the effective coefficients of friction, f_c', were computed from the water surface profile drawn through the experimental results, and they are compared with the coefficient of friction for corresponding uniform flow for the same surface and slope. The results show no consistent relationship since the raindrop impact disturbs and hastens the change of flow from the regular laminar to the irregular turbulent condition.

However, a method of computing the water surface profile during rainfall is developed for practical use. Since this study of overland flow was carried out under certain restricted conditions, the results of this study and the suggested methods of use are only valid under similar conditions.

The original experimental data sheets and the detailed computation sheets are not shown in this thesis; they are filed in the Civil Engineering Department of the University of Michigan. Sample data sheets and computations for each purpose are included for reference.

INTRODUCTION

In ordinary open-channel flow the vertical velocity gradient and the intensity of turbulence depend on the depth, the velocity, the fluid properties, the boundary roughness, and the wind velocity. Rain falling on open channels having a considerable depth of water might have only a minor effect in the flow conditions. However, in overland flow, the depths are small because the only source of supply is the rain itself, and with these small depths the impact effect of the rainfall becomes of very great importance. Furthermore, at very small depths, the effect of boundary roughness becomes much greater than in the case of larger depths.

An experimental investigation of the hydraulics of overland flow with natural rainfall on natural surfaces presents nearly insurmountable difficulties. One could conceivably construct a number of test plots in the open, but great difficulties would be involved in making accurate measurements of depths and discharge. Completely automatic recording equipment would be required because it would not be practical to have personnel on hand waiting for suitable rains to occur. Furthermore, it would require many years of records to obtain a few data due to the infrequent occurrence of rains of high intensities. Because the intensity of rainfall varies with both time and location, it would be difficult to obtain results for a particular set of conditions. The variability of wind direction and velocity would further complicate tests with natural rainfall. Another factor influencing flow conditions would be the variation in the rate at which flowing water would infiltrate into the soil. It was therefore

decided to undertake a series of laboratory tests in which controlled rain intensity could be applied to impermeable surfaces having various slopes and roughnesses. However, in order to accomplish this, it was first necessary to develop a method of producing realistic raindrops artificially. It is believed that the laboratory techniques developed here will be of assistance to future investigators in this field.

Water surface profiles were determined for 117 combinations of conditions in which the variables were rain intensity, bottom surface roughness, and slope. Of these, seventy-eight were compared with profiles derived analytically. It is believed that the results will provide a contribution toward a better understanding of the hydraulics of overland flow. Due to the vast scope of the problem, this study covers only the flow of small Reynolds' number, corresponding to the laminar condition of steady uniform flow.

Review of Past Literature

Brief reviews of the past studies on this subject and those closely related are presented in the following paragraphs.

In 1925, J. Hinds (1) first presented the rational equation and the method of computing the water surface profile in the side channel spillway based on the principle of momentum. The effect of channel friction was estimated separately. His work was checked by experiments.

Later, in 1933, H. Favre (2), based on the same principle, derived the water surface profile equation including the friction term and a consideration of the effects of the velocity component of the inflow and the change of vertical velocity distribution. His work was also checked by experiments.

K. H. Beij (3), in 1934, did the same for the roof gutter problems and offered a rational solution for one condition of frictionless surface and zero slope. His analysis checked well with experiments.

R. E. Horton (4), in 1938, derived the equations of depth and discharge of overland flow from the storage equation plus the simple assumption that the profile of overland flow for all conditions, from laminar to full turbulent, is of parabolic form, but of different order. Some question of consistency in the procedure of derivation was discussed by Professor E. F. Brater (5).

T. R. Camp (6), in 1939, following the same procedure as Hinds, derived the equation of water surface profile in a lateral spillway channel by including the term giving the friction effect.

G. H. Keulegan's (7) 1944 analytical solution of the nonuniform and unsteady runoff over a sloping plane contained two equations: the equation of continuity, and the dynamical equation of motion. Every effect was considered individually in deriving the flow equation.

C. F. Izzard (8), in 1944, presented his experimental work on this subject by using three different kinds of surface 75 feet in length, and two rainfall intensities: 1.8 and 3.6 inches per hour. To create rain in the laboratory he used the popular Type-F rainfall applicator. This apparatus has the weakness of producing decreasing raindrop sizes as the rainfall intensity is increased, which is contrary to the natural condition (9). Since the raindrop impact is one of the most important factors in this study, this procedure seems hardly satisfactory. His method of obtaining the water surface profile from the average depth through total detention did involve error, especially for shorter distance because of the more changes in water depth at the upper end. Consequently the coefficient of friction computed from this water surface profile failed to represent the true value.

D. A. Parsons (10), in 1949, based on his experimental results, believed that the average depth of overland flow within the range of laminar and transition regime could be expressed simply by the product of corresponding depth for pure laminar flow and a constant factor which is different for different surface material. This does not take into account the fact that the raindrop impact effect is not uniform, but varies inversely with the water depth.

E. F. Brater (11), in 1950, indicated that Manning's formula can be used to express laminar flow in open channel just as Darcy-Weisbach's turbulent pipe flow formula related to Hagen-Poiseuille law for laminar flow in pipe. The relationship of $n^2/y^{1/3} = 0.206/N_R$ for uniform thin flow was well checked by the experimental data. This proves that the existing open-channel flow formulas do relate to the Reynolds' number both for turbulent and laminar flow conditions in the same way as that of pipe flow.

Entire empirical equations for overland flow from experiments were reported by W. I. Hicks (12) and C. F. Izzard (13). Their use is limited to the same conditions under which the tests were conducted.

Of the rational analyses mentioned above, Keulegan's is the most general and complete treatment which includes all factors involved except infiltration and the raindrop impact. The other analyses apply only to the case where the discharge is constant with respect to time. By using the same notations and assuming that the coefficient of kinetic energy C_e is equal to unity and that the surface slope is small, the equations for equilibrium flow derived by different authors are practically the same after some adjustment, except for a different form of the friction term if it is included.

All the experimental work heretofore was carried out with the use of a Type-F rainfall applicator or even simpler apparatus, and

the water depths on impervious surfaces were measured indirectly through average detention. Thus none of the earlier work provides information as to actual water surface profiles for overland flow.

CHAPTER I

THEORETICAL ANALYSIS

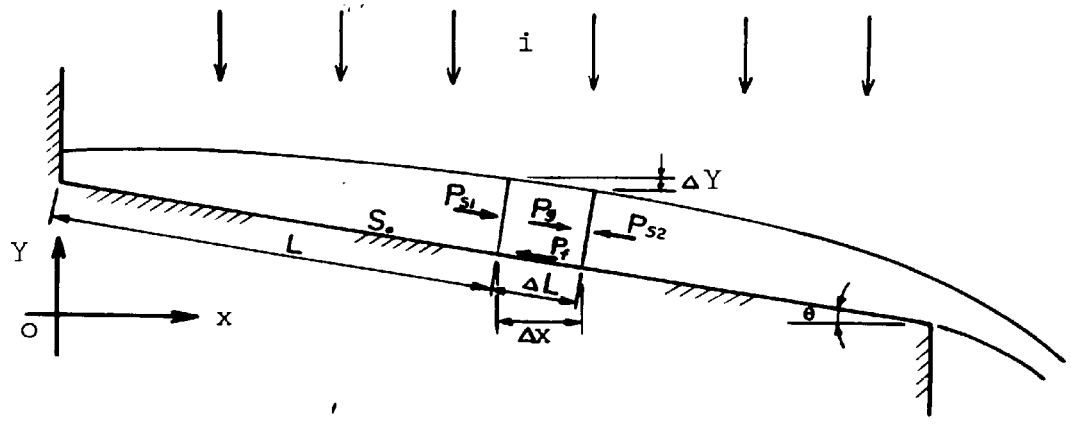
The Equation of Water Surface Profile Without the Raindrop Impact Effect

The following assumptions are made:

1. The rainfall is uniform and constant.
2. The surface is impervious and has an infinite width.
3. The slope of the surface is uniform and small (less than 10°).
4. The surface friction is the same as that of corresponding uniform flow.
5. The coefficient of momentum, C_m, equals unity.
6. The dynamic effect of falling rain is neglected.
7. The flow is in equilibrium condition.

The derivation of this equation follows closely the procedure used by Hinds (1) in his paper for side channel spillway, and Camp (6) in the paper on lateral spillway channels. The basic principle is the momentum theorem that the effective force is equal to the rate of change of momentum, $F = dM/dt$.

For a surface of infinite width, a reach 1-2 of unit width is taken.



At section 1:

the water depth perpendicular to the channel bottom, y_1	$= y$
the discharge per unit width, $q_1 = i\ x$	$= q$
the mean velocity, $V_1 = \frac{q_1}{y_1}$	$= V$
the momentum, $M_1 = \frac{q_1\ w\ \Delta t}{g}\ V_1$	$= \frac{q\ w\ \Delta t}{g}\ V$

At section 2:

the water depth perpendicular to the channel bottom, y_2	$= y + \Delta y$
the discharge per unit width, $q_2 = i\ (x + \Delta x)$	$= q + \Delta q$
the mean velocity, $V_2 = \frac{q_2}{y_2}$	$= V + \Delta V$
the momentum, $M_2 = \frac{q_2\ w\ \Delta t}{g}$	$= \frac{(q+\Delta q)w\ \Delta t}{g}(V+\Delta V)$

For reach 1-2

the water depth perpendicular to the channel bottom, mean in the reach, $y_m = 1/2\ (y_1 + y_2)$	$= y + \frac{\Delta y}{2}$
the discharge per unit width, mean in the reach, $q_m = 1/2\ (q_1 + q_2)$	$= q + \frac{\Delta q}{2}$
the mean velocity, mean in the reach, $V_m = \frac{q_m}{y_m}$	$= \frac{q + \frac{\Delta q}{2}}{y + \frac{\Delta y}{2}}$

then

$$\Delta M = M_2 - M_1 = \frac{\Delta t\ w}{g}\left[(q_1 + \Delta q)(V_1 + \Delta V) - q_1 V_1\right]$$

$$= \frac{\Delta t\ w}{g}\ (q_1\ \Delta V + V_2\ \Delta q) \quad \ldots\ldots\ldots\ldots\ldots\ldots (1)$$

or

$$\frac{\Delta M}{\Delta t} = \text{accelerating force} = \frac{w}{g}\ (q_1\ \Delta V + V_2\ \Delta q) \quad \ldots\ldots\ldots (2)$$

For the net external force on reach 1-2,

$$F = (P_{s1} - P_{s2}) + P_g - P_f \quad \ldots\ldots\ldots\ldots\ldots\ldots\ldots (3)$$

P_{s1} and P_{s2} are static pressures at sections 1 and 2

$$P_{s1} = 1/2\ w\ y_1^2$$

$$P_{s2} = 1/2\ w\ y_2^2$$

and $$P_{s1} - P_{s2} = 1/2\ w\ (y_1^2 - y_2^2) \quad \ldots\ldots\ldots\ldots\ldots\ldots (4)$$

P_g is the component of the gravitational force of the water column ΔL parallel to the bottom surface,

$$P_g = 1/2\ w\ (y_1 + y_2)\ \Delta L\ \text{Sin}\ \theta \quad \ldots\ldots\ldots\ldots\ldots\ldots (5)$$

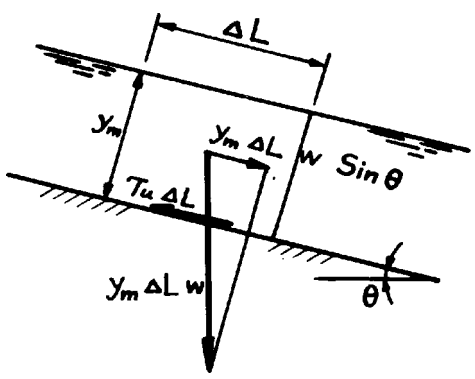
P_f is the frictional force at the bottom surface,

$$P_f = \tau \Delta L \quad \ldots\ldots\ldots\ldots\ldots\ldots\ldots\ldots\ldots\ldots (6)$$

where τ, the shearing stress at the bottom surface, is related to the velocity head as follows.

$$\tau = K_s \frac{V_m^2}{2g} w \quad \ldots\ldots\ldots\ldots\ldots\ldots\ldots\ldots\ldots\ldots (7)$$

The coefficient K_s varies with the Reynolds' number and the boundary roughness. It may be evaluated from the uniform flow condition as follows.



$\sum F$ (in the direction of flow under equilibrium) = 0

$$y_m\ \Delta L\ w\ \text{Sin}\ \theta = \tau_u\ \Delta L$$

when θ is small, Sin θ = tan θ = S_o (slope of bottom surface), and for uniform flow S_o = S (slope of energy gradient), then

$$\tau_u = y_m\ w\ S_o = y_m\ w\ S \quad \ldots\ldots (8)$$

From Darcy-Weisbach's formula of energy loss for pipe,

$$h_f = f_p \frac{L}{D} \frac{V^2}{2g}$$

by using D = 4 R (R is hydraulic radius) and R = y for wide channel, it is obtained for open channel

$$h_f = f_p \frac{L}{4y} \frac{V^2}{2g} = \frac{f_p}{4} \frac{L}{y} \frac{V^2}{2G}$$

or

$$h_f = f_c \frac{L}{y} \frac{V^2}{2g} \quad \ldots\ldots\ldots\ldots (9)$$

where f_c (= 1/4 f_p) is the coefficient of friction for open channel with uniform flow. Now in this case, the slope of energy gradient, S, is

$$S = \frac{h_f}{L} = f_c \frac{1}{y_m} \frac{V_m^2}{2g} \quad \ldots\ldots\ldots (10)$$

Substituting equation (10) into equation (8) gives

$$\tau_u = y_m \, w \, f_c \, \frac{1}{y_m} \, \frac{V_m^2}{2g} = f_c \, \frac{V_m^2}{2g} \, w \quad \ldots\ldots\ldots\ldots (11)$$

By assuming $\tau = \tau_u$, then from equations (11) and (7), it gives

$$K_s = f_c$$

and the frictional force, from equation (6) is

$$P_f = f_c \, \Delta L \, w \, \frac{V_m^2}{2g} \quad \ldots\ldots\ldots\ldots\ldots\ldots\ldots\ldots (12)$$

The net force **F** is then, from equations (3), (4), (5), and (12),

$$F = \frac{w}{2} (y_1^2 - y_2^2) + \frac{w}{2} (y_1 + y_2) \, \Delta L \, \text{Sin} \, \theta - f_c \, \Delta L \, w \, \frac{V_m^2}{2g}$$

or

$$F = y_m \, w \, (y_1 + \Delta L \, \text{Sin} \, \theta - y_2) - f_c \, \Delta L \, w \, \frac{V_m^2}{2g} \quad \ldots\ldots (13)$$

As $\mathbf{F} = \frac{\Delta M}{\Delta t}$, equating equations (2) and (13) gives

$$\frac{w}{g} (q_1 \, \Delta V + V_2 \, \Delta q) = w \left[y_m \, (y_1 + \Delta L \, \text{Sin} \, \theta - y_2) - f_c \, \Delta L \, \frac{V_m^2}{2g} \right]$$

or

$$\frac{1}{g} (q_1 \, \Delta V + V_2 \, \Delta q) = y_m (y_1 + \Delta L \, \text{Sin} \, \theta - y_2) - \frac{f_c \, \Delta L \, V_m^2}{2 \, g} \quad \ldots (14)$$

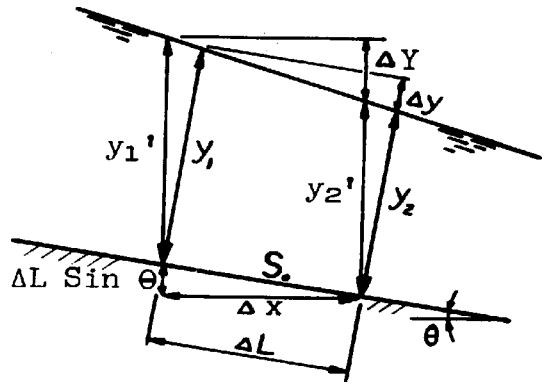
For practical purpose of convenience in computation, equation (14) for small bottom surface **slopes can** be modified by substituting numerically

x (horizontal distance) = L (distance along the surface)

$\Delta x = \Delta L$

and $S_o = \tan \theta = \text{Sin} \, \theta$,

and since $y = y'$ (y' is vertical water depth) for small angle θ, then



$$\Delta Y = y_1' + \Delta L \sin\theta - y_2'$$

$$= y_1 + \Delta L \sin\theta - y_2 .$$

Thus equation (14) becomes

$$\frac{1}{g}\left(q_1\,\Delta V + V_2\,\Delta q\right) = y_m\,\Delta Y - \frac{f_c\,\Delta x\,V_m^2}{2g}$$

or

$$\Delta Y = \frac{1}{g\,y_m}\left(q_1\,\Delta V + V_2\,\Delta q + \frac{f_c\,\Delta x\,V_m^2}{2}\right)$$

If Δq is replaced by $i\,\Delta x$, then

$$\Delta Y = \frac{1}{g\,y_m}\left(q_1\,\Delta V + i\,\Delta x\,V_2 + \frac{f_c\,\Delta x\,V_m^2}{2}\right) \quad \ldots\ldots\ldots (15)$$

or

$$\frac{\Delta Y}{\Delta x} = \frac{1}{g\,y_m}\left(q_1\,\frac{\Delta V}{\Delta x} + i\,V_2 + \frac{f_c\,V_m^2}{2}\right) \quad \ldots\ldots\ldots (16)$$

By substituting $y_m = y + 1/2\,\Delta y$, $q_1 = q$, $i = q/x$, $V_2 = V + \Delta V$ and $V_m = 1/2\,\Delta V + V$, equation (16) becomes

$$\frac{\Delta Y}{\Delta x} = \frac{1}{g(y + 1/2\,\Delta y)}\left[q\,\frac{\Delta V}{\Delta x} + \frac{q}{x}\left(V + \Delta V\right) + \frac{f_c}{2}\left(V + 1/2\,\Delta V\right)^2\right] \quad \ldots (17)$$

When $\Delta x \to 0$, then Δy and $\Delta V \to 0$, $\frac{\Delta Y}{\Delta x} = \frac{dY}{dx}$ and $\frac{\Delta V}{\Delta x} = \frac{dV}{dx}$, hence from equation (17)

$$\frac{dY}{dx} = \frac{1}{g\,y}\left(q\,\frac{dV}{dx} + \frac{q}{x}\,V + \frac{f_c}{2}\,V^2\right)$$

or

$$g\,\frac{dY}{dx} = V\,\frac{dV}{dx} + \frac{V^2}{x} + \frac{f_c\,V^2}{2\,y} \quad \ldots\ldots\ldots\ldots\ldots\ldots (18)$$

This is the exact equation of water surface profile of thin sheet flow without raindrop impact effect. Unfortunately a direct solution of it cannot be made because of mathematical difficulties. For practical use, therefore, equation (15) is employed to obtain the approximate water surface profile which does represent very closely the exact profile if Δx is kept small.

The Approximate Equation of Water Surface Profile Without the Raindrop Impact Effect

To solve ΔY from equation (15) the water depth at both ends of section Δx must be obtained. Actually only one depth is known. Although equation (15) may be expressed in terms of one known depth y and known quantities of S_o, g, i, f_c, x, and Δx through the following substitution,

$$* \quad y_2 = y + S_o \Delta x - \Delta Y$$

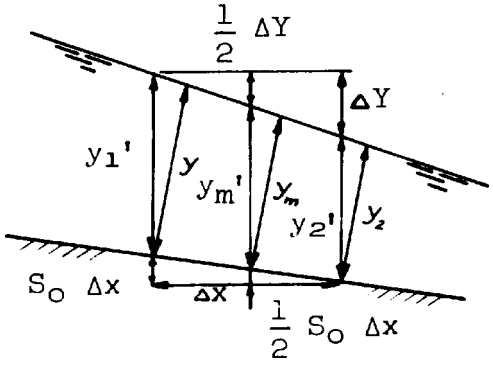
$$* \quad y_m = y + 1/2\, S_o \Delta x - 1/2\, \Delta Y$$

$$q_1 = i\, x = q$$

$$q_2 = i\,(x + \Delta x)$$

$$q_m = 1/2\,(q_1 + q_2) = 1/2[i\, x + i\,(x + \Delta x)] = i\,(x + 1/2\, \Delta x)$$

---

* 

$$y_2' = y_1' + S_o \Delta x - \Delta Y$$

$$\therefore y_2 = y_2' = y + S_o \Delta x - \Delta Y$$

$$y_m' = y_1' + S_o \Delta x - 1/2\, S_o \Delta x - 1/2\, \Delta Y$$

$$= y_1' + 1/2\, S_o \Delta x - 1/2\, \Delta Y$$

$$\therefore y_m = y_m' = y + 1/2\, S_o \Delta x - 1/2\, \Delta Y$$

$$V_1 = \frac{q_1}{y_1} = \frac{i\ x}{y}$$

$$V_2 = \frac{q_2}{y_2} = \frac{i\ (x + \Delta x)}{(y + S_o\ \Delta x - \Delta Y)}$$

$$V_m = \frac{q_m}{y_m} = \frac{i\ (x + 1/2\ \Delta x)}{(y + 1/2\ S_o\ \Delta x - 1/2\ \Delta Y)}$$

$$\Delta V = V_2 - V_1 = \frac{i\ (x + \Delta x)}{(y + S_o\ \Delta x - \Delta Y)} - \frac{i\ x}{y}$$

the reduced equation

$$\Delta Y\ g\ (y + 1/2\ S_o\ \Delta x - 1/2\ \Delta Y) = q\left[\frac{i\ (x + \Delta x)}{(y + S_o\ \Delta x - \Delta Y)} - \frac{i\ x}{y}\right] + i\ \Delta x\ \frac{i\ (x + \Delta x)}{(y + S_o\ \Delta x - \Delta Y)} + \frac{f_c\ \Delta x}{2}\left[\frac{i\ (x + 1/2\ \Delta x)}{(y + 1/2\ S_o\ \Delta x - 1/2\ \Delta Y)}\right]^2 \quad \ldots(19)$$

is very difficult to solve for ΔY.

Therefore, to use the method of successive approximations to obtain water surface profile from equation (15) seems to the writer still the best answer. The procedure consists of: first, assuming a trial ΔY, then from this value and the known depth y_1, values of y_2, y_m, V_2, and ΔV are computed; then, using these values together with the known quantities to compute the ΔY from equation (15). Another trial is needed whenever the computed ΔY differs from the trial ΔY.

$$\Delta Y = \frac{1}{g\ y_m}\left(q_1\ \Delta V + i\ \Delta x\ V_2 + \frac{f_c\ \Delta x\ V_m^2}{2}\right) \quad \ldots\ldots\ldots(15)$$

A similar detail example showing the step-by-step computation can be found in Chapter IV on pages 61 to 65.

CHAPTER II

EXPERIMENTAL WORK

In this chapter the experimental apparatus and the detailed testing procedure are described, and the experimental results are presented.

The experimental arrangement consists of two main parts: the artificial rainfall applicator, and the testing flume, together with the measuring devices necessary for recording the results. Photograph 1 on page 179 illustrates the general arrangement.

The testing procedure divides into two steps: the adjustment of the experimental arrangement to get the best possible results and the actual tests of roughness factor and the effect of raindrop impact on thin flow.

Artificial Rainfall Applicator

From their measurements of natural raindrops, Laws and Parsons (14) found that the median drop diameter (the raindrop diameter dividing the drops of larger and smaller diameter into groups of equal volume) increases with the rainfall intensity. The relation between median drop diameter, D_{50} (mm), and rainfall intensity, i (in. per hr.), can be represented by the equation $D_{50} = 2.23\ i^{0.182}$. Concerning the velocity of waterdrops, Laws (9) found that in still air there is a definite height required to gain its terminal velocity. If distance through which waterdrop falls is less

than this limiting height, the velocity varies with the height. A perfect artificial rainfall applicator for laboratory use must produce uniform rainfall and perform exactly according to the above findings, but unfortunately it has not been developed.

Artificial rainfall applicators were first made by different experiment stations for infiltration and erosion tests. In September, 1936, soil conservation service started a program to develop a sprinkling apparatus for simulating rainfall on experimental plots of 200 or 300 square feet. A total of seven kinds (from Type-A to Type-FA) of apparatus were produced either by modifying those already in use or making entirely new ones. Though most of them are good for field test, none truly simulates natural rainfall. A brief description of the history of the development of these devices can be found in Parsons' discussion about Wilm's work (15).

Today Type-F artificial rainfall applicator (16) is the most widely used device and also has been used quite often in laboratory study of thin sheet flow. It consists of three orifice discs and two sleeves alternately enclosed and confined to definite positions by a cylindrical shell. The base acts as a housing for a standardized entrance arrangement composed of a helix mounted rigidly within an entrance brass tube. When water passes through this narrow spiral base and is forced out from the last disc, it forms a spray containing comparative larger drops and covering an area of about 6 feet square. The main weakness of this apparatus lies in the fact that the drop sizes decrease when the rainfall intensity is increased, because the higher water pressure destroys the chance of occurrence of larger water particles. Figure 1 on page 15 shows the drop size distribution curve for two pressures, 15 and 35 pounds per square inch, made by the United States Soil Conservation Service. Also,

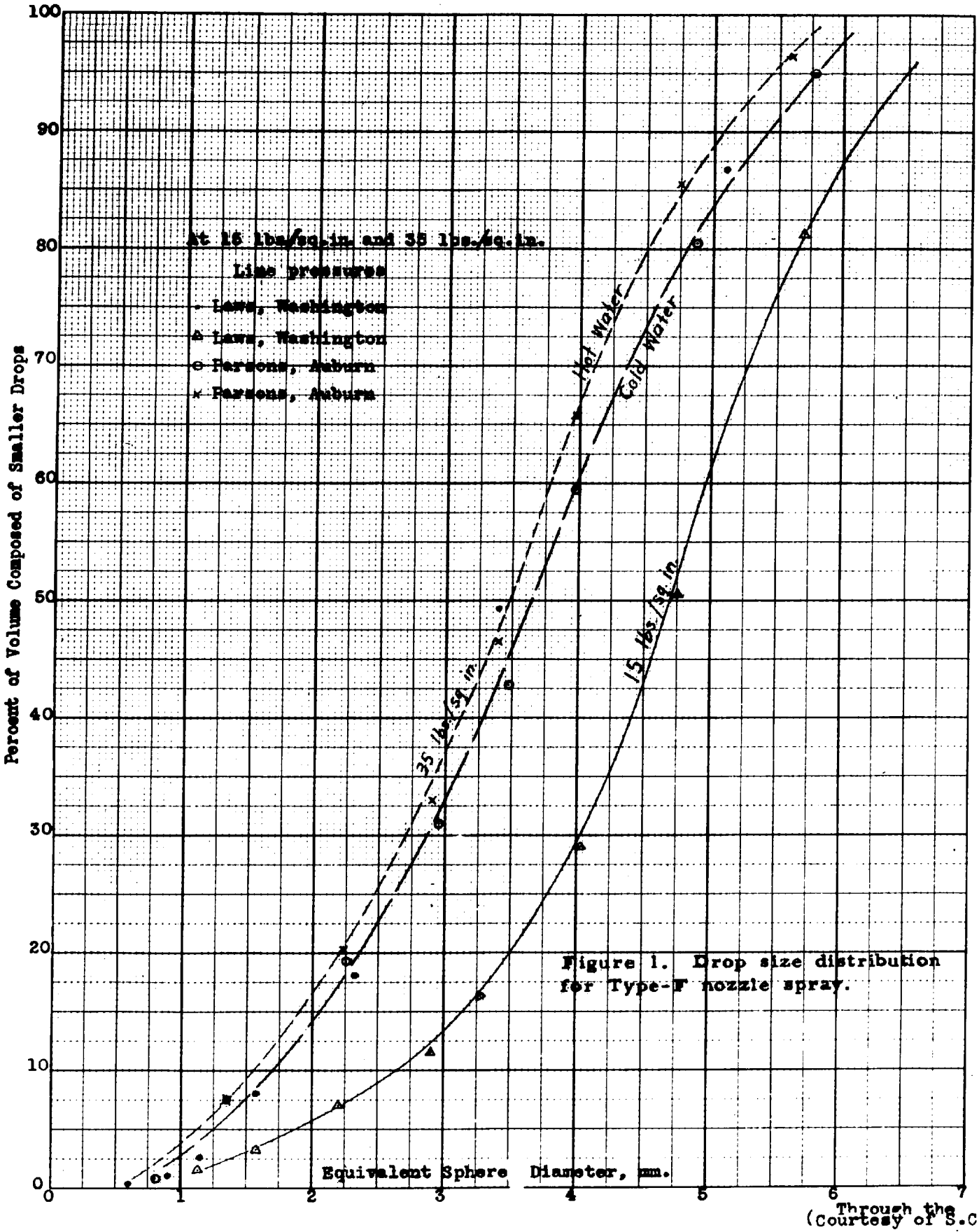


Figure 1. Drop size distribution for Type-F nozzle spray.

(Courtesy of S.C.S.)

Through the

this device does not give as uniform rainfall as is desired for precise laboratory research.

Author's Improved Rainfall Applicator

In order to understand the basic effect of raindrop impact on overland flow, this study requires a fairly uniform rainfall with drops of one size for different rainfall intensities. For these reasons, the Type-F rainfall applicator was considered unsuitable for the experimental work. Considerable time had been spent in trying different methods before this final improved rainfall applicator was adopted. It was derived by modifying the one used by J. J. Goodman (17) in his study of soil characteristics, and also by W. D. Ellison and Pomerene (18), which was also called the Type-C dripolator or stalactometer (15). The principle was to spray water uniformly over a layer of cheesecloth supported by a coarse wire screen, then waterdrops fell from yarns hung underneath. The quantity of spray above controlled the rainfall intensity, and the mattress governed the size of waterdrops.

The spray above the cheesecloth was emitted from nozzles. After many tests for the design and position of the nozzles (see Appendix I) to give a uniform spray pattern, thirty-three of the final design were set in a line above the center of the cheesecloth and spaced 1 foot apart, each with an angle of 35° dip from the horizontal position. Because the spray pattern changed with the water pressure, it was not possible to produce different uniform rainfall intensities just by changing the water pressure in the pipe line. Instead, the nozzles were connected to four pipe lines in such a way that three rainfall intensities could be obtained by turning on one pipe with one-fourth of the nozzles in operation for light rain,

two pipes with half of the nozzles in operation for medium rain, and all four pipes with all the nozzles in operation for heavy rain. In all three cases, the water pressure was almost the same for all nozzles, the difference between the last and the first being 2 pounds per square inch. A small drain was provided directly under each nozzle to take away the dripping water from the nozzle. Detail arrangement of nozzles is shown on Drawing 2 on page 177, while Photographs 3 to 5 on page 180 furnish the detail views of the cheesecloth mattress and the nozzle with drain.

The cheesecloth was supported by wire screen consisting of fencing material made of wire spaced at 2-inch intervals in each direction. A piece of yarn 3/32 inch in diameter and approximately 1-1/2 inch long was fastened to the cheesecloth at the center of each 2-inch square formed by the wire mesh. The total area covered was 35 feet 2 inches long and 2 feet 4 inches wide. This design of mattress produced waterdrops of the average size of 4.5 millimeters in diameter of corresponding sphere (actually the waterdrop was not in spheric shape). Although the size of waterdrop was controlled by the size of mesh spacing, the thickness of the cheesecloth layer, the degree of middle depression, and the diameter of the yarn, yet the smallest possible size was limited by the surface tension of water. The mattress must be set strictly in horizontal position to avoid any concentration of water due to different elevation.

The whole applicator was supported on five wooden frames 8 feet 3 inches apart, with the mattress about 1 foot below the nozzles. About 6 feet 6 inches underneath this mattress laid the testing flume.[1] Muslin strips were hung from the ceiling to the floor

[1] The distance between the upper end of the flume and the mattress was decreased while the flume slope was increased. The effect of this varying height to the waterdrop impact on flowing water is discussed at the end of Chapter III.

on both sides of these frames to prevent the sprayed water from wetting other portions of the laboratory. For detail arrangement see Drawing 1 on page 176.

The Testing Flume

An existing redwood flume of 29 feet 7 inches long by 6-1/4 inches wide was used to catch the rain. Since the maximum depth of flow was recorded at 0.45 inch, the maximum ratio of depth to width was less than one-tenth, the side-wall should have little effect on the center flow. Thus the measured water surface profile along the center line of the flume should represent very closely the overland flow condition.

The flume was rested on four supports, of which three were attached to threaded bars at both ends for adjusting transverse flatness as well as longitudinal slope. The flume was lined up with the mattress of the rainfall applicator so that three lines of raindrops would fall within the side walls along the entire flume length. For flume detail see Drawing 1 on page 176, and Photographs 1 and 2 on page 179.

Surface Condition

No attempt was made to simulate a particular land surface; instead, three materials were used to represent three general classifications of surface roughness--smooth, rough, and very rough.

Smooth surface (Surface "A"): The existing redwood flume was chosen to represent the smooth surface.

Rough surface (Surface "B"): Due to the difficulty of putting a new bottom in the existing flume, a new shallow flume of the same

length and width made of marine plywood with a Masonite board as the bottom was supported on the existing flume. The Masonite bottom was used with the rough side of the Masonite turned up. A thin coating of floor sealer was applied on the Masonite bottom for waterproofing. For the setup see Photograph 2 on page 179.

Very rough surface (Surface "C"): Sand screened between sieves number 16 and 20 with an average size of 1 millimeter in diameter were glued on the Masonite bottom to form this very rough surface. See Photograph 15 on page 185.

Measuring Devices

Water Surface Profile

Along the center line of the testing flume bottom twelve holes were drilled at 4-foot intervals near the middle part of the flume, with smaller intervals at both ends where the changes in water depth were more rapid. For the purpose of checking the side wall effect, two additional holes were drilled on both sides of one center line hole at about the middle of the flume length. In each hole a piece of 8-millimeter glass tube about 6 inches long was carefully glued with the smooth top and just flat with the flume bottom to avoid causing any disturbance of the flowing water. The lower end of the tube was connected by rubber tubing to the manometer bank. For detail see Drawing 1 on page 176, and Photographs 2 and 6 on pages 179 and 181.

The inclined-tube manometer bank

Since this experiment dealt with very thin flow, high accuracy was required in measuring the water depth. Hence the manometers were set at an angle so that they could be read to 0.005 inch on a scale placed parallel to the tubes. The position of this bank in the vertical direction was fixed by a plumb line and a vertical position line marked on the right side of this bank. Because of the inclined scale used to gain sensitivity, the initial reading of each tube for flume at horizontal position was not the same. Consequently these manometers could not be used to adjust the flume flatness, and also the initial readings for each flume slope did not directly indicate the actual bottom slope. For the same reason, this device did not show the actual water surface profile on the manometer bank but gave the static pressures or the water depths along the center line.

Discharge

The water from the flume at the lower end was discharged into a volumetric tank, converted from a 10-gallon corrugated garbage tank 13 inches in diameter. A simple aluminum sliding gate was used to open and close this tank, while a portable point gage was set at a marked position on the upper edge of this tank to measure the water surface elevation. From the calibration curve the quantity of water was obtained. To prevent this tank from receiving the direct rain during operation, a removable aluminum shelter plate extending from the lower end of the flume covered the tank area. See Photographs 1 and 7 on pages 179 and 181 for detail.

Flume Slope

At each flume support, except the lower end one, two stainless steel rods, one at each side of the supporting block, were erected vertically on the base plank. The marks for the flume elevation at different testing slopes at each support were computed from the horizontal distance between the center of supports and painted on the rods. Around each rod a small piece of brass plate fixed on the side of the supporting block was used as the indicator. See Photograph 8 on page 182 for detail.

Rainfall Distribution

Beakers of 6-inch diameter were placed 1 foot 3 inches center to center in the flume. Then depths of water caught in the beakers after a certain time interval of rainfall showed the rainfall distribution along the testing flume. See Photograph 9 on page 182 for detail.

Testing Procedure

Nozzle and Rainfall Distribution

The success of the improved rainfall applicator to produce a uniform rainfall largely depended upon the performance of the nozzles; whether they could give an even spray or not. A great deal of work had been done on this phase of the research before the test actually began. Rainfall distributions were measured at various stages of the experimental work and curves representing these results are shown in Figure 5 on page 92.

Waterdrop Size Measurement

From high-speed photographs Laws (9) showed the actual shape of a falling waterdrop in still air, and that the shape is continuously changing due to the air friction. It is further complicated by the influence of wind in natural rainfall. But for the simplicity and practical convenience in use, the diameter of a sphere of corresponding mass of water was adopted by the former researchers and is used here as the representing dimension of waterdrop size. It was determined by weighing and computing the water of twenty drops from a particular yarn. A total of fourteen measurements were made from different yarns for different rainfall intensities. The results showed a variation from 4.22 millimeters to 4.6 millimeters; generally speaking, it was a little bit larger for larger rainfall intensity; the average size was 4.5 millimeters.

Calibration of Volumetric Tank

With the portable point gage set at the marked position on the top edge of the volumetric tank, the initial reading for the empty tank was taken, and the weight with the dry empty tank was determined. The tank was gradually filled with water to different elevations until nearly full and then it was gradually emptied. In each case the elevation of the water surface and the corresponding weight were recorded, and the net weight of the water was computed and converted to volume. The results were plotted and a curve was drawn to represent the calibrated relation between elevation and volume of water in this tank.

The Test

The entire test consisted of three kinds of bottom surface (smooth, rough, and very rough); each at thirteen different slopes (0, 0.001, 0.002, 0.003, 0.004, 0.006, 0.008, 0.010, 0.015, 0.020, 0.040, 0.060, and 0.075); and each slope subjected to two parts of test (Part 1, the roughness coefficient test, and Part 2, the rainfall test; the latter contained three rainfall intensities--light, medium, and heavy rain).

For any test, the manometer bank position was checked frequently to make sure it was in the right position, and the initial reading was taken carefully before and after each test. The latter was done by adding water to the hole at each station until the water surface was above the flume bottom, then a piece of cloth was used to absorb the water around the station until the water surface in the hole was just flush with the flume bottom and the corresponding manometer reading was taken immediately. The average initial reading at each station was subtracted from the average reading during the tests to obtain water depths. The actual slope of the flume during each test was obtained by subtracting the corrected initial manometer readings when the flume was horizontal from the average initial readings for this test. In the series of tests of Surface "C," the readings thus obtained were measured to the surface of the Masonite board (see Photograph 15 on page 185), then a correction of 0.04 inch (equivalent to 1 millimeter, the average sand size) was added to the initial reading of each station as the corrected initial reading, which represented the location of the top of the sand particles.

Checks and adjustments of bottom slope of the flume and the rainfall distribution

Before and after each series of tests, the bottom slope of the flume and the rainfall distribution were checked and adjusted.

Adjusting flume flatness.--Before the start of a series of tests, the bottom of the flume was brought to a horizontal position by means of a level and rod longitudinally, and carpenters' level transversely. Then the initial manometer reading with water surface at the level of the flume bottom was obtained as described above. Because of the inclined-tube manometers adopted, the initial readings cannot be used directly for precise adjustment of the bottom flatness; therefore, the following still water surface method was employed. The lower end of the flume was sealed and water was discharged into it to form a shallow still pond, the first manometer readings were taken; then more water was added into the pond; after waiting for the water to be in still condition again, the second manometer readings were taken; and by the same procedure the third manometer readings were taken. If the flume bottom were perfectly horizontal, then the water depth obtained for one still water surface would be the same at all stations. (Three still water surfaces were used to minimize the error in manometer reading which is described in the next item.) It was not possible to achieve this ideal condition, but the bottom was adjusted and readjusted until all stations were within ±0.02 inch of a horizontal plane. The manometer reading at each station was corrected to the value which would correspond to a perfect horizontal plane. These corrected zero slope manometer readings were then used to determine the actual slopes of the flume bottom for slopes other than horizontal.

After completing a series of tests, the flume was again lowered to the zero slope condition; the bottom condition was again checked with this still water surface method. This latter reading was only used to examine whether there was any error in the former reading and any big change due to the disturbance in the process of raising and lowering the flume.

Maximum error in manometer reading.--Theoretically, during the adjustment of flume flatness with still water surface method, the increment of water surface elevation at all the stations between first and second readings should be the same, so did those between second and third or first and third readings, since all the three still water surfaces were absolutely flat and parallel to each other. In each case, the results showed that most of the stations had equal increments, occasionally differing by 0.005 inch, but never over 0.01 inch. This indicated that a maximum possible error in this manometer arrangement was only ±0.005 inch. Also, the manometer reading was checked with the portable point gage reading several times for different discharges on different slopes of different bottom surfaces during the Part 1 roughness test (due to the disturbance of waterdrops on the water surface, it was impossible to do this measurement during Part 2 rainfall test). Each time the point gage was set right over the station, so the water depth obtained could be directly compared with that from the corresponding manometer. The results again showed close agreement.

Checking rainfall distribution.--Though the uniform rainfall distribution had been very deliberately adjusted before the Surface "A" test, a complete set of data for all three rainfall intensities before and after each series of tests was still considered necessary

for checking the performance of all thirty-three nozzles and to insure that the nozzles were free from complete or partial plugging. As the nozzle hole was so small that a tiny piece of dirt in the pipe line would block it and thus change the spray pattern and consequently destroy the uniform rainfall distribution which is a vital requirement of this study. The good result of this check-up can assure the value of the experimental data recorded, and form the reliable base of analysis. (See Figure 5 on page 92 for rainfall distribution curves.)

Part 1: roughness test

In this test, water was introduced from a constant head tank through a rubber hose to the upper end of the flume (Photograph 10 on page 183). For further increase of the supply, another hose connected to the municipal supply line was added, and most of these runs were made in the evenings and nights when the pressure in the supply line was quite steady. The amount of supply was controlled by gate valves. The procedure for this test consisted of taking the manometer readings and measuring the corresponding discharge. Usually after the control valve was turned on, an interval of two minutes or more for small discharges was required to allow the condition of steady uniform flow to be formed. The interval for discharging water into the volumetric tank varied from ten seconds to eleven minutes, the time needed to fill up this tank. As Stations 1, 2, and 14 were located at sections of nonuniform flow, only eleven of the fourteen readings were recorded for each run. From the recorded data, a further examination was made to select those which would most probably represent the actual uniform flow (usually Stations 6, 8, and 10 at the middle part of the flume). From these the average value was used as the depth of uniform flow. For each slope,

five or more runs of different discharges were made. Room and water temperatures were taken for each run. Original experimental data sheets are filed in the Civil Engineering Department of the University of Michigan. One sample data sheet of this test is shown on page 72 for reference.

Part 2: rainfall test

In this test, rainfall was the only source of water for the flow in the flume. This rainfall applicator was able to produce three kinds of uniform rain: light, medium, and heavy. Since this applicator was designed for a nozzle spray pattern resulting from a pressure of 40 to 45 pounds per square inch, a constant pressure near this value had to be maintained. It was found that this condition could be obtained from the municipal supply line in the evening and at night when the water consumption was much lower in the buildings where this experimental work was being carried out. For these reasons, the tests were performed from 7:00 p.m. to 5:00 a.m. Photograph 11 on page 183 shows the test (especially the formation of artificial rain) in general, while Photographs 12 to 14 and 16 to 18 on pages 184 to 187 show the flow in the flume for all three rainfall intensities on two extreme slopes (S_o = 0 and 0.075) of Surface "C."

The general procedure for the tests consisted of taking the manometer readings and measuring the corresponding discharge. An interval of at least fifteen minutes was required to obtain equilibrium conditions in the flume after the beginning of rainfall or after changing the rainfall to a new intensity. For each slope six runs were made, two for each intensity, in the following order: light, medium, heavy, light, medium, and heavy. Manometer readings were taken for each run, but discharges were measured only for the last

three runs of every other or every third slope since little change was shown for two consecutive sets of data. From the discharge readings, the actual uniform rainfall intensities were computed, while interpolated values were used for unmeasured slopes. Original experimental data sheets are filed in the Civil Engineering Department of the University of Michigan. One sample data sheet of this test is shown on page 74 for reference.

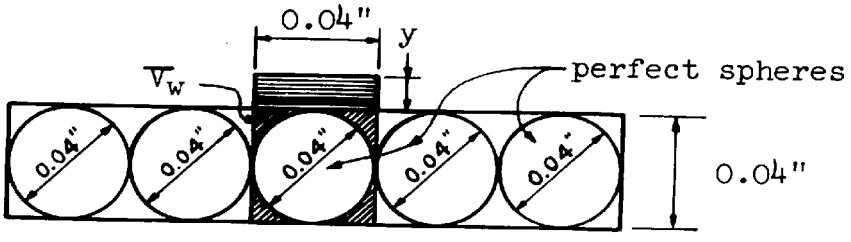
Presentation of Results

Abandoning Surface "A" Data

Because of the considerable difference in elevation of the channel bottom at the flume section connections the water surface profiles, in many cases especially in higher slopes, were not fully continuous, thus subjected to great percentage of error. Therefore the data on Surface "A" were not used.

Water Depth in Surface "C" Tests

The water depth in Surface "C" was first measured from the top of the sand particles, and then corrected for the void water flowing between the sand. This correction is estimated from the ideal condition of perfect spheres.



Assume the sand particles are of perfect spherical shape with a diameter of 0.04 inch,

$$k_s = 0.04 \text{ inch}$$

then the volume of each sand particle is

$$\forall_s = \frac{1}{6} \pi k_s^3 = 0.524 k_s^3$$

For a bottom area of 0.04 inch by 0.04 inch, and a depth of 0.04 inch, the volume of the void water is

$$\forall_w = \forall - \forall_s = k_s^3 - 0.524 k_s^3 = 0.476 k_s^3$$

its corresponding water depth over this same area would be,

$$y = \frac{\forall_w}{A} = \frac{\forall_w}{k_s^2} = \frac{0.476 k_s^3}{k_s^2} = 0.476 k_s = 0.019 \text{ inch}$$

But because the actual sand particles were not exactly spherical in shape and not of exactly uniform diameter, these irregularities would make the sand bottom more compact. The actual amount of this void water, therefore, would not be as large as that computed above from ideal conditions. As a result, a correction of +0.010 inch was added to all the recorded depths except those of zero depths at the upper end of the flume for steeper slopes. In the latter case, the correction of 0.010 inch was added only to the last zero depth.

The Experimental Results

The results of roughness tests were summarized in Columns (3) to (6) of Table I. It includes all the tests made on Surfaces "B" and "C," except for a few on the smallest slopes of Surface "C." In these cases, the data showed that the discharges were too large to allow uniform flow to be formed.

A part of the results of rainfall tests were summarized in Table II. The measured water depths and the water surface profiles were plotted in Figures 11 to 36 on pages 100 to 125.

All the water depths listed or plotted for Surface "C" tests are corrected depths for void water between sand particles.

Table III is a summary of experimental conditions under which this experimental work was done. It gives the actual range and average conditions, and serves as a good reference for those who intend to use the results in this thesis.

TABLE I

RESULTS OF ROUGHNESS TESTS

Surface	Slope S_o	Unit Discharge q (cfs)	Water Depth y (in.)	Water Temp. T_{H_2O} (°C)	Reynolds' No. N_R	Coeff. of Friction f_c	Manning's "n"
(1)	(2)	(3)	(4)	(5)	(6)	(7)	(8)
B	0.001	.002683	.185	18.8	239	.0328	.0161
		.00889	.26	17.5	768	.00829	.0094
		.0163	.405	17.4	1403	.00933	.0094
		.0374	.645	17.5	3230	.00716	.00848
		.0463	.765	17.8	4030	.00776	.00889
	0.002	.00471	.175	19.2	424	.018	.01195
		.01275	.28	17.1	1091	.00981	.00941
		.03075	.515	17.3	2640	.0108	.0103
		.0457	.66	17.8	3980	.01028	.01015
		.07	.87	16.9	5950	.01	.01015
	0.003	.001538	.105	19.0	138	.0547	.02
		.00748	.185	17.0	638	.01265	.0101
		.01495	.30	17.1	1280	.01353	.01095
		.0464	.555	17.4	4000	.00888	.00939
		.0733	.805	16.9	6240	.01086	.01054
	0.004	.0042	.135	18.1	368	.0208	.01255
		.00627	.165	17.3	539	.01705	.01162
		.01653	.28	17.4	1425	.012	.01026
		.02607	.37	16.9	2220	.01113	.01015
		.0469	.58	17.0	4000	.01323	.01147
		.0746	.73	16.7	6320	.01042	.0103
	0.006	.003096	.10	19.0	277	.02335	.01305
		.0084	.155	16.9	715	.01178	.00961
		.02356	.34	16.6	1990	.0159	.01205
		.0482	.545	17.2	4130	.0156	.01242
		.0761	.685	16.5	6410	.0124	.0112
	0.008	.00238	.09	18.9	213	.0383	.0167
		.01123	.205	16.8	953	.0204	.01293
		.0472	.465	17.2	4050	.01345	.0114
		.0668	.585	16.7	5660	.0134	.01153
		.0883	.69	16.8	7500	.0126	.01128

TABLE I--Continued

Surface	Slope S_o	Unit Discharge q (cfs)	Water Depth y (in.)	Water Temp. T_{H_2O} (°C)	Reynolds' No. N_R	Coeff. of Friction f_c	Manning's "n"
(1)	(2)	(3)	(4)	(5)	(6)	(7)	(8)
B	0.010	.00266	.10	17.3	229	.0527	.0196
		.00643	.125	17.1	551	.0176	.01015
		.02545	.30	17.0	2170	.01555	.01176
		.0461	.41	17.1	3950	.01207	.01072
		.0923	.57	18.0	8075	.0081	.00896
	0.015	.002323	.065	17.6	201	.01312	.0284
		.00865	.115	17.3	744	.00906	.01136
		.01994	.19	17.1	1705	.00877	.00963
		.0471	.34	16.9	4010	.00954	.00953
		.0936	.50	17.2	8030	.0088	.00797
	0.020	.00536	.09	17.1	459	.0189	.0117
		.015	.155	17.2	1285	.01235	.00984
		.02825	.215	17.3	2430	.00928	.00879
		.0471	.315	17.5	4075	.0105	.00969
		.099	.47	17.5	8550	.00792	.00875
	0.040	.00521	.07	16.7	441	.019	.011
		.04515	.245	16.5	3805	.01075	.00954
		.05395	.295	16.3	4520	.01315	.0108
		.0805	.36	16.5	6775	.01078	.00998
	0.060	.00519	.065	17.2	445	.0228	.01175
		.0492	.25	17.1	4215	.0144	.01105
		.068	.295	17.0	5800	.01245	.0105
		.0861	.33	17.1	7380	.01083	.01088
		.09275	.36	17.4	7980	.01215	.0106
	0.075	.01468	.11	16.3	1230	.0173	.01117
		.03685	.185	16.4	3100	.01305	.01015
		.07125	.27	16.1	5940	.01085	.00973
		.082	.325	16.4	6885	.0143	.01138
		.0964	.335	16.1	8035	.01135	.01017
C	0.001	.000786	.145	16.5	66	.184	.037
		.002345	.195	16.0	195	.0502	.02
		.0097	.31	15.2	789	.0118	.0103

TABLE I--Continued

Surface	Slope S_o	Unit Discharge q (cfs)	Water Depth y (in.)	Water Temp. T_{H_2O} (°C)	Reynolds' No. N_R	Coeff. of Friction f_c	Manning's "n"
(1)	(2)	(3)	(4)	(5)	(6)	(7)	(8)
C	0.002	.00614	.21	18.8	547	.0183	.01215
		.01198	.295	15.8	992	.0133	.01085
		.0166	.375	14.8	1340	.01425	.0145
		.02165	.45	14.4	1730	.0115	.0118
	0.003	.002017	.145	15.6	166	.084	.025
		.00673	.19	15.5	553	.0169	.0115
		.0126	.30	15.1	1025	.01905	.013
		.02097	.40	14.7	1687	.0163	.01235
		.04655	.695	14.2	3695	.01735	.01325
	0.004	.002323	.13	15.0	188	.0608	.0208
		.00446	.16	14.2	354	.0308	.0153
		.00611	.18	13.9	482	.0233	.0135
		.02397	.43	13.6	1870	.0207	.01405
		.0477	.65	13.5	3720	.018	.0135
	0.006	.003834	.14	15.0	311	.0418	.01755
		.0089	.21	14.2	707	.0262	.0145
		.01747	.315	14.1	1384	.023	.01435
		.02756	.43	13.9	2188	.0234	.01495
		.0485	.595	13.7	3795	.0201	.01415
	0.008	.0058	.145	14.9	469	.027	.01415
		.0115	.23	14.4	919	.0274	.01505
		.02106	.32	14.1	1670	.022	.0141
		.02295	.36	14.0	1811	.0264	.0156
		.0481	.55	13.7	3768	.0214	.0146
	0.010	.00213	.11	11.4	157	.1095	.0269
		.00506	.145	10.9	367	.0445	.0182
		.00724	.16	10.7	523	.0291	.0149
		.00997	.215	10.6	718	.0374	.01735
		.00921	.20	14.2	732	.0351	.01675
		.01492	.27	10.7	1080	.0329	.0168
		.01558	.26	13.7	1221	.027	.0151
		.01825	.305	11.0	1330	.0318	.01675
		.0224	.34	13.4	1740	.0292	.0164
		.0472	.52	13.3	3664	.0235	.0152
		.0741	.685	13.8	5820	.0218	.0149

TABLE I--Continued

Surface	Slope S_o	Unit Discharge q (cfs)	Water Depth y (in.)	Water Temp. T_{H_2O} (°C)	Reynolds' No. N_R	Coeff. of Friction f_c	Manning's "n"
(1)	(2)	(3)	(4)	(5)	(6)	(7)	(8)
C	0.015	.002256	.105	11.6	167	.1275	.0287
		.00433	.125	11.1	316	.0582	.0203
		.00445	.12	16.6	367	.0488	.01825
		.00731	.16	10.8	530	.0429	.01805
		.00868	.185	10.6	626	.047	.0192
		.01483	.25	10.6	1070	.0398	.01835
		.01437	.23	13.8	1130	.033	.0165
		.01904	.29	11.1	1393	.0376	.0182
		.02665	.355	13.5	2178	.0352	.018
		.0521	.525	13.6	4075	.0298	.01715
		.0921	.69	13.1	7100	.0217	.01485
	0.020	.001824	.095	11.8	136	.193	.0344
		.004275	.115	11.2	313	.062	.0204
		.0071	.15	10.9	516	.05	.01945
		.0108	.195	10.9	785	.0475	.0194
		.01177	.195	13.9	928	.04	.0178
		.01477	.235	11.0	1076	.0443	.01925
		.01835	.265	11.6	1360	.0412	.01865
		.02033	.26	13.1	1570	.0317	.0164
		.0456	.445	12.8	3490	.0316	.0174
		.0668	.535	12.8	5110	.0256	.0166
		.0948	.64	12.3	7160	.0217	.0148
	0.040	.001812	.075	12.1	136	.1915	.0334
		.00437	.095	11.3	321	.0671	.0203
		.0069	.125	11.0	503	.0611	.0208
		.0093	.145	10.9	676	.0527	.0198
		.01158	.17	10.8	840	.0547	.0205
		.01666	.205	11.1	1220	.0464	.01925
		.0197	.175	13.4	1530	.0207	.0127
		.0235	.25	12.4	1780	.0422	.0189
		.04425	.36	12.3	3340	.0356	.0181
		.0635	.435	12.3	4800	.0305	.017
		.0895	.555	11.9	6690	.0318	.01775

TABLE I--Continued

Surface	Slope S_o	Unit Discharge q (cfs)	Water Depth y (in.)	Water Temp. T_{H_2O} (°C)	Reynolds' No. N_R	Coeff. of Friction f_c	Manning's "n"
(1)	(2)	(3)	(4)	(5)	(6)	(7)	(8)
C	0.060	.001795	.065	10.9	131	.1905	.0366
		.00759	.115	10.0	538	.0592	.0199
		.01208	.165	10.0	857	.0689	.0288
		.01618	.20	10.0	1048	.0683	.0234
		.0296	.285	10.2	2110	.0592	.0226
		.02808	.24	13.1	2165	.0392	.0182
		.03924	.315	11.2	2880	.0455	.0202
		.0437	.34	12.3	3300	.0461	.0205
		.05435	.385	12.1	4080	.0432	.02
		.0808	.475	11.8	6020	.0368	.0189
		.0991	.53	11.8	7380	.0339	.0183
	0.075	.001904	.07	13.5	148	.265	.0397
		.00595	.11	13.2	460	.1055	.0263
		.00833	.13	13.1	642	.0885	.0251
		.01213	.15	13.1	936	.0641	.022
		.02113	.215	13.3	1637	.0623	.0225
		.02915	.27	13.7	2280	.0648	.0236
		.03886	.335	12.7	2960	.0697	.0251
		.0465	.33	13.0	3580	.0465	.0205
		.0546	.395	12.4	4140	.0578	.0232
		.07115	.45	11.7	5280	.0503	.022
		.0869	.49	11.6	6440	.0436	.0206
		.1017	.53	11.6	7540	.0403	.0199

TABLE II

PART OF THE RESULTS OF RAINFALL TEST

Surface	Slope S_o	Rainfall Intensity i					
		Light		Medium		Heavy	
		Recorded	Interpolated	Recorded	Interpolated	Recorded	Interpolated
		in./hr.	in./hr.	in./hr.	in./hr.	in./hr.	in./hr.
(1)	(2)	(3)	(4)	(5)	(6)	(7)	(8)
B	0.000		1.87		3.22		5.31
	0.001	1.87		3.22		5.31	
	0.002		1.84		3.15		5.28
	0.003		1.81		3.08		5.25
	0.004	1.79		3.02		5.22	
	0.006		1.73		2.98		5.14
	0.008		1.68		2.94		5.06
	0.010	1.62		2.90		4.98	
	0.015		1.61		2.85		4.91
	0.020		1.6		2.8		4.84
	0.040	1.60		2.76		4.77	
	0.060		1.62		2.81		4.75
	0.075	1.64		2.88		4.74	
C	0.000		1.72		3.08		5.17
	0.001	1.72		3.08		5.17	
	0.002		1.69		3.06		5.34
	0.003	1.67		3.06		5.42	
	0.004		1.64		3.01		5.29
	0.006		1.61		2.96		5.15
	0.008	1.57		2.92		5.01	
	0.010		1.55		2.87	5.17	
	0.015		1.52		2.82	4.88	
	0.020	1.49		2.77		4.94	
	0.040		1.49		2.80	4.96	
	0.060		1.48		2.84	4.89	
	0.075	1.48		2.88		5.05	

TABLE II--Continued

Water Temperature T_{H_2O}			Water Pressure		
Light Rain	Medium Rain	Heavy Rain	Light Rain	Medium Rain	Heavy Rain
°C (9)	°C (10)	°C (11)	psi (12)	psi (13)	psi (14)
		17.1	47-48	47-48.5	45-47
17.6	17.6	17.6	46-47	46-47	44-45.5
		17.5	46-47.5	46-47	44-45
		19.0	48-49	48	45-47
18.0	18.5	18.2	47-48	47-47.5	44-45
		17.3	46	45-46	43-45
		18.6	47	46.5	44-44.5
17.2	16.8	17.0	47-47.5	46-47	45
		17.6	45-45.5	44.5-45.5	43
		16.9	46.5-47.5	45.5-47	44.5-45
16.3	16.3	16.5	47.5-48	47.5	45.5
		17.0	48	47.5	45-45.5
16.9	16.9	17.0	48-50	48-49	46-47.5
		15.3	48-48.5	47.5-48	46-46.5
15.2	14.9	14.8	47.5-48	45.5-48	45-46.5
		14.2	47	46-47	45
14.9	14.0	13.8	48.5	47.5-48	45-46.5
		13.3	48-48.5	47-48	45.5-46.5
		13.6	49-50	48.5	47.5
14.0	13.9	13.8	48-50	48.5	46-47.5
		13.7	47-49	47-48	45-46
		13.9	47-48	46-47.5	44-46
14.8	14.6	14.3	46-47	46-47	44-46
		13.6	46-48	46-47	45.5
		14.8	45-48	44-47	44-46
14.6	14.7	14.4	45-47	45-46.5	44.5

TABLE III

SUMMARY OF EXPERIMENTAL CONDITIONS

Item	Surface "B"			
	Part 1		Part 2	
	Average	Range	Average	Range
Raindrop diameter			4.5 mm	
Raindrop ht.				
S_o = 0				6'5"-6'5"
S_o = 0.075				4'2"-6'5"
(*Raindrop velocity				
S_o = 0				(5.65)
S_o = 0.075)				(4.8-5.65)
Rainfall intensity				
Light			1.72	1.6-1.87
Medium			2.97	2.76-3.22
Heavy			5.05	4.74-5.31
Surface length	29'7"	29'7"	29'7"	29'7"
Rain-covered length			29'4"	29'4"
Surface slope		0-0.075		0-0.075
Surface roughness				
Smooth				
Rough		Masonite		Masonite
Very rough				
Water temperature	17.6	16.1-19.2	17.2	15.4-19.0
Water pressure			46	43-49
Room temperature	22.5	20-25	22.5	20-25.1

* From J. O. Laws paper (9).

TABLE III--Continued

Surface "C"				
Part 1		Part 2		Average
Average	Range	Average	Range	
		4.5 mm	4.5 mm (0.18")	4.5 mm (0.18")
			6'5"-6'5"	6'5"
			4'2"-6'5"	5'4"
			(5.65)	(5.65 mps)
			(4.8-5.65)	(5.23 mps)
		1.59	1.48-1.72	1.65 in./hr.
		2.94	2.77-3.08	2.95 in./hr.
		5.11	4.88-5.42	5.08 in./hr.
29'7"	29'7"	29'7"	29'7"	29'7"
		29'4"	29'4"	29'4"
	0-0.075		0-0.075	0-0.075
	Sand (1 mm diameter)		Sand (1 mm diameter)	Red wood Masonite Sand (1 mm diameter)
14.4	10-18.8	14.3	13.3-15.3	15.9°C
		47	44-50	46.5 psi
20.2	17.8-22.5	19.2	17.2-21.2	21.1°C

CHAPTER III

ANALYSIS OF EXPERIMENTAL DATA AND DISCUSSION OF RESULTS

From the nature of this study, the analysis of the experimental data may be divided into two parts, the coefficient of friction for uniform flow and the water surface profiles. In the latter portion the water surface profiles without raindrop impact effect are computed from theoretical equations and compared with the measured profiles. A detailed investigation is made on the effect of raindrop impact on water surface profiles and on the coefficient of friction.

Part 1: Coefficient of Friction for Uniform Flow

From the principle of laminar flow, Horton (19) derived the mean velocity equation for the open channel

$$V = \frac{g S_o y^2}{3\nu} \quad \ldots\ldots\ldots\ldots\ldots\ldots\ldots\ldots\ldots\ldots (20)$$

which can be written as

$$S_o = \frac{3 V\nu}{g y^2} = \frac{6\nu}{V y^2} \frac{V^2}{2 g} = \frac{6}{y N_R} \frac{V^2}{2 g} \quad \ldots\ldots\ldots\ldots (21)$$

Since for uniform flow, $S = S_o$ and $S = h_f/L$, then

$$\frac{h_f}{L} = \frac{6}{y N_R} \frac{V^2}{2 g}$$

or

$$h_f = \frac{6}{N_R} \frac{L}{y} \frac{V^2}{2g} \quad \ldots\ldots\ldots\ldots\ldots\ldots\ldots \quad (22)$$

In general form,

$$h_f = f_c \frac{L}{y} \frac{V^2}{2g} \quad \ldots\ldots\ldots\ldots\ldots\ldots\ldots \quad (23)$$

where h_f is the head lost by boundary friction through a distance of L with a uniform depth and average velocity of y and V. f_c is the coefficient of friction. Although equation (22) was derived from the principle of laminar flow, it is believed that the general equation (23) can also be used in turbulent flow.

This equation is now used in this study of overland flow for computing the energy lost in all flow conditions. The relationship of this coefficient of friction with Reynolds' number is the object of the study of Part 1.

Rearranging equation (21) and using f_c in place of $6/N_R$ yield

$$f_c = \frac{2 g S_o y}{V^2}$$

After replacing g = 32.2 and V = Q/by, it is obtained

$$f_c = \frac{64.4 S_o b^2 y^3}{Q^2} \quad \ldots\ldots\ldots\ldots\ldots\ldots \quad (24)$$

From this equation the coefficient of friction, f_c, is computed for different discharges (or Reynolds' numbers) and slopes. The value of y used is the mean water depth in the middle section of the flume in most cases, except for larger discharges on small slopes of Surface "C" test, where, because of the high roughness of the surface, no uniform flow formed for this flume length. The results

for Surfaces "B" and "C" are shown in Column (7) of Table I and plotted in Figures 6 and 7 on pages 94 and 95, whence the relationship between f_c and N_R is derived.

Discussion of Results

From the basic principle of laminar flow in open channel it is shown (on page 41) that the theoretical relationship between f_c and N_R should be

$$f_c = \frac{6}{N_R}$$

The experimental results for the rough surface fall along a line of $f_c = 7.7/N_R$. This relationship is used in the analysis of water surface profiles and raindrop impact effect for Surface "B."

For the very rough surface, the experimental results show that the coefficient of friction, f_c, increases with increasing bottom surface slope, though they still follow the relationship of a straight line with the same slope as for $f_c = 6/N_R$. The relationship between f_c and N_R for each slope is estimated by the following procedure: first, the value of C ($f_c = C/N_R$) for each slope, S_o, is determined from the experimental results; then, plotting S_o against C/S_o a smooth curve is drawn as shown in Figure 10 on page 98. From this curve the values of C are modified except those for $S_o = 0.000$, 0.001, and 0.003, which are estimated from extending the curve of S_o against the modified C values. The computing table and the curve of S_o versus modified C are also shown in Figure 10. The reason for this increasing discrepancy of value of C in the laminar flow from the theoretical relationship with increasing roughness of bottom surface roughness is not known; since this is not in the scope of this study, no further research has been attempted.

The experimental arrangement only permitted to reach a maximum Reynolds' number of 9000 (or corresponding to 9000 x 4 = 36000 for pipe flow), and the experimental results of f_c versus N_R within the turbulent flow condition up to this limit are quite scattering, but with a tendency to get closer for higher Reynolds' numbers. As a reference, the Manning's "n" are also computed; the results are shown in Column (8) of Table I and plotted against N_R (see Figures 8 and 9 on pages 96 and 97); they show less scattering. Since this study deals with the laminar flow, it leaves this fully turbulent flow for future study.

Part 2: Water Surface Profiles

It consists of two steps: first, to compute the water surface profiles without considering the raindrop impact effect; then, to find the raindrop impact effect on the water surface profiles under different conditions.

Computed Water Surface Profiles Without Raindrop Impact Effect

This analysis is based on equation (15) and the actual coefficient of friction, f_c, obtained in the test of Part 1. From the tests of uniform flow, it was learned that within the laminar range, f_c varies with N_R along a straight line of the same slope as that in the pipe flow. By replacing $f_c = \frac{C}{N_R} = \frac{C}{\frac{q_m}{\nu}} = \frac{C\nu}{q_m}$ and $V_m = \frac{q_m}{y_m}$, equation (15) can be written as

$$\Delta Y = \frac{1}{g\, y_m}\left(q_1\, \Delta V + i\, \Delta x\, V_2 + \frac{C\nu\, \Delta x\, q_m}{2\, y_m^2}\right) \quad \ldots\ldots\ldots \quad (25)$$

In order to apply this equation to compute the water surface profile (also see page 12), it is necessary first to know one water depth together with its location, which is called the starting point.

Methods of determining starting point by use of the critical depth

For slopes less than the critical slope for the discharge at the lower end of the flume.--From the hydraulics of nonuniform flow, it is learned that the critical depth occurs at the free-fall end of a slope which is less than the critical slope. However, little is known about the exact location of critical depth with respect to the end of the flume or the ratio of the depth at the fall to critical depth. These factors vary to some extent with the discharge, bottom roughness, and slope. Only limited work was done, by M. P. O'Brien (20) and H. Rouse (21), for the condition of zero slope under steady flow conditions.

For unsteady flow, this picture is more complicated. Since this study deals with flow of small depths, the friction term (equation 25) controls the shape of water surface profile to such an extent that a small error in assuming the position of critical depth would yield only a negligible error in the computed profile. It was found that an error of 2 or 3 inches in locating critical depth only influences the computed profile to a small extent, for a distance of approximately 20 inches upstream from critical depth. Therefore, in the calculation of the water surface profiles for slopes less than the critical slope, the critical depth corresponding to the discharge at the lower end of flume was always assumed at 352 inches from the upper end of the flume (or 3 or 4 inches from the free-fall end of flume).

For slopes greater than the critical slope for the discharge at the lower end of the flume.--As the bottom slope increases to greater than the critical slope for the discharge at the lower end of the flume, the assumed starting point must be found in another manner. This is because critical depth no longer tends to occur very near to the fall, but occurs at some other location. Hinds' approximate method of locating the position of critical depth was used. The detailed procedure is:

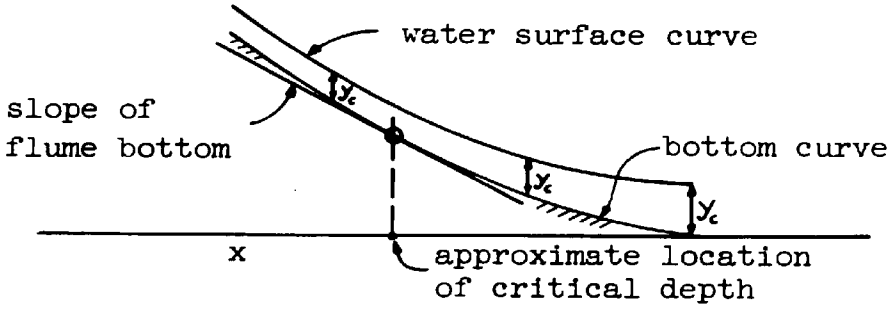
1. Assume the water depths throughout the length of flume are all critical depths.

2. Use equation (25) to compute ΔY between successive critical depths.

3. Plot this critical depth water surface and the bottom curves.

4. Locate the point on the bottom curve which has the same slope as the actual bottom slope. This is the position of critical depth.

This procedure is illustrated by the following sketch.



Owing to the fact that the friction term dominates in the computation of the water surface profile, the starting point does not require the exact location of the critical depth, as the error involved is easily minimized after smoothing the connection between the two parts, upstream and downstream from this point, of the computed water surface profile.

The detailed computations of all the water surface profiles without raindrop impact effect by using equation (25) are filed in the Civil Engineering Department of the University of Michigan. A set of sample sheets of computations including both the conditions mentioned above are shown on pages 77 to 83. All the computed water surface profiles without raindrop impact effect together with the curves of critical depth for corresponding uniform flow when the slope is greater than the critical are shown in Figures 11 to 36 on pages 100 to 125.

The effect of Δx value on water surface profile

Values of Δx must be chosen arbitrarily in the solution of equation (25) for water surface profiles. A detailed investigation was made to determine the effect of using different values of Δx in the calculations. For a particular set of conditions, the water surface profile was computed for three different values of Δx. It was found that no appreciable difference occurred for values of Δx up to 48 inches. In each case values of Δx were made gradually short near the ends of the flume where changes in depth were more rapid.

The water surface profiles, shown in Figures 11 to 36 on pages 100 to 112 and 113 to 125 were established by plotting the average depth ($y_m = \frac{1}{2}(y_1+y_2)$) for each reach ($\Delta x$) at the center of the reach. Values of y_m were used because they are more consistent than the y values at the two ends of the section Δx. This method of plotting the profile eliminates most of the errors which resulted from the choosing of the approximate location of the critical depth and the arbitrary value of Δx. As a result, it represents more the

true form of the water surface profile without the raindrop impact effect.

The Raindrop Impact Effect

The raindrop impact effect consists of:

(1) changing the momentum of the flowing water;

(2) increasing the intensity of turbulence of the flowing water;

(3) changing the heat energy of the flowing water; and

(4) changing the pressure on the land surface.

Little is known about how each one changes mechanically, but from the knowledge of fundamental physics and hydraulics, the following qualitative analysis can be made.

The effect on total momentum of the flowing water

This consists of two parts: the change of momentum of the increased quantity of flow or the rainfall and the change of the momentum of the original quantity of flow.

The first part of this effect can be estimated from the summation of the individual raindrops falling within the reach under consideration. When one raindrop hits the flowing water, it breaks into small parts which bounce out in all directions with different velocities. The sum of the products of the masses of the parts of each drop with their corresponding velocity components in the direction of flow gives the net increase in momentum due to one raindrop in the direction of flow. This raindrop momentum varies with the size, shape, and velocity of the raindrop; the angle between the rainfall direction and bottom surface; and the intensity of the rainfall.

Among them the slope of the bottom surface stands much more important than the rest of the factors.

The second part of this effect is represented by the change of vertical velocity distribution of the original flowing water. Ordinarily the maximum velocity occurs near the water surface. Now the raindrop impact cancels a part of the energy of the flowing water and thus reduces its velocity. This effect is more serious near the top of the water surface vertically. Its magnitude again depends upon the rainfall characteristics; the depth and velocity of the flowing water; and the angle between the rainfall direction and bottom surface.

The effect on the intensity of turbulence of the flowing water

The continuous pounding on the flowing water by the raindrops not only affects the momentum, but also changes the intensity of turbulence of the flowing water. It causes the disturbances in laminar flow and increases the intensity of turbulence in turbulent flow. Because of this consistent local disturbance, the viscous stress of the originally laminar flow is not sufficient to quell such fluctuations. As a consequence, in this study, there no longer exists the pure laminar flow. The whole flow is a turbulent flow of increasing intensity of turbulence with increasing distance from the upper end. Therefore, Reynolds' number does not indicate any more the different stages of conditions of flow, but the intensity of turbulence of the flow. The roughness factor should have a continuous relationship against all Reynolds' numbers. Again this effect varies with the rainfall characteristics and the depth of the flowing water.

The effect on heat energy of the flowing water

Resulting from the difference of temperatures of the raindrops and the flowing water, this effect is usually small unless the difference is large. Also, a part of the kinetic energy of the raindrop is converted into heat loss. The latter one is so small that it has no practical significance.

The effect on the pressure on the bottom surface

The dynamic force of the raindrop impact transfers through the flowing water to the bottom surface. Because of the high velocity of the raindrops and the shallow depth of the overland flow this is one of the most important factors in the soil erosion problem during rainfall. This pressure again changes with the rainfall characteristics; the angle between the raindrop direction and the water surface or bottom surface; and the depth and velocity of the flowing water. Since this is not in the scope of this study, no effort was tried to investigate this effect.

From the above analysis it is quite clear that all these effects are interrelated and depend upon the characteristics of the rainfall and the flowing water, and the roughness of the bottom surface. A separate study for each effect seems almost impossible, especially at this stage, since the fundamental mechanics dealing with a single raindrop have not been studied. Fortunately, under certain conditions, many of these factors have only a minor effect, such as the effect of change of momentum of the raindrops on the momentum of the flowing water is negligible in this study, because of the small slope of

the bottom surface, with a maximum of 7.5 percent or 5 degrees. In order to further simplify this study by eliminating as many variables as possible, the raindrops were maintained at the same size and nearly equal velocity throughout the experiments. Since rainfall is the only source of supply, the effect on heat energy of the flowing water is nil.

The studies reported here serve to evaluate the gross effect on the water surface profile of the raindrop by comparing measured profiles with profiles computed by means of equation (25). The practical result is a series of values of the roughness factor (f_c'--the effective coefficient of friction) which, when compared with values of f_c for steady flow, show the gross effect of the raindrop impact. Values of f_c' were computed for various reaches of the measured water surface profiles using equation (15) rearranged as follows.

$$f_c' = \frac{2}{\Delta x \left(\frac{q_m}{y_m}\right)^2} (g\, y_m\, \Delta Y - q_1\, \Delta V - i\, \Delta x\, V_2) \quad \ldots\ldots (26)$$

The computations of f_c' for all the measured profiles are filed in the Civil Engineering Department of the University of Michigan; a sample is shown on page 85. The results can be found in Figures 41 to 66 on pages 132 to 157.

Discussion of results

When the experimental values of f_c' are plotted against N_R as shown in Figures 67 to 72 on pages 159 to 164, no consistent relationship occurs. This is in contrast to the relation between f_c and N_R (Figures 6 and 7 on pages 94 and 95) which occurs during steady flow conditions in the laminar range. This is not difficult to understand since the raindrop impact disturbs and hastens the change of

flow from the regular laminar condition to the irregular turbulent condition, for which no fundamental rule has been developed. However, the following conclusions can be drawn for the general tendencies:

1. For rough surface the relationship between f_c' and N_R differs from the steady flow relationship more than for smooth surfaces (because turbulent flow starts more easily on rough surfaces, this is seen from comparing the f_c' versus N_R curves of Surfaces "B" and "C").

2. The impact effect is greater for small depths and small values of N_R (because the disturbance has much more influence on the manner of flow, as illustrated in Figures 67 to 72 on pages 159 to 164, from the curved upper end part of the f_c' versus N_R curves).

3. The corresponding f_c' values for the same N_R decrease with increasing slope for very small slopes, but do not follow this rule for steeper slopes.

4. When N_R is large, values of f_c' (for a certain roughness and slope) are greater for the heavier rains, while for small values of N_R the larger values of f_c' occur during light rains (as illustrated from f_c' versus N_R curves for constant slope).

5. For rougher surfaces, high rainfall intensities and steep slopes (because the water depth is smaller on steep slopes), the relationship between f_c' and N_R tends to follow a straight line. This may be reasoned from the combining results of (1) and (2).

The feasibility of equation (26)

In Chapter I, it is indicated that equation (15) only applies to the computation of water surface profiles without raindrop impact effect. This equation is also subjected to the restrictions of several

other assumptions imposed during the derivation. Now whether this equation, in the form of equation (26), can also be used to determine the raindrop impact effect needs to be proved. Analytical investigations have been made. They include two parts: the direct effect of raindrop impact to the total momentum of the flowing water, and the effect on the coefficient of momentum, C_m. From these discussions it is concluded that those effects are of minor importance and the use of equation (26) to find the gross effect of raindrop impact is justified.

Detailed treatment for each factor are included in the appendixes:

Appendix II: The Consideration of Actual Change of Momentum.

Appendix III: Modifying the Derivation of Equation (15) to Include the Coefficient of Momentum.

The Use of Actual Rainfall and Actual Slope of Bottom Surface

All the computations are based on the conditions of uniform rainfall and uniform bottom surface slope. Neither of these conditions could be easily obtained due to the technical difficulties. The question would naturally arise as to how seriously these variations would affect the computed profiles. Therefore, profiles were computed for actual rainfall and actual bottom surface slopes for two slopes, 0.002 and 0.020, and on both Surfaces "B" and "C." The actual rainfall for a particular intensity, slope, and bottom surface was computed from the recorded discharge and the use of rainfall distribution curves before and after each bottom surface test, as shown in Figure 5 on page 92. The actual bottom surface slopes for each test were obtained by subtracting the corrected initial manometer

readings when the flume was horizontal from the initial reading for this test, as explained on page 24.

The results show that the water depths are more sensitive to the actual bottom surface slopes than the actual rainfall, and the maximum difference between the water depth computed from ideal conditions and that of actual conditions are not more than 10 percent of the ideal condition. Since the difference between these two conditions are not consistent, but rather following closely the actual local surface slope, greater depth for slope less than the ideal one and vice versa, the water surface profile of the average actual conditions can be well represented by that of the ideal conditions. Sample computations are shown on page 87, and the results are plotted in Figures 37 to 40 on pages 127 to 130.

The Simplified Approximate Equation

Equation (15) on page 10 can be simplified by neglecting the first two terms on the right side as follows:

$$\Delta Y = \frac{1}{g\, y_m}\left(\frac{f_c\, \Delta x\, V_m^2}{2}\right) = \frac{f_c\, \Delta x\, q_m^2}{2\, g\, y_m^3} \quad \ldots\ldots\ldots \quad (27)$$

The terms neglected are momentum terms. Therefore, equation (27) is based on the assumption that the profile is determined entirely by friction. This equation gives smaller water depths than equation (15), the difference decreases with increasing surface slope and roughness, and increases with the rainfall intensity. For small slopes and near the exit of the flume, considerable smaller depths are obtained. Examples of using this equation are made and results plotted for slopes 0.002 and 0.020 of Surfaces "B" and "C" (see Figures 37 to 40 on pages 127 to 130). Sample computations are shown on page 89.

The Minimum and Zero Water Depth

When the depth of the flowing water becomes very small, a point is reached where the continuous sheet of water is broken up into small segments and thereafter flow proceeds from one segment of water to another and might be described as discontinuous. This lower limit of depth depends upon the surface tension of water and nature of the bottom surface. It also changes with the rainfall intensity and the size and velocity of the raindrop, as raindrop impact helps to break up the water. Under this situation, the surface uniformity or evenness has a great effect on the manner in which the water flows. For this reason, when zero depth is recorded it means that flow is discontinuous. It usually happens at the upper end of the flume for steeper slopes.

The Wave Motion and Supercritical Flow

During the experimental tests, it was noted that, when the slope reached 0.075 for Surface "B" and 0.060 for Surface "C," the flow started to possess a wave motion which was more prominent for heavy rainfall. Horton (4) also noted this phenomenon on steep slopes during heavy rainfall and described it as a rain-wave-train. In both cases, the flow was near critical and in the supercritical condition. The cause of the formation of this wave motion is yet unknown. A possible explanation might be that as high velocity flow in thin sheets is struck by heavy rainfall, it is disturbed abruptly by the high impact force of the raindrops and its local velocity is temporarily reduced. However, the undisturbed parts of the flow still push forward with their original velocity. This intermittent pounding by raindrops causes fluctuations of local velocity which then

grow into visible wave motions. Since this motion occurred only on the three steepest slopes, it is not believed important enough in this study to receive any further investigation.

An Investigation of the Kinetic Energy of Waterdrops

In general, the raindrop impact effect is proportional to the kinetic energy of the rainfall which depends upon the raindrop velocity. However, this kinetic energy cannot be represented simply by the product of the quantity of rainfall and the raindrop velocity because the intensity of impact is also influenced by raindrop size. In order to determine the real relationship further investigation with different waterdrop sizes and velocities is required. For reference purposes, it is of interest to compare the kinetic energy of a single waterdrop of natural rain with that of corresponding rainfall intensity in this experimental work (see Table IV on the next page).

TABLE IV

COMPARISON OF KINETIC ENERGY OF A SINGLE WATERDROP OF NATURAL RAIN WITH THAT OF EXPERIMENTAL RAIN

Rainfall Intensity (in./hr.)	Waterdrop Diameter (mm.)	Height of Drop	Velocity m./sec.	Kinetic Energy 10^{-6} ft.-lb.
Natural Rain				
Light (1.65)	2.45[a]	12 m.	7.25[b]	0.68
Medium (2.95)	2.75[a]	14 m.	7.75[b]	1.1
Heavy (5.08)	3.1[a]	16 m.	8.2[b]	1.76
Experimental Rain				
Light (1.65)	4.5[c]	6'5''[d]	5.65	2.55
		4'2''-6'5''[e]	4.8-5.65	1.84-2.55
Medium (2.95)	4.5[c]	6'5''	5.65	2.55
		4'2''-6'5''	4.8-5.65	1.84-2.55
Heavy (5.08)	4.5[c]	6'5''	5.65	2.55
		4'2''-6'5''	4.8-5.65	1.84-2.55

[a] Median-diameter from Laws and Parsons' paper (14).

[b] Terminal velocity for corresponding median-diameter from Laws' paper (9).

[c] Uniform waterdrop diameter.

[d] When $S_o = 0$.

[e] When $S_o = 0.075$.

CHAPTER IV

PRACTICAL APPLICATIONS

The results of this study are used to obtain the water surface profiles during rainfall on impermeable surfaces under various conditions within the experimental limites of this study. Although the conditions under which the results are obtained are ideal (uniform rainfall and uniform bottom surface slope) and the height of rainfall is not enough to allow waterdrop to gain its maximum velocity, it is believed that those factors do not reduce their actual value in practical use. It is believed that the results could also be applied with reasonable accuracy to permeable surface. The procedure is, first, to correct the run-off for infiltration loss by means of the infiltration curve to get the net supply. The effective coefficients of friction can then be used by the method described in the following paragraphs to determine the water surface profile. From the water surface profile can be obtained the mean velocity at any place which indicates the transporting and erosive ability of the flow, two vital factors in the soil erosion study. Following is a description of the methods of obtaining the water surface profile during rainfall on impermeable surfaces.

Computing Water Surface Profiles During Rainfall

Friction Factors

In order to compute a water surface profile it is first necessary to determine values of the effective coefficient of friction (f_c') for the particular set of conditions. Values of f_c' differ from corresponding quantities for uniform flow (f_c) and vary with rainfall

intensity, slope, and bottom surface roughness. Figures 41 to 66 on pages 132 to 144 and 145 to 157 give values of f_c' as a function of N_R and also show how f_c' differs from f_c for various bottom surface slopes, roughnesses, and rainfall intensities. Each plate gives results for three rainfall intensities and one bottom surface slope. Figures 41 to 53 on pages 132 to 144 show values for bottom Surface "B," and Figures 54 to 66 on pages 145 to 157 give values for bottom Surface "C." It is interesting to note that for small slopes f_c' is larger than f_c and this difference increases with rainfall intensity. However, for steeper slopes, f_c' is smaller than f_c for small Reynolds' numbers and the difference is larger for heavy rainfall intensity; this condition is gradually reversed for larger Reynolds' numbers.

Figures 67 to 69 on pages 159 to 161 show how f_c' is affected by slope for each rainfall intensity on Surface "B." Values of f_c' at the very upper end and near the downstream end are not included because they are not reliable and affected by the lower end conditions. The straight line of $f_c = 7.7/N_R$ represents the relationship between the Reynolds' number and the coefficient of friction for uniform laminar flow on this surface (see Figure 6 on page 94). From these curves it is learned that, for slopes smaller than 0.6 percent, f_c' is larger than f_c. The increase in the value of coefficient of friction due to rainfall impact is the largest on the smallest slope and decreases as the slope increases. The relationship between f_c' and N_R for each of these small slopes can be closely represented by a straight line parallel to that of the uniform flow. For slopes steeper than 0.6 percent, the values of f_c' at upper ends for small Reynolds' numbers begin to drop. This decrease is more evident and extends further downstream when the slope increases. Consequently, the relationship between f_c' and N_R for each slope follows a curve line

with a general slope smaller than that of uniform flow which gradually decreases with increasing bottom slopes. However, it does not have a consistent change with bottom slopes: the values of f_c' for 2 percent slope are smaller than that for 6 percent. This general pattern of variation is more aggravated by heavy rainfalls. The irregularity of the variation between f_c' and N_R for different slopes makes the attempt of deriving any general law impossible. Figures 70 to 72 on pages 162 to 164 show the results on Surface "C." The straight line of $9.6/N_R$ with a slope of 1 to 1 represents the relationship of f_c and N_R for uniform flow on 0.001 slope of this Surface "C" (see Figure 7 on page 95). In this case the results are further complicated by the continuous change of relationship between coefficient of friction and Reynolds' number with bottom surface slopes for uniform laminar flow. Because of the complex relationship between f_c' and N_R, bottom surface slope and rainfall intensity, the most accurate method of finding values of f_c' is to read values directly from the curve of Figures 67 to 72.

The C' Curves

The relationships involving f_c' with N_R, bottom surface slope and rainfall intensity can be expressed in simpler form if very small Reynolds' numbers are neglected. These small Reynolds' numbers occur at the upper end of the runoff area where depths and discharges are very small. Under these conditions depths tend to be so thin that flow is affected by surface tension--which may break the flow into small segments. Therefore, neglecting the experimental results on the upper third of the testing flume,[1] the

[1] For the sake of consistency in comparison, the middle section of the flume, x = 102 to 246 inches from the upper end, is

relationship between f_c' and N_R can be best fitted by straight lines (with 1 to 1 slope on log-log coordinates) parallel to the corresponding line for uniform undisturbed flow. Thus, for a particular rainfall intensity and on the same surface, a family of straight lines with different interceptions C' is obtained. C' is defined by equation (28):

$$f_c' = \frac{C'}{N_R} \quad \ldots\ldots\ldots\ldots\ldots\ldots\ldots\ldots \quad (28)$$

By comparing C' for the light rainfall (designated as C_L') to the corresponding C for uniform undisturbed flow, $f_c = C/N_R$, a curve of C_L'/C can be drawn against S_o, the slope of the bottom surface. Likewise, by comparing C' for the medium rainfall (designated as C_M') to C, a curve of C_M'/C versus S_o is drawn. And so is the curve of C_H'/C versus S_o, where C_H' is C' for the heavy rainfall. From these three curves the effect of the raindrop impact on values of C are clearly expressed. The effect of different rainfall intensities on values of C' are represented by curves of C_M'/C_L' and C_H'/C_L' versus S_o as shown in Figures 73 and 74 on pages 166 and 167.

The Method

From the above conclusion a method of computing the water surface profile during rainfall is developed for practical use. First,

---

used for the determination for C' values. The range of average N_R corresponding to this section for three rainfall intensities are:

	Surface "B"	Surface "C"
for light rain	29-70	25-60
for medium rain	50-121	46-111
for heavy rain	85-206	80-192

the coefficient of friction of the particular surface and slope for uniform flow must be known and also the rainfall intensity to be used; then from the C'/C curves, Figures 73 and 74 on pages 166 and 167, the C' value for this particular condition can be determined. By using this value of C' in place of C in equation (25), the profile can be computed. Examples of profiles computed by this method are shown in Figures 2 to 4 on pages 66 to 68, and the sample sheet of computation on page 64. All computations are filed in the Civil Engineering Department of the University of Michigan.

Following is an example of detailed procedure of computation of water surface profile during rainfall. Take the condition of light rainfall (1.87 inches per hour or 0.000518 inch per second) on Surface "B" with a slope of 0.001 (see the computation sheet on page 64).

1. From Figure 73 on page 166, the value of C_L'/C for S_o = 0.001 is found to be 1.72.

2. Since the value of C for uniform flow is equal to 7.7 (see Figure 6 on page 94), then $C_L' = 1.72\ C = 1.72 \times 7.7 = 13.2$.

3. By using this value, 13.2, as the value of C, equation (25) can be written:

$$\Delta Y = \frac{1}{g\ y_m}\left(q_1\ \Delta V + i\ \Delta x\ V_2 + \frac{13.2\ \nu\ \Delta x\ q_m}{2\ y_m^2}\right)$$

4. Since the slope of bottom surface in this example (S_o = 0.001) is smaller than the critical slope (see page 44), the critical depth is assumed to occur at x = 352 inches from the upper end. This is computed as y_c = 0.0442 inch.

5. Then the values of Δx are fixed. Because the change of water surface is more rapid at both ends of the flume, the Δx selected are varying from 7 to 48 inches at lower end and then

gradually reduced from 48 to 9 inches at the upper end (see column 3 on page 64).

6. By taking the bottom surface elevation at x = 352 inches as zero and assuming that the slope is uniform, the rest of the values in column (4) are computed.

7. By assuming that the distribution of rainfall is uniform, the quantities of water received within each Δx are computed (see column 14), from which the rate of flow at each point and the average rate for each Δx are computed (see columns 9 and 10).

8. Since the quantities at x = 352 inches are known, the computation is started at x = 345 inches. A trial ΔY of 0.11 inch is assumed first, then step by step (the computation sheet is self-explanatory) the ΔY is computed as 0.0558 inch in column (19). This value does not agree with the trial ΔY of 0.11 inch, hence a new trial ΔY of 0.08 inch is assumed and the computation is repeated. After the fourth trial, the computed ΔY of 0.0817 inch coincides with the trial ΔY, then the corresponding value of y for this trial, 0.1189 inch, is the water depth at x = 345 inches.

By the same procedure the values of y in column (7) are obtained. As explained previously (near the bottom of page 46), values of y_m in column (8) are used to plot the water surface profile which is shown together with the one through experimental results on page 66.

Water Surface Profiles During Rainfall Obtained from Experimental Graphs

Figures 75 to 80 on pages 169 to 174 are the summary of the experimental results of water surface profiles on Surfaces "B" and "C." Water depth is plotted against distance along the flume for

each rainfall intensity and surface roughness. Values of Reynolds' number are also shown for each location except near the downstream end where end conditions affect the depth. The broken line represents the position of critical depth; to its left side the velocity is subcritical and to the right side it is supercritical. From these curves the water surface profile for any condition within the experimental limits can be obtained very easily. Although this method gives a truer profile than could be obtained from computation, it is strictly empirical and would require extensive experimental data to cover all possible conditions.

WATER SURFACE PROFILE DURING RAINFALL — Surface "B" Light rain

11-20-1955

$$\Delta Y = \frac{1}{g y_m}\left(q_1 \Delta V + i \Delta x V_2 + \frac{C_L' \nu \Delta x q_m}{2 y_m^2}\right)$$

x	x_m	Δx	Bottom Elev.	Trial ΔY	Surface Elevation	y	y_m	q	q_m
(1)	(2)	(3)	(4)	(5)	(6)	(7)	(8)	(9)	(10)
352			0		0.0442	0.0442		0.1823	
345	348.5	7	0.007	0.11	0.1542	0.1472	0.0957	0.1788	0.1807
				0.08	0.1242	0.1172	0.0807		
				0.0818	0.126	0.119	0.0816		
				0.0817	0.1259	0.1189			
336	340.5	9	0.016	0.023	0.1489	0.1329	0.1259	0.174	0.1764
				0.0234	0.1493	0.1333	0.1261		
318	327	18	0.034	0.034	0.1833	0.1493	0.1413	0.1647	0.1694
				0.0328	0.1821	0.1481	0.1407		
				0.0322	0.1815	0.1475	0.1404		
294	306	24	0.058	0.032	0.2135	0.1555	0.1515	0.1522	0.1585
				0.0318	0.2133	0.1553	0.1514		
246	270	48	0.106	0.05	0.2633	0.1573	0.1563	0.1274	0.1398
				0.0504	0.2637	0.1577	0.1565		
				0.0505	0.2638	0.1578	0.1566		
198	222	48	0.154	0.044	0.3078	0.1538	0.1558	0.1025	0.115
				0.0428	0.3066	0.1526	0.1552		
				0.0427	0.3065	0.1525			
150	174	48	0.202	0.0394	0.3459	0.1439	0.1482	0.0777	0.0901
				0.0386	0.3451	0.1431	0.1478		
102	126	48	0.25	0.035	0.3801	0.1301	0.1366	0.0528	0.06525
				0.0353	0.3804	0.1304	0.1368		
54	78	48	0.298	0.031	0.4114	0.1134	0.1219	0.028	0.0404
				0.0309	0.4113	0.1133			
30	42	24	0.322	0.0108	0.4221	0.1001	0.1067	0.01554	0.02177
				0.012	0.4233	0.1013	0.1073		
				0.0121	0.4234	0.1014	0.1074		
12	21	18	0.34	0.0068	0.4302	0.0902	0.0958	0.0062	0.01087
				0.0064	0.4298	0.0898	0.0956		
3	7.5	9	0.349	0.0012	0.431	0.082	0.0859	0.001554	0.00388

$\frac{C_L'}{C}$ = 1.72

C_L' = 1.72 x 7.7 = 13.2

S_o = 0.001

i = 0.000518 in./sec.

y_c = 0.0442 in.(x = 352 in.)

T_{H_2O} = 17.6°C

ν = 1.663 x 10^{-3} in.^{2}/sec.

g = 386.4 in./sec.^{2}

V	ΔV	$q_1\Delta V$ (a)	i Δx	$i\Delta x V_2$ (b)	$\frac{C_L'\nu\Delta x q_m}{2}$	$\frac{C_L'\nu\Delta x q_m}{2y_m^2}$ (c)	(a) + (b) + (c)	ΔY
(11)	(12)	(13)	(14)	(15)	(16)	(17)	(18)	(19)
4.125								
1.215	2.91	0.53	0.003625	0.015	0.01391	1.518	2.063	0.0558
1.526	2.599	0.465				2.135	2.615	0.0838
1.503	2.622	0.469				2.09	2.574	0.0816
1.503	2.622	0.469				2.09	2.574	0.0817
1.31	0.193	0.034	0.00466	0.007	0.01749	1.103	1.144	0.0235
1.305	0.198	0.034				1.1	1.141	0.0234
1.103	0.202	0.033	0.00933	0.012	0.03357	1.68	1.725	0.0316
1.112	0.193	0.032				1.696	1.74	0.032
1.117	0.188	0.031				1.703	1.746	0.0322
0.979	0.138	0.021	0.01243	0.014	0.04185	1.823	1.858	0.0317
0.98								
0.81	0.17	0.022	0.02486	0.024	0.0738	3.02	3.066	0.0508
0.808	0.172	0.022				3.014	3.06	0.0506
0.666	0.142	0.015	0.02486	0.02	0.0607	2.503	2.538	0.0421
0.672	0.136	0.014				2.52	2.554	0.0426
0.54	0.132	0.01	0.02486	0.017	0.0476	2.166	2.193	0.0383
0.543	0.129	0.01				2.18	2.207	0.0387
0.406	0.137	0.007	0.02486	0.014	0.0345	1.85	1.871	0.0355
0.405	0.138	0.007				1.843	1.864	0.0353
0.247	0.158	0.004	0.02486	0.01	0.02137	1.439	1.453	0.0309
0.155	0.092	0.001	0.01243	0.003	0.00575	0.506	0.51	0.0124
0.153	0.094	0.001				0.5	0.504	0.0121
0.069	0.084	0.005	0.00933	0.0014	0.002157	0.235	0.237	0.0064
						0.236	0.238	0.0064
0.019	0.05	0.0001	0.00466	0.0003	0.000384	0.052	0.0524	0.0012

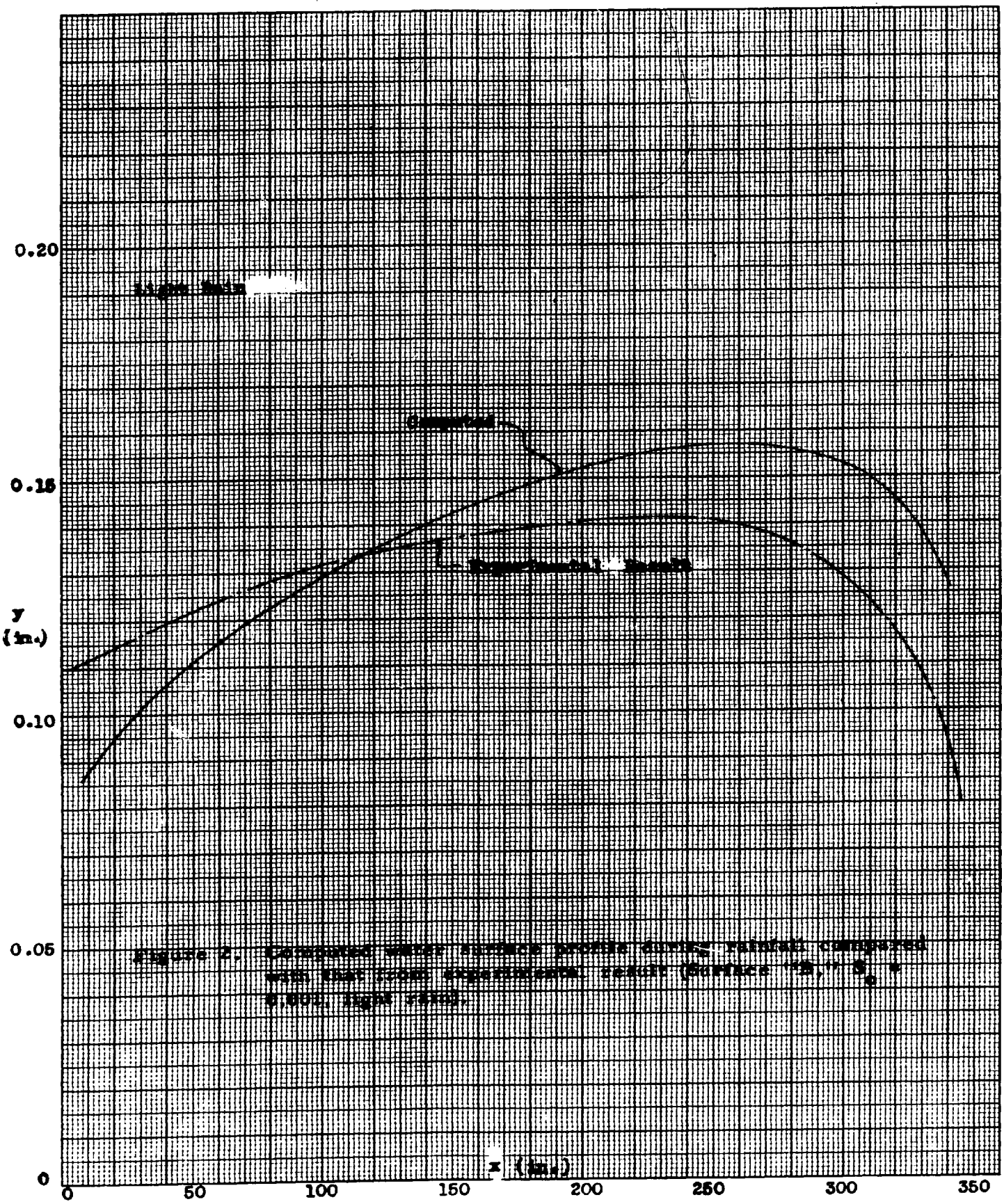


Figure 2. Computed water surface profile during rainfall compared with that from experiments, result (Surface "B," S_o = 0.005, light rain).

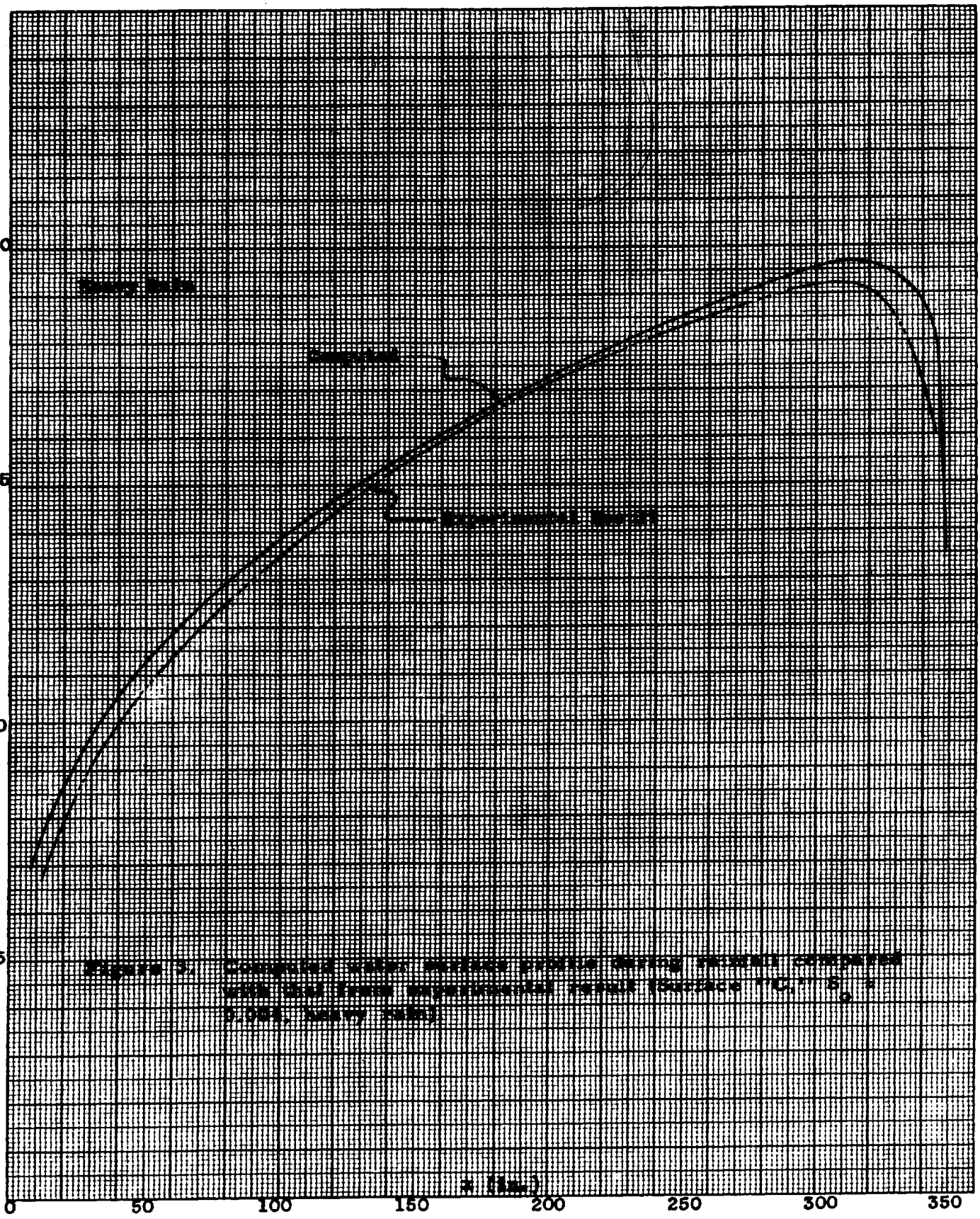
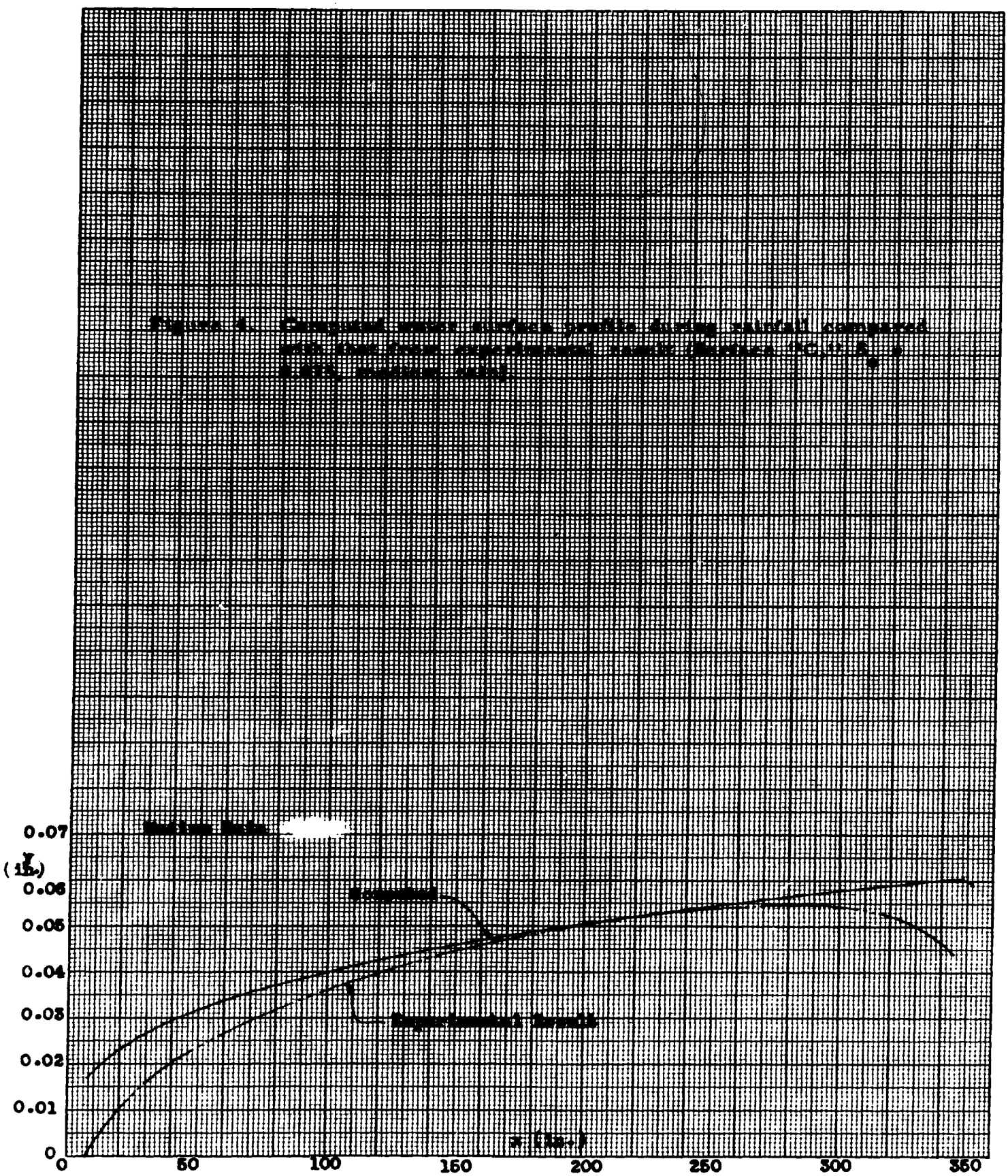


Figure 3. Computed wake profile during transit compared with data from experimental result (Surface $\pi C_f = \delta_o^+ = 0.001$, heavy rule).


0.07
0.06
0.05
0.04
0.03
0.02
0.01
0
0
50
100
150
200
250
300
350

CHAPTER V

SUMMARY

In this study the artificial rainfall applicator method of producing controlled uniform rainfall is described. The idea of this method is not new, but the applicator is believed to be the first one ever developed for the purpose of studying overland flow in laboratory research. Theoretical analysis for overland flow neglecting the effect of raindrop impact was made by means of which water surface profiles for different conditions were computed. By comparing with the experimental results for corresponding conditions it shows that the raindrop impact does have a vital effect on the shape of the water surface profiles. A method of computing the water surface profile during rainfall under any particular condition is suggested. This study involved a range of conditions such that for some cases all depths were less than critical while for others all depths were greater than critical. A range was covered which for ordinary flow (without raindrop impact) would all have been in the laminar range. Due to the rainfall impact the relation between Reynolds' number and the modified friction factor exhibit characteristics which are normally associated with turbulent flow.

This study covers only a very small part of the subject of overland flow and is carried out under certain restricted conditions; therefore, the results of this study and the suggested methods of use are only valid under similar conditions. Before any general law can be derived and applied, a more complete and thorough study must be

made. The future researches on this subject should contain the effect of rainfall characteristics, the effect of physical characteristics of bottom surface, the effect of permeability, the effect of properties of soil and the effect of cultivating. Although quite a few studies for some of the variables have been undertaken by some special groups, mostly in agricultural engineering, they are limited to their own interest. The results would be more valuable for general use if they were connected with the principles of hydraulic engineering. Therefore, it is the opinion of the author that since this problem of overland flow lies between hydraulic engineering and agricultural engineering, future researchers are required to have vast basic knowledge of both fields to piece together all the existing information and carry out a systematic study for all the factors involved.

SAMPLE DATA SHEETS

Notes

* The depth of uniform flow was obtained by taking the average value at Stations 6, 8, and 10.

** This Manning's coefficient of roughness "n" was computed by using the formula $n = \frac{K'}{Q} b^{8/3} S_o^{1/2}$ and Tables 92, 95, and 97 of King's Handbook of Hydraulics (revised by E. F. Brater, 1954).

*** From equation (24), $f_c = \frac{64.4\, S_o\, b^2\, y^3}{Q^2}$

**** $i = \frac{Q\ (cfs) \times 12}{\frac{352}{12} \times \frac{6.25}{12}} \times 60 \times 60 = 2830\, Q$

PART 1 - ROUGHNESS TEST
Date: 10-1-53
Flume width, b = 6.25 inches

Station	Water Depth y in Inches				
	Initial Reading			Q_1	
	Before Test	After Test	Avg.		y
3	6.58	6.57	6.575	7.11	0.535
4	6.675	6.67	6.675	7.21	0.535
5	6.36	6.355	6.36	6.86	0.50
6	6.075	6.075	6.075	6.58	0.505
7	5.85	5.845	5.85	6.36	0.51
8	6.37	6.365	6.37	6.87	0.50
9	6.85	6.85	6.85	7.34	0.49
10	6.61	6.61	6.61	7.11	0.50
11	6.395	6.39	6.395	6.92	0.525
12	6.555	6.55	6.555	7.045	0.49
13	6.76	6.76	6.76	7.24	0.48
	* Depth of uniform flow				0.50

Temp.(H_2O)° C		17.2	
Remarks		no	
Discharge Q	Initial	3.532	0.228
	Final	4.344	0.958
	Interval (sec.), t	15	0.73
	Q (cfs)	0.0487	
	N_R	8030	
	y/b	0.08	
	$S^{1/2} = S_o{}^{1/2}$	0.1225	
	K'	0.02	
**	n ($b^{8/3} = 0.175$)	0.0088	
***	f_c	0.00797	

Surface "B"
Temperature: Room 23°C
Slope, S_o = 0.015

Water Depth y in Inches							
Uniform Flow							
Q_2		Q_3		Q_4		Q_5	
	y		y		y		y
6.915	0.34	6.755	0.18	6.69	0.115	6.64	0.065
7.015	0.34	6.87	0.195	6.785	0.11	6.74	0.065
6.68	0.32	6.53	0.17	6.455	0.095	6.425	0.065
6.405	0.33	6.255	0.18	6.18	0.105	6.14	0.065
6.195	0.34	6.055	0.20	5.98	0.13	5.94	0.09
6.715	0.345	6.565	0.195	6.49	0.12	6.445	0.75
7.185	0.335	7.045	0.195	6.965	0.115	6.915	0.065
6.955	0.345	6.81	0.20	6.73	0.12	6.675	0.065
6.745	0.35	6.585	0.19	6.495	0.10	6.455	0.06
6.89	0.335	6.74	0.185	6.66	0.105	6.615	0.06
7.09	0.33	6.935	0.175	6.855	0.095	6.815	0.055
	0.34		0.19		0.115		0.065
16.9		17.1		17.3		17.6	
no		negligible		It seems all stations are not affected.			
3.523	0.22	3.555	0.248	3.566	0.257	3.540	0.233
4.340	0.954	4.247	0.87	4.166	0.797	4.426	1.031
30	0.734	60	0.622	120	0.54	660	0.798
0.02447		0.01037		0.0045		0.001209	
4010		1705		744		201	
0.0544		0.0304		0.0184		0.0104	
0.01089		0.00424		0.0019		0.00074	
0.00954		0.00877		0.00906		0.01312	
0.00953		0.00963		0.01136		0.0284	

PART 2 - RAINFALL TEST
Date: 9-30-53
Flume width, b = 6.25 inches

Station	Water Depth y in Inches		
	Initial Reading		
	Before Test	After Test	Avg.
1	4.21	4.22	4.22
2	4.61	4.61	4.61
3	4.96	4.97	4.965
4	5.16	5.175	5.17
5	5.10	5.105	5.10
6	5.07	5.07	5.07
7	5.09	5.095	5.095
8	5.60	5.61	5.605
9	6.085	6.10	6.095
10	6.09	6.09	6.09
11	6.10	6.105	6.105
12	6.38	6.385	6.385
13	6.67	6.655	6.67
14	7.085	7.10	7.095

Temp.(water °C)

Pressure (psi)

Remarks

Discharge

Initial

Final

(cu. ft.), ∇

Interval (min.), t

Q (cfs)

**** Intensity (in./hr.), i

Surface "B"
Temperature: Room 23°C
Slope, S_o = 0.010

Water Depth y in Inches								
Steady Condition								
Rainfall I (L)			Rainfall II (M)			Rainfall III (H)		
	Avg.	y		Avg.	y		Avg.	y
4.225	4.225	0.005	4.225	4.225	0.005	4.225	4.23	0.01
4.22			4.225			4.23		
4.625	4.625	0.15	4.625	4.63	0.02	4.63	4.635	0.025
4.625			4.63			4.635		
4.99	4.99	0.025	4.995	5.00	0.035	5.00	5.005	0.04
4.99			5.00			5.005		
5.21	5.21	0.04	5.215	5.22	0.05	5.22	5.225	0.055
5.21			5.22			5.23		
5.145	5.145	0.045	5.15	5.155	0.055	5.165	6.17	0.07
5.14			5.155			5.17		
5.115	5.115	0.045	5.125	5.13	0.06	5.145	5.15	0.08
5.115			5.13			5.15		
5.15	5.15	0.055	5.16	5.16	0.065	5.185	5.185	0.09
5.15			5.16			5.18		
5.655	5.66	0.055	5.67	5.67	0.065	5.70	5.705	0.10
5.66			5.67			5.705		
6.13	6.13	0.035	6.145	6.15	0.055	6.17	6.175	0.08
6.13			6.15			6.175		
6.145	6.15	0.06	6.165	6.165	0.075	6.19	6.19	0.10
6.15			6.165			6.19		
6.16	6.16	0.055	6.175	6.175	0.07	6.21	6.21	0.105
6.16			6.175			6.21		
6.43	6.435	0.05	6.45	6.455	0.07	6.48	6.485	0.10
6.435			6.455			6.485		
6.72	6.72	0.05	6.735	6.735	0.065	6.76	6.76	0.09
6.72			6.715			6.75		
7.14	7.14	0.045	7.16	7.16	0.065	7.19	7.19	0.095
7.14			7.16			7.19		
17.2			16.8			17.0		
47			46-47			45		
47.5			47			45		

3.516	0.213	37	3.563	0.254	16	3.482	0.183	20
3.976	0.624	49	4.245	0.868	26	4.070	0.71	25
	0.411	12		0.614	10		0.527	5
12	y_c=.0401	N_R	10	y_c=.0591	N_R	5	y_c=.0849	N_R
	0.000571	89		0.001023	159.5		0.001757	274
	1.62			2.90			4.98	

SAMPLE COMPUTATION SHEETS

Notes

* From Part 1 f_c vs N_R curve; $f_c = C/N_R = 7.7/N_R$ for N_R up to 400.

** Total discharge (cfs) from experimental data is converted to average rainfall intensity (in./hr.).

*** y_c is computed from $(q^2/g)^{1/3}$.

WATER SURFACE PROFILE WITHOUT RAINDROP IMPACT EFFECT

Surface "B"
Light rain

4-14-1955

$$\Delta Y = \frac{1}{g y_m}\left(q_1 \Delta V + i \Delta x V_2 + \frac{Cv \Delta x q_m}{2 y_m^2}\right)$$

x	x_m	Δx	Bottom Elev.	Trial ΔY	Surface Elevation	y	y_m	q	q_m
352			0		0.0399	0.0399			
345	348.5	7	0.14	0.1594	0.1993	0.0593	0.0496	0.1565	0.155
				0.1597	0.1996	0.0596	0.0498	0.1534	
				0.1598	0.1997	0.0597			
336	340.5	9	0.32	0.1642	0.3639	0.0439	0.0518	0.1494	0.1514
				0.1634	0.3631	0.0431	0.0514		
318	327	18	0.68	0.3728	0.7359	0.0559	0.0495	0.1414	0.1454
294	306	24	1.16	0.4662	1.2021	0.0421	0.049	0.1308	0.1361
246	270	48	2.12	0.969	2.1711	0.0511	0.0466	0.1094	0.1201
198	222	48	3.08	0.9458	3.1169	0.0369	0.044	0.08805	0.09873
				0.9456	3.1167	0.0367	0.0439		
150	174	48	4.04	0.9678	4.0845	0.0445	0.0406	0.0667	0.07738
				0.9674	4.0841	0.0441	0.0404		
				0.9671	4.0838	0.0438	0.0403		
102	126	48	5.0	0.9454	5.0292	0.0292	0.0365	0.04535	0.05603
				0.945	5.0288	0.0288	0.0363		
				0.9451	5.0289	0.0289	0.0364		
54	78	48	5.96	0.964	5.9929	0.0329	0.0309	0.02402	0.03469
				0.9638	5.9927	0.0327	0.0308		
30	42	24	6.44	0.465	6.4577	0.0177	0.0252	0.01334	0.01868
				0.4652	6.4579	0.0179	0.0253		
				0.4653	6.458	0.018	0.0254		
12	21	18	6.8	0.364	6.822	0.022	0.02	0.005334	0.009337
				0.3636	6.8216	0.0216	0.0198		
				0.3637	6.8217	0.0217	0.0199		
3	7.5	9	6.98	0.166	6.9877	0.0077	0.0147	0.001334	0.003334
				0.1658	6.9875	0.0075	0.0146		
				0.1656	6.9873	0.0073	0.0145		

*C = 7.7
S_o = 0.020

**i = $\frac{0.000566 \times 12^3}{6.25 \times 352}$ = 0.0004447 in./sec.

***y_c = 0.0399 in. (x = 352 in.)

T_{H_2O} = 16.9°C

$\nu = 1.692 \times 10^{-3}$ in.^{2}/sec.

g = 386.4 in./sec.^{2}

V	ΔV	$q_1 \Delta V$ (a)	i Δx	$i \Delta x V_2$ (b)	$\frac{C\nu\Delta x q_m}{2}$	$\frac{C\nu\Delta x q_m}{2y_m^2}$ (c)	(a) + (b) + (c)	ΔY
3.92								
2.587	1.333	0.205	0.00311	0.012	0.00707	2.87	3.087	0.161
2.573	1.347	0.207				2.857	3.076	0.16
2.57								
3.405	-0.835	-0.125	0.004	0.01	0.00888	3.308	3.193	0.1596
3.465	-0.895	-0.134				3.365	3.241	0.1632
2.53	0.935	0.132	0.008	0.028	0.01706	6.96	7.12	0.3724
3.105	-0.575	-0.075	0.01067	0.027	0.02128	8.86	8.812	0.466
2.14	0.965	0.106	0.02134	0.066	0.03755	17.28	17.452	0.969
2.385	-0.245	-0.022	0.02134	0.046	0.03087	15.95	15.974	0.939
2.4	-0.26	-0.023				16.03	16.053	0.946
1.5	0.9	0.06	0.02134	0.051	0.0242	14.67	14.781	0.942
1.512	0.888	0.059				14.83	14.94	0.957
1.522	0.878	0.059				14.94	15.05	0.967
1.553	-0.031	-0.001	0.02134	0.033	0.01753	13.15	13.182	0.934
1.574	-0.052	-0.002				13.31	13.341	0.951
1.57								
0.73	0.84	0.02	0.02134	0.033	0.01085	11.36	11.413	0.956
0.735	0.835	0.02				11.44	11.493	0.965
0.754	-0.019	-	0.01067	0.008	0.00292	4.6	4.608	0.4725
0.746						4.56	4.568	0.467
0.741								
0.242	0.499	0.003	0.008	0.006	0.001095	2.738	2.747	0.3554
0.247						2.795	2.804	0.3664
0.246						2.78	2.789	0.3637
0.173	0.073	0.0001	0.004	0.001	0.0001955	0.905	0.9061	0.1595
						0.917	0.9181	0.1628
						0.93	0.9311	0.1662

WATER SURFACE PROFILE WITHOUT RAINDROP IMPACT EFFECT

Surface "B"
Medium rain

4-15-1955

$$\Delta Y = \frac{1}{gy_m}\left(q_1 \Delta V + i \Delta x V_2 + \frac{C \nu \Delta x q_m}{2y_m^2}\right)$$

x	x_m	Δx	Bottom Elev.	Trial ΔY	Surface Elevation	y	y_m	q	q_m
352			0		0.0579	0.0579		0.2737	
345	348.5	7	0.14	0.1466	0.2045	0.0645	0.0612	0.2682	0.271
336	340.5	9	0.32	0.172	0.3765	0.0565	0.0605	0.2612	0.2647
				0.173	0.3775	0.0575	0.061		
				0.1732	0.3777	0.0577	0.0611		
318	327	18	0.68	0.3646	0.7423	0.0623	0.06	0.2473	0.2543
				0.3647	0.7424	0.0624	0.0601		
294	306	24	1.16	0.4724	1.2148	0.0548	0.0586	0.2285	0.2379
				0.473	1.2154	0.0554	0.0589		
				0.4731	1.2155	0.0555	0.059		
246	270	48	2.12	0.9614	2.1769	0.0569	0.0562	0.1913	0.2099
				0.9616	2.1771	0.0571	0.0563		
				0.9618	2.1773	0.0573	0.0564		
198	222	48	3.08	0.9514	3.1287	0.0487	0.053	0.154	0.1727
				0.9512	3.1285	0.0485	0.0529		
150	174	48	4.04	0.9606	4.0891	0.0491	0.0488	0.1166	0.1353
				0.9604	4.0889	0.0489	0.0487		
				0.9603	4.0888	0.0488			
102	126	48	5.0	0.9498	5.0386	0.0386	0.0437	0.0793	0.098
				0.9502	5.039	0.039	0.0439		
				0.95	5.0388	0.0388	0.0438		
54	78	48	5.96	0.9572	5.996	0.036	0.0374	0.042	0.06065
				0.9569	5.9957	0.0357	0.0373		
30	42	24	6.44	0.4696	6.4653	0.0253	0.0305	0.02333	0.03267
12	21	18	6.8	0.3582	6.8235	0.0235	0.0244	0.00933	0.01633
				0.3576	6.8229	0.0229	0.0241		
				0.3575	6.8228	0.0228			
3	7.5	9	6.98	0.1686	6.9914	0.0114	0.0171	0.002333	0.005832
				0.1691	6.9919	0.0119	0.0174		
				0.1692	6.992	0.012			

$C = 7.7$

$S_o = 0.020$

$i = \frac{0.00099 \times 12^3}{6.25 \times 352} = 0.0007775$ in./sec.

$y_c = 0.0579$ in. ($x = 352$ in.)

$T_{H_2O} = 16.9°C$

$\nu = 1.692 \times 10^{-3}$ in.^{2}/sec.

$g = 386.4$ in./sec.^{2}

V	ΔV	$q_1\Delta V$ (a)	$i\,\Delta x$	$i\Delta x V_2$ (b)	$\frac{C\nu\Delta x q_m}{2}$	$\frac{C\nu\Delta x q_m}{2y_m^2}$ (c)	(a) + (b) + (c)	ΔY
4.725								
4.16	0.565	0.152	0.00544	0.026	0.01235	3.3	3.478	0.147
4.62	-0.46	-0.12	0.007	0.029	0.01553	4.243	4.152	0.1777
4.543	-0.383	-0.1				4.175	4.104	0.174
4.52	-0.36	-0.094				4.16	4.095	0.1734
3.968	0.552	0.136	0.014	0.063	0.02983	8.285	8.484	0.3658
3.96	0.56	0.138				8.26	8.461	0.3644
4.17	-0.21	-0.048	0.01866	0.112	0.0372	10.82	10.884	0.4805
4.13	-0.17	-0.039				10.725	10.798	0.4745
4.12	-0.16	-0.037				10.71	10.785	0.4735
3.36	0.76	0.145	0.03733	0.154	0.06565	20.78	21.079	0.971
3.35	0.77	0.147				20.72	21.021	0.966
3.34	0.78	0.149				20.67	20.973	0.962
3.16	0.18	0.028	0.03733	0.125	0.054	19.23	19.383	0.946
3.174	0.166	0.026				19.31	19.461	0.952
2.375	0.799	0.093	0.03733	0.119	0.0423	17.78	17.992	0.954
2.385	0.789	0.092				17.84	18.051	0.958
2.39								
2.054	0.336	0.027	0.03733	0.089	0.03066	16.04	16.156	0.956
2.034	0.356	0.028				15.92	16.037	0.946
2.043								
1.167	0.876	0.037	0.03733	0.076	0.01898	13.58	13.693	0.946
1.176	0.867	0.036				13.68	13.792	0.9575
0.922	0.254	0.006	0.01866	0.022	0.00511	5.49	5.518	0.4685
0.397	0.525	0.005	0.014	0.013	0.001915	3.215	3.233	0.343
0.407						3.297	3.315	0.356
0.409						3.307	3.325	0.358
0.205	0.204	0.001	0.007	0.003	0.000342	1.17	1.174	0.1778
						1.136	1.14	0.17
						1.13	1.134	0.1687

HINDS' METHOD OF LOCATING y_c FOR $S_o > S_c$

Surface "B"
Heavy rain

$$\Delta Y = \frac{1}{g y_m}\left(q_1 \Delta V + i \Delta x V_2 + \frac{C \nu \Delta x q_m}{2 y_m^2}\right)$$

4-17-1955

x	Δx	y_c	y_m	q	q_m	V	ΔV	$q_1 \Delta V$ (a)
352		0.0832		0.472		5.67		
345	7	0.0822	0.0827	0.463	0.4675	5.63	0.04	0.019
336	9	0.0808	0.0815	0.451	0.457	5.58	0.05	0.023
318	18	0.0778	0.0793	0.427	0.439	5.49	0.09	0.038
294	24	0.0739	0.0758	0.3947	0.4109	5.34	0.15	0.062
246	48	0.0656	0.0698	0.3303	0.3625	5.03	0.31	0.102
198	48	0.0568	0.0612	0.2658	0.2981	4.675	0.355	0.094
150	48	0.0472	0.052	0.2013	0.2336	4.26	0.415	0.084
102		0.0364		0.1369				
54		0.0239		0.0725				
30		0.0162		0.04025				
12		0.0088		0.01611				
3		0.0034		0.004025				

$C = 7.7$
$S_o = 0.020$
$i_{y_c} = 0.001342$ in./sec.

$T_{H_2O} = 16.9°C$
$\nu = 1.692 \times 10^{-3}$ in.^{2}/sec.
$g = 386.4$ in./sec.^{2}

$i\,\Delta x$	$i\Delta x V_2$ (b)	$\frac{C\nu\Delta x q_m}{2}$	$\frac{C\nu\Delta x q_m}{2y_m^2}$ (c)	(a) + (b) + (c)	ΔY	Bottom Elev.	Surface Elevation
						0	0.083
0.0094	0.053	0.0213	3.116	3.188	0.0967	0.098	0.18
0.01208	0.068	0.0268	4.034	4.125	0.131	0.23	0.311
0.02415	0.135	0.0515	8.19	8.363	0.273	0.506	0.584
0.03222	0.177	0.06425	11.095	11.334	0.387	0.897	0.971
0.06444	0.344	0.11335	23.27	23.716	0.88	1.785	1.851
0.06444	0.324	0.0932	24.9	25.318	1.07	2.864	2.921
0.06444	0.301	0.073	27.0	27.385	1.363	4.237	4.284

WATER SURFACE PROFILE WITHOUT RAINDROP IMPACT EFFECT

Surface "B"
Heavy rain

4-17-1955

$$\Delta Y = \frac{1}{g y_m}\left(q_1 \Delta V + i \Delta x V_2 + \frac{C \nu \Delta x q_m}{2 y_m^2}\right)$$

x	x_m	Δx	Bottom Elev.	Trial ΔY	Surface Elevation	y	y_m	q	q_m
				0.3177	0.0748	0.0748	0.0737		
				0.3178	0.0747	0.0747	0.0736		
				0.3174	0.0751	0.0751	0.0738		
352	344	16	0	0.3168	0.0757	0.0757	0.0741	0.472	0.4615
				0.36	0.3925	0.0725	0.0725		
				0.3602	0.3923	0.0723	0.0724		
336	327	18	0.32	0.3606	0.3919	0.0719	0.0722	0.451	0.439
				0.5962	0.7525	0.0725	0.0706		
318	303	30	0.68	0.5966	0.7521	0.0721	0.0704	0.427	0.4069
288	273	30	1.28	0.599	1.3487	0.0687	0.0682	0.3867	0.3666
258			1.88		1.9477	0.0677		0.3464	
228	243	30	2.48	0.596	2.5437	0.0637	0.0657	0.3061	0.3263
				0.5959	2.5436	0.0636	0.0656		
				0.5958	2.5435	0.0635			
198	213	30	3.08	0.5952	3.1387	0.0587	0.0611	0.2658	0.286
				0.5972	3.1407	0.0607	0.0621		
				0.5985	3.142	0.062	0.0628		
150	174	48	4.04	0.9528	4.0948	0.0548	0.0584	0.2013	0.2336
				0.9532	4.0952	0.0552	0.0586		
				0.9533	4.0953	0.0553	0.0587		
102	126	48	5.0	0.9546	5.0499	0.0499	0.0526	0.1369	0.1691
				0.9547	5.05	0.05	0.0527		
54	78	48	5.96	0.95	6.00	0.04	0.045	0.0725	0.1047
				0.9499	5.9999	0.0399	0.0449		
				0.9498	5.9998	0.0398			
30	42	24	6.44	0.4734	6.4732	0.0332	0.0365	0.04025	0.05638
12	21	18	6.8	0.3518	6.825	0.025	0.0291	0.01611	0.02818
				0.3517	6.8249	0.0249			
3	7.5	9	6.98	0.1714	6.9963	0.0163	0.0206	0.004025	0.01007
				0.1716	6.9965	0.0165	0.0207		
				0.1717	6.9966	0.0166	0.0208		

$C = 7.7$
$S_o = 0.020$
$i = \frac{0.001708 \times 12^3}{6.25 \times 352} = 0.001342$ in./hr.
$y_c = 0.0677$ in. ($x = 258$ in.)

$T_{H_2O} = 16.9°C$
$\nu = 1.692 \times 10^{-3}$ in.^{2}/sec.
$g = 386.4$ in./sec.^{2}

V	ΔV	$q_1 \Delta V$ (a)	$i \Delta x$	$i \Delta x V_2$ (b)	$\frac{C\nu\Delta x q_m}{2}$	$\frac{C\nu\Delta x q_m}{2y_m^2}$ (c)	(a) + (b) + (c)	ΔY
6.32	0.1	0.045		0.136		8.885	9.066	0.3186
6.29	0.07	0.032		0.135		8.84	9.007	0.3154
6.235	0.015	0.007	0.02147	0.134	0.04813	8.77	8.911	0.3113
6.22	0.33	0.141		0.15		9.79	10.081	0.36
6.24	0.35	0.149		0.151		9.82	10.12	0.3614
6.27	0.38	0.162	0.02415	0.152	0.0515	9.88	10.194	0.365
5.89	0.268	0.114				15.94	16.293	0.5965
5.92	0.298	0.115	0.04026	0.239	0.0795	16.05	16.404	0.603
5.622	0.507	0.176	0.04026	0.226	0.07165	15.4	15.802	0.599
5.115								
4.8	0.315	0.096	0.04026	0.206	0.0638	14.78	15.082	0.594
4.813	0.302	0.093				14.8	15.099	0.595
4.82								
4.525	0.295	0.078	0.04026	0.194	0.0559	14.97	15.242	0.649
4.378	0.442	0.117				14.5	14.811	0.617
4.285	0.535	0.142				14.18	14.516	0.5985
3.673	0.612	0.123	0.06444	0.276	0.073	21.43	21.829	0.967
3.644	0.641	0.129				21.25	21.655	0.957
3.64	0.645	0.13				21.21	21.616	0.9535
2.743	0.897	0.125	0.06444	0.234	0.0529	19.11	19.467	0.957
2.738	0.902	0.123				19.06	19.417	0.954
1.812	0.926	0.067	0.06444	0.176	0.03275	16.17	16.413	0.945
1.818	0.92	0.067				16.22	16.463	0.948
1.822								
1.212	0.61	0.025	0.03222	0.059	0.0088	6.607	6.691	0.4744
0.645	0.567	0.009	0.02415	0.029	0.003305	3.9	3.938	0.35
0.647						3.914	3.952	0.352
0.247	0.4	0.002	0.01208	0.008	0.00059	1.39	1.4	0.1757
						1.376	1.386	0.1732
						1.37	1.38	0.172

f_c' FROM RAINDROP IMPACT EFFECT

Surface "B"
Light rain

$$f_c' = (g\, y_m\, \Delta Y - q_1\, \Delta V - i\, \Delta x\, V_2) \frac{2}{\Delta x \left(\frac{q_m}{y_m}\right)^2}$$

6-9-1954

x	x_m	Δx	Bottom Elev.	ΔY	Surface Elevation	Depth y	y_m	$gy_m\Delta Y$ (a)	Discharge q	N_R
352									0.1797	108
345	348.5	7	0.014		0.089	0.075			0.1761	106
336	340.5	9	0.032	0.0285	0.1175	0.0855	0.0803	0.884	0.1716	103
318	327	18	0.068	0.0525	0.17	0.102	0.0938	1.904	0.1623	97
294	306	24	0.116	0.061	0.231	0.115	0.1085	2.557	0.1501	90
246	270	48	0.212	0.095	0.326	0.114	0.1145	4.205	0.1256	75
198	222	48	0.308	0.092	0.418	0.11	0.112	3.98	0.1011	61
150	174	48	0.404	0.091	0.509	0.105	0.1075	3.78	0.0766	46
102	126	48	0.5	0.091	0.6	0.10	0.1025	3.608	0.0521	31
54	78	48	0.596	0.088	0.688	0.092	0.096	3.264	0.02757	16.5
30	42	24	0.644	0.039	0.727	0.083	0.0875	1.318	0.01532	9.2
12	21	18	0.68	0.024	0.751	0.071	0.077	0.714	0.006125	3.7
3	7.5	9	0.698	0.007	0.758	0.06	0.0655	0.177	0.001532	0.9

S_o = 0.002

i = 0.000511 in./sec.

T_{H_2O} = 17.5°C

ν = 1.667×10^{-3} in.^{2}/sec.

g = 386.4 in./sec.^{2}

q_m	Velocity V	ΔV	$q_1 \Delta V$ (b)	$i \Delta x$	$i \Delta x V_2$ (c)	(a) - (b) - (c)	$\frac{q_m}{y_m}$	f_c'	N_R (for q_m)
0.1779	2.348			0.003576					107
0.1739	2.007	0.341	0.0585	0.0046	0.0108	0.8147	2.165	0.0386	104
0.167	1.591	0.416	0.0675	0.0092	0.0185	1.818	1.78	0.0637	100
0.1562	1.305	0.286	0.0429	0.01226	0.0195	2.4946	1.439	0.1004	94
0.1379	1.102	0.203	0.0255	0.02452	0.032	4.1475	1.204	0.119	83
0.1134	0.92	0.182	0.0184	0.02452	0.027	3.9346	1.013	0.1597	68
0.0889	0.729	0.191	0.0146	0.02452	0.0225	3.7429	0.827	0.228	53
0.0644	0.521	0.208	0.0108	0.02452	0.0179	3.5793	0.628	0.378	39
0.03984	0.3	0.221	0.0061	0.02452	0.0128	3.2451	0.415	0.785	24
0.02145	0.1846	0.1154	0.0018	0.01226	0.0037	1.3125	0.245	1.822	13
0.01072	0.0863	0.0983	0.0006	0.0092	0.0017	0.7117	0.1391	4.085	6.4
0.003829	0.0255	0.0608	0.0001	0.0046	0.0004	0.1765	0.058511.46		2.3

WATER SURFACE PROFILE WITHOUT RAINDROP IMPACT EFFECT (from actual rainfall distribution and surface elevation) 4-22-1955 Surface "B" Light rain

$$\Delta Y = \frac{1}{g y_m}\left(q_1 \Delta V + i \Delta x V_2 + \frac{C \nu \Delta x q_m}{2 y_m^2}\right)$$

x	x_m	Δx	Bottom Elev.	Trial ΔY	Surface Elevation	y	y_m	q	q_m
352			0		0.0438	0.0438			
345	348.5	7	0.015	0.071	0.1148	0.0998	0.0718	0.1797	0.178
				0.0712	0.115	0.1	0.0719	0.1762	
336	340.5	9	0.045	0.0274	0.1424	0.0974	0.0987	0.1719	0.1741
318	327	18	0.095	0.0542	0.1966	0.1016	0.0995	0.1618	0.1669
				0.0532	0.1956	0.1006	0.099		
				0.0526	0.195	0.1	0.0987		
				0.0527	0.1951	0.1001	0.0988		
294	306	24	0.135	0.0526	0.2477	0.1127	0.1064	0.1524	0.1571
				0.0529	0.248	0.113	0.1066		
246	270	48	0.19	0.067	0.315	0.125	0.119	0.1263	0.1394
				0.0672	0.3152	0.1252	0.1191		
198	222	48	0.295	0.0716	0.3868	0.0918	0.1085	0.1029	0.1146
150	174	48	0.37	0.0834	0.4702	0.1002	0.096	0.0787	0.0908
102	126	48	0.52	0.1081	0.5783	0.0583	0.0793	0.05447	0.06659
				0.1077	0.5779	0.0579	0.0792		
				0.1076	0.5778	0.0578	0.0791		
54	78	48	0.62	0.1166	0.6944	0.0744	0.0661	0.0293	0.04189
				0.1168	0.6946	0.0746	0.0662		
30	42	24	0.69	0.0412	0.7358	0.0458	0.0602	0.01571	0.02251
				0.0413	0.7359	0.0459	0.0603		
12	21	18	0.67	0.0132	0.7491	0.0791	0.0625	0.005546	0.01063
3	7.5	9	0.72	0.003	0.7521	0.0321	0.0556	0.001346	0.003446

$C = 7.7$ $\quad T_{H_2O} = 17.5°C$

$S_o = 0.002$

$q_{352} = 0.1797$ in.^{3}/sec. $\quad \nu = 1.667 \times 10^{-3}$ in.^{2}/sec.

$y_c = 0.0438$ in. ($x = 352$ in.) $\quad g = 386.4$ in./sec.^{2}

V	ΔV	q_1 ΔV (a)	i Δx	$i\Delta x V_2$ (b)	$\frac{C\nu\Delta x q_m}{2}$	$\frac{C\nu\Delta x q_m}{2y_m^2}$ (c)	(a) + (b) + (c)	ΔY
4.1								
1.766	2.334	0.411	0.003407	0.014	0.008	1.552	1.977	0.0713
1.762	2.338	0.412				1.548	1.974	0.0711
1.74	0.022	0.004	0.00447	0.008	0.01005	1.032	1.044	0.0274
1.592	0.148	0.024	0.01011	0.018	0.01926	1.946	1.988	0.0517
1.608	0.132	0.021				1.963	2.002	0.0523
1.618	0.122	0.02				1.977	2.015	0.0528
1.353	0.265	0.04	0.00942	0.015	0.0242	2.136	2.191	0.0532
1.35	0.268	0.041				2.13	2.186	0.053
1.01	0.34	0.043	0.0261	0.035	0.04293	3.033	3.111	0.0676
1.009	0.341	0.043				3.022	3.1	0.0673
1.12	-0.111	-0.013	0.02332	0.024	0.03528	3.0	3.011	0.0717
0.785	0.335	0.026	0.02426	0.027	0.02797	3.036	3.089	0.0833
0.934	-0.149	-0.008	0.02423	0.019	0.0205	3.263	3.274	0.1069
0.94	-0.155	-0.008				3.274	3.285	0.1074
0.941	-0.156	-0.009				3.278	3.288	0.1076
0.394	0.547	0.016	0.02517	0.024	0.0129	2.947	2.987	0.117
0.393	0.548	0.016				2.942	2.982	0.1167
0.343	0.05	0.001	0.0136	0.005	0.003467	0.957	0.963	0.0414
0.342								
0.07	0.272	0.002	0.01016	0.004	0.001228	0.314	0.32	0.0132
0.042	0.028	-	0.0042	0.0003	0.000199	0.0643	0.0646	0.003

WATER SURFACE PROFILE WITHOUT RAINDROP EFFECT (from simplified equation)

Surface "B"
Light rain

4-24-1955

$$\Delta Y = \frac{1}{gy_m}\left(\frac{C\ \nu\ \Delta x\ q_m}{2y_m^2}\right)$$

x	x_m	Δx	Bottom Elev.	Trial ΔY	Surface Elevation	y
352			0		0.0438	0.0438
345	348.5	7	0.014	0.0638	0.1076	0.0936
336	340.5	9	0.032	0.0274	0.135	0.103
318	327	18	0.068	0.042	0.177	0.109
294	306	24	0.116	0.048	0.225	0.109
246	270	48	0.212	0.0908 0.091	0.3158 0.316	0.1038 0.104
198	222	48	0.308	0.0892 0.089	0.4052 0.405	0.0972 0.097
150	174	48	0.404	0.088	0.493	0.089
102	126	48	0.5	0.086 0.0862	0.579 0.5792	0.079 0.0792
54	78	48	0.596	0.0828	0.662	0.066
30	42	24	0.644	0.0377 0.0378	0.6997 0.6998	0.0557 0.0558
12	21	18	0.68	0.025 0.0251	0.7248 0.7249	0.0448 0.0449
3	7.5	9	0.698	0.0087	0.7336	0.0356

$C = 7.7$
$S_o = 0.002$
$i = \frac{0.00065 \times 12^3}{6.25 \times 352} = 0.000511$ in./sec.
$y_c = 0.0438$ in. ($x = 352$ in.)

$T_{H_2O} = 17.5°C$
$\nu = 1.667 \times 10^{-3}$ in.^{2}/sec.
$g = 386.4$ in./sec.^{2}

y_m	q	q_m	$\frac{C\nu\Delta x q_m}{2}$	$\frac{C\nu\Delta x q_m}{2y_m^2}$	ΔY
	0.1797				
0.0687	0.1761	0.1779	0.00799	1.693	0.0638
0.0983	0.1716	0.1739	0.01004	1.039	0.0274
0.106	0.1623	0.167	0.0193	1.717	0.0419
0.109	0.1501	0.1562	0.02406	2.025	0.0481
0.1064 0.1065	0.1256	0.1379	0.04245	3.75 3.742	0.0911 0.0909
0.1006 0.1005	0.1011	0.1134	0.0349	3.447 3.454	0.0887 0.0889
0.093	0.0766	0.0889	0.02736	3.16	0.088
0.084 0.0841	0.0521	0.0644	0.01983	2.81 2.803	0.0866 0.0862
0.0726	0.02757	0.03984	0.01227	2.326	0.0829
0.0609	0.01532	0.02145	0.003306	0.8925 0.891	0.038 0.0378
0.0503 0.0504	0.006125	0.01072	0.001239	0.49	0.0252
0.0403	0.001532	0.003829	0.000221	0.1364	0.0088

FIGURES

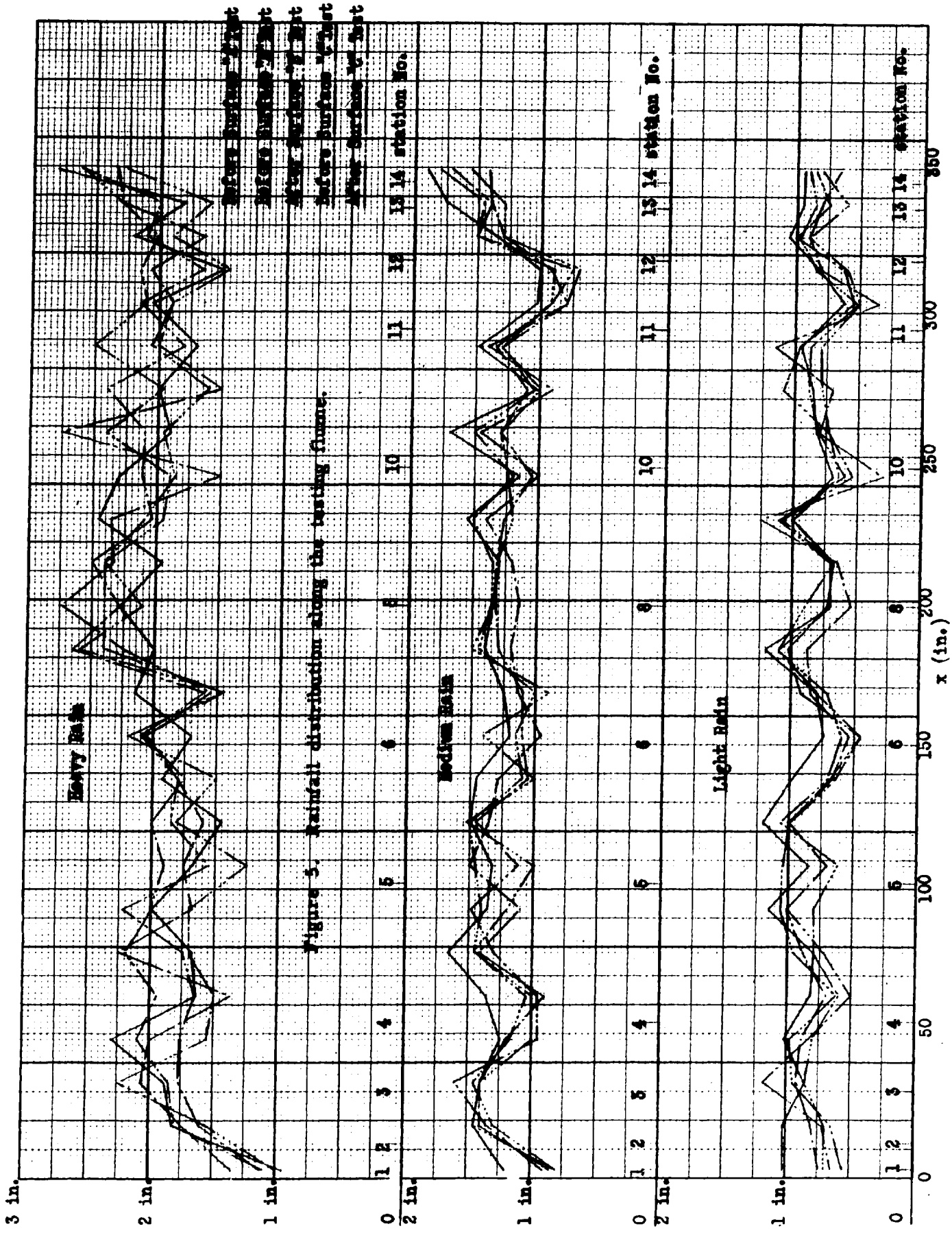
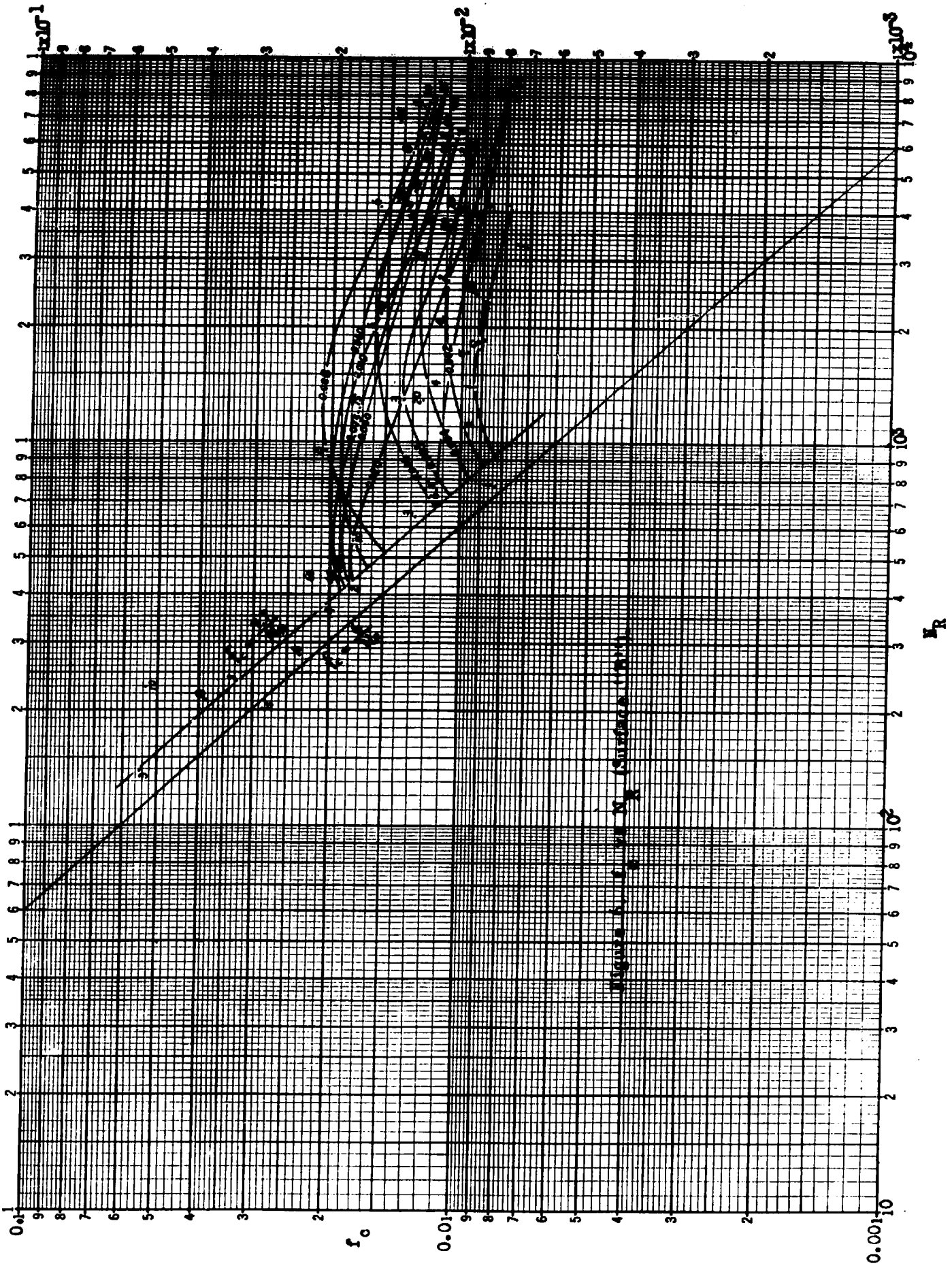


Figure 5. Rainfall distribution along the basin flume.

COEFFICIENTS OF FRICTION FOR UNIFORM FLOW

Legend

$\bullet^{3}$ Experimental Result for $S_o = 0.003$


f_c
K_R
0.1
0.01
0.001
$\times 10^{-1}$
$\times 10^{-2}$
$\times 10^{-3}$

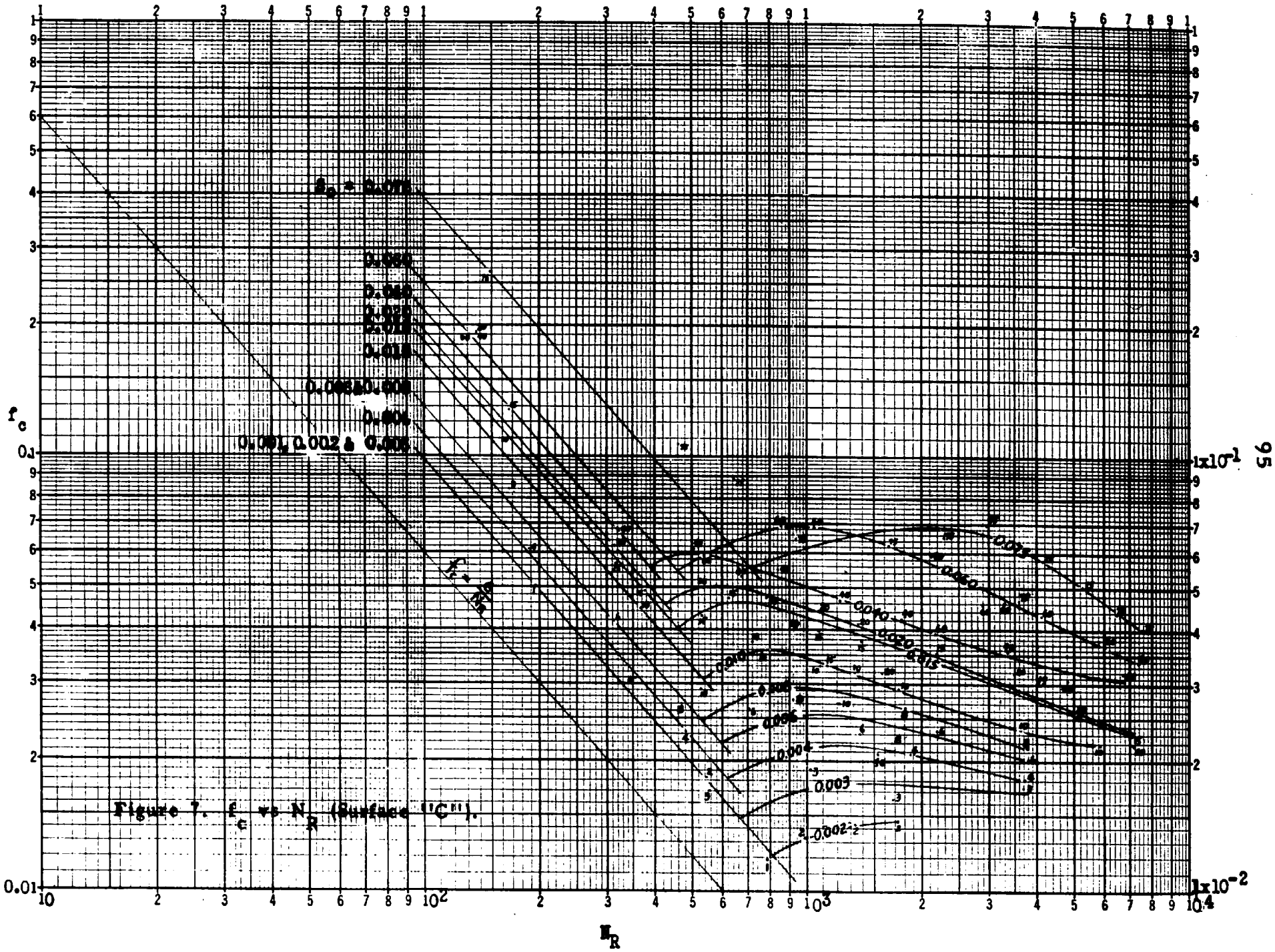


Figure 7. f_c vs N_R (Surface "C").

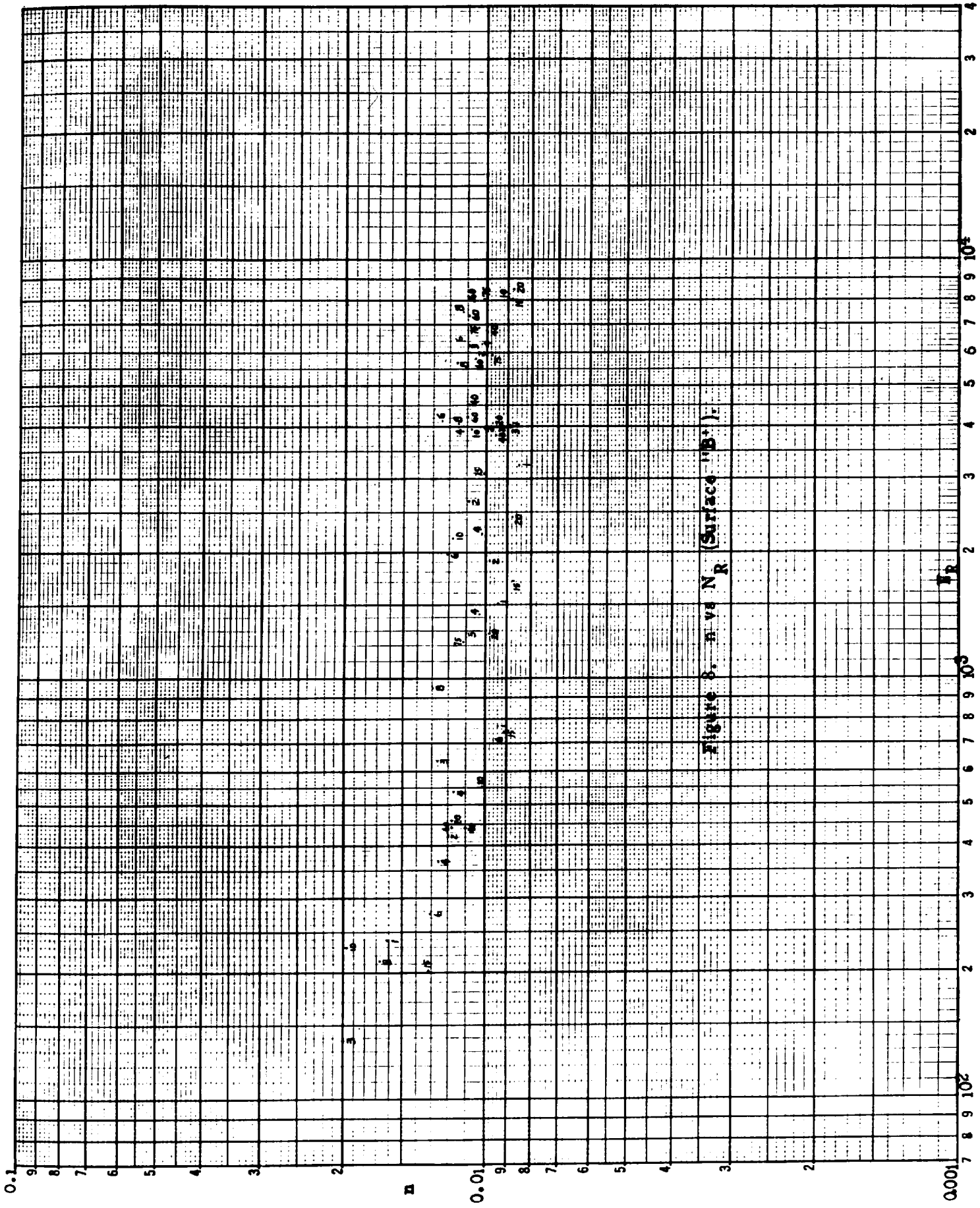


Figure 8. n vs N_R (Surface $^{11}B^+$ I)

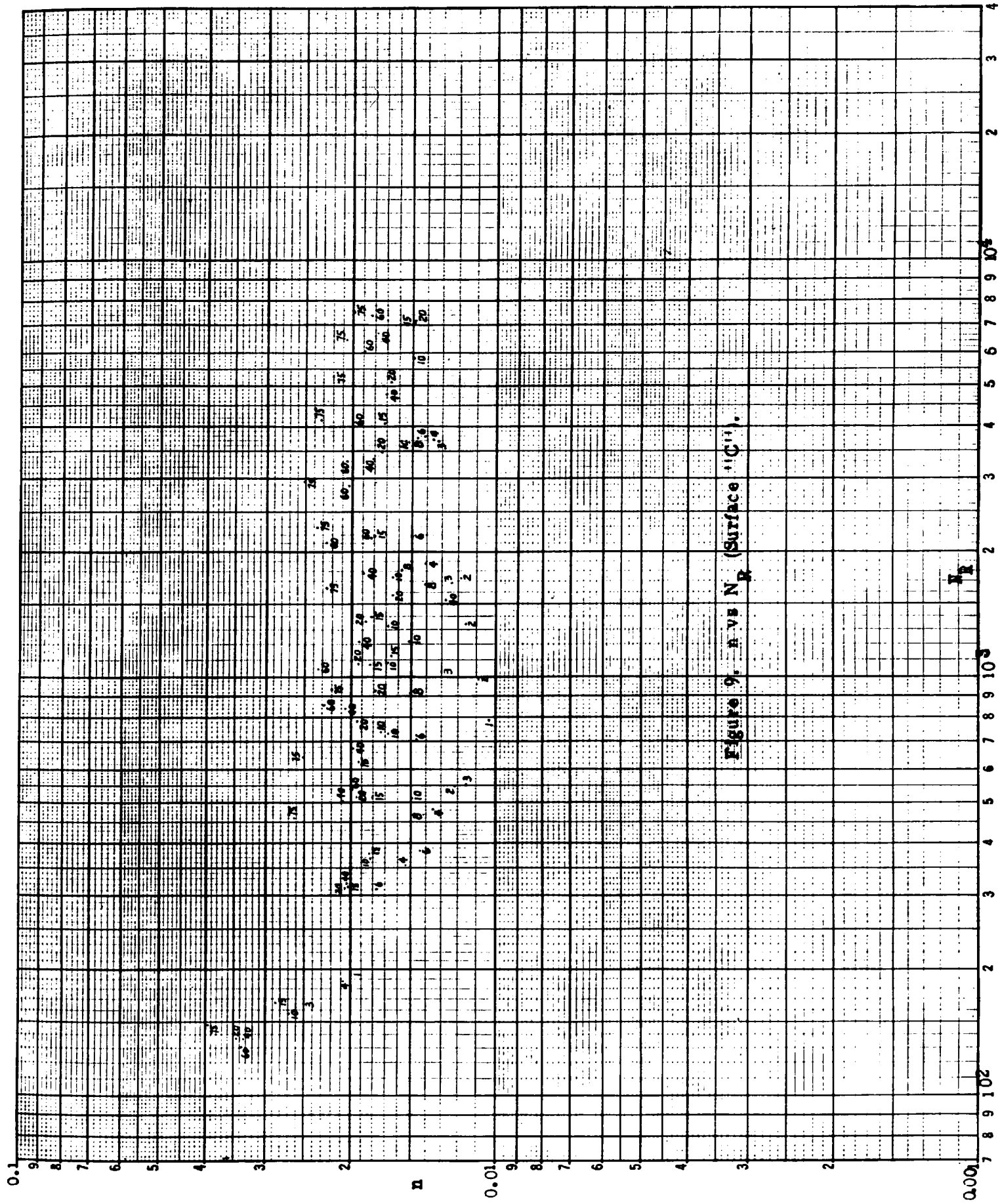
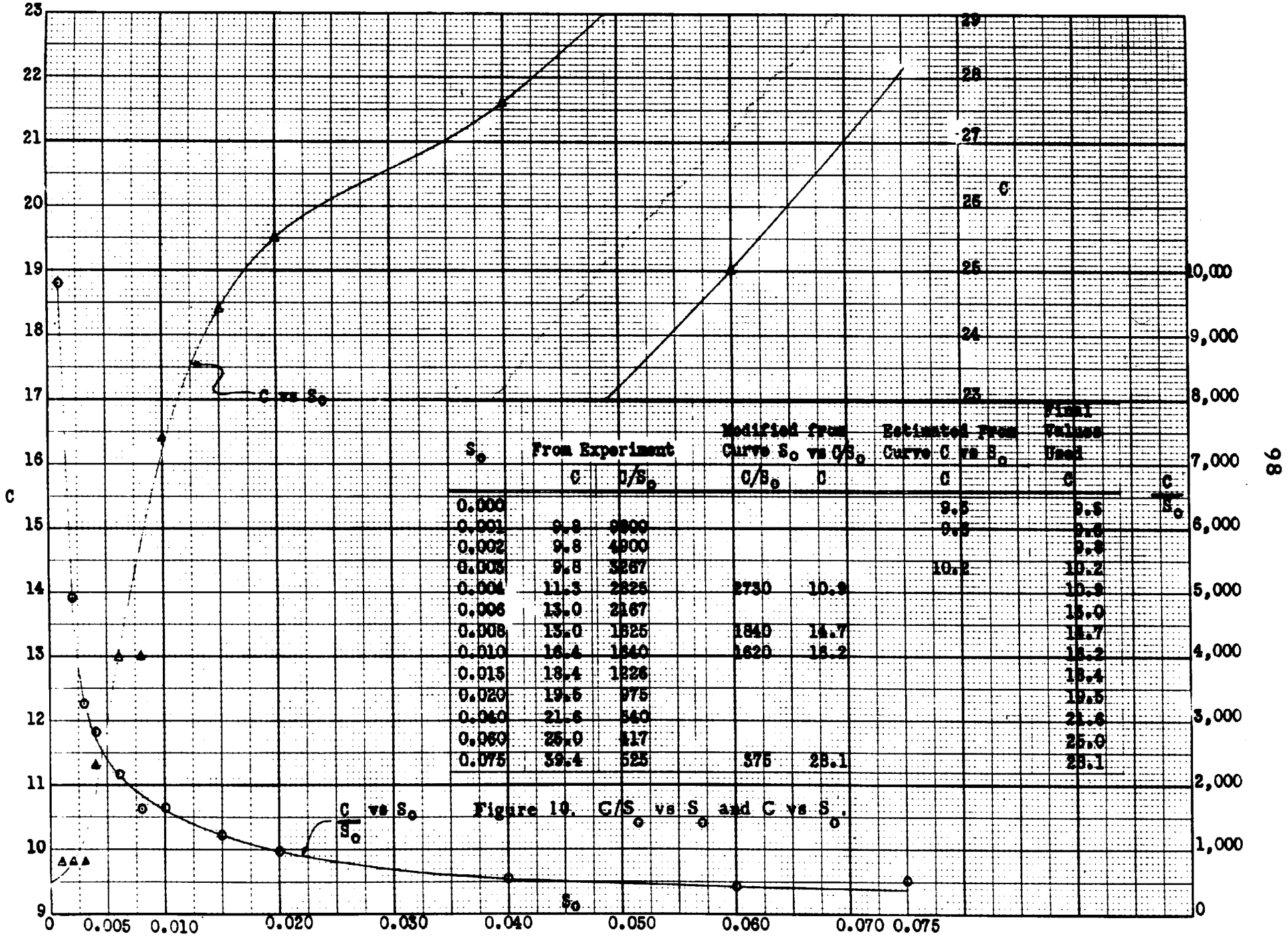


Figure 9. n vs N_R (Surface "C").



S_o	From Experiment C	From Experiment C/S_o	Modified from Curve S_o vs C/S_o C/S_o	Modified from Curve S_o vs C/S_o C	Estimated from Curve C vs S_o C	Final Values Used C	Final Values Used $\frac{C}{S_o}$
0.000					9.5	9.5	
0.001	9.8	9800			9.6	9.6	
0.002	9.8	4900				9.8	
0.003	9.8	3267			10.2	10.2	
0.004	11.3	2825	2730	10.9		10.9	
0.006	13.0	2167				13.0	
0.008	13.0	1625	1640	13.7		13.7	
0.010	16.4	1640	1620	16.2		16.2	
0.015	18.4	1226				18.4	
0.020	19.5	975				19.5	
0.040	21.6	540				21.6	
0.060	25.0	417				25.0	
0.075	39.4	525	575	28.1		28.1	

Figure 10. C/S_o vs S_o and C vs S_o.

WATER SURFACE PROFILES

Legend

—L— Computed water surface profile (without raindrop impact effect) for light rain.

—M— Computed water surface profile (without raindrop impact effect) for medium rain.

—H— Computed water surface profile (without raindrop impact effect) for heavy rain.

—·— Experimental water surface profile for light rain.

—··— Experimental water surface profile for medium rain.

—···— Experimental water surface profile for heavy rain.

------ Profile of critical depth.

× Measured water depth for light rain.

⊙ Measured water depth for medium rain.

⊛ Measured water depth for heavy rain.

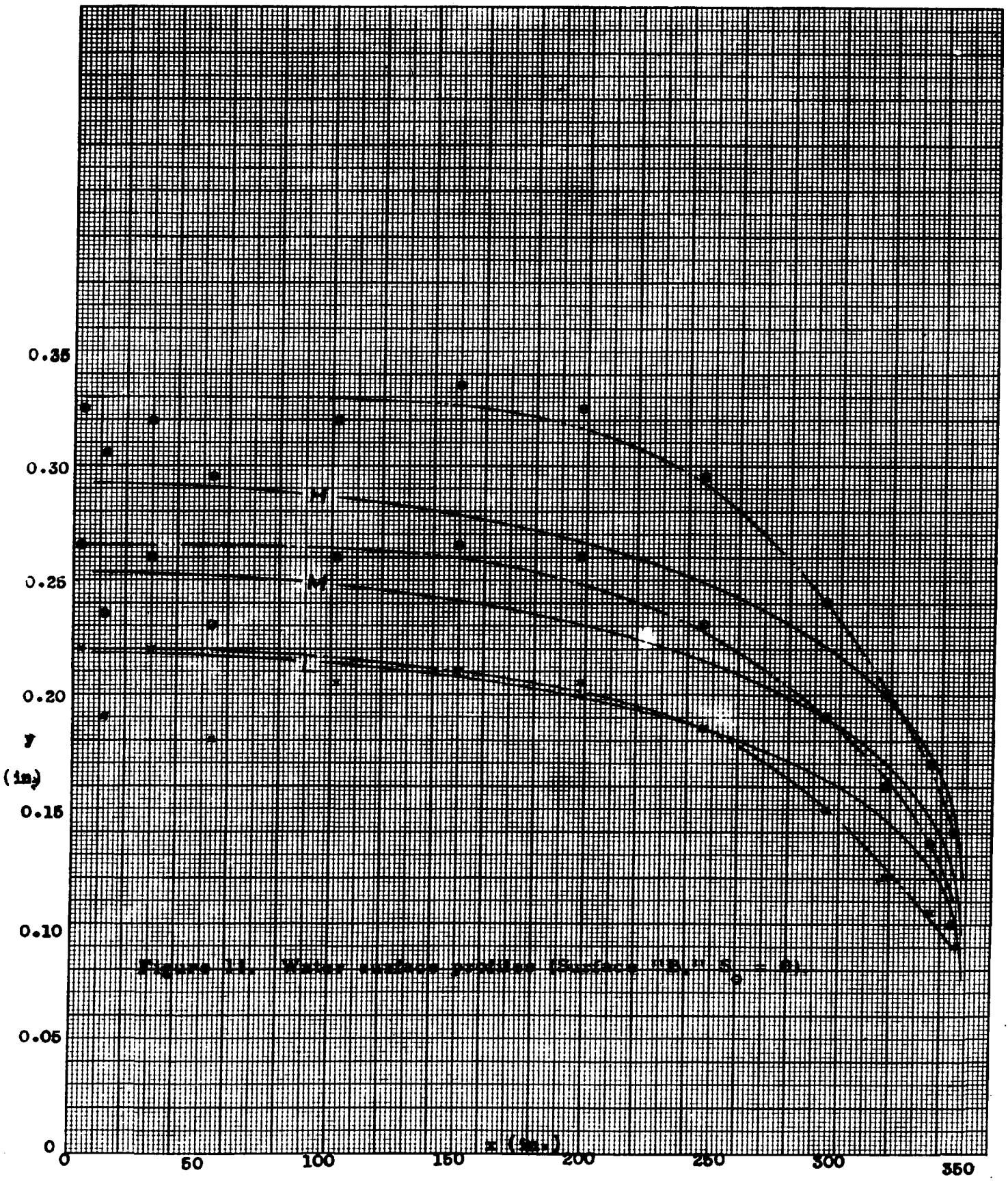


Figure 14. Water surface profiles (Surface "B," $S_o = 0$).

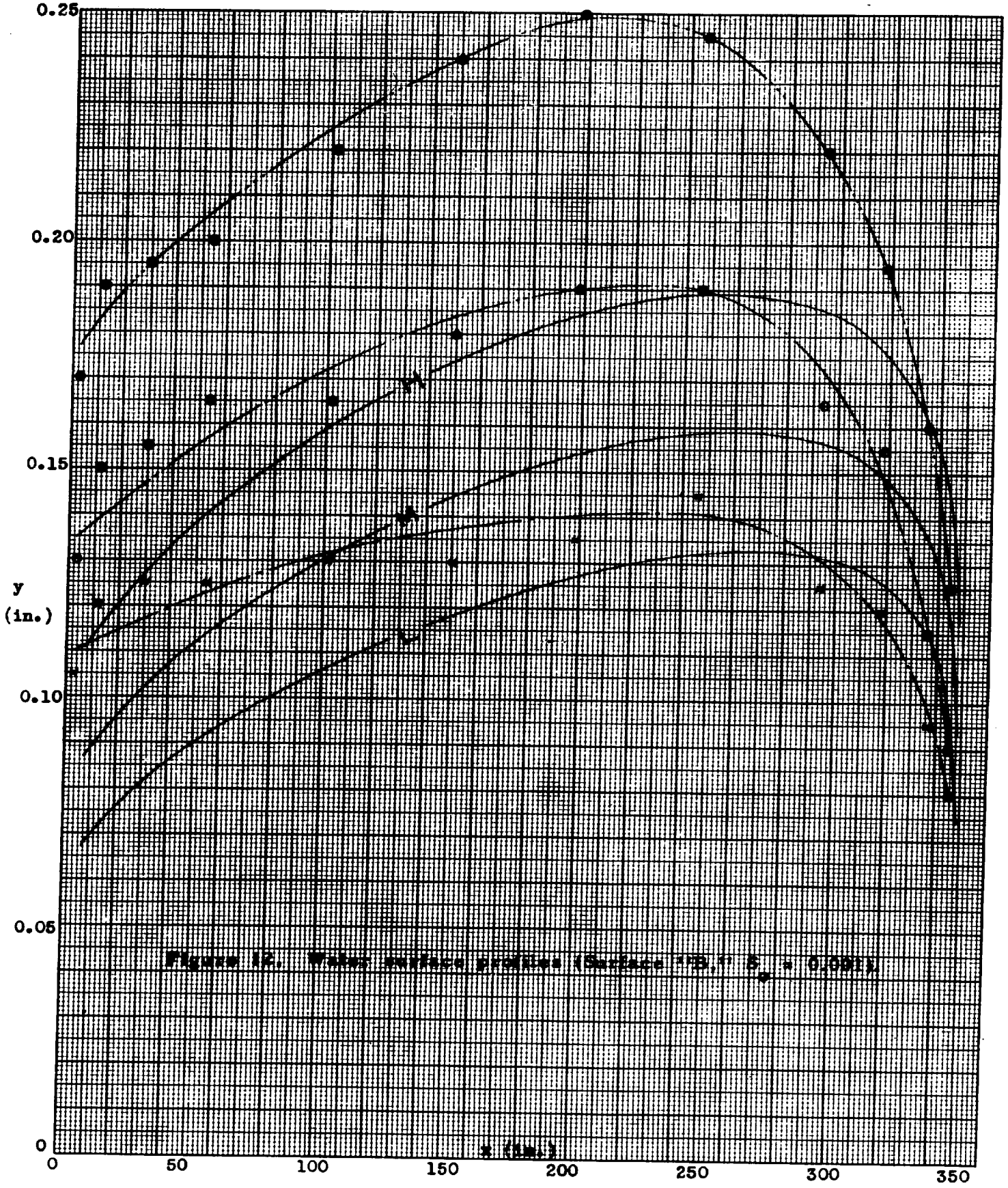


Figure 12. Water surface profiles (Surface "B," S_o = 0.0015)

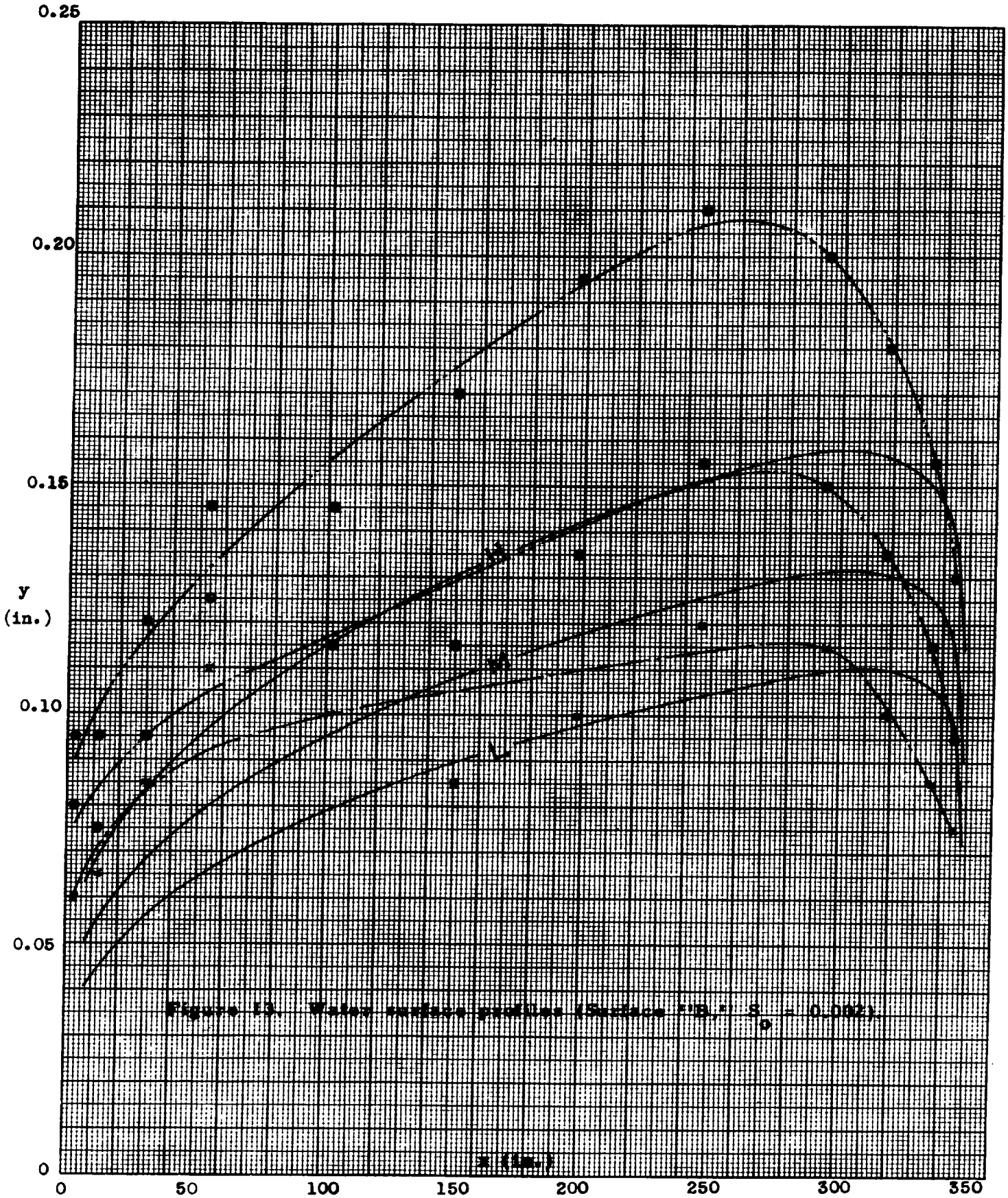


Figure 19. Water surface profiles (Section "B," S_o = 0.002).

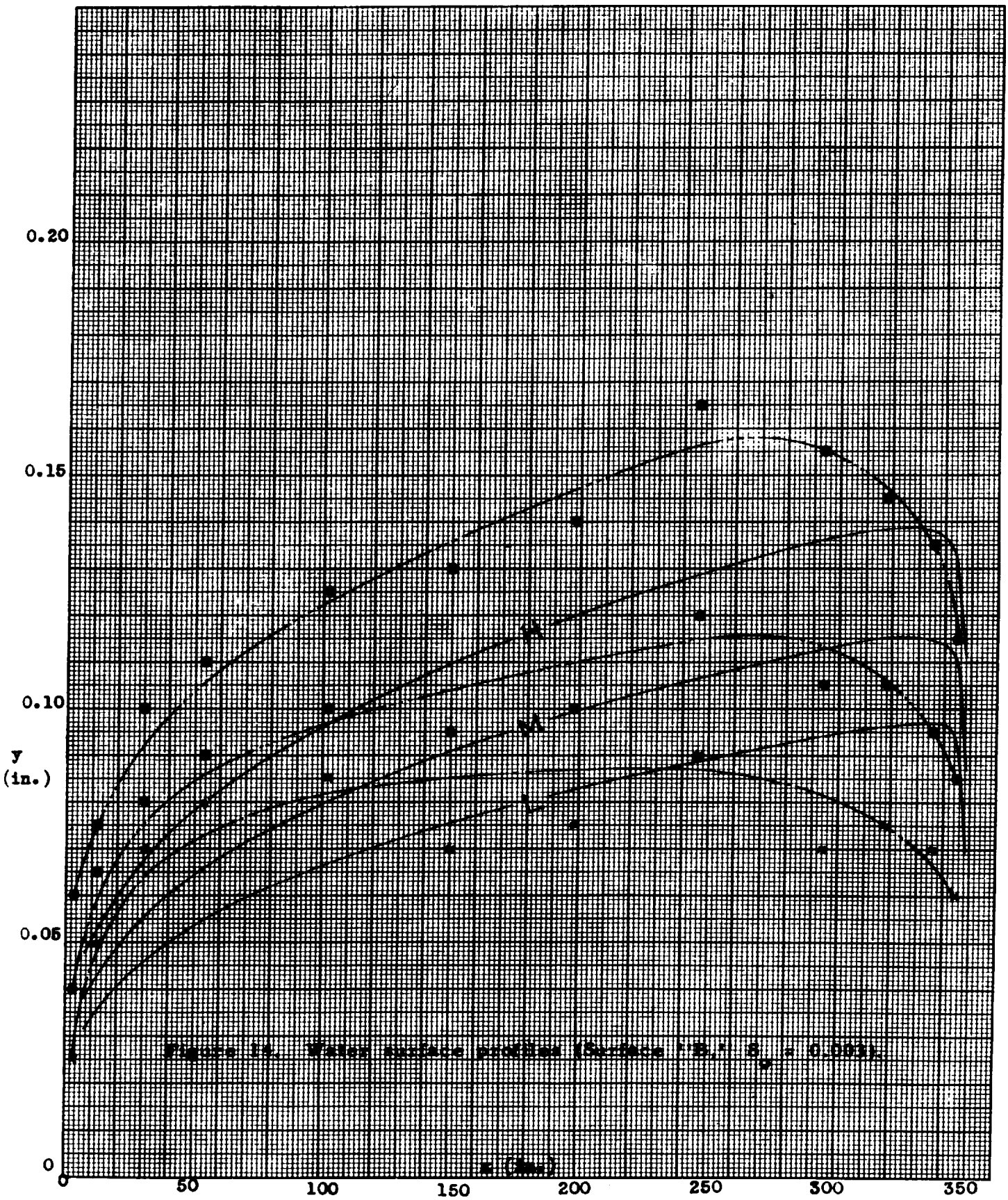


Figure 14. Water surface profiles (Surface "B," S_w = 0.003).

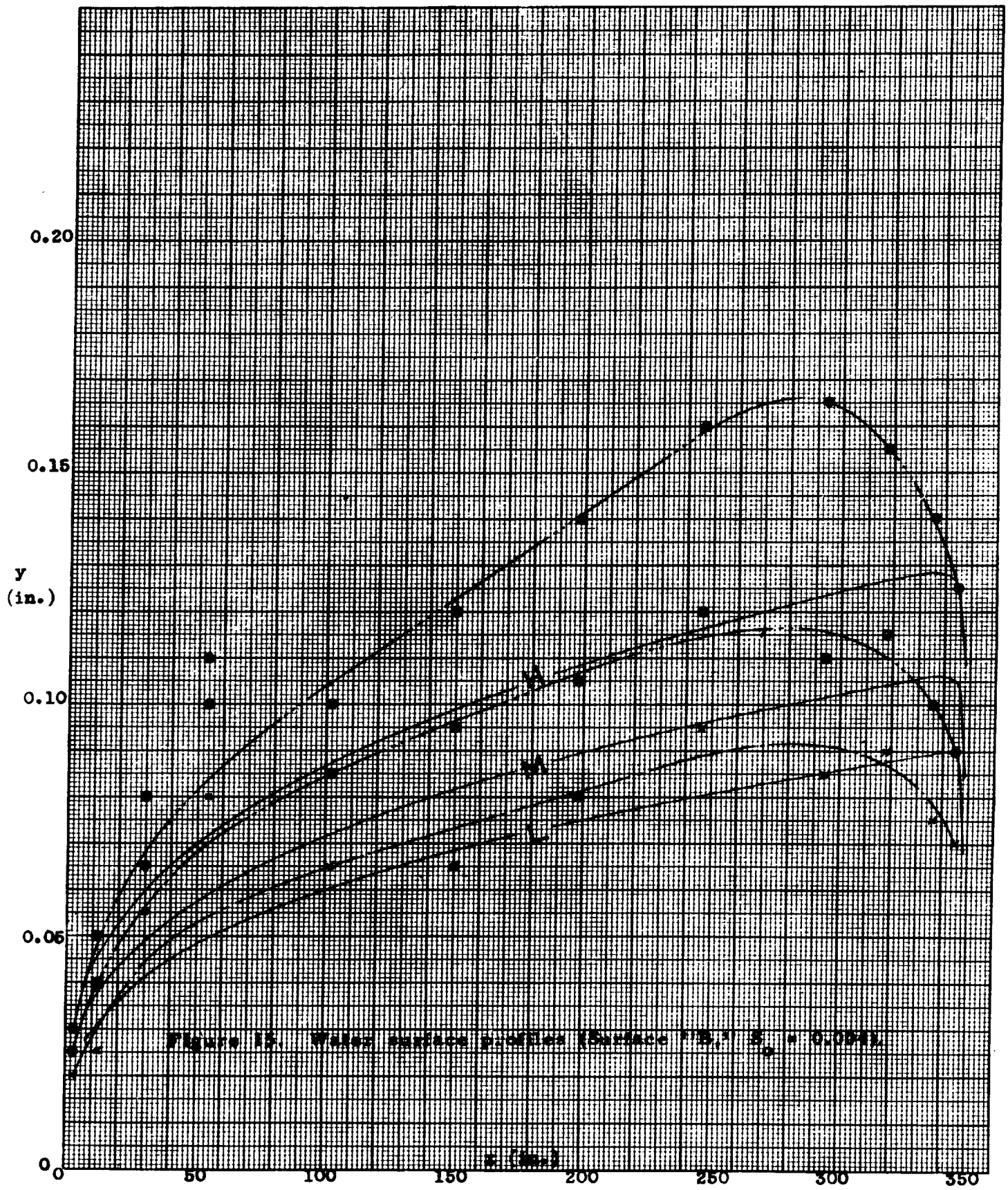
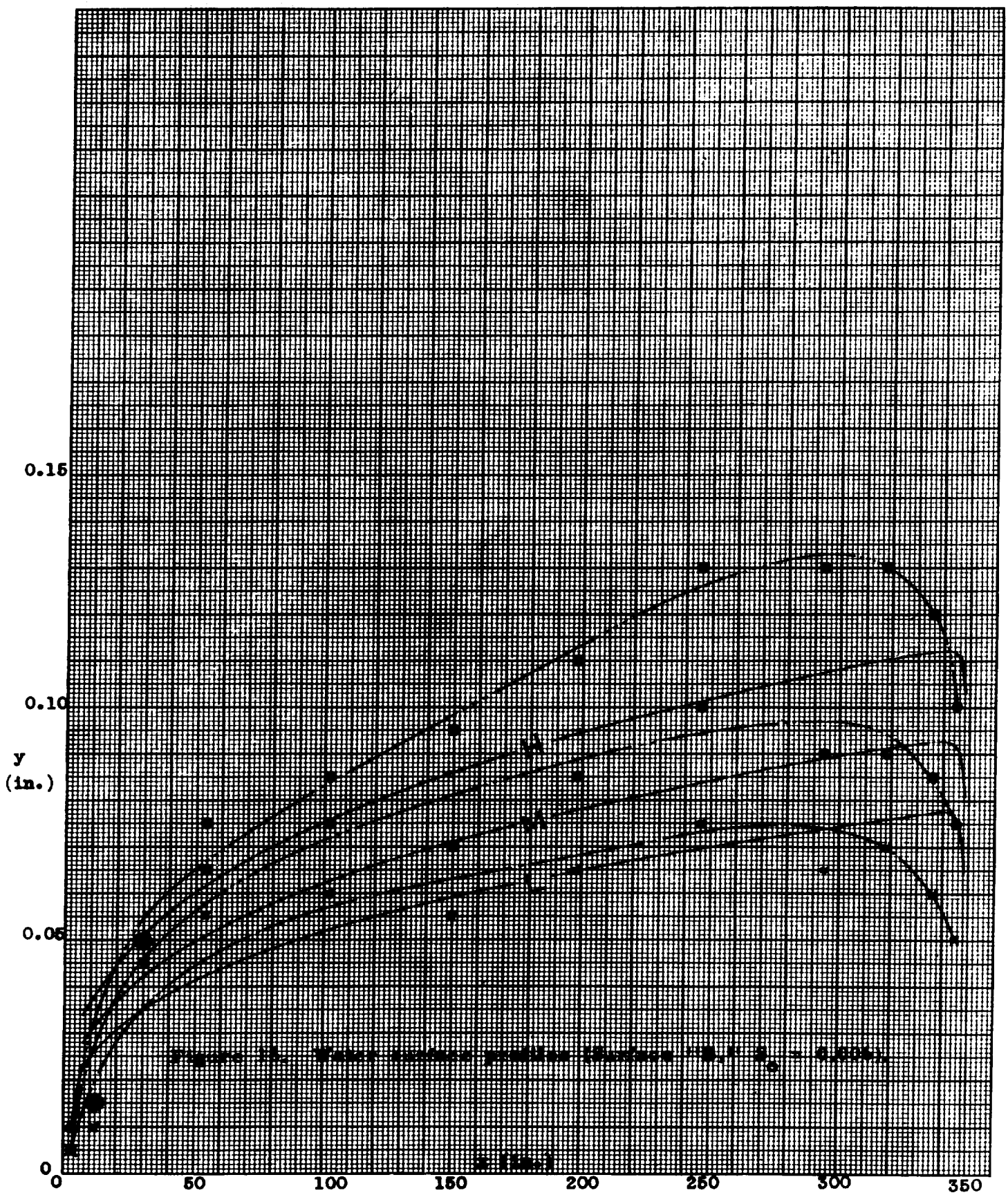


Figure 15. Water surface profiles (Surface TB, 1) $S_o = 0.005$


0.15
0.10
0.05
0
y
(in.)
0
50
100
150
200
250
300
350

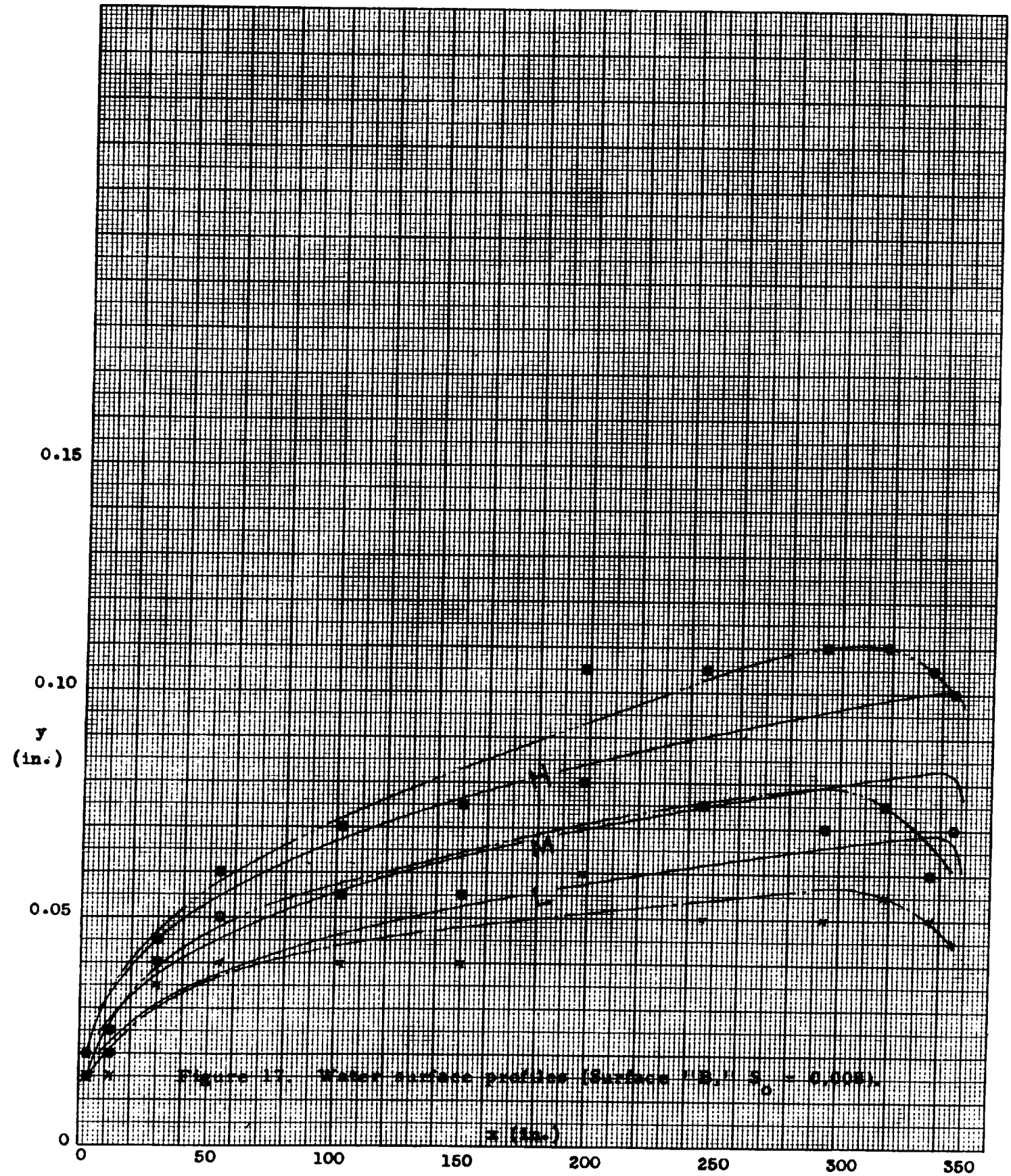


Figure 17. Water surface profiles (Surface "B," S_o = 0.008).

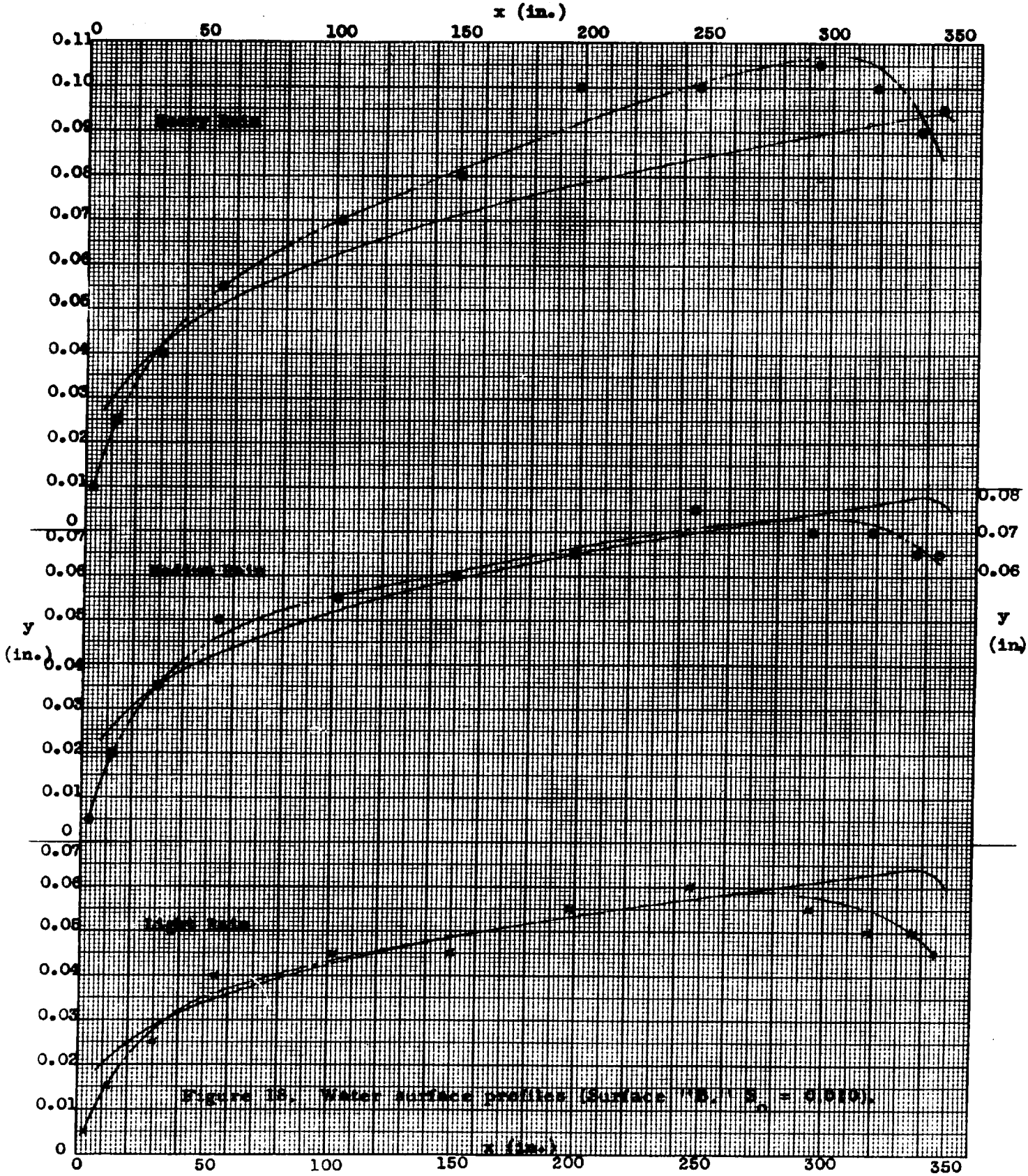


Figure 18. Water surface profiles (Surface "B," S_o = 0.010).

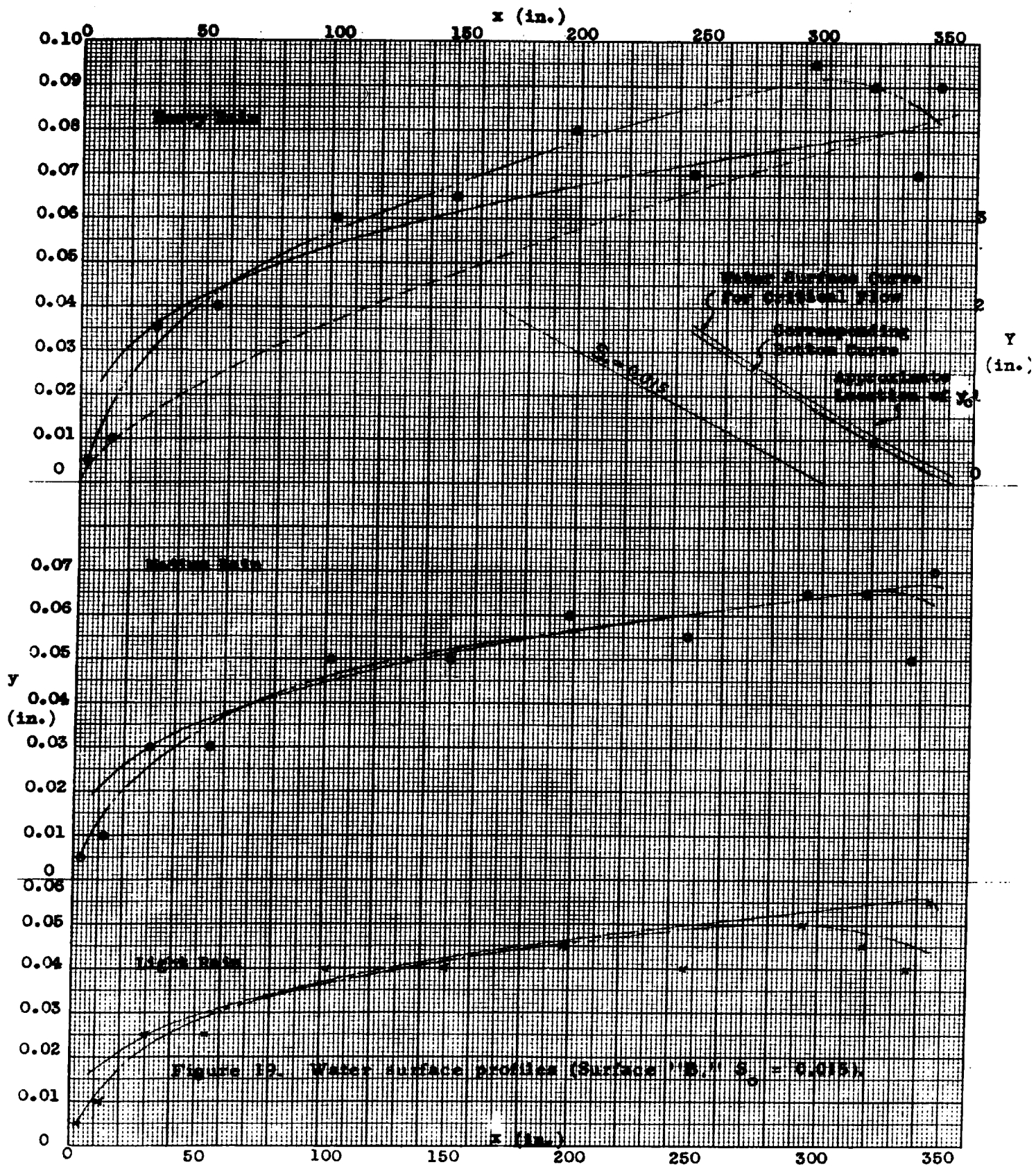


Figure 12. Water surface profiles (Surface "B," S_o = 0.015).

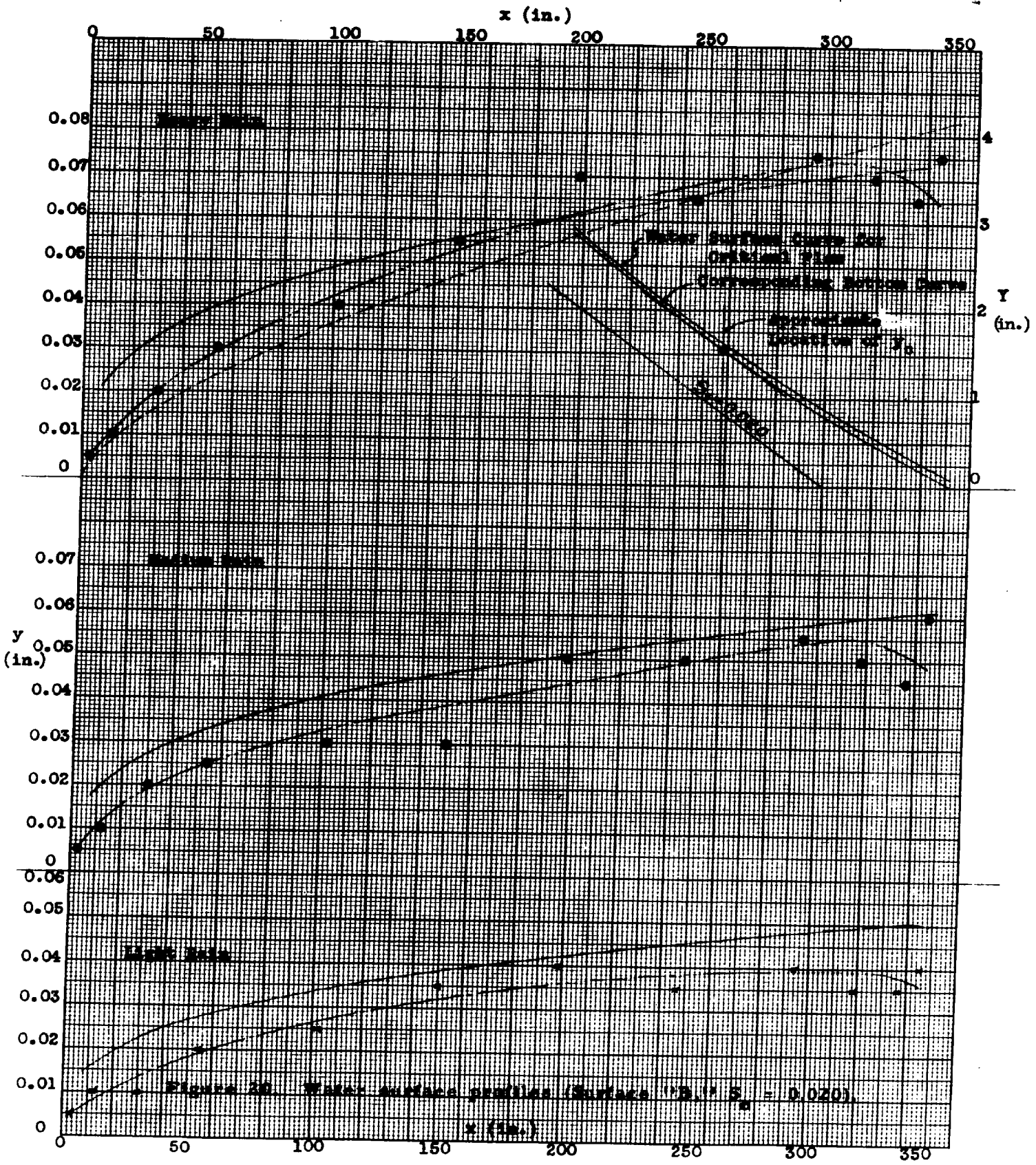


Figure 20. Water surface profiles (Surface "B," S_o = 0.020).

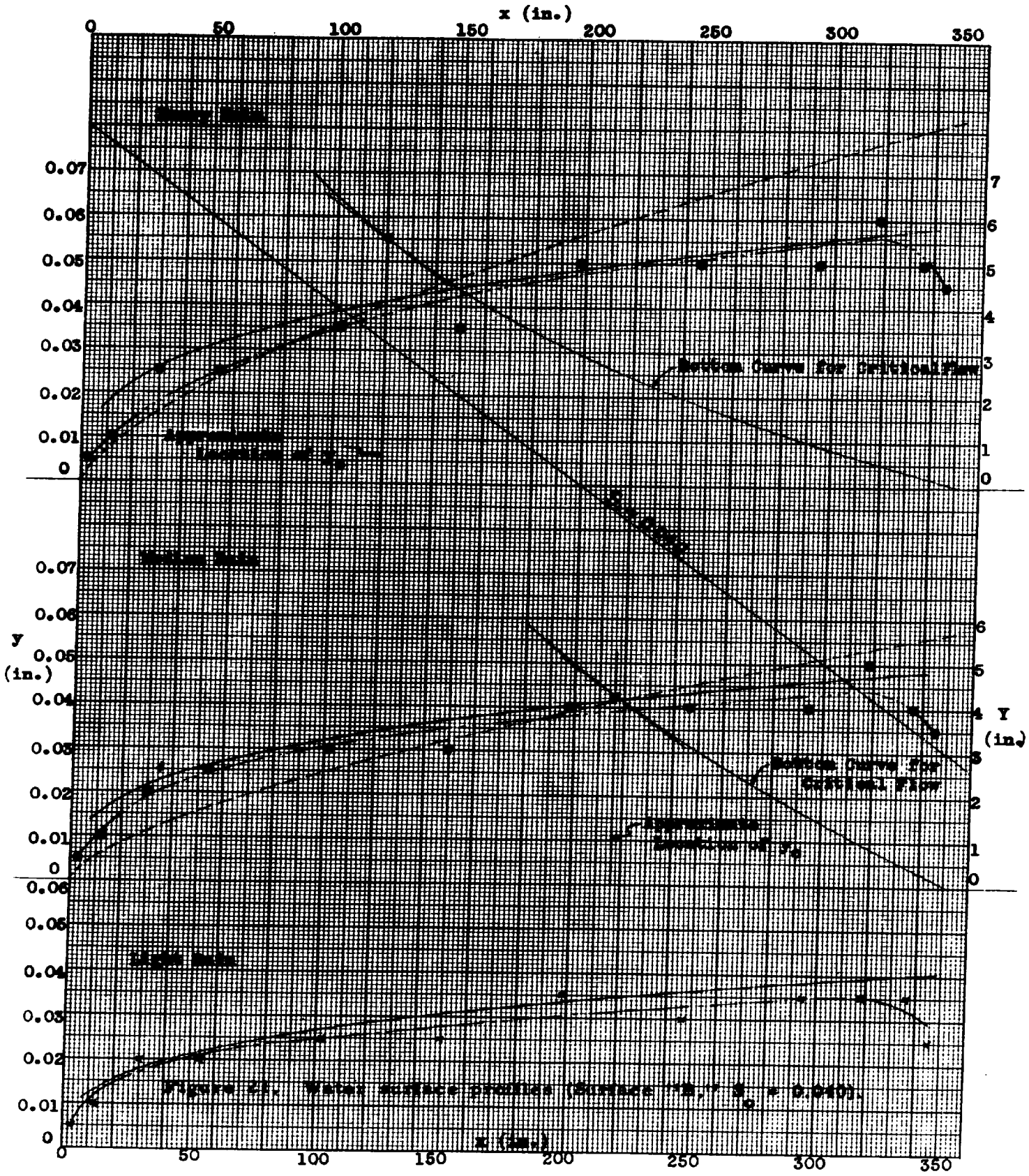


Figure 21. Water surface profile (Slope "B," S_o = 0.0400).

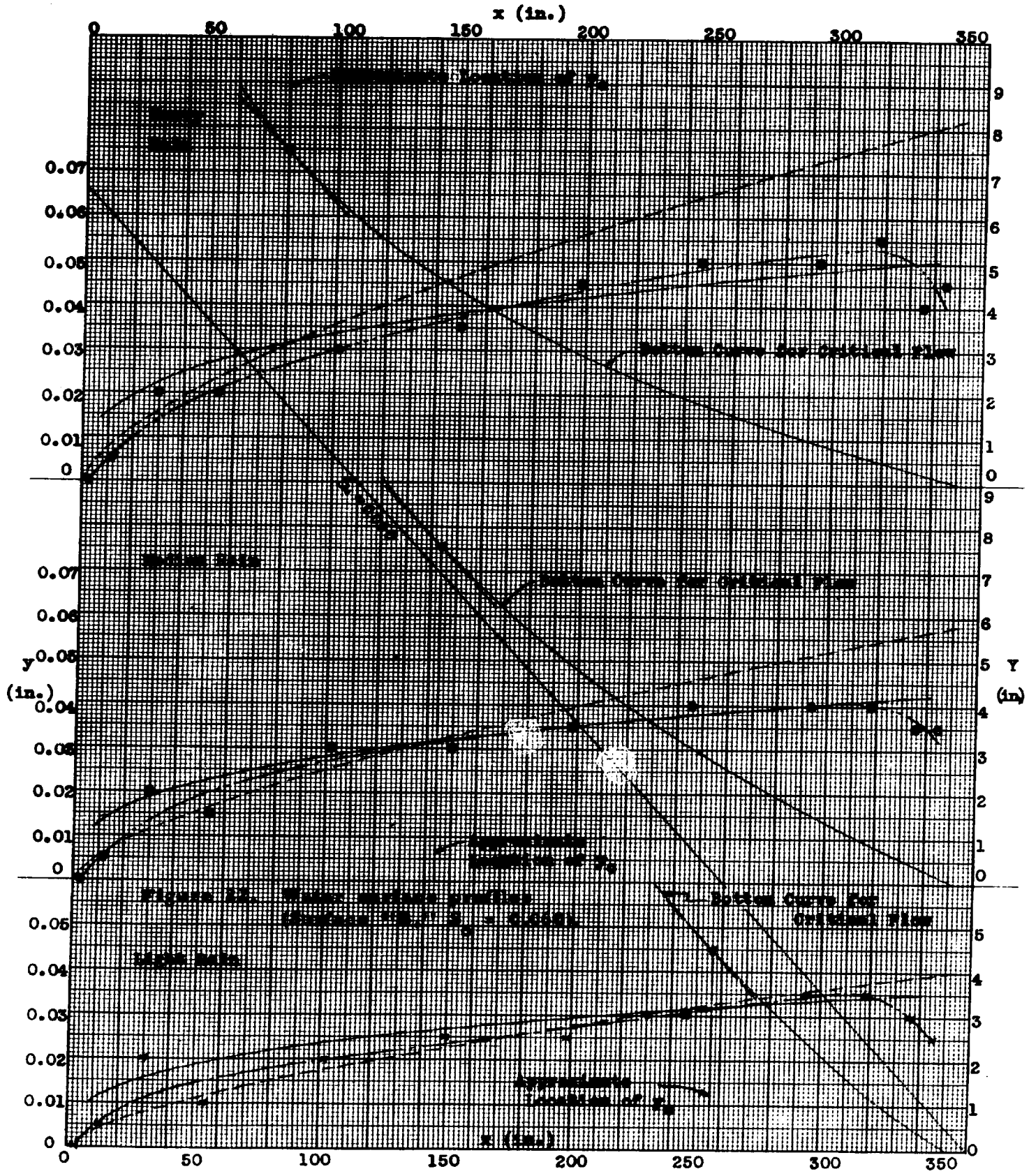
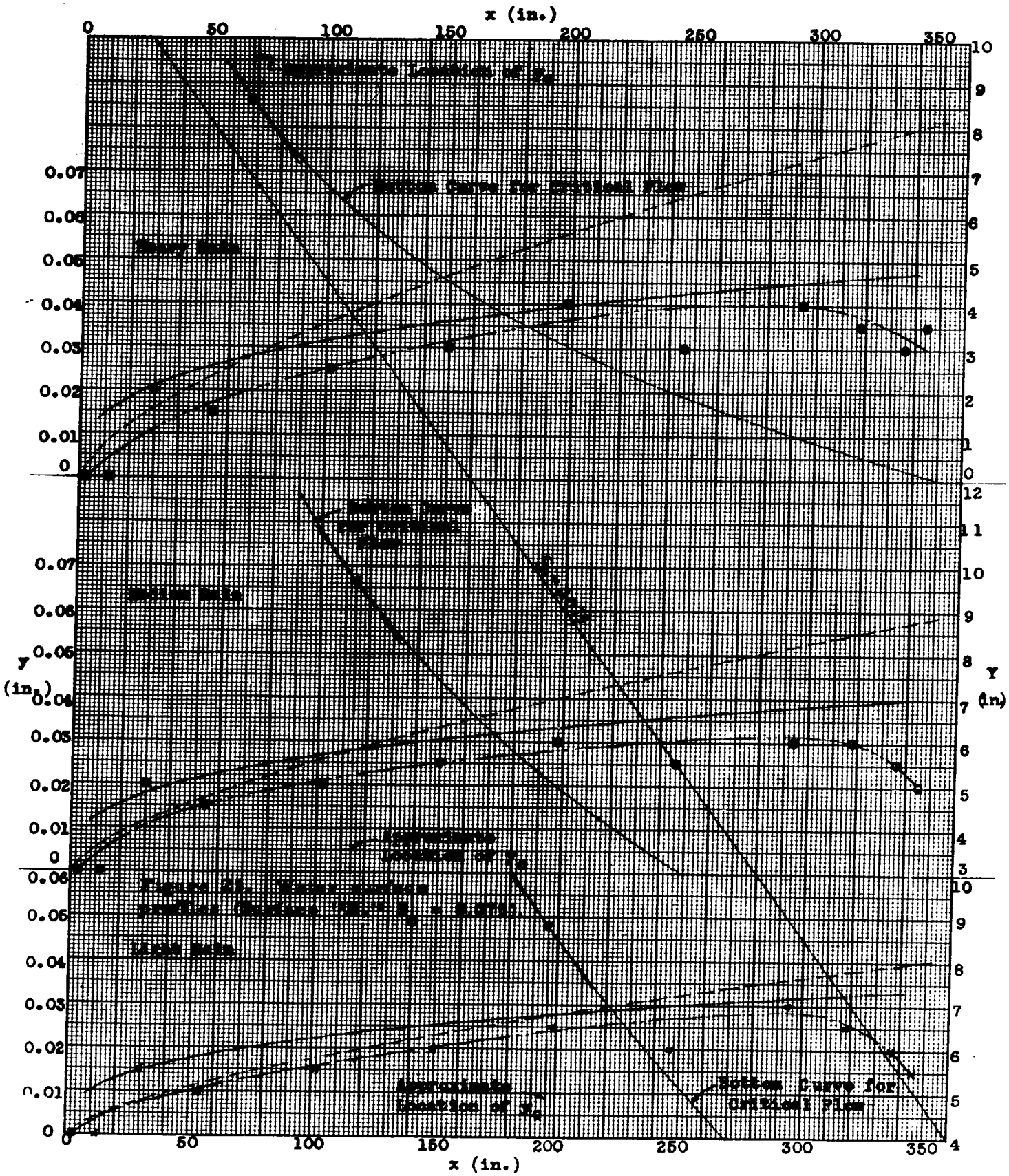


Figure 22. Water surface profile


x (in.)
0
50
100
150
200
250
300
350
Approximate Location of y_c
Bottom Curve for Critical Flow
Base Data
Bottom Curve for Critical Flow
Base Data
y (in.)
Y (in.)
Approximate Location of Y_c
Figure 24. Water Surface Profiles (Bottom Width = 4 in.)
Base Data
Approximate Location of Y_c
Bottom Curve for Critical Flow
x (in.)

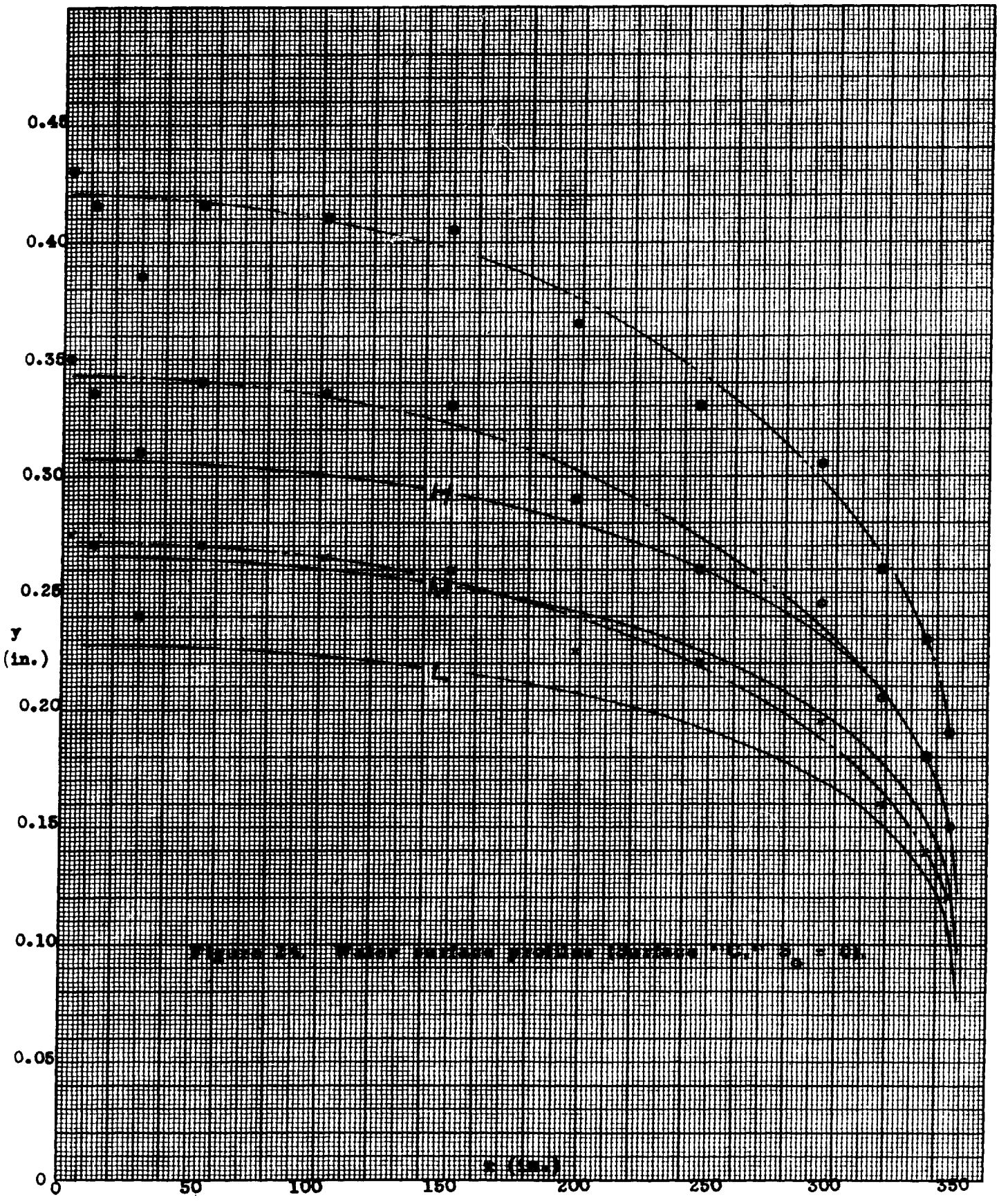


Figure 24. Water surface profiles (Series "C," $\theta_0 = 0°$)

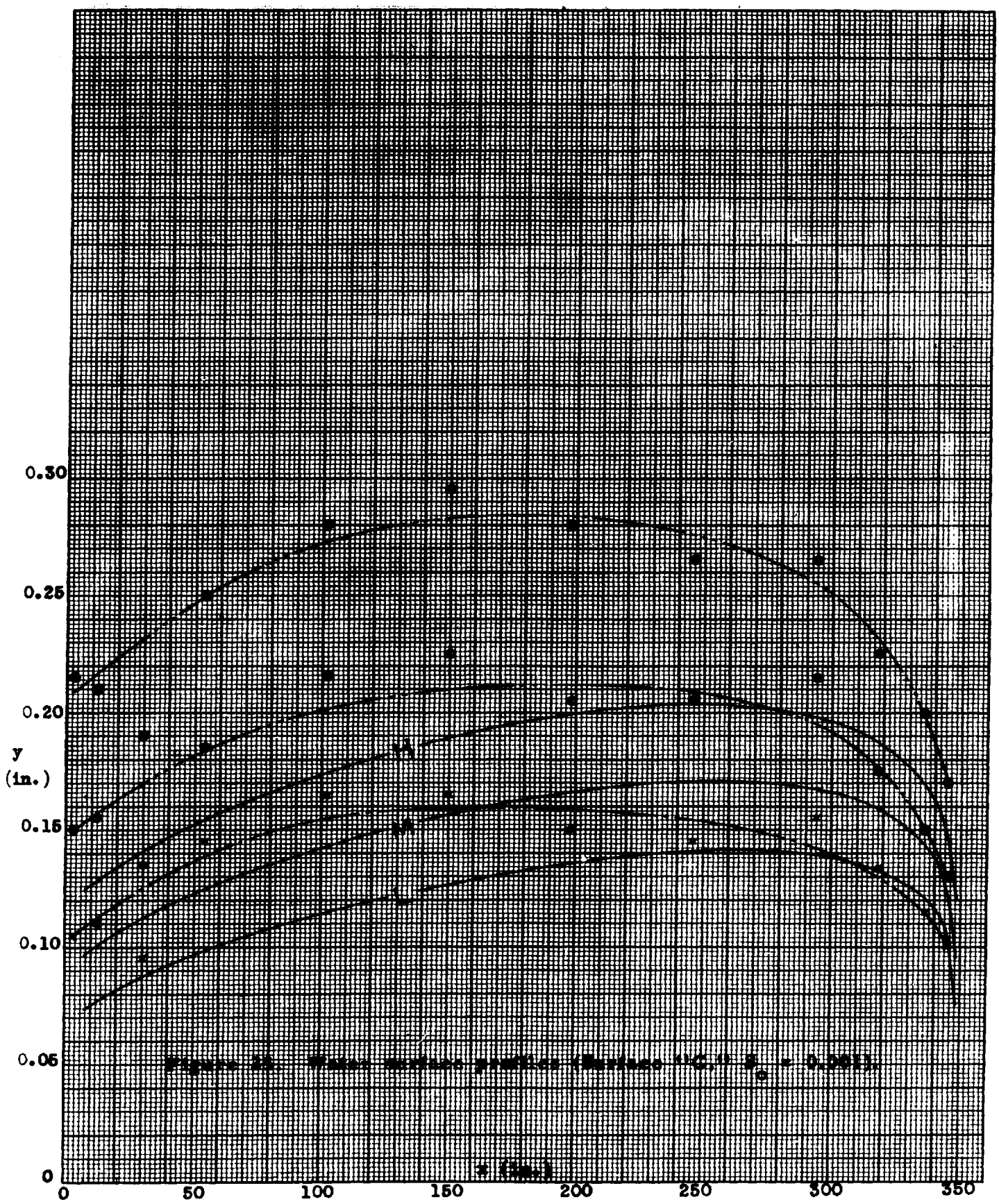


Figure 24. Water surface profiles (Series 10C, S_o = 0.001).

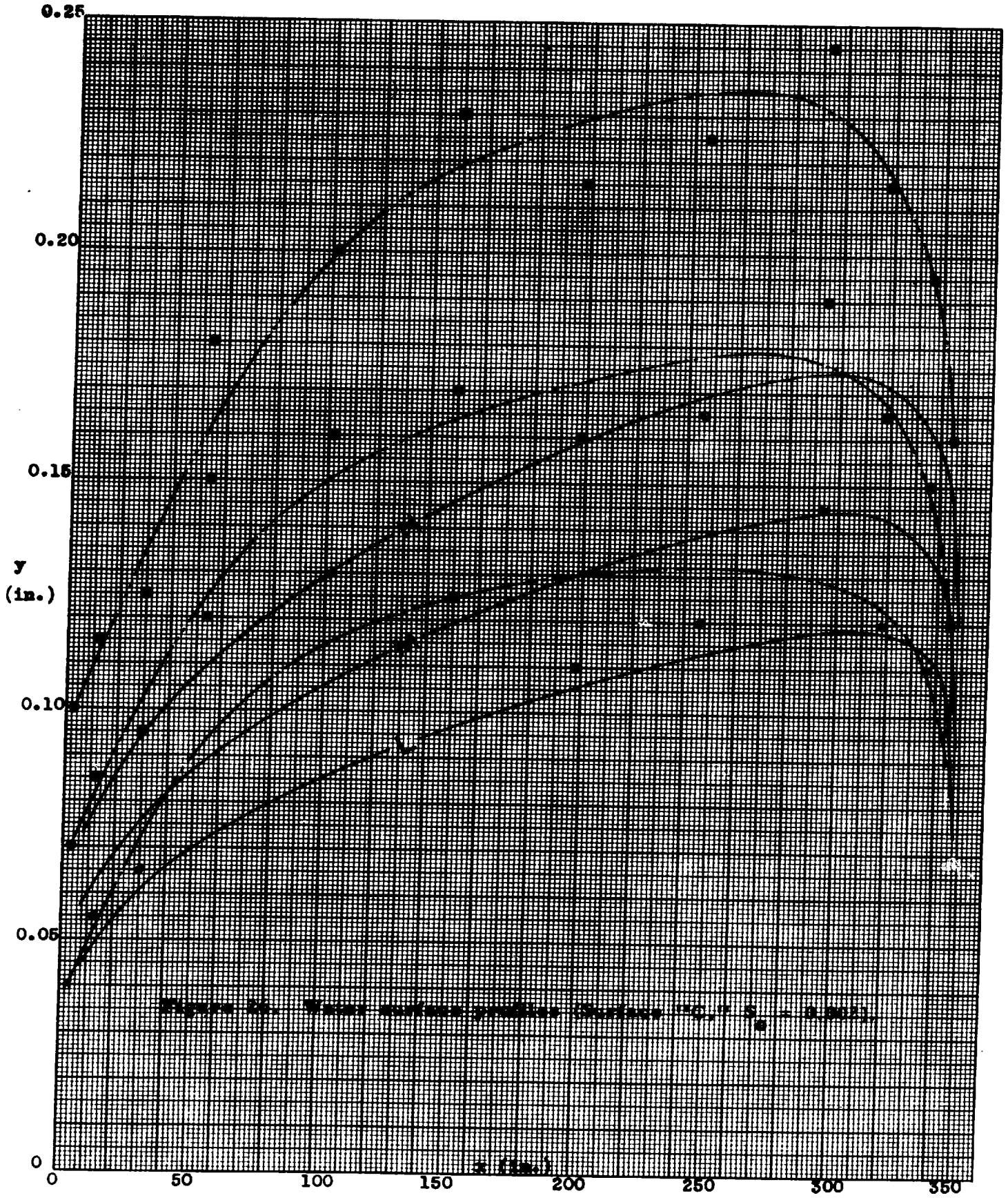


Figure 46. Wear surface profiles (Surface [illegible], S_g = 0.80%).

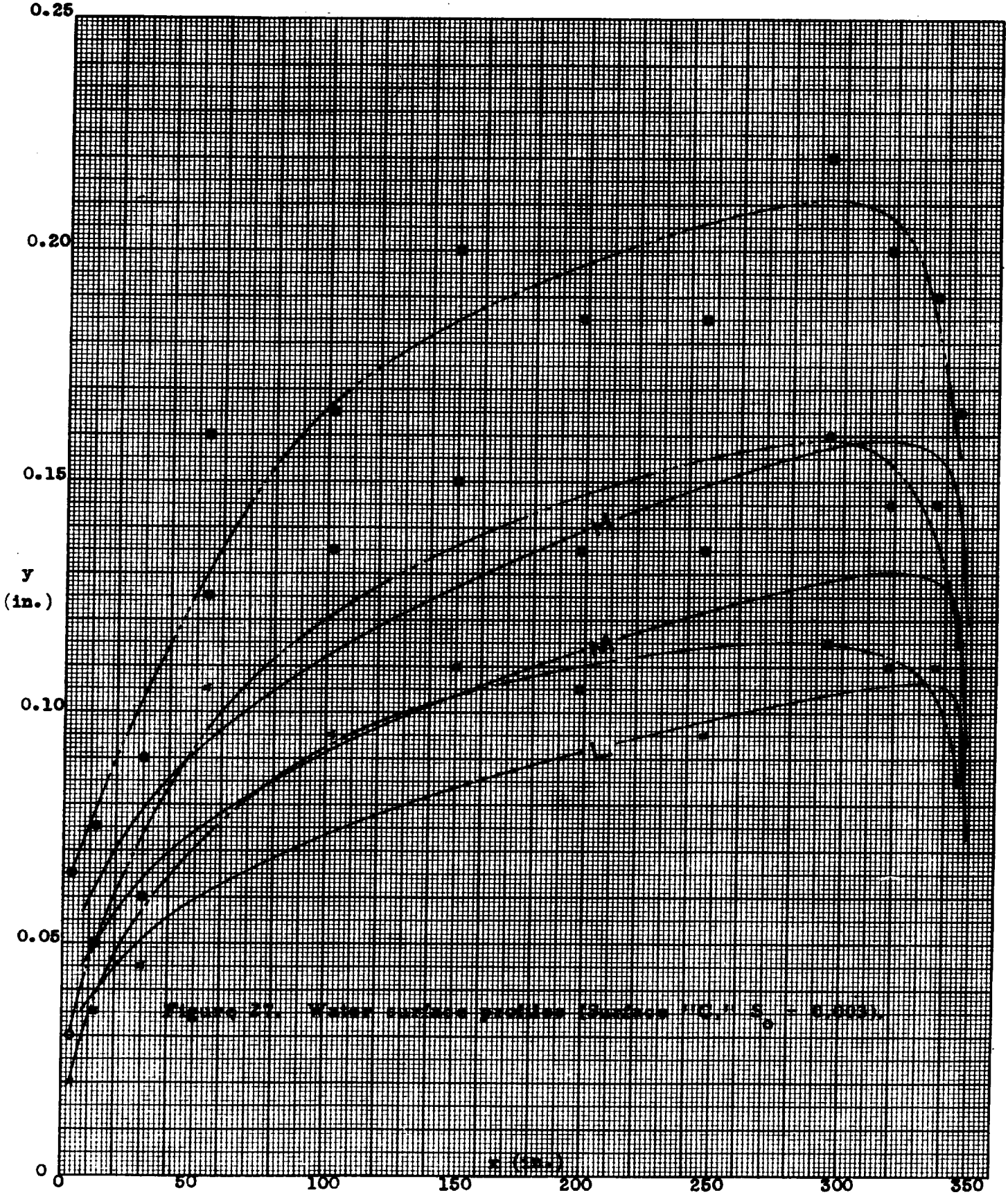


Figure 21. Water surface profiles (Sandusa rig, S_o = 0.003).

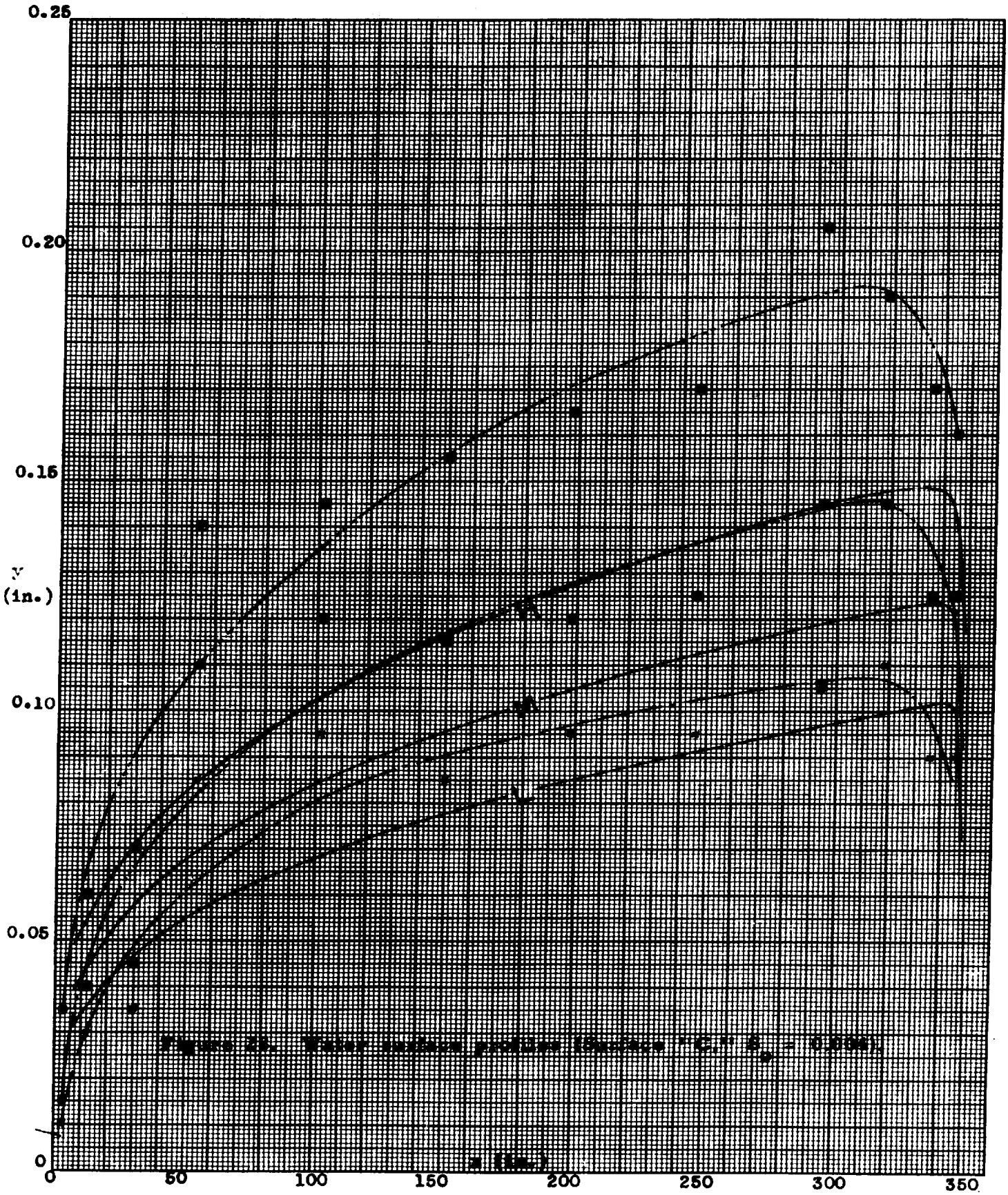


Figure 28. Water surface profiles (Series F-C, F_D = 0.006).

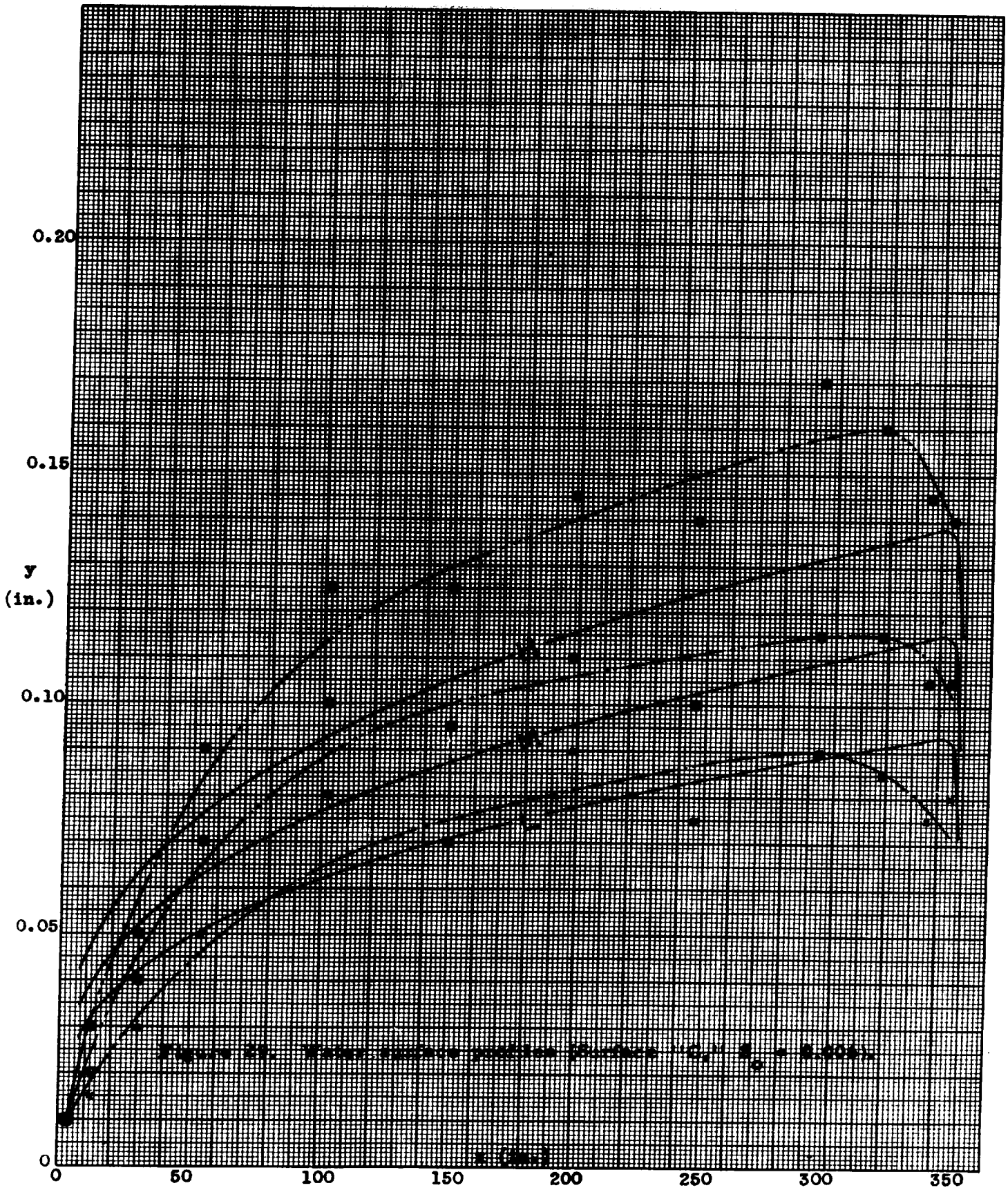


Figure 29. Water surface profile plotted [illegible]

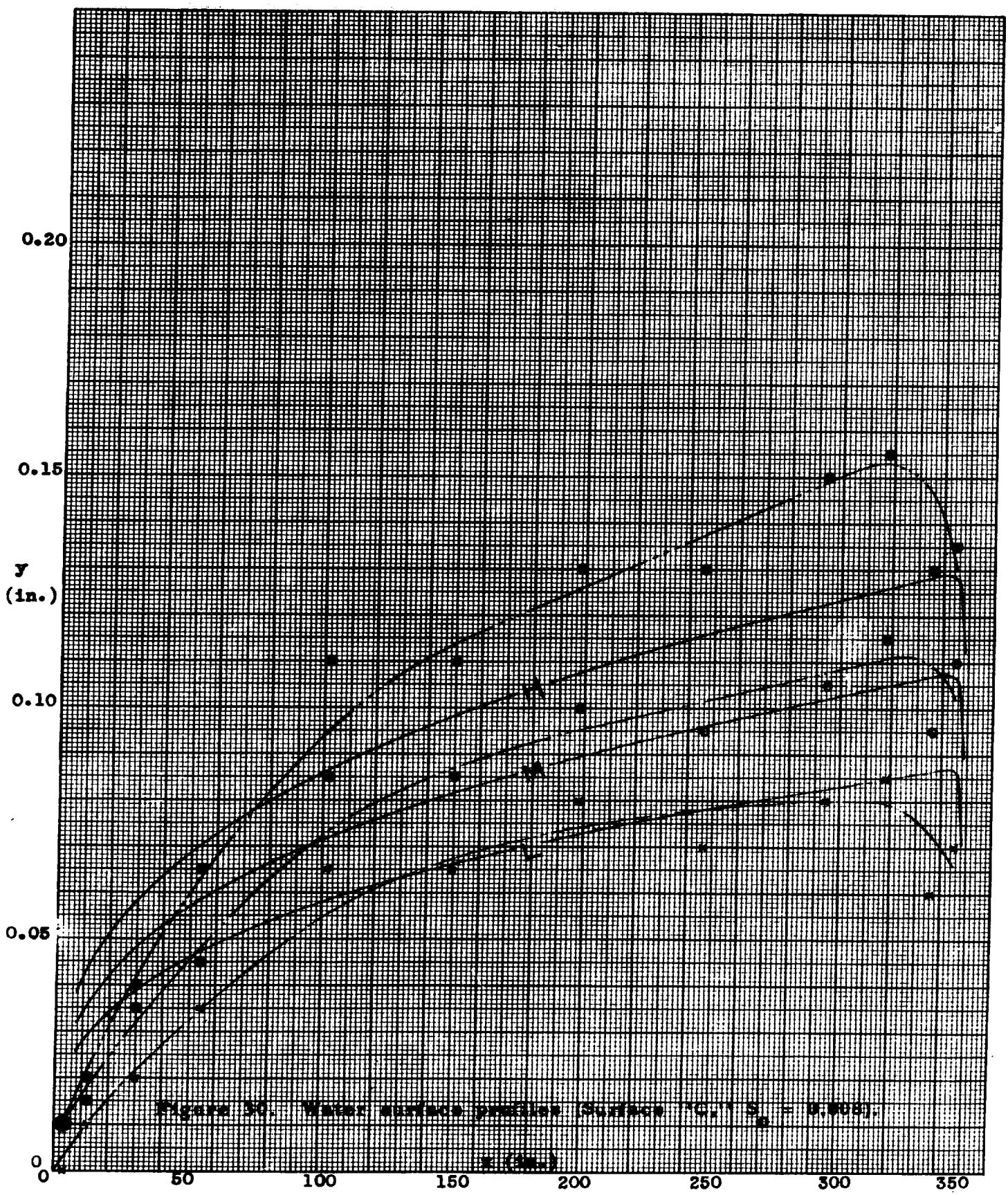


Figure 30. Water surface profiles (Surface °C., S_o = 0.008).

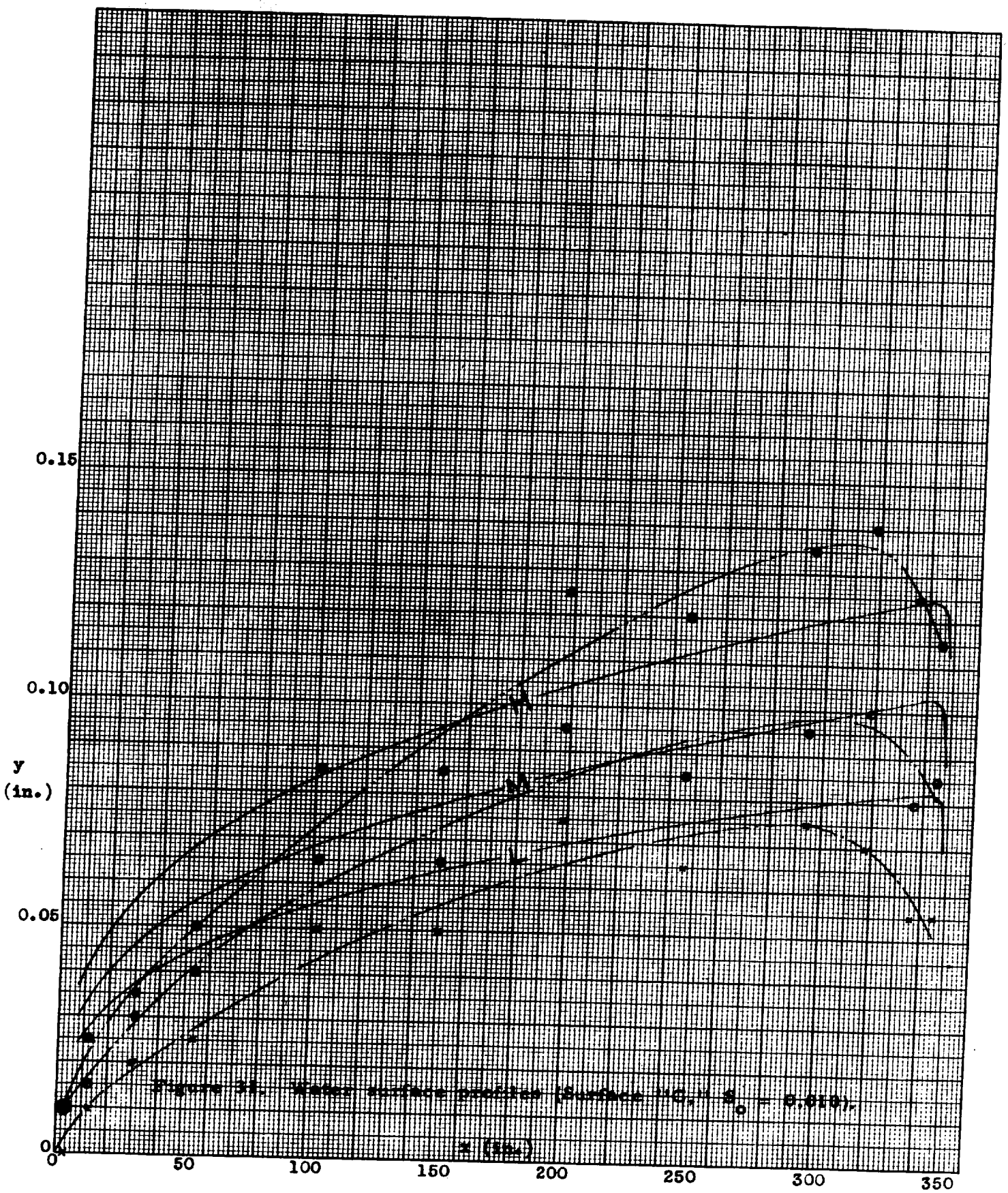


Figure 31. Water surface profiles (Surface 1, $S_o = 0.010$).

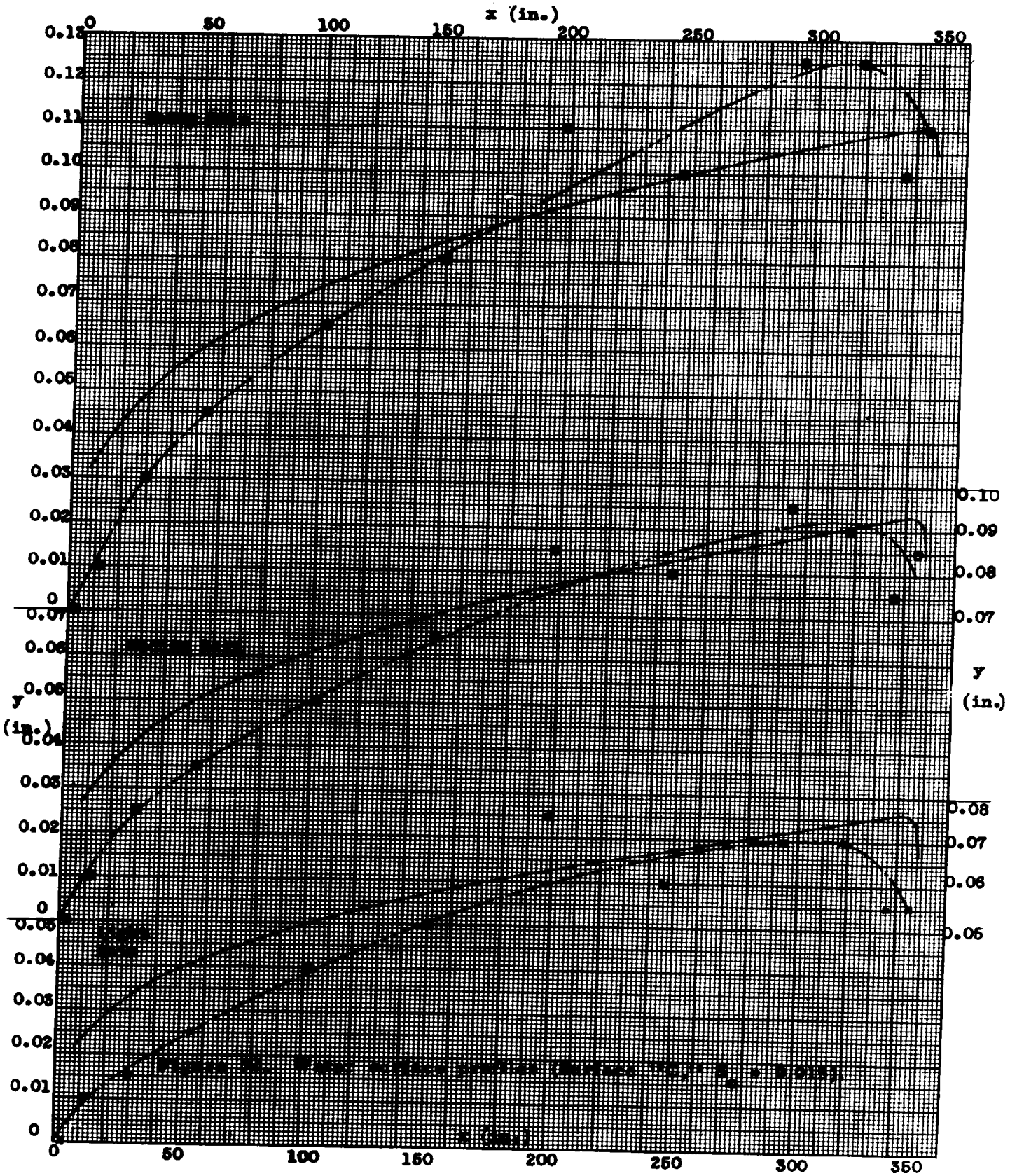


Figure 32. Wake surface profile (Series test 3, $\alpha = 0.2$)

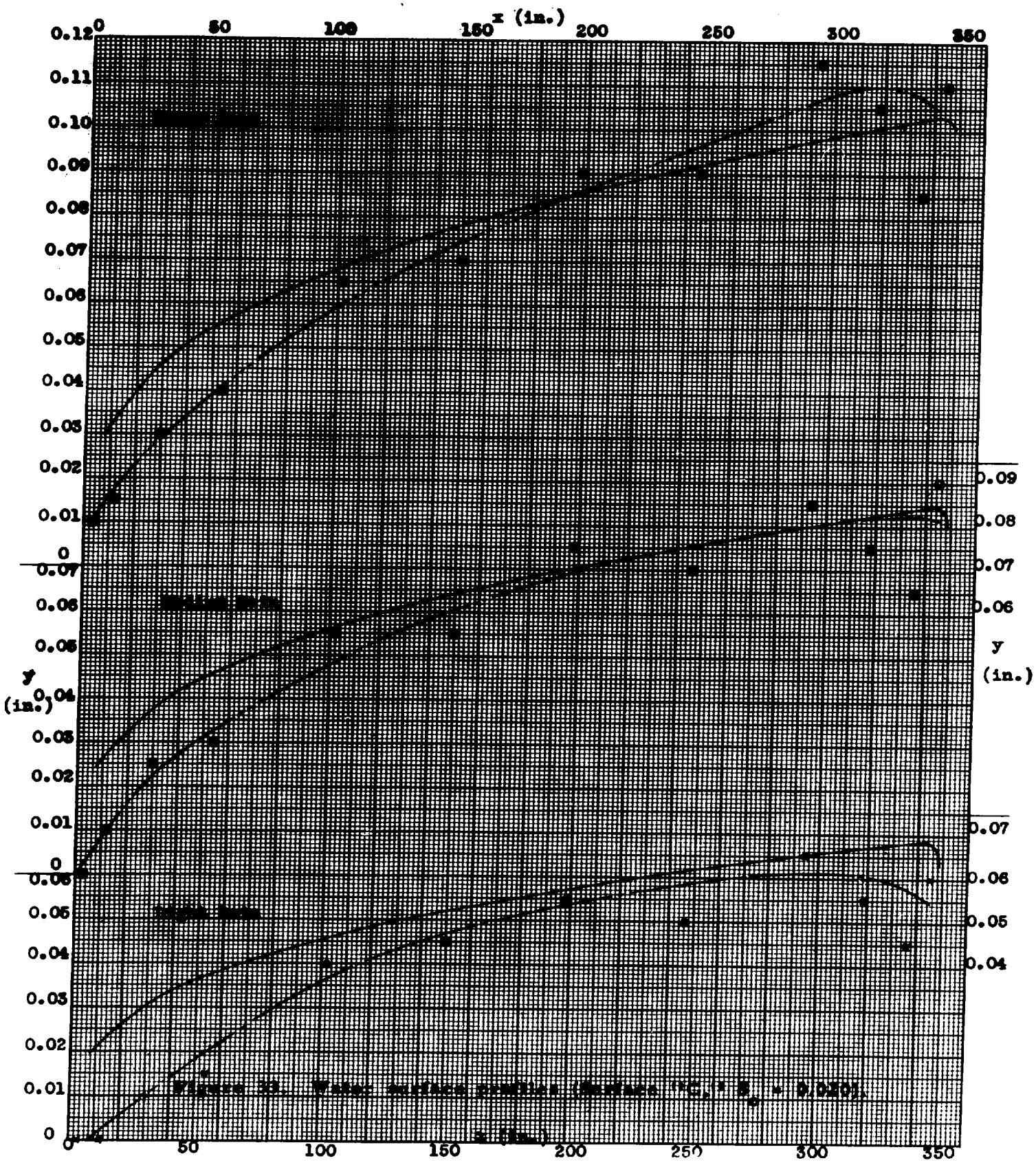
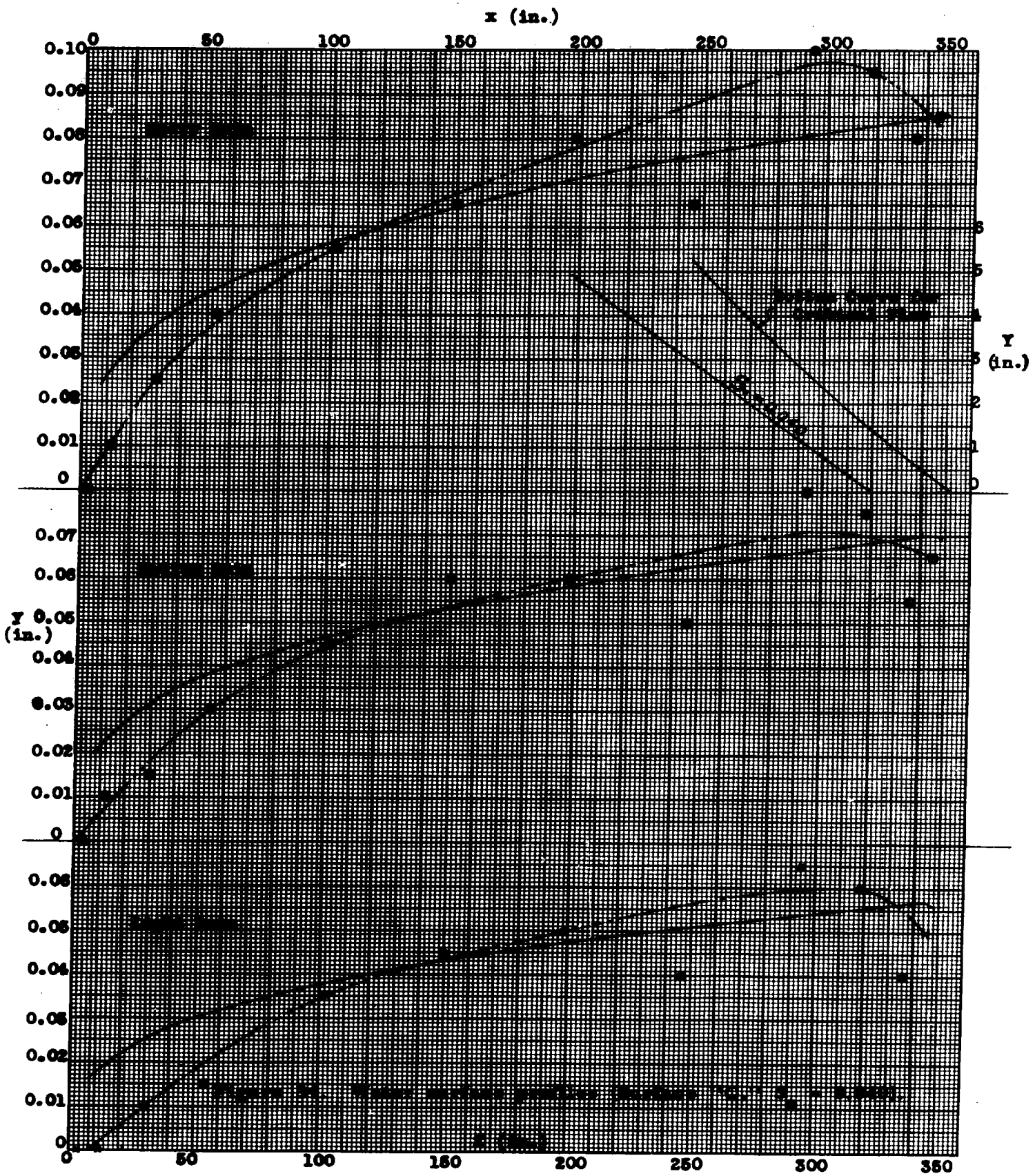


Figure 39. Water surface profiles (Series $^{\circ}C_1$, $S_o = 0.020$).


x (in.)
0
50
100
150
200
250
300
350
0.10
0.09
0.08
0.07
0.06
0.05
0.04
0.03
0.02
0.01
0
Y (in.)
Y (in.)
0
1
2
3
4
5
6

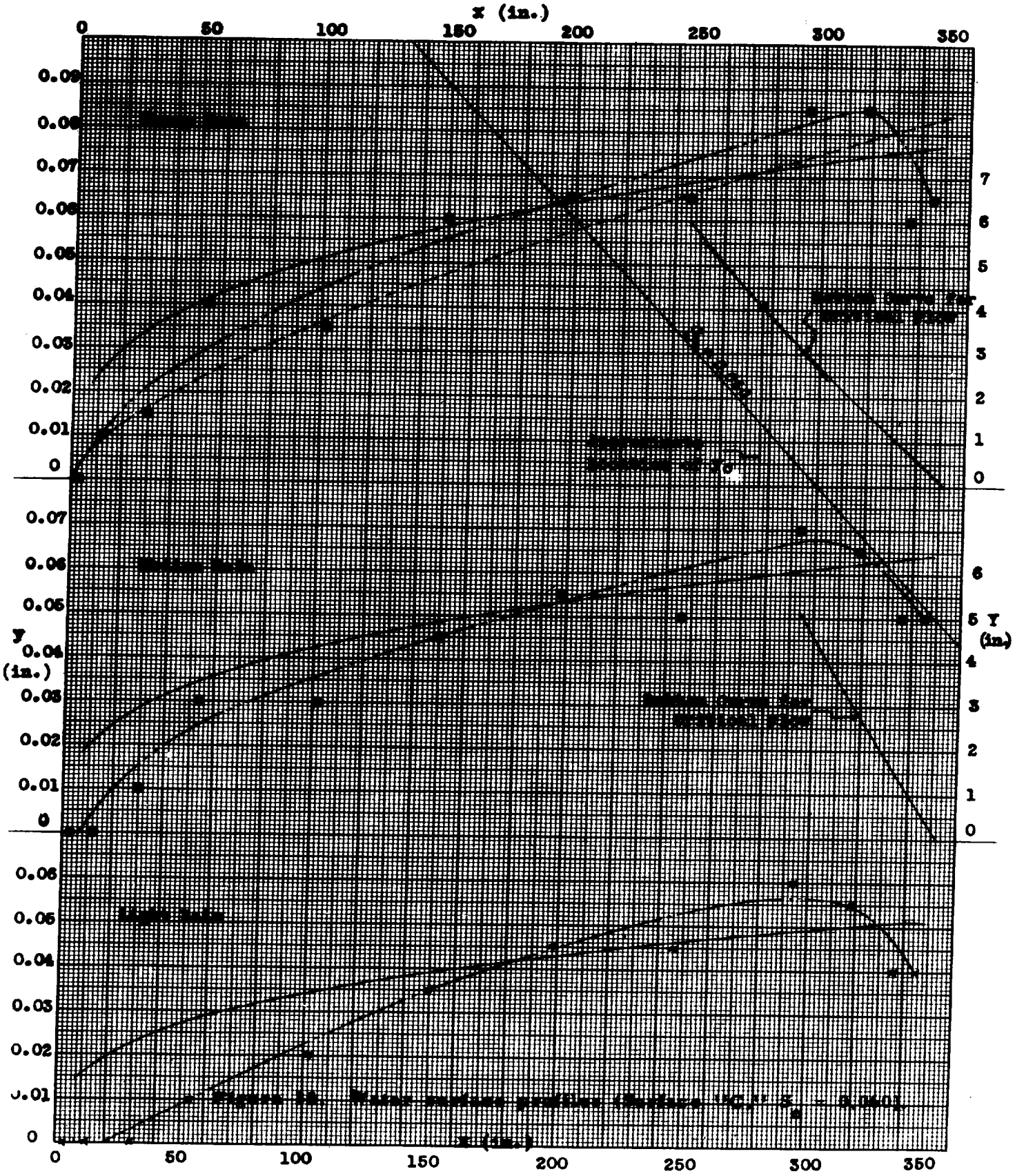


Figure 18. Mean-motion profiles (Surface $^{15}C_{17}$, δ_i = 0.040)

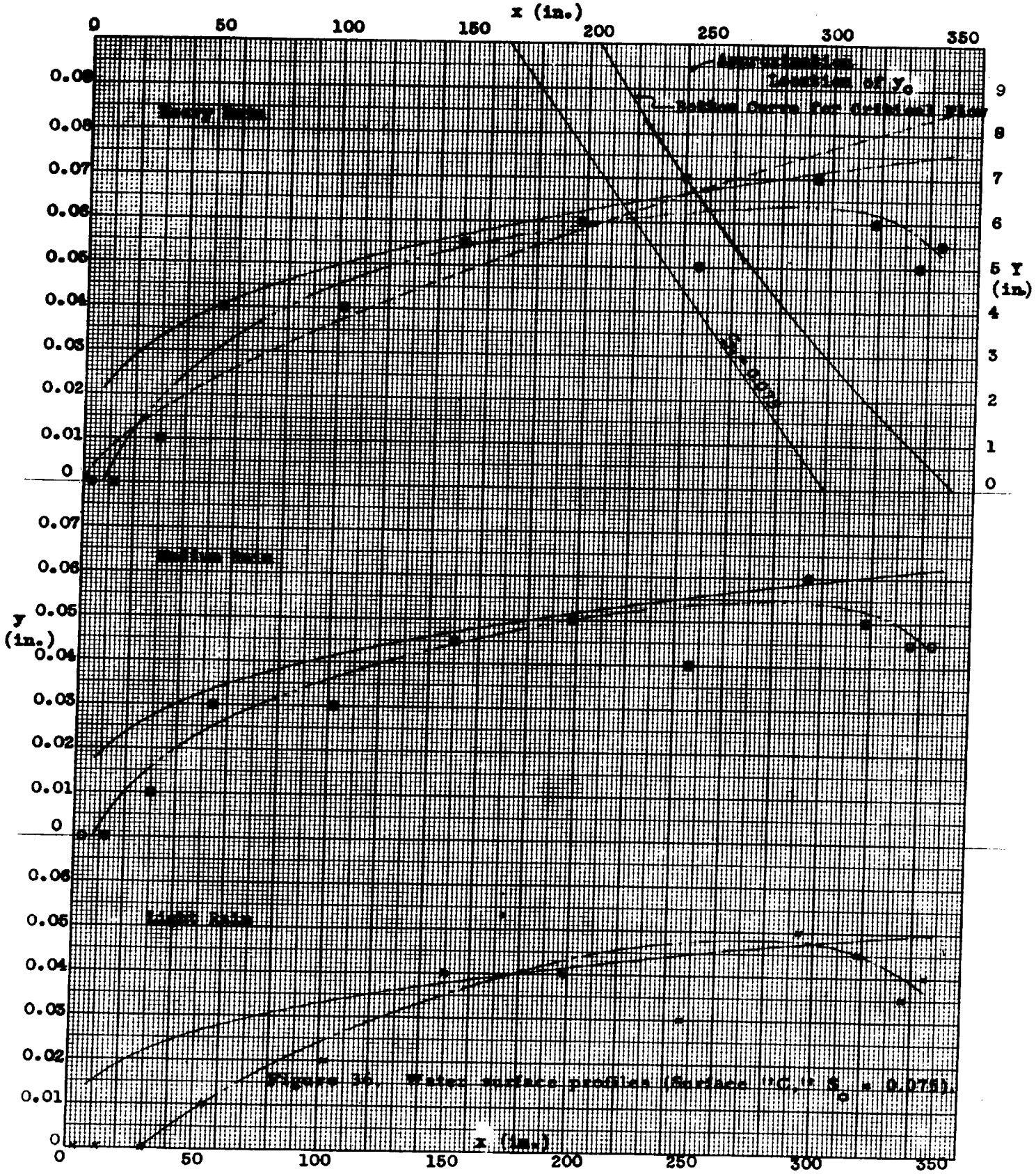


Figure 36. Water surface profiles (Surface 1'C, S_o = 0.075).

WATER SURFACE PROFILES COMPUTED FROM ACTUAL EXPERIMENTAL CONDITIONS AND SIMPLIFIED EQUATION (27)

Legend

—L— Computed (from equation 15) water surface profile for light rain.

—M— Computed (from equation 15) water surface profile for medium rain.

—H— Computed (from equation 15) water surface profile for heavy rain.

• Computed water depth for light rain based on actual rainfall distribution and actual bottom elevation.

▣ Computed water depth for medium rain based on actual rainfall distribution and actual bottom elevation.

△ Computed water depth for heavy rain based on actual rainfall distribution and actual bottom elevation.

Water depth for light rain computed from the simplified equation (27).

Water depth for medium rain computed from the simplified equation (27).

Water depth for heavy rain computed from the simplified equation (27).

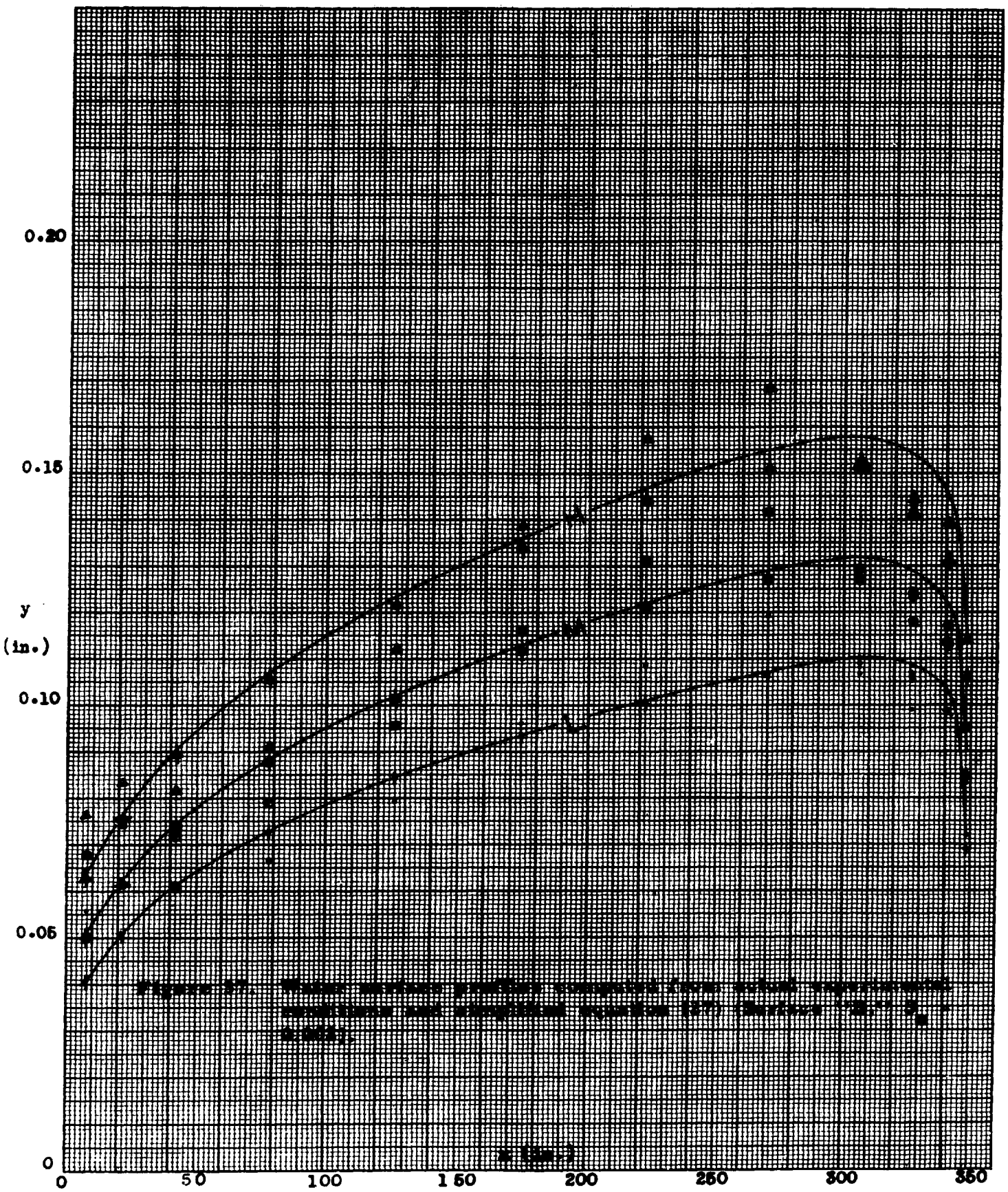
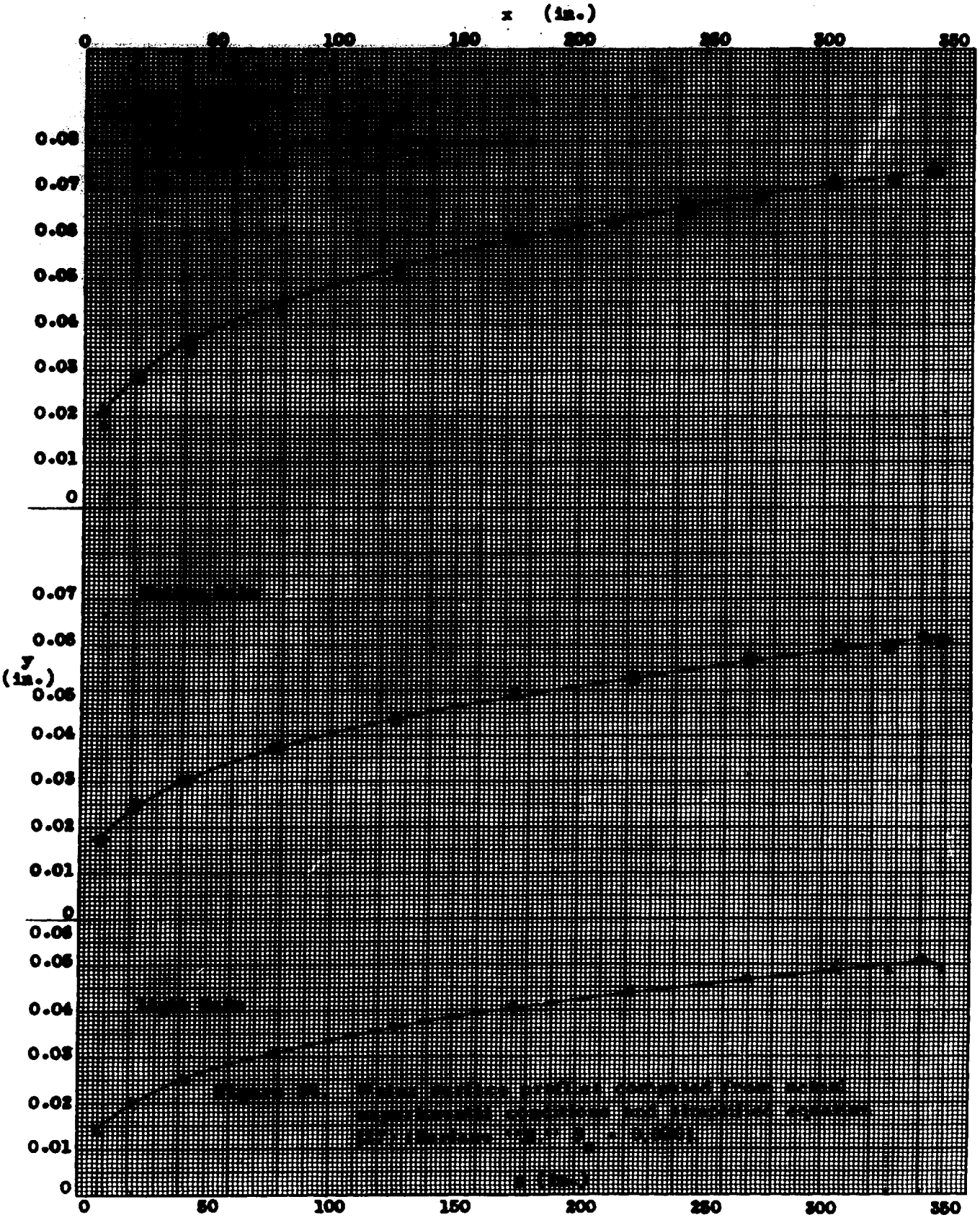


Figure 37. Water surface profiles, computed from method of characteristics and empirical equation (37) (Series 2, S_o = 0.015).


x (in.)
0
50
100
150
200
250
300
350
0.08
0.07
0.06
0.05
0.04
0.03
0.02
0.01
0
y (in.)

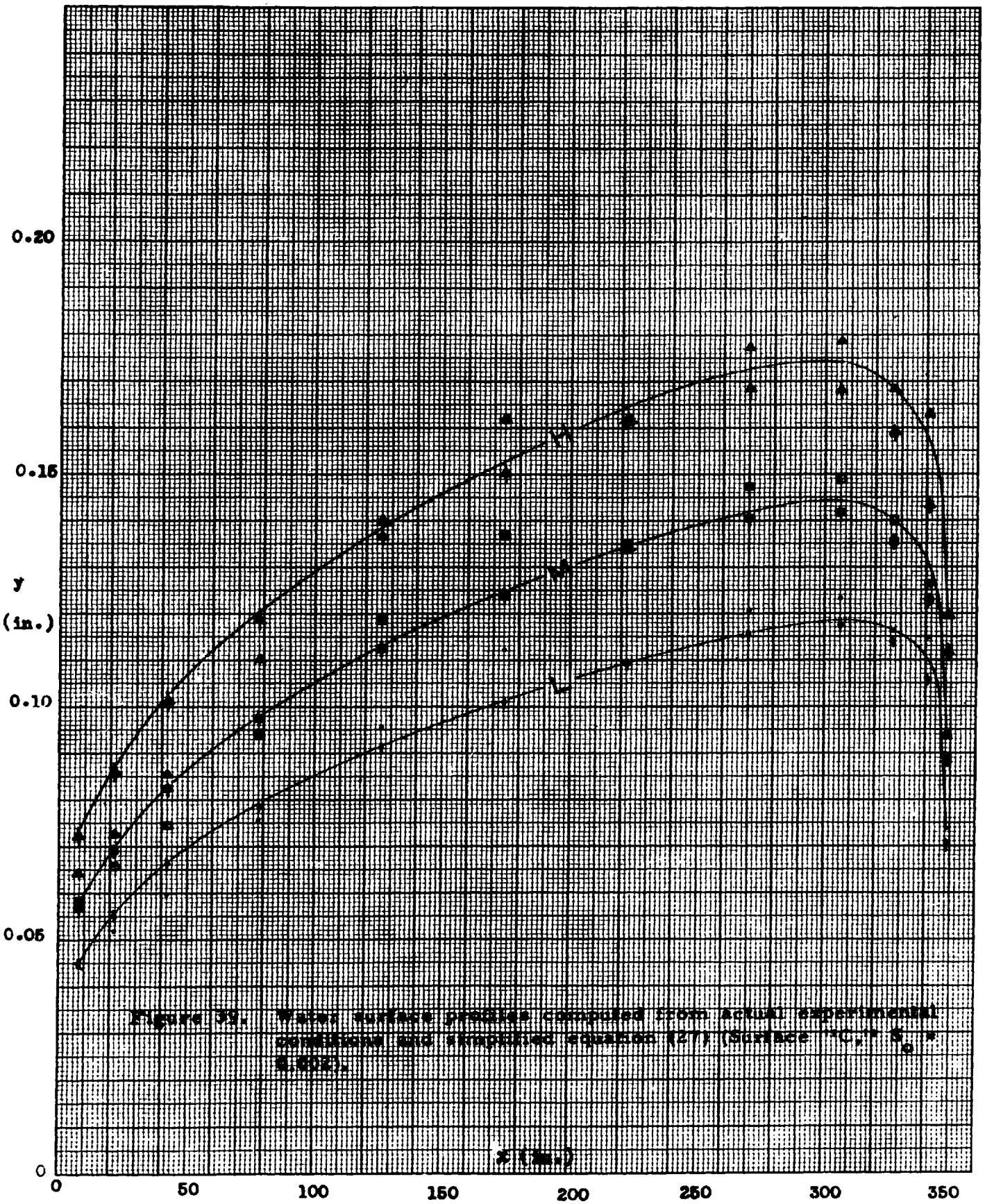


Figure 39. Water surface profiles computed from actual experimental conditions and simplified equation (27) (Surface $^{\circ}C_f$ = S_o = 0.002).

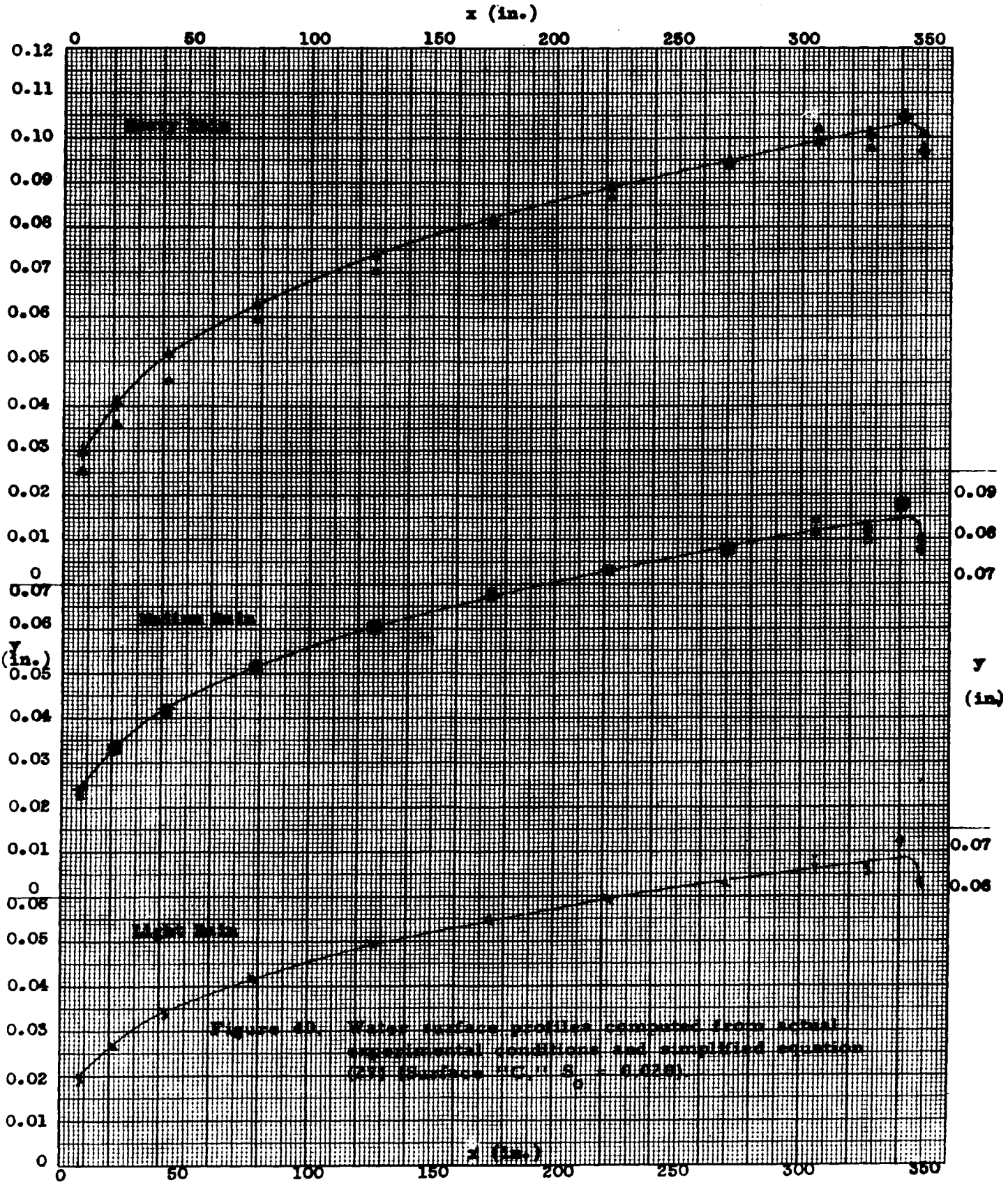


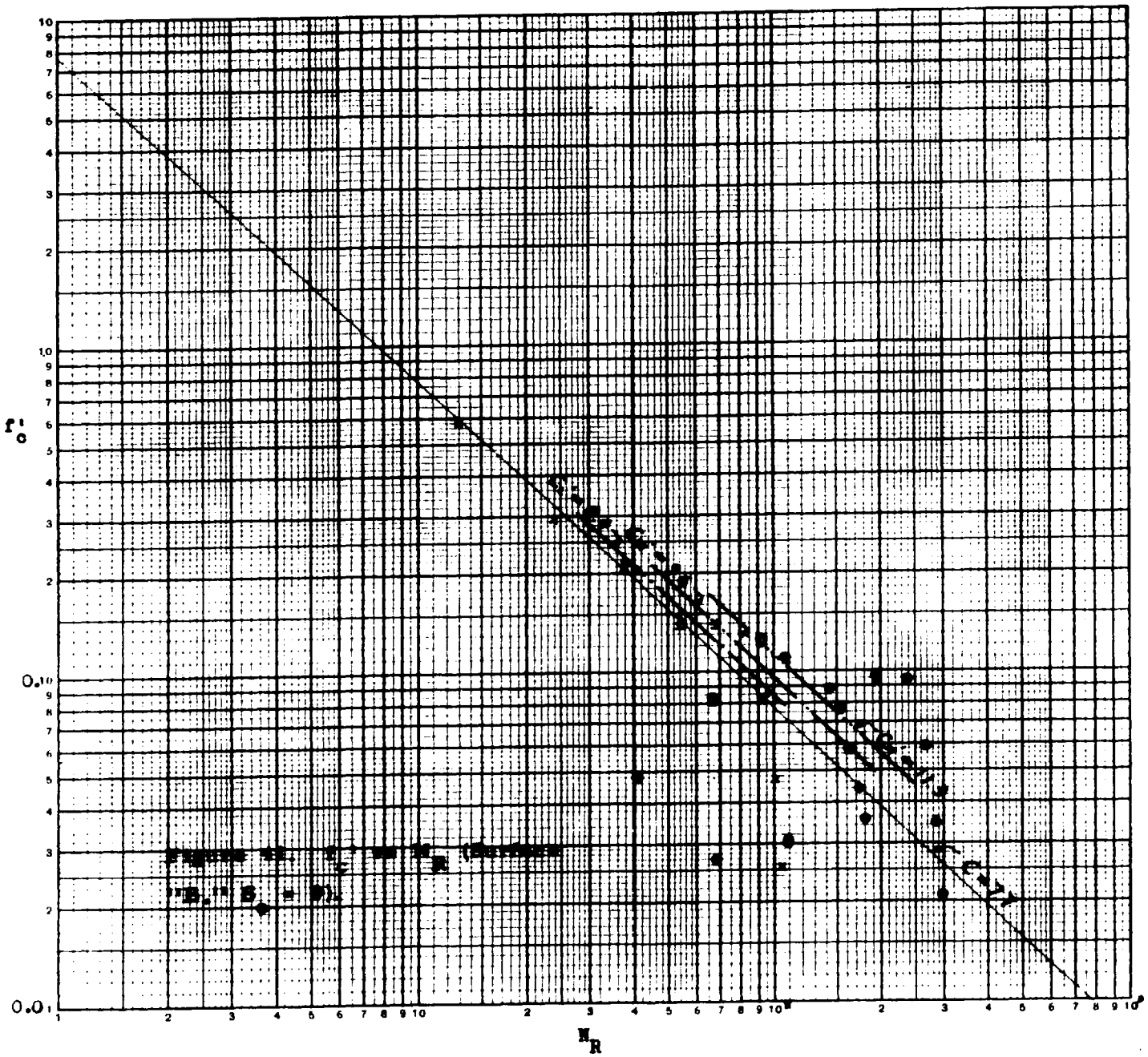
Figure 4b. Water surface profiles computed from actual experimental conditions and simplified equation (2) (Surface n_c, n', S_0 = 0.028).

EFFECT OF RAINDROP IMPACT ON COEFFICIENT OF FRICTION

f_c' vs N_R

Legend

x	For light rain.
⊙	For medium rain.
⊛	For heavy rain.
$\underline{x}$	Those used to determine C_L'.
$\underline{\odot}$	Those used to determine C_M'.
$\underline{\circledast}$	Those used to determine C_H'.


f'_c
N_R

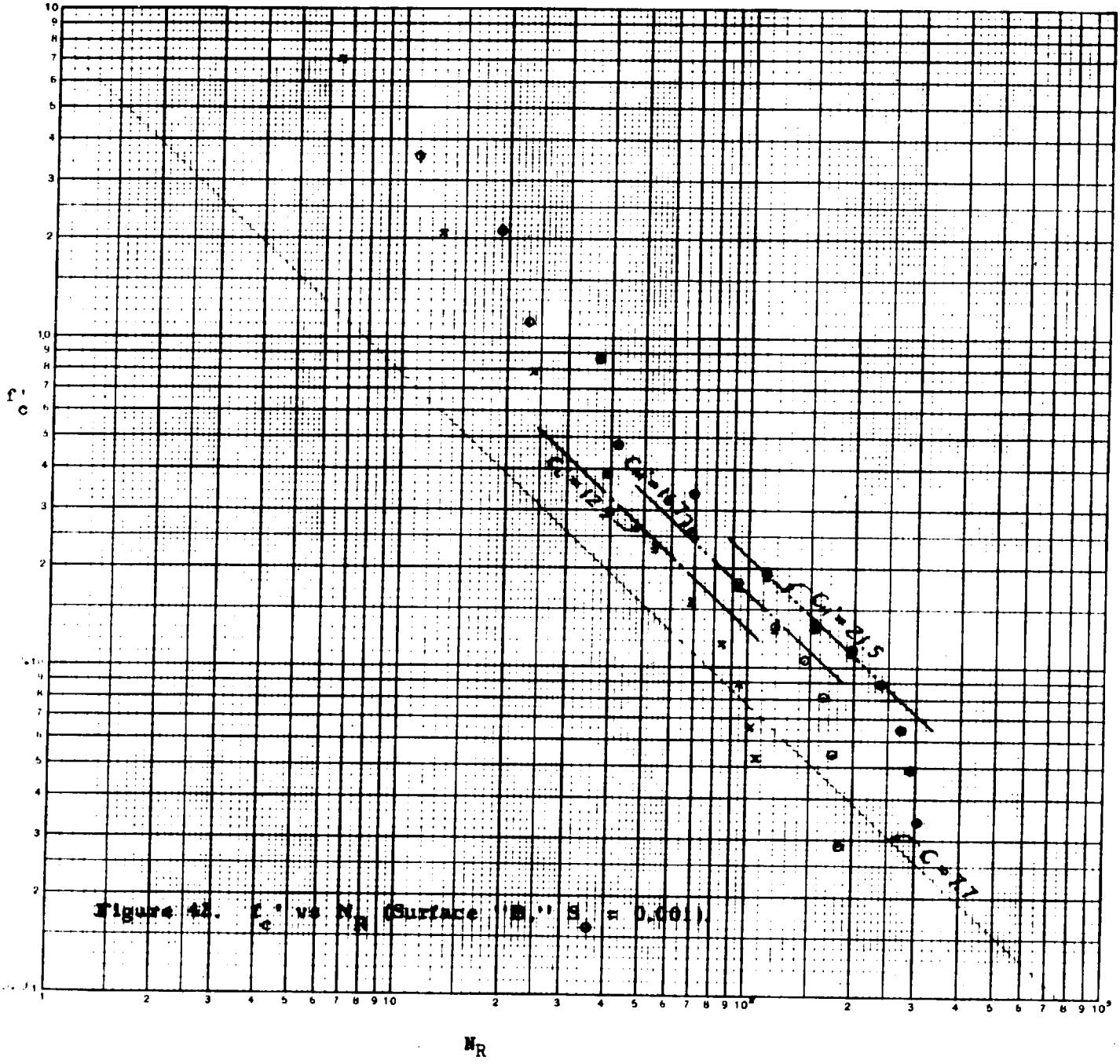
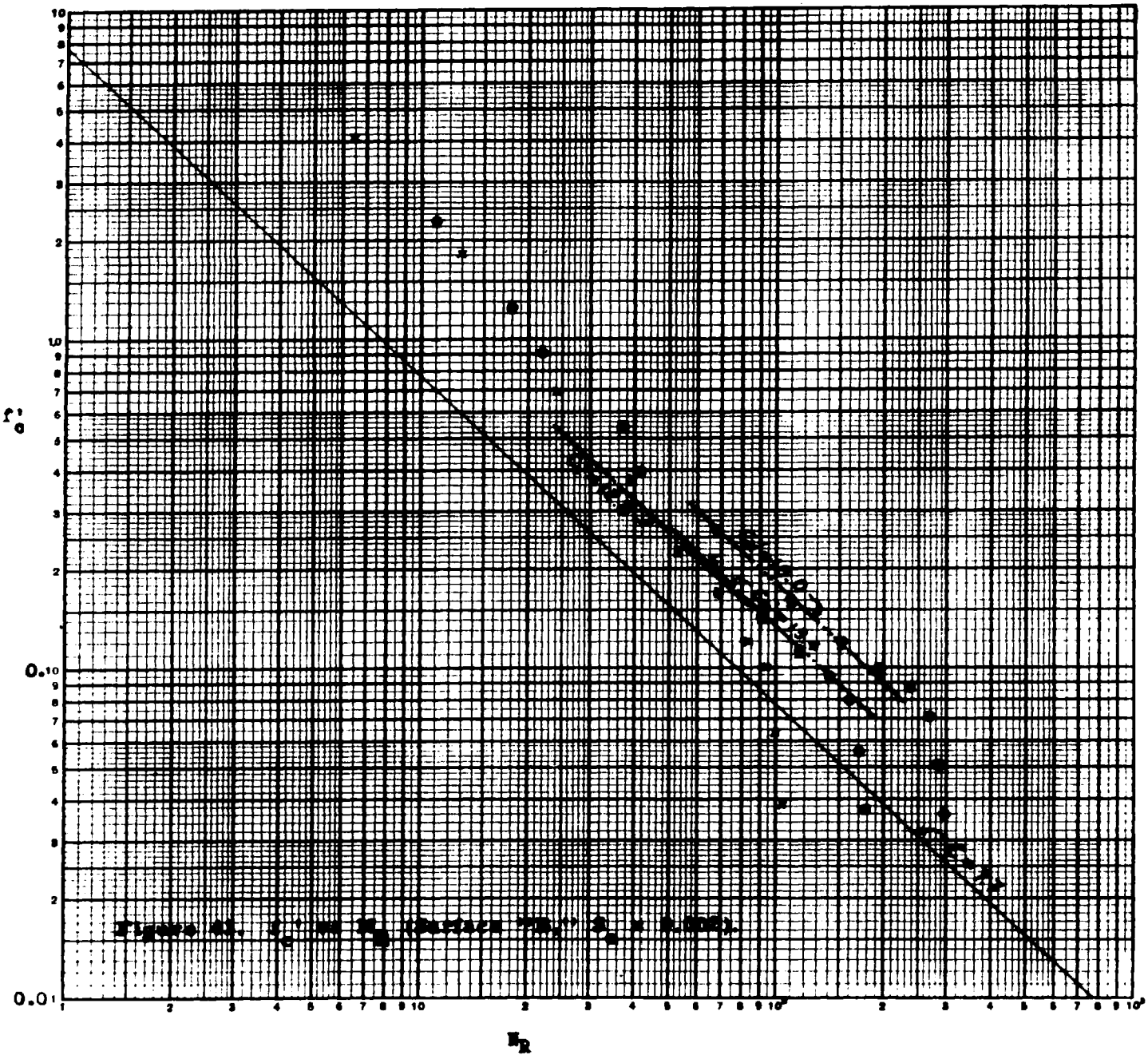


Figure 42. f_c' vs N_R (Surface "B," S_r = 0.001)


f'_a
R_R
0.01
0.10

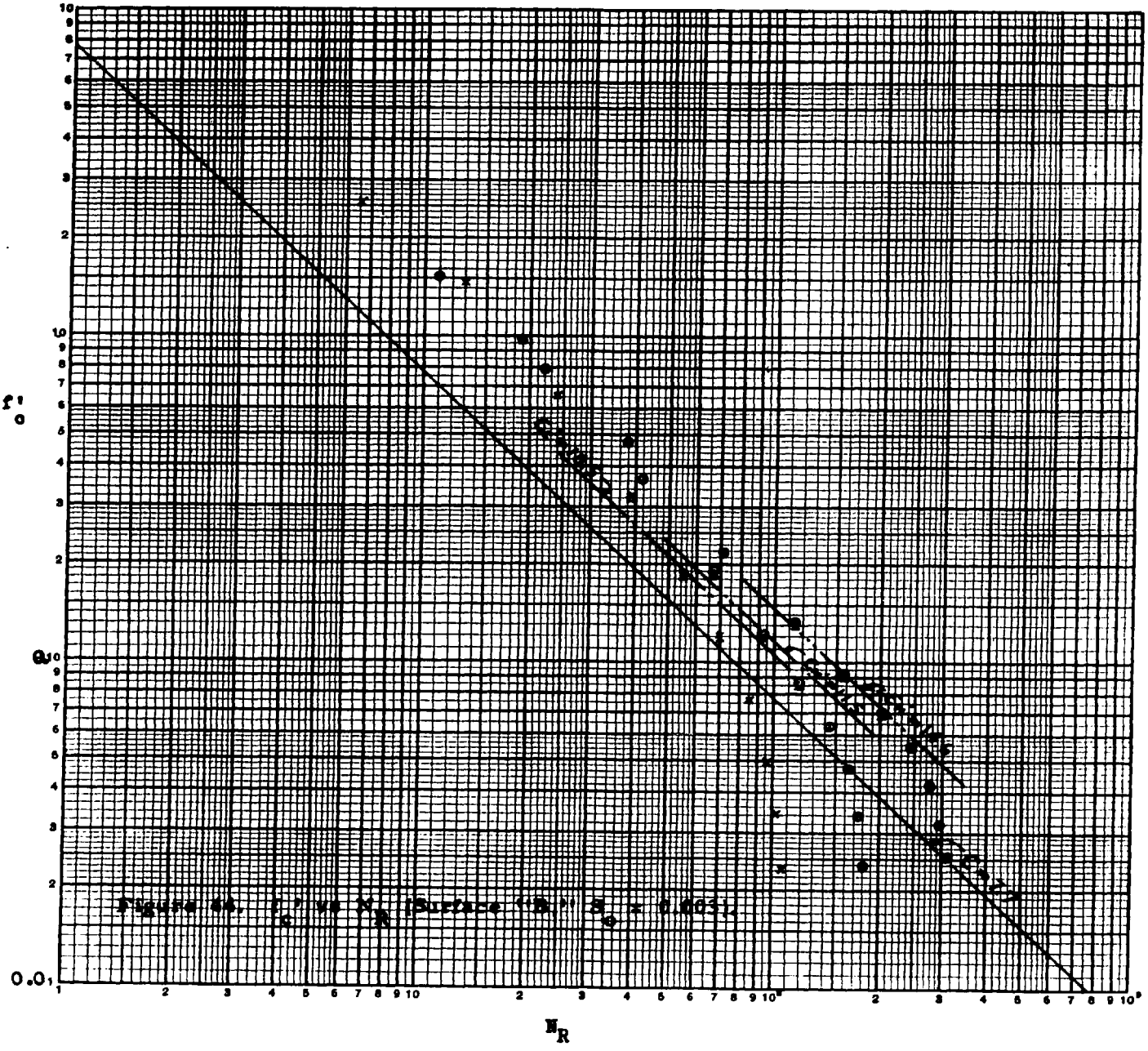


Figure 44. f'_o vs N_R (Surface "B", $N_{Re_\theta} \approx 0.6 \times 10^6$)

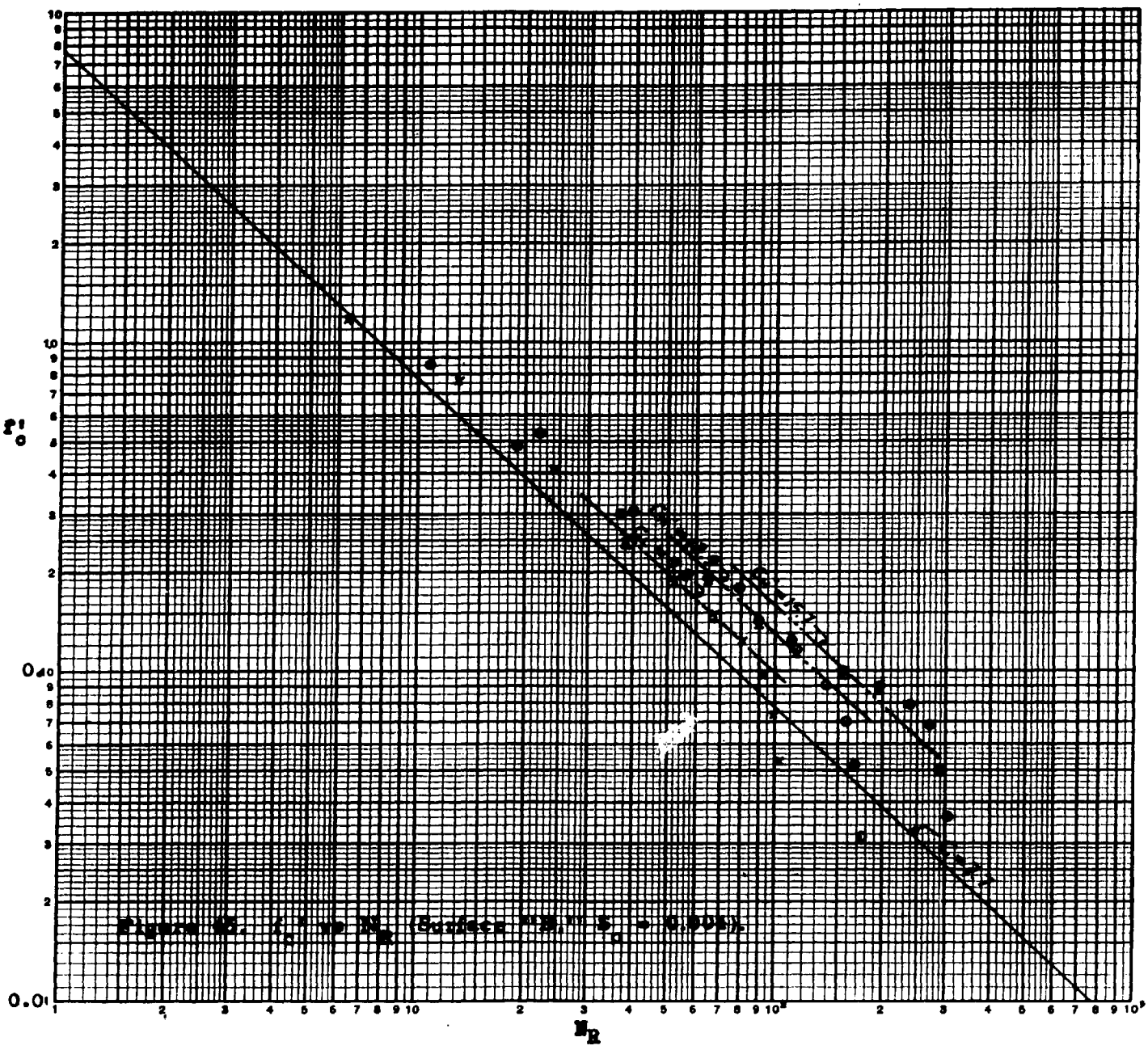


Figure 45: f'_c vs N_R (Surface "B", $\bar{s}_a$ = 0.005)

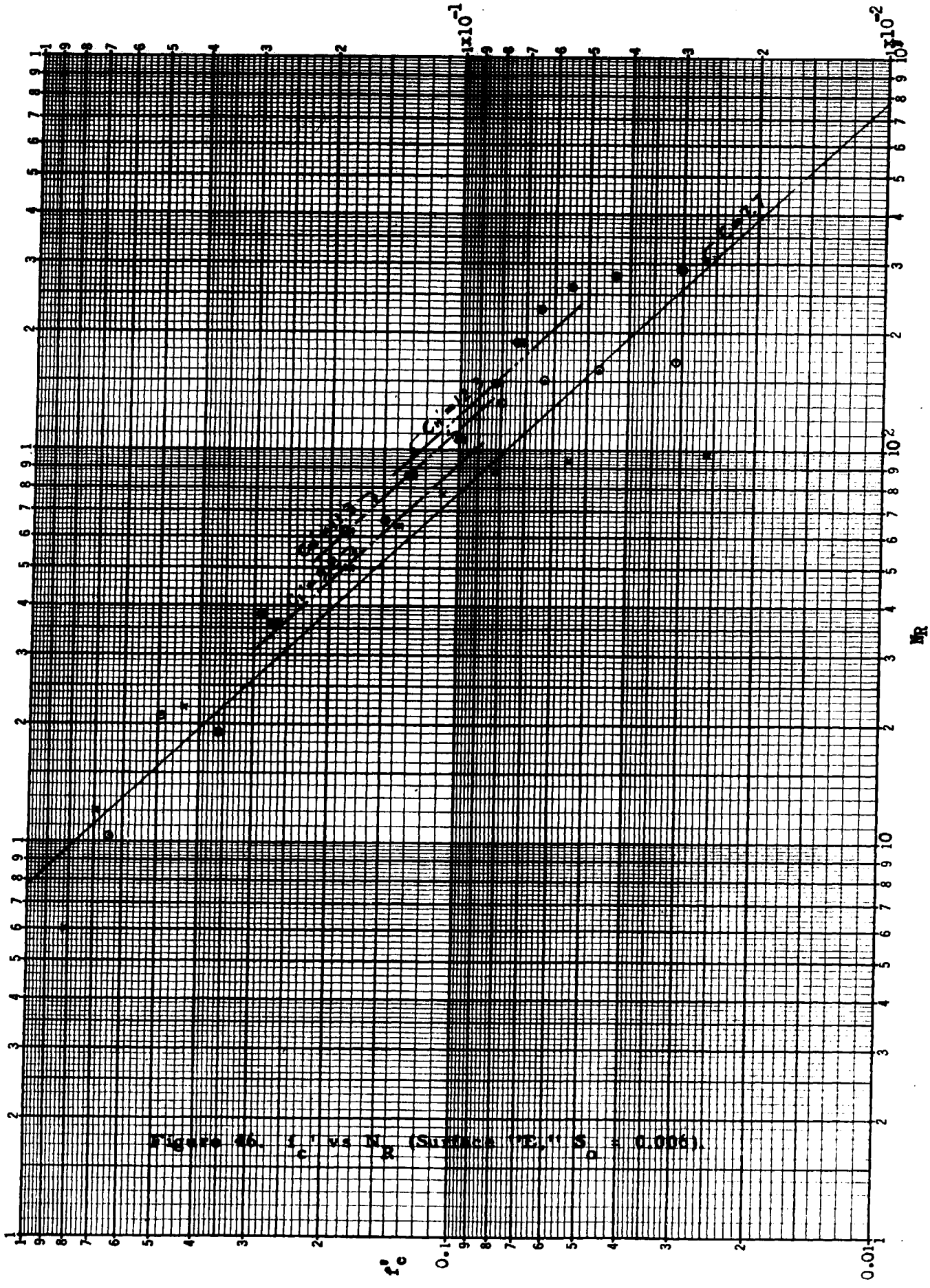


Figure 46. f'_c vs N_R (Surface "E," S_D = 0.006).

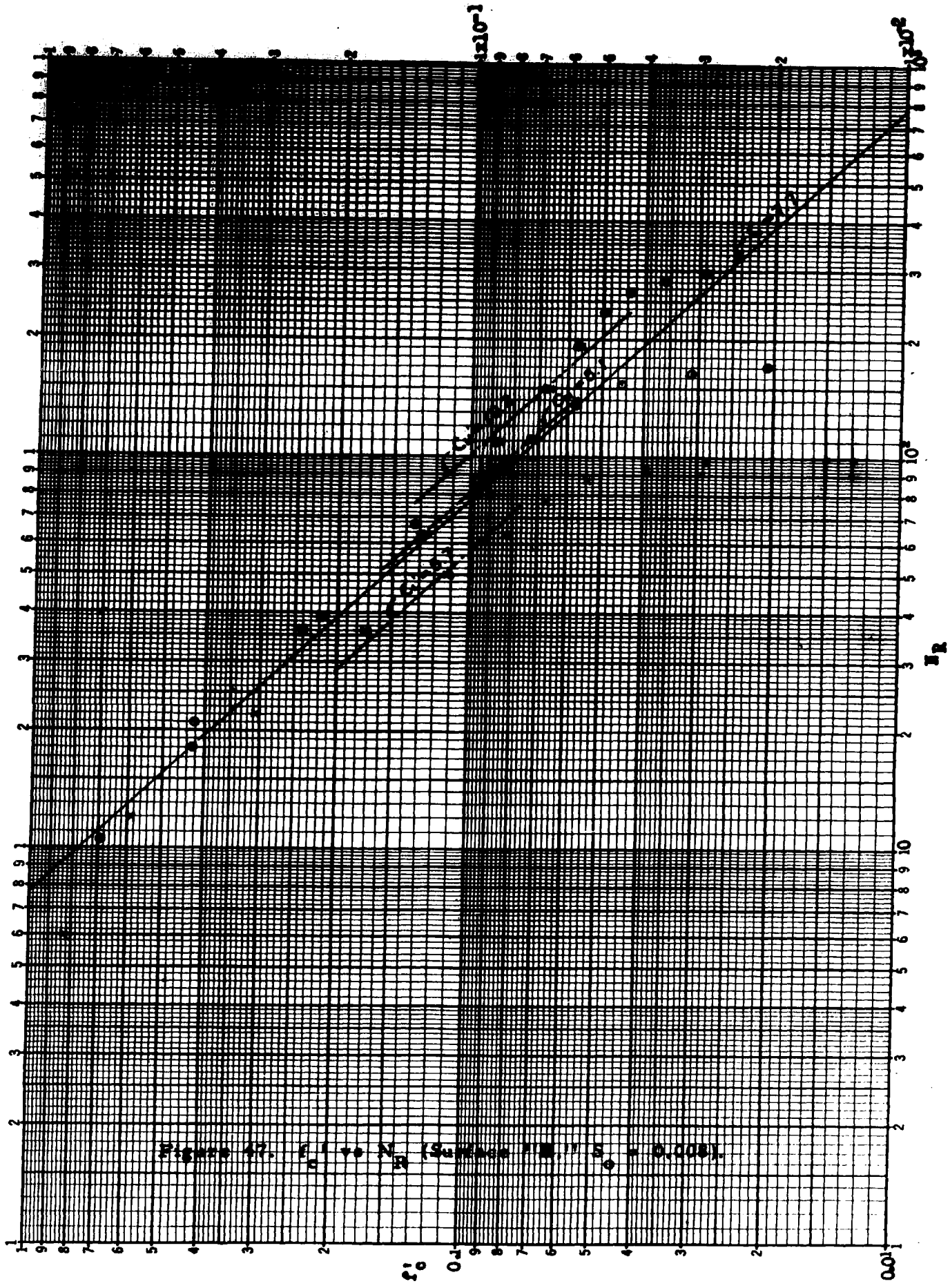


Figure 47. f_c' vs N_R (Surface "B", S_ϕ = 0.008).

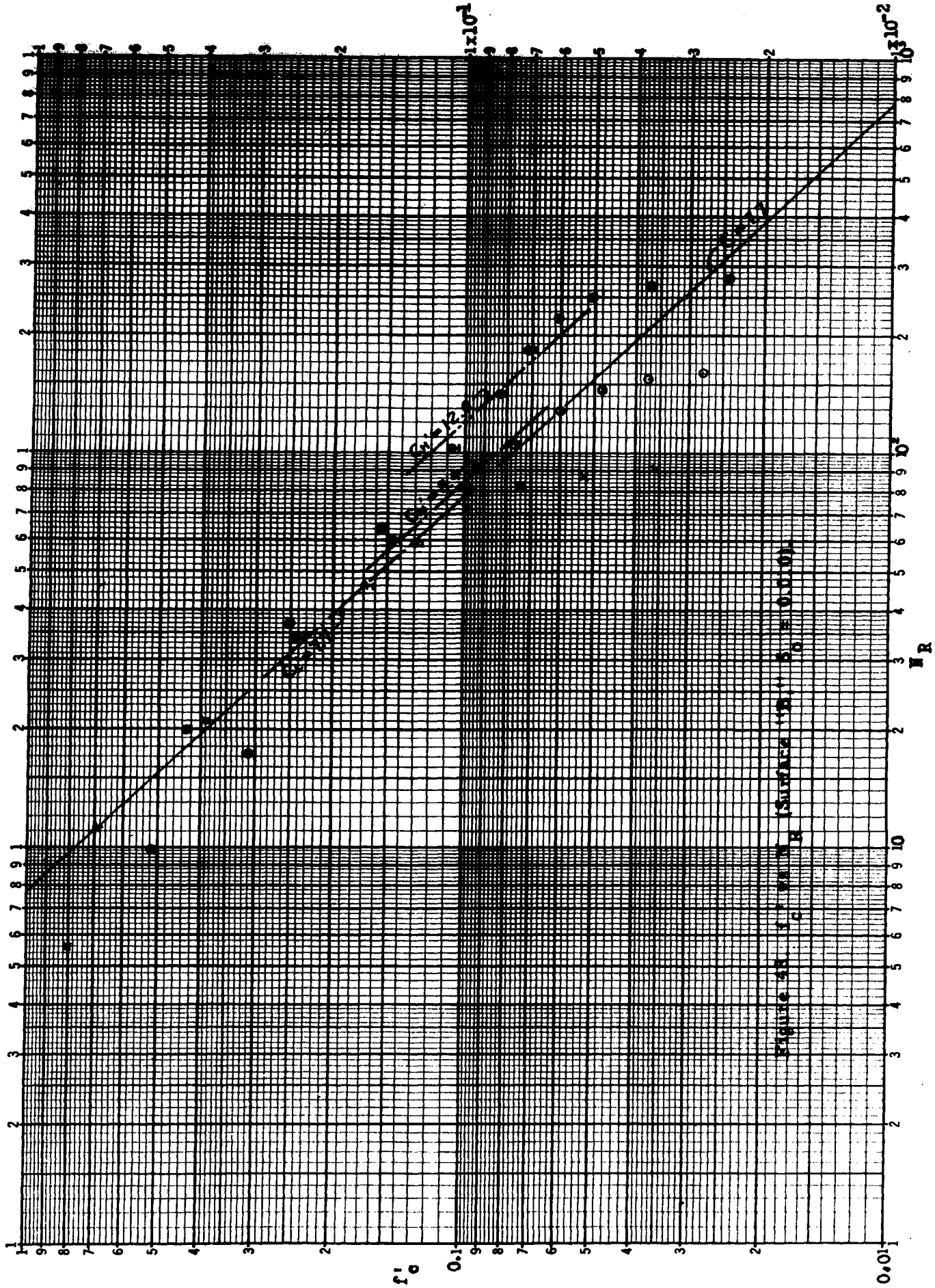


Figure 48. f'_o vs N_R Isentropic, $\gamma_o = 0.01$

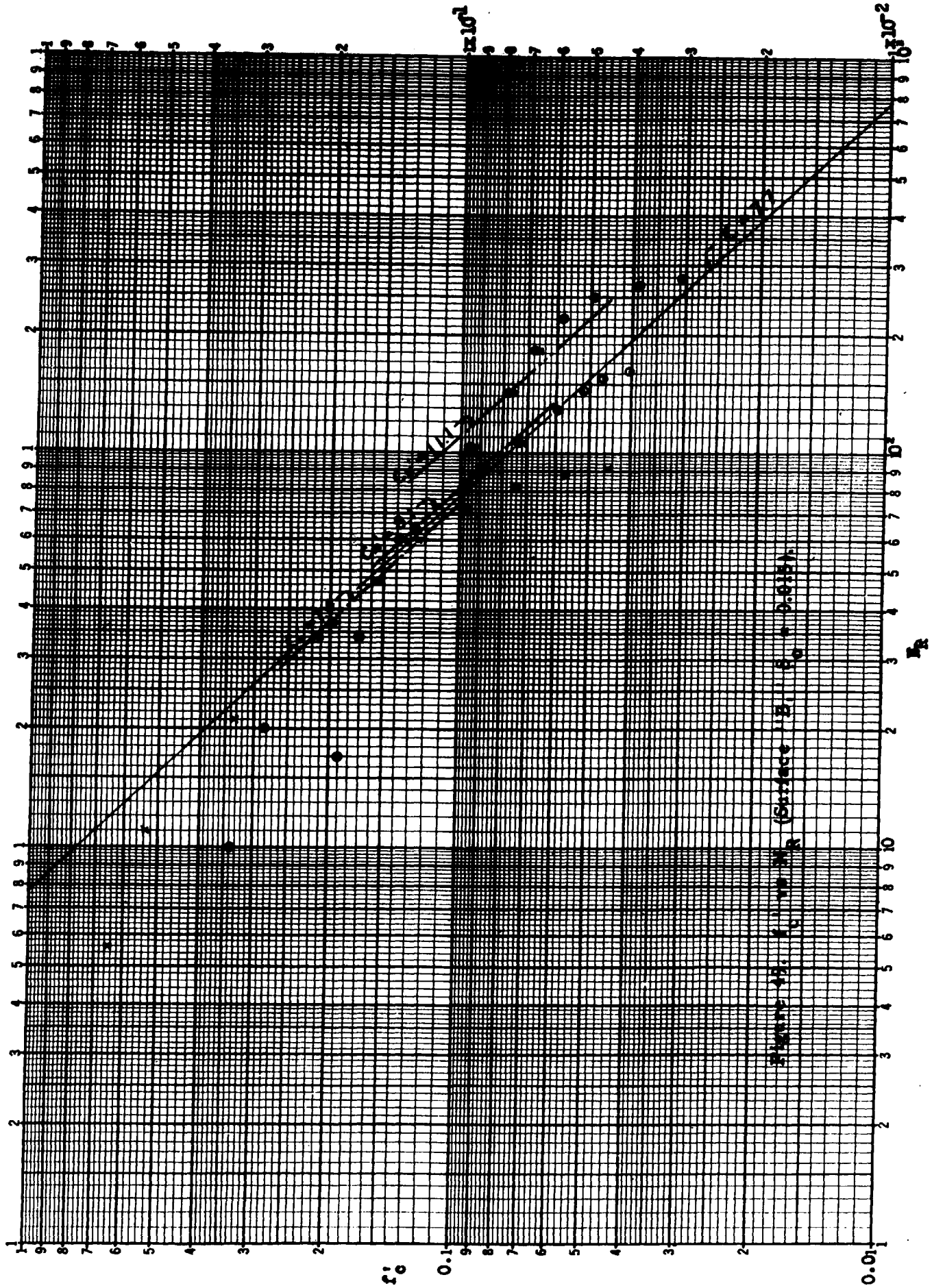


Figure 44. f'_c vs F_R (Surface - B, C, D, E, F)

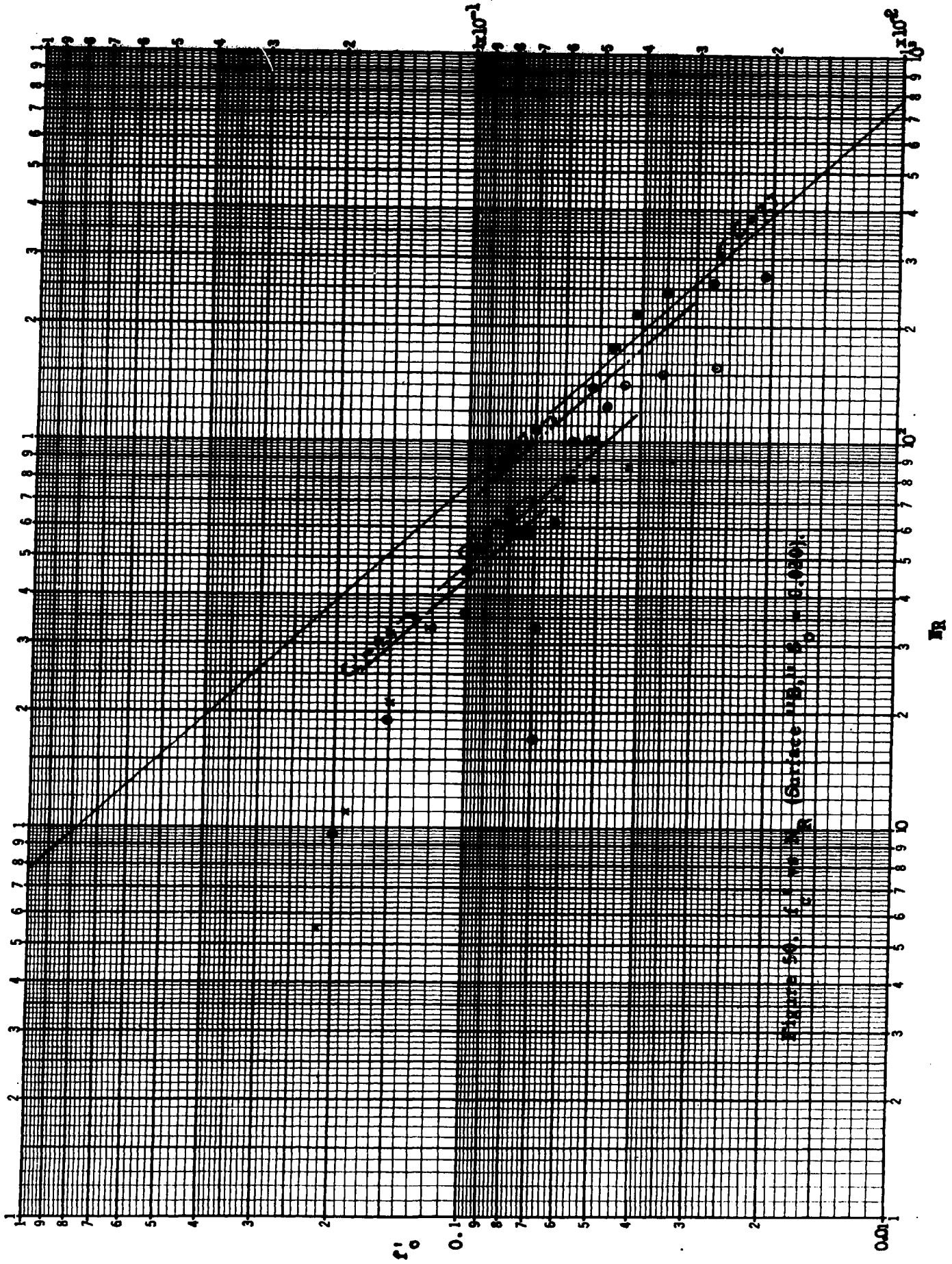


Figure 54. f'_o vs N_R (Surface tension, ϕ_p = 0.00).

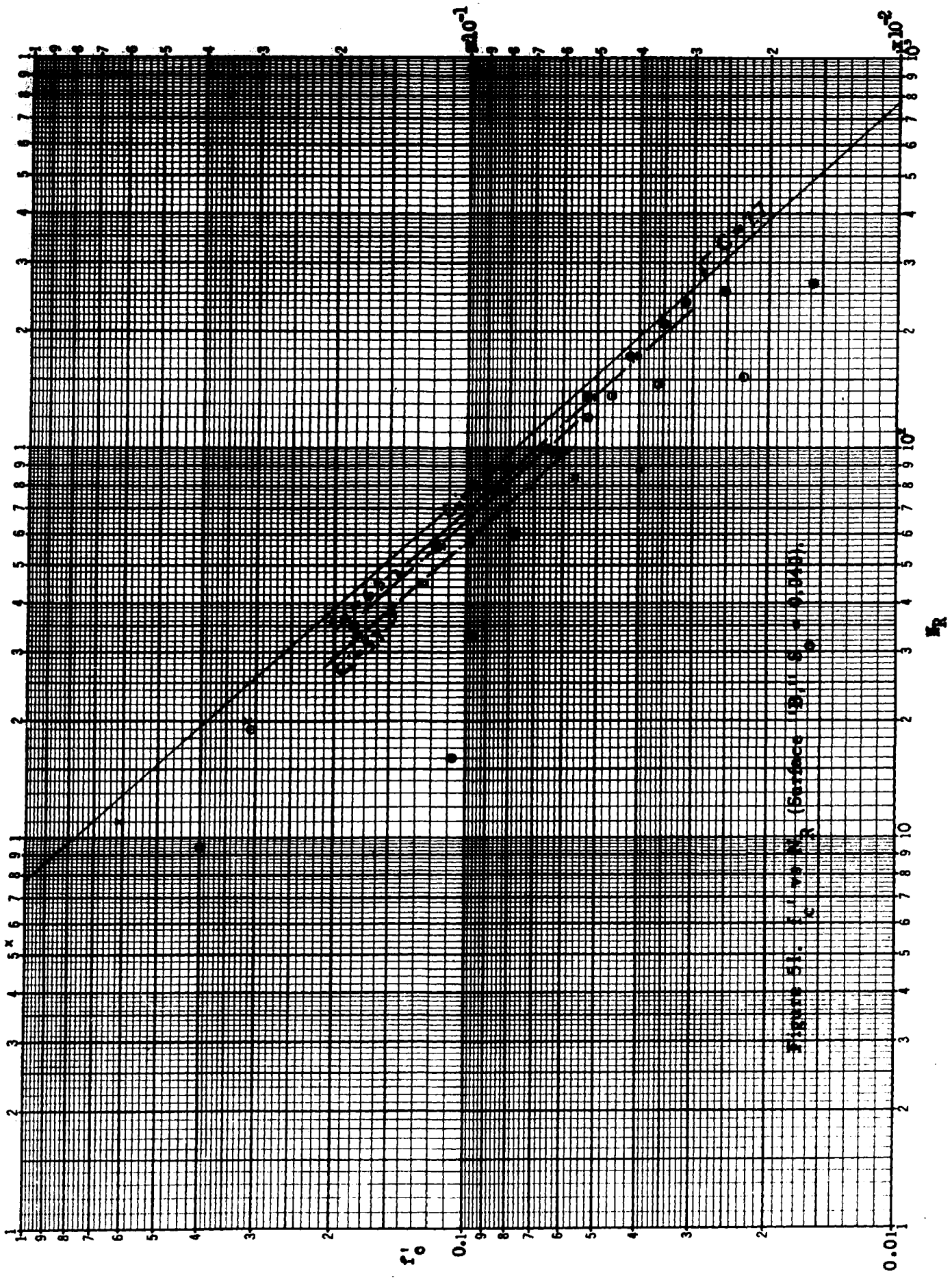


Figure 5.11. f'_o vs N_R (Surface $(B_{r'})_{max}$ = 0.040).

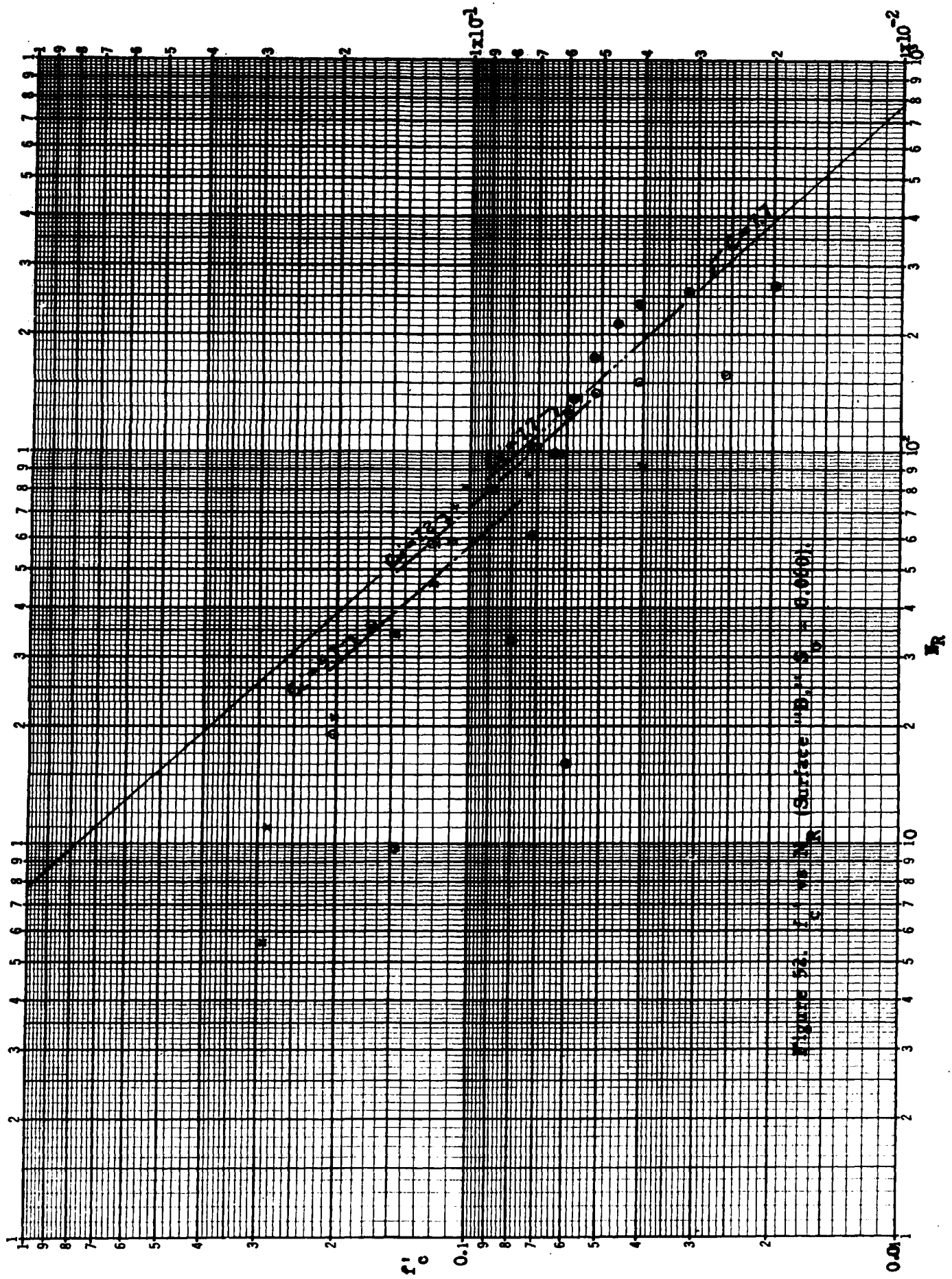


Figure 52. f'_c vs K_R (Surface "D", $\beta_D = 0.001$)

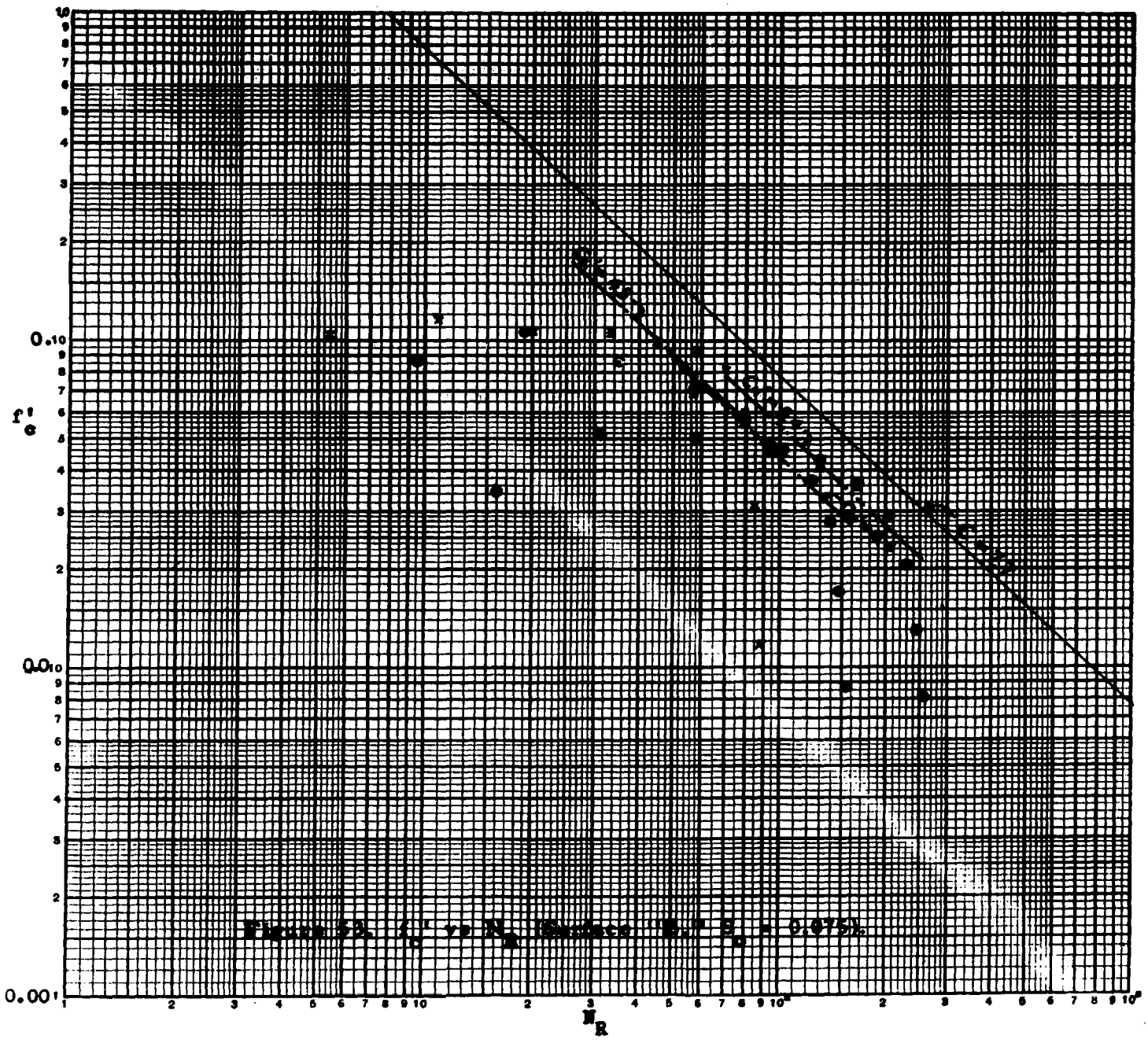
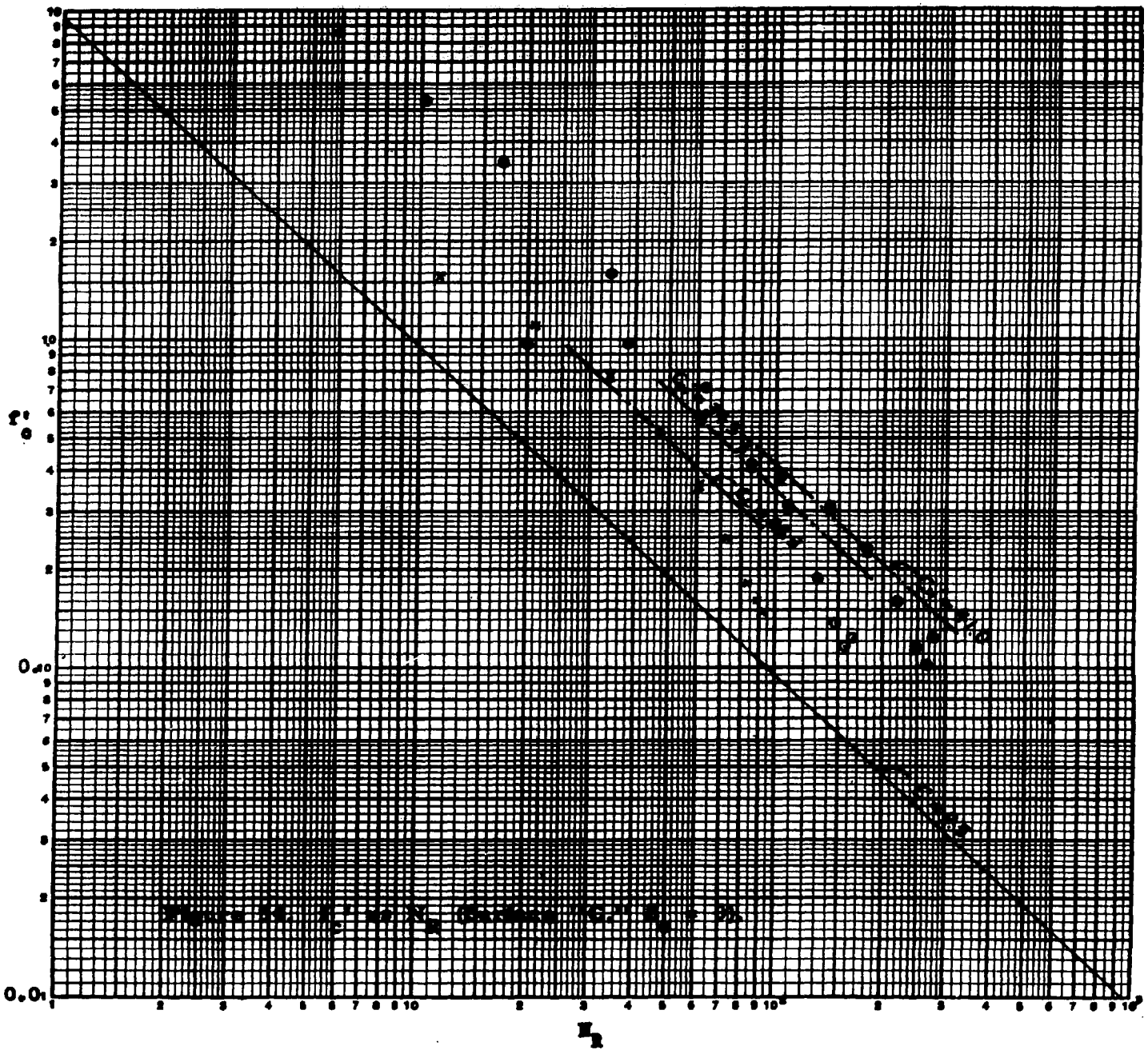
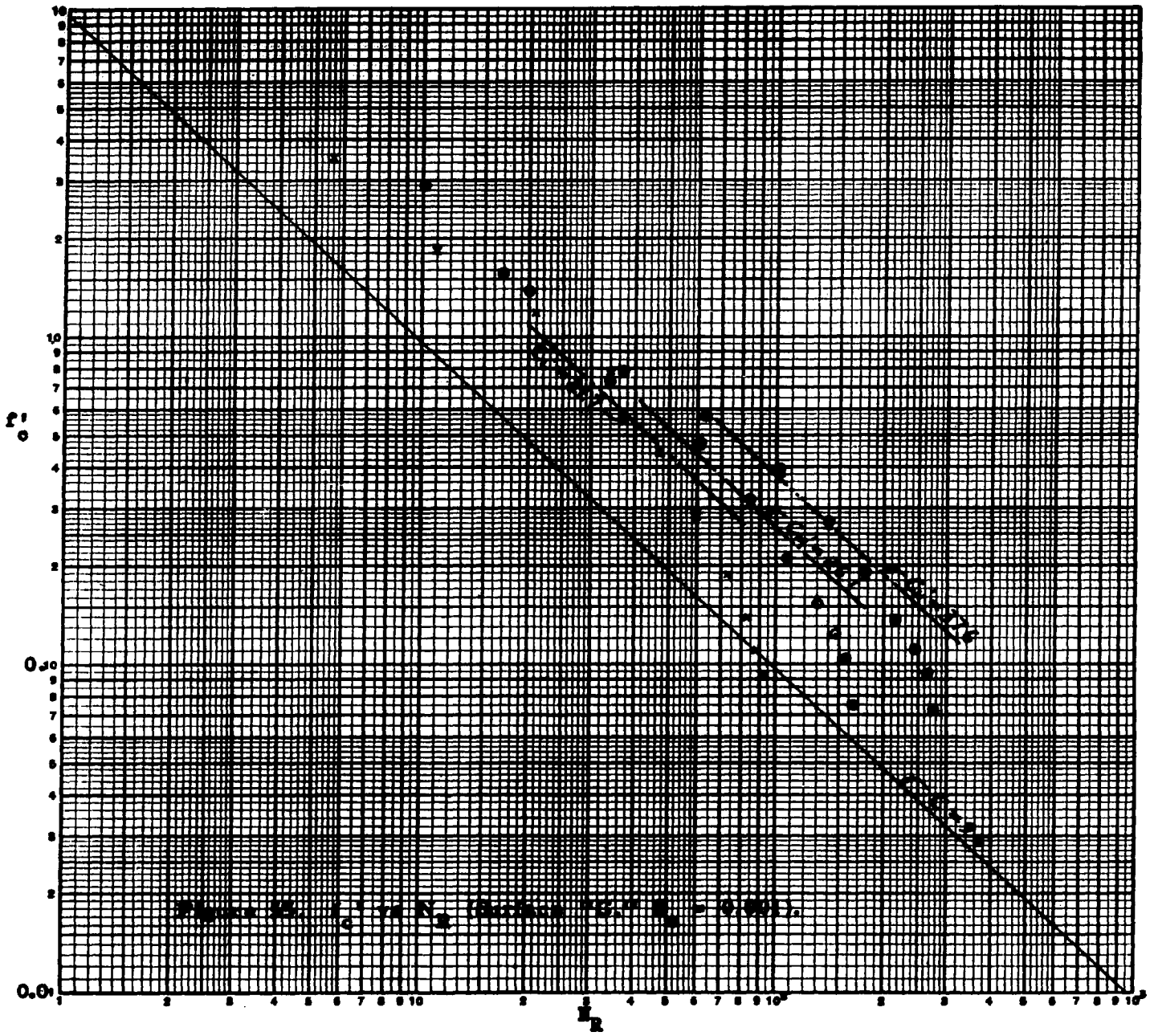
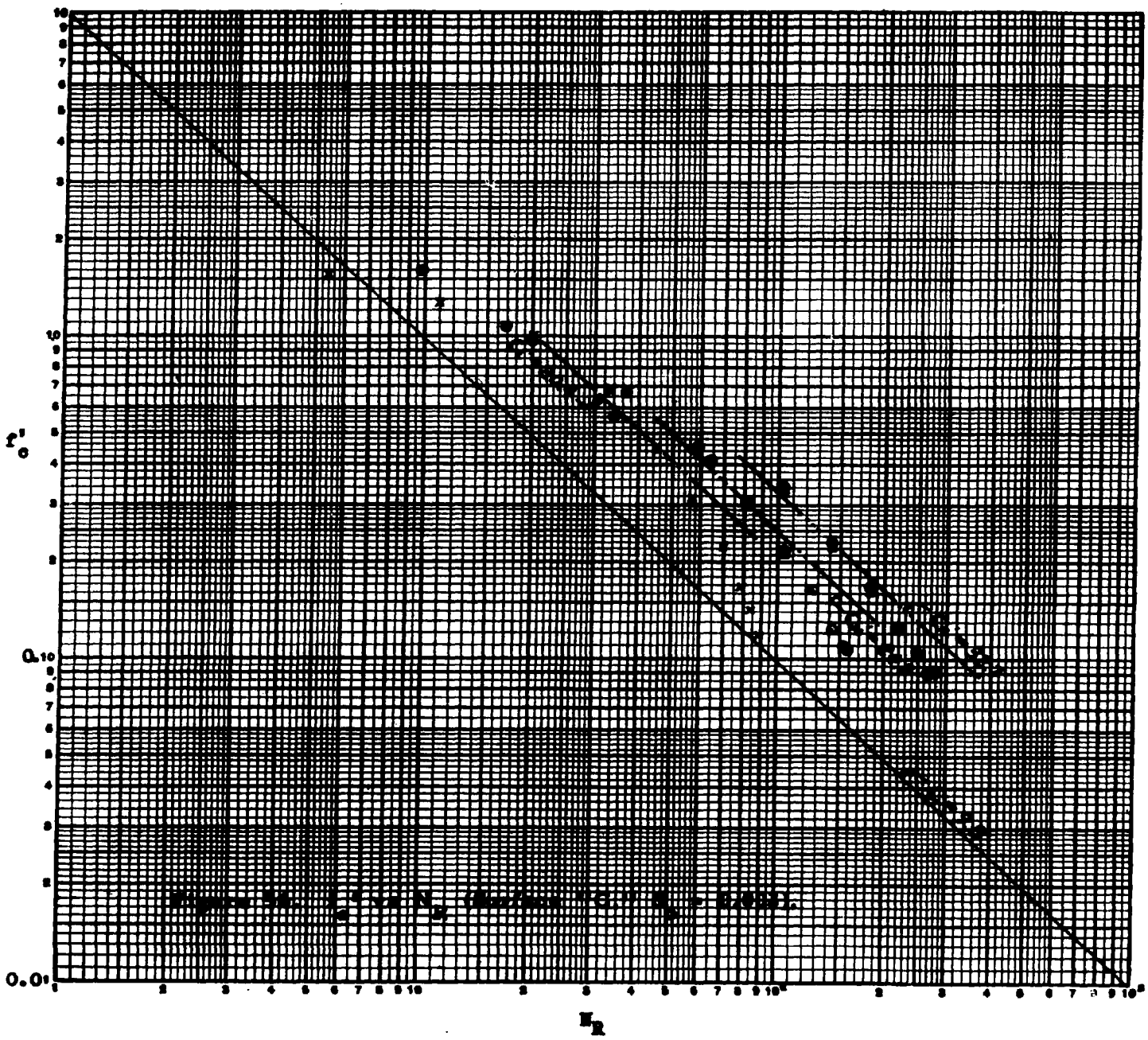
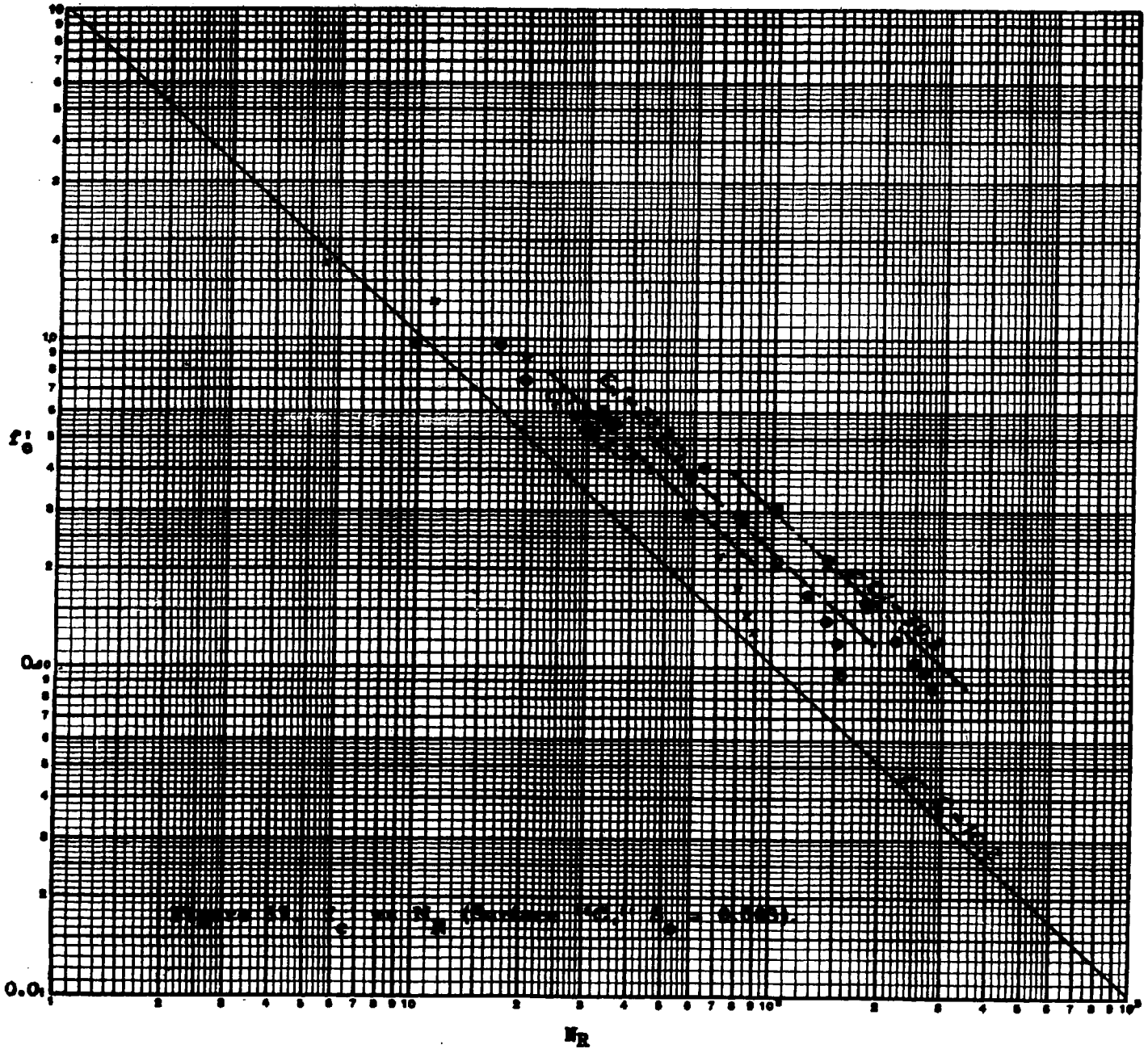


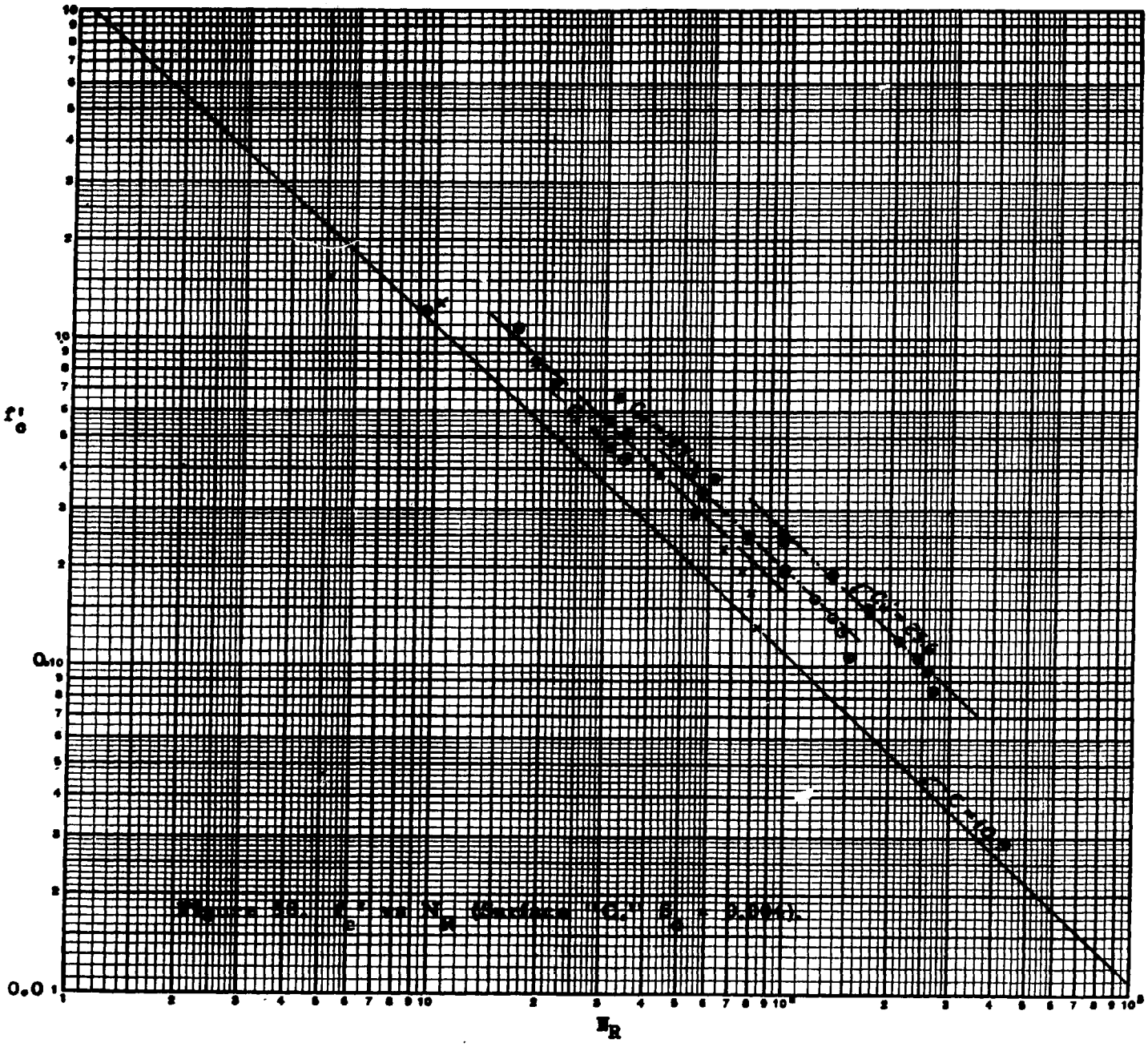
Figure 52. f'_c vs N_R (Surface R_a = 0.075)




f'_c
N_R


f'_o
N_R
0.01


f'_0
0.01
R_R


f'_0
Q_{10}
0.0
N_R

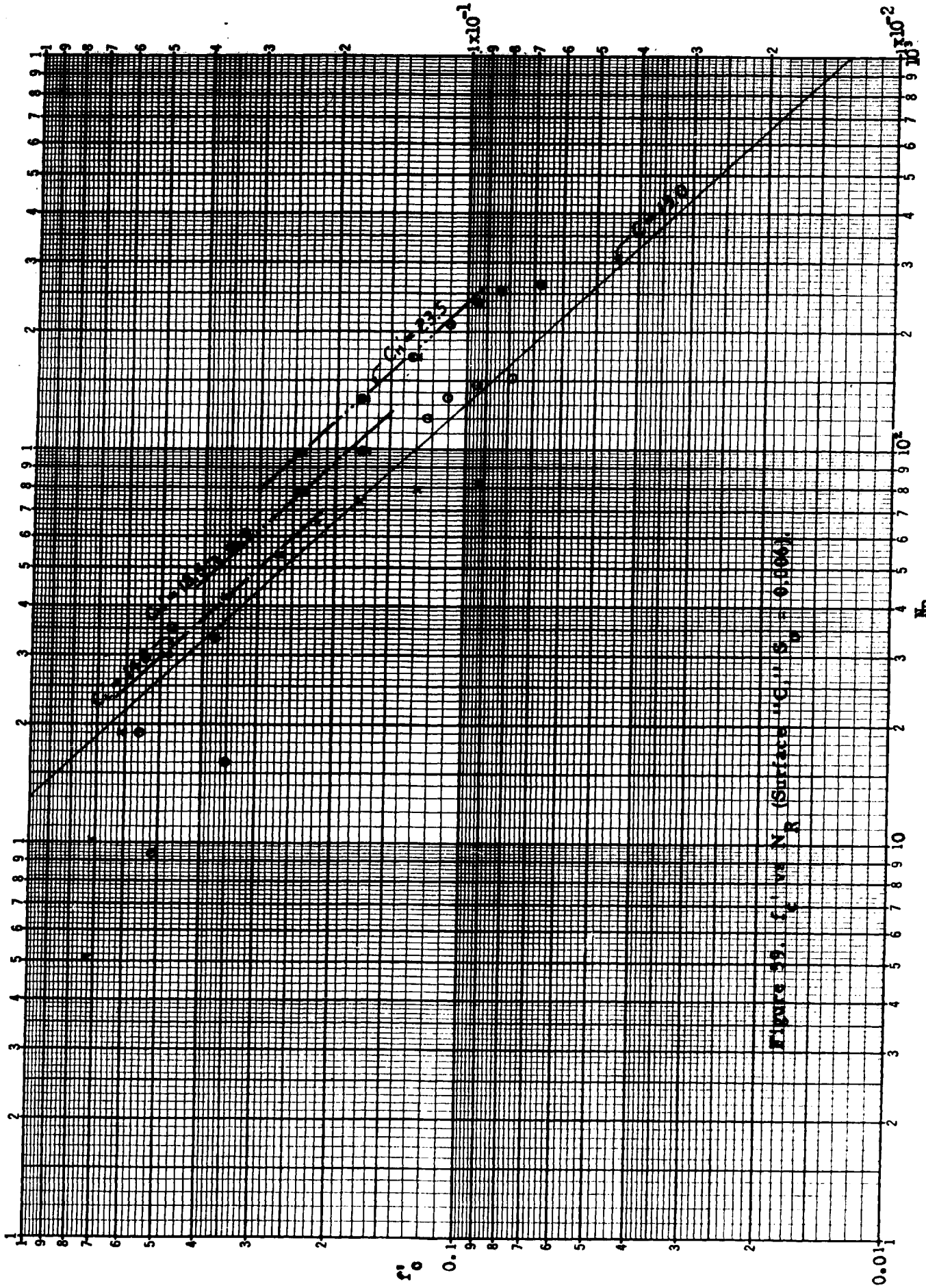


Figure 59. f_o vs N_R (Surface "C", $S_o = 0.0001$)

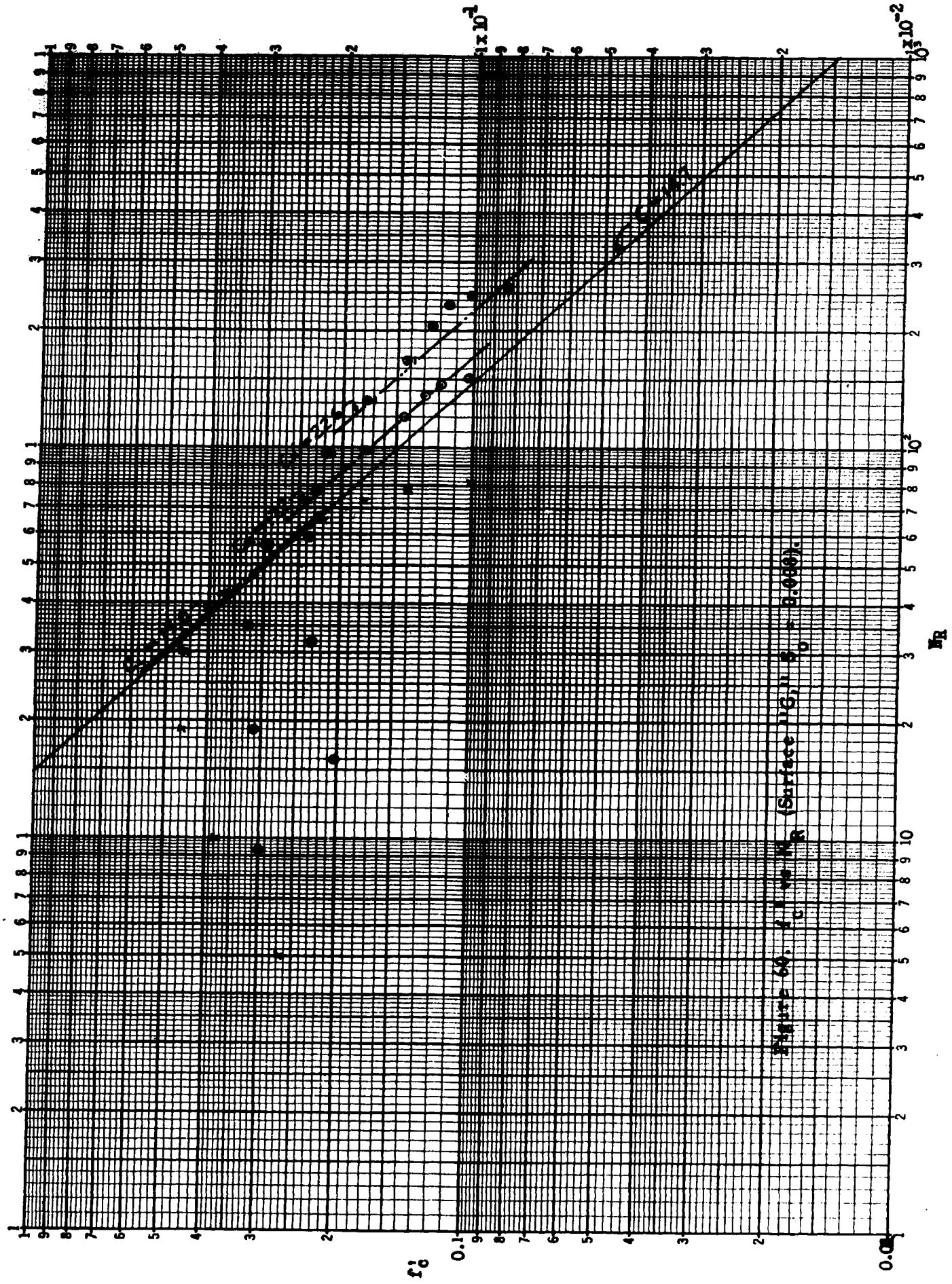


Figure 60. f'_c vs N_R (Surface 116, ϕ_o = 0.000)

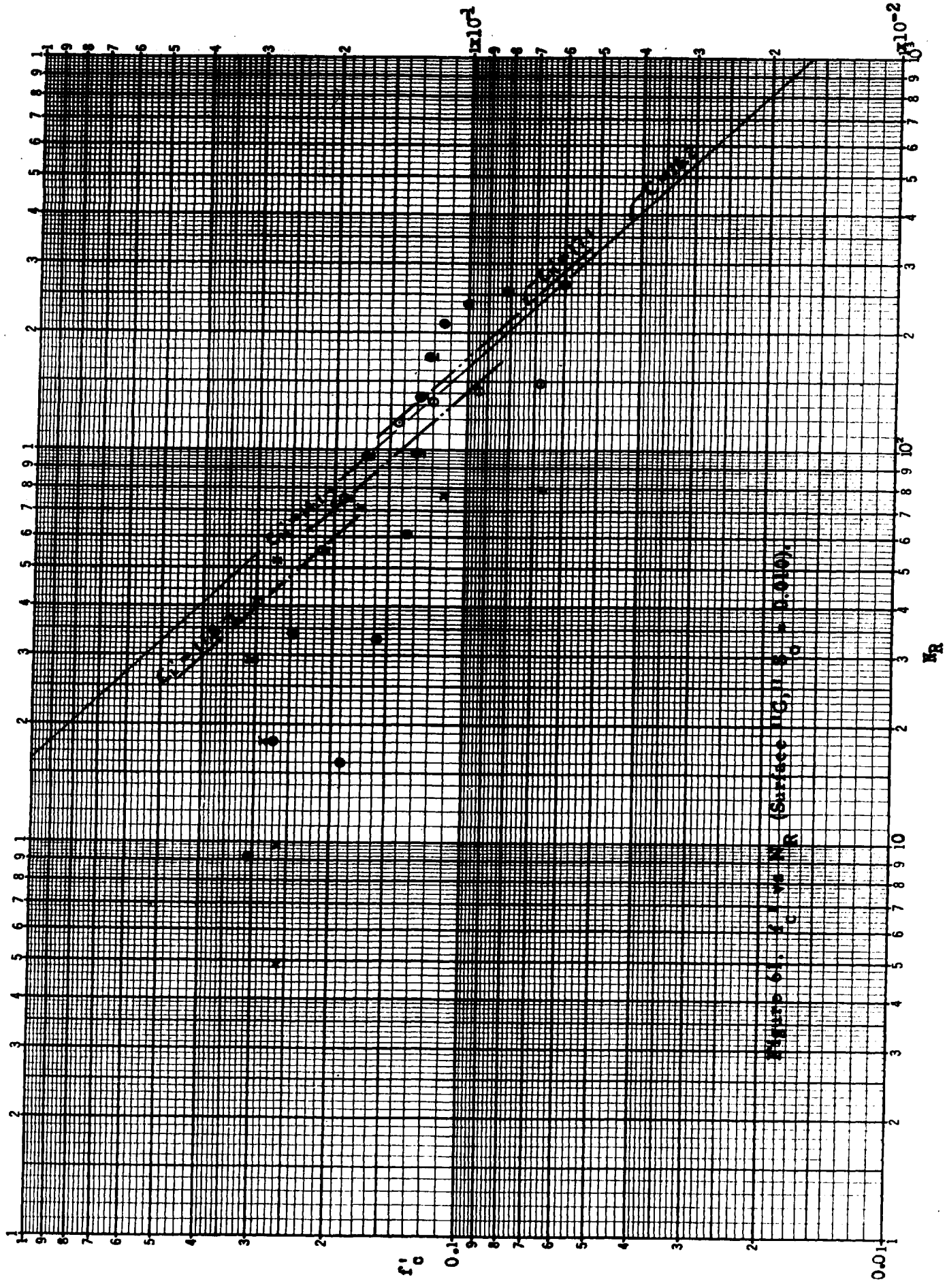


Figure 61. f'_o vs N_R (Surface 11, ϕ_o = 0.010)

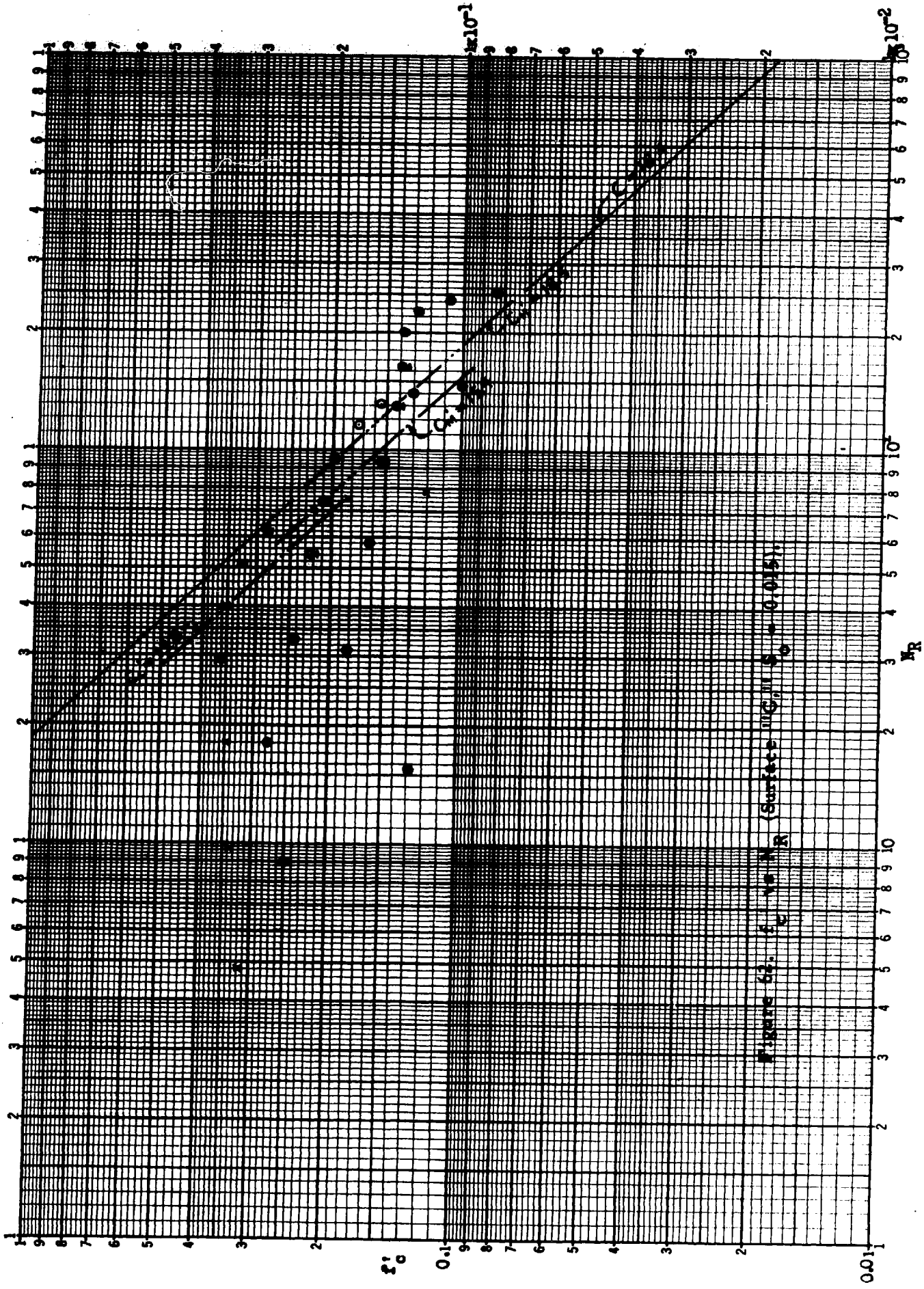


Figure 62. f'_o vs N_R (Surface $\overline{G'_{11}}$ Φ = 0.015)

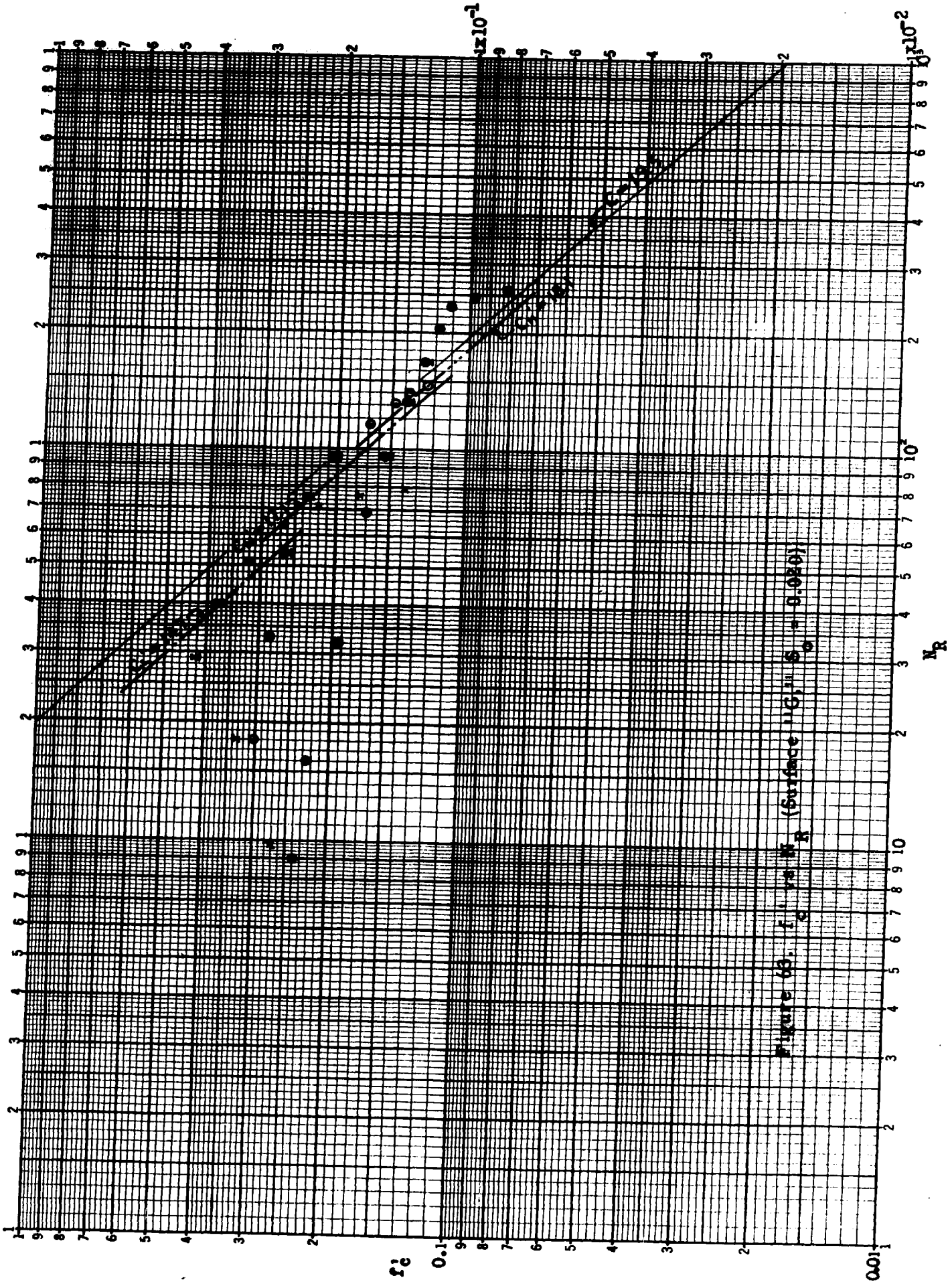


Figure 69. f_c vs N_R (Surface #6, ϕ = 0.0801)

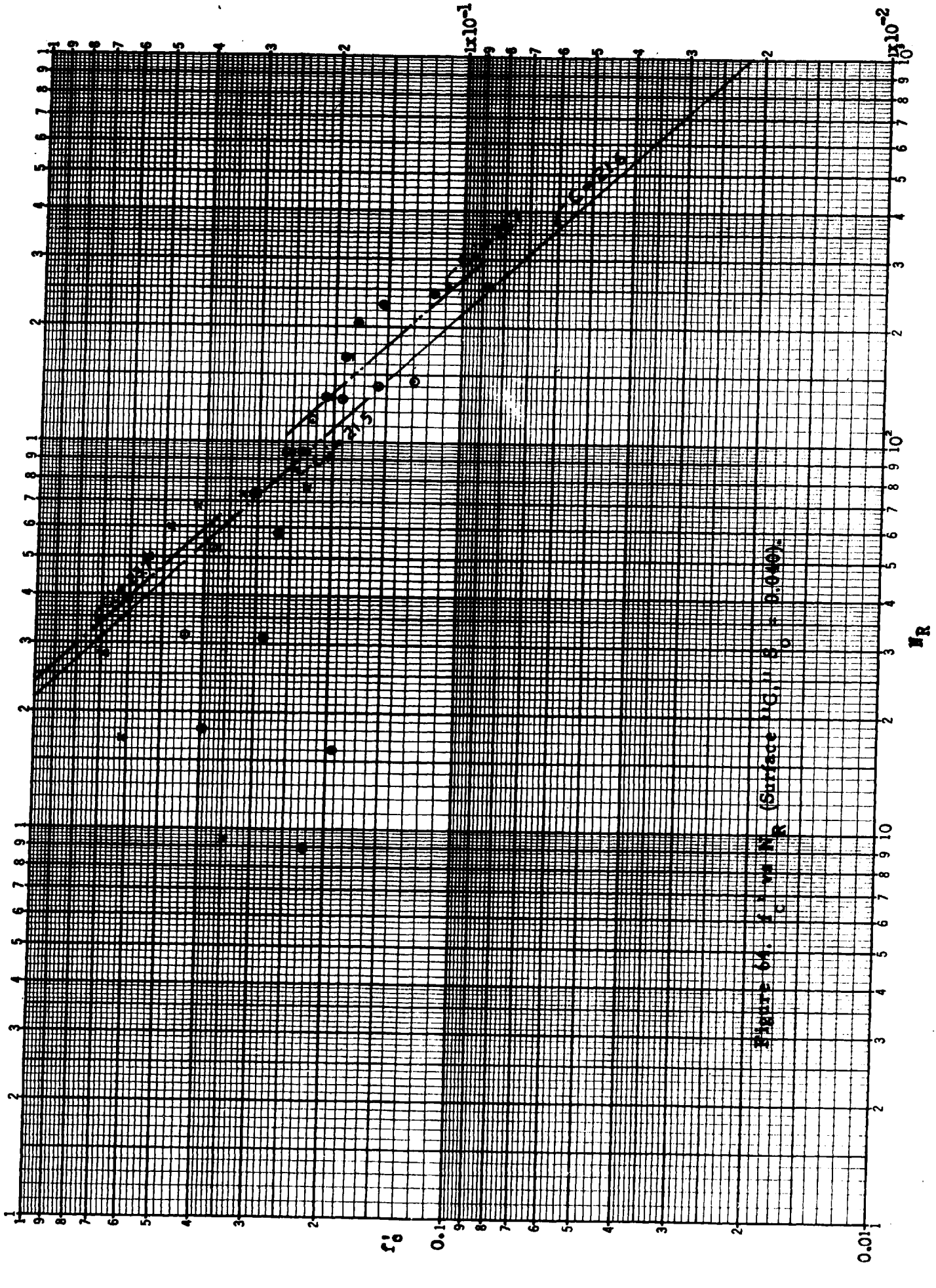
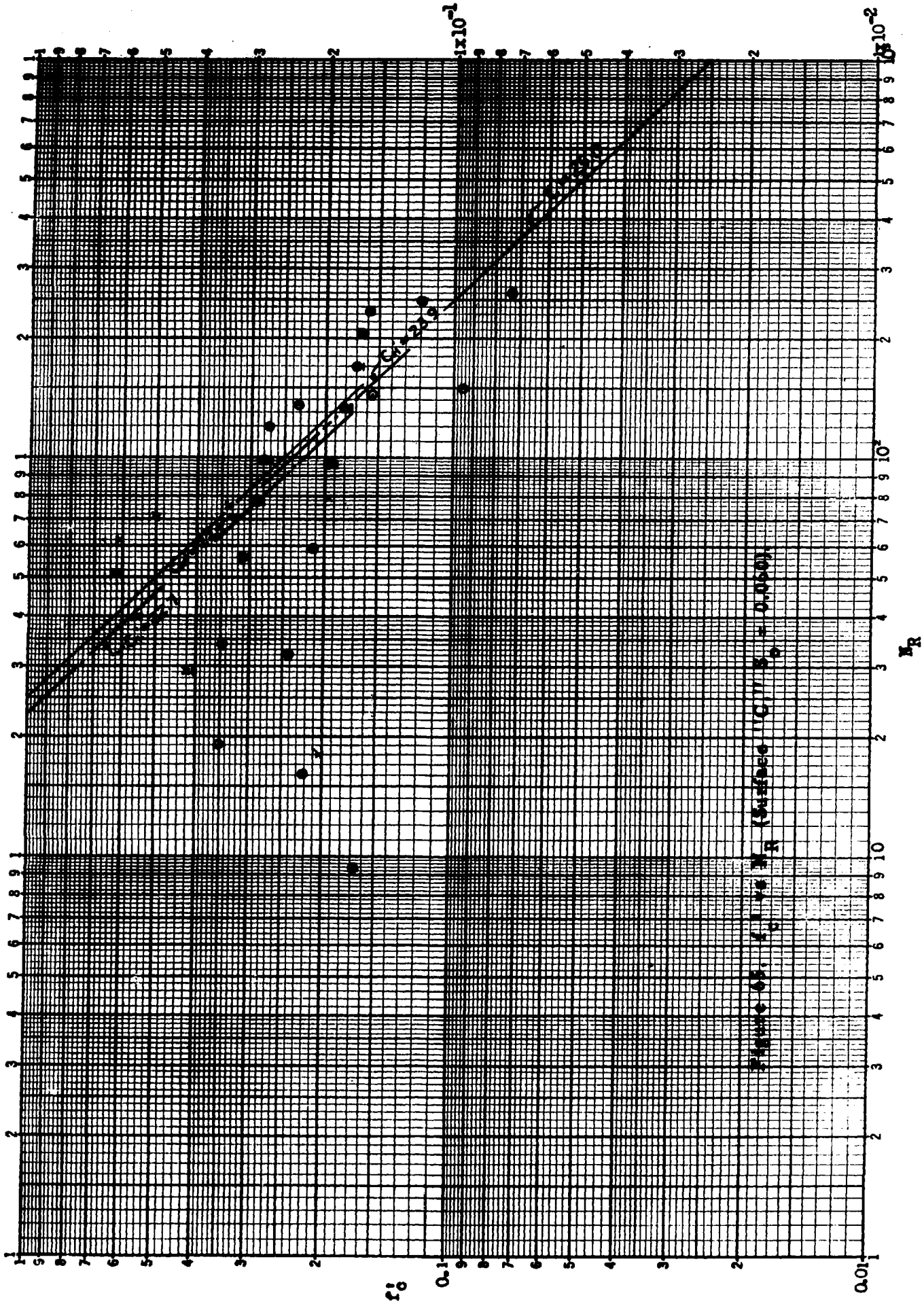


FIGURE 64. f'_o VS N_R (Surface 1G, θ_o = 0.040).


1×10^{-1}
1×10^{-2}
10^{-2}
K_R
f_o
0.1
0.01
$C_f = 2.2 \times 10^{-3}$
$C_f = 2.0 \times 10^{-3}$
$C_f = 1.8 \times 10^{-3}$
$C_f = 1.6 \times 10^{-3}$
$C_f = 1.4 \times 10^{-3}$
$C_f = 1.2 \times 10^{-3}$
$C_f = 1.0 \times 10^{-3}$
$C_f = 0.8 \times 10^{-3}$
$C_f = 0.6 \times 10^{-3}$
$C_f = 0.4 \times 10^{-3}$
$C_f = 0.2 \times 10^{-3}$
$C_f = 0.0 \times 10^{-3}$
Figure 46. f_o vs K_R for $C_f = 0.0001$

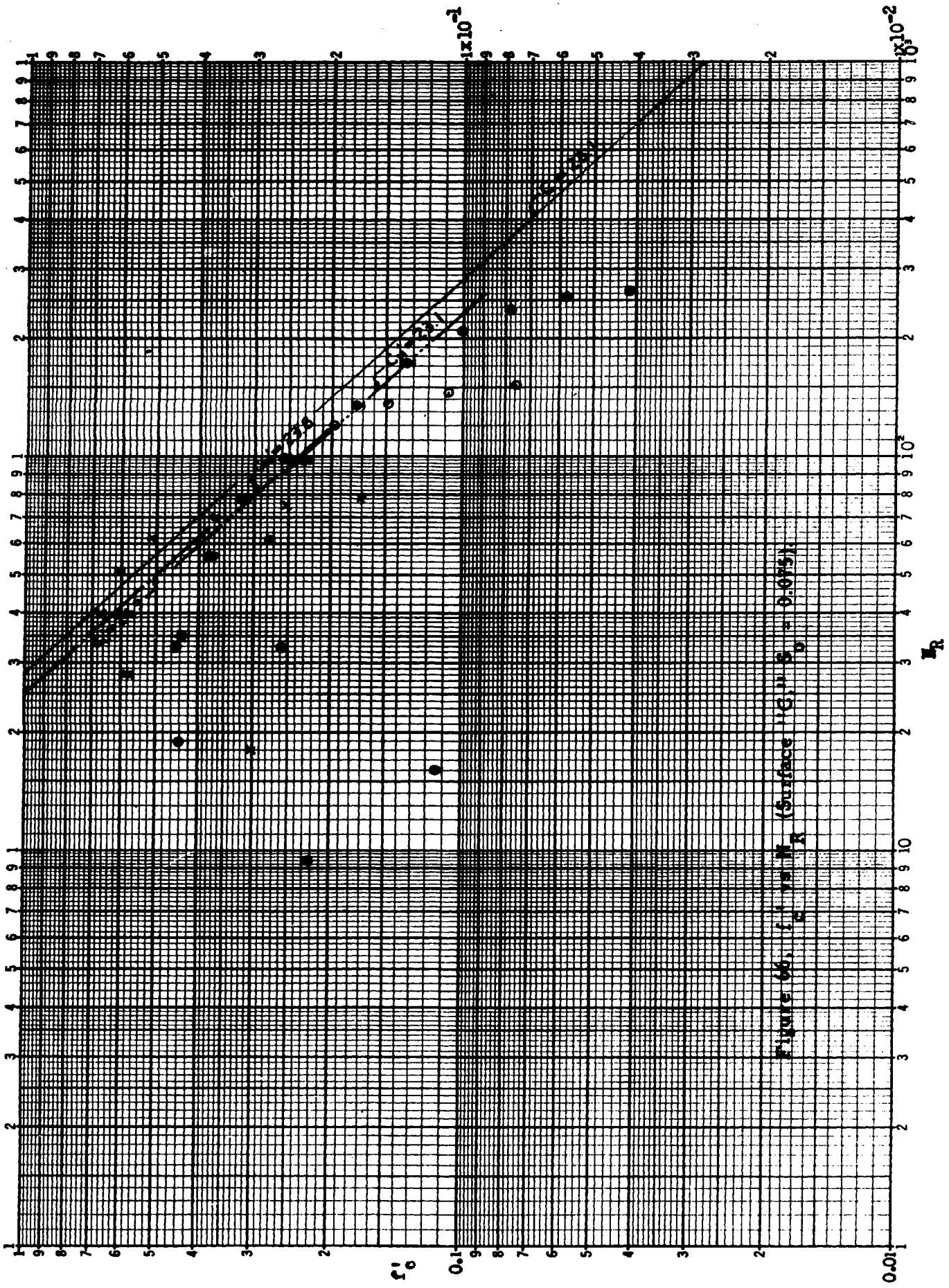


Figure 66. f'_o vs N_R (Surface $(C_u, S_u = 0.05)$)

EFFECT OF RAINDROP IMPACT ON COEFFICIENT OF FRICTION

f_c' vs N_R

(condensed)

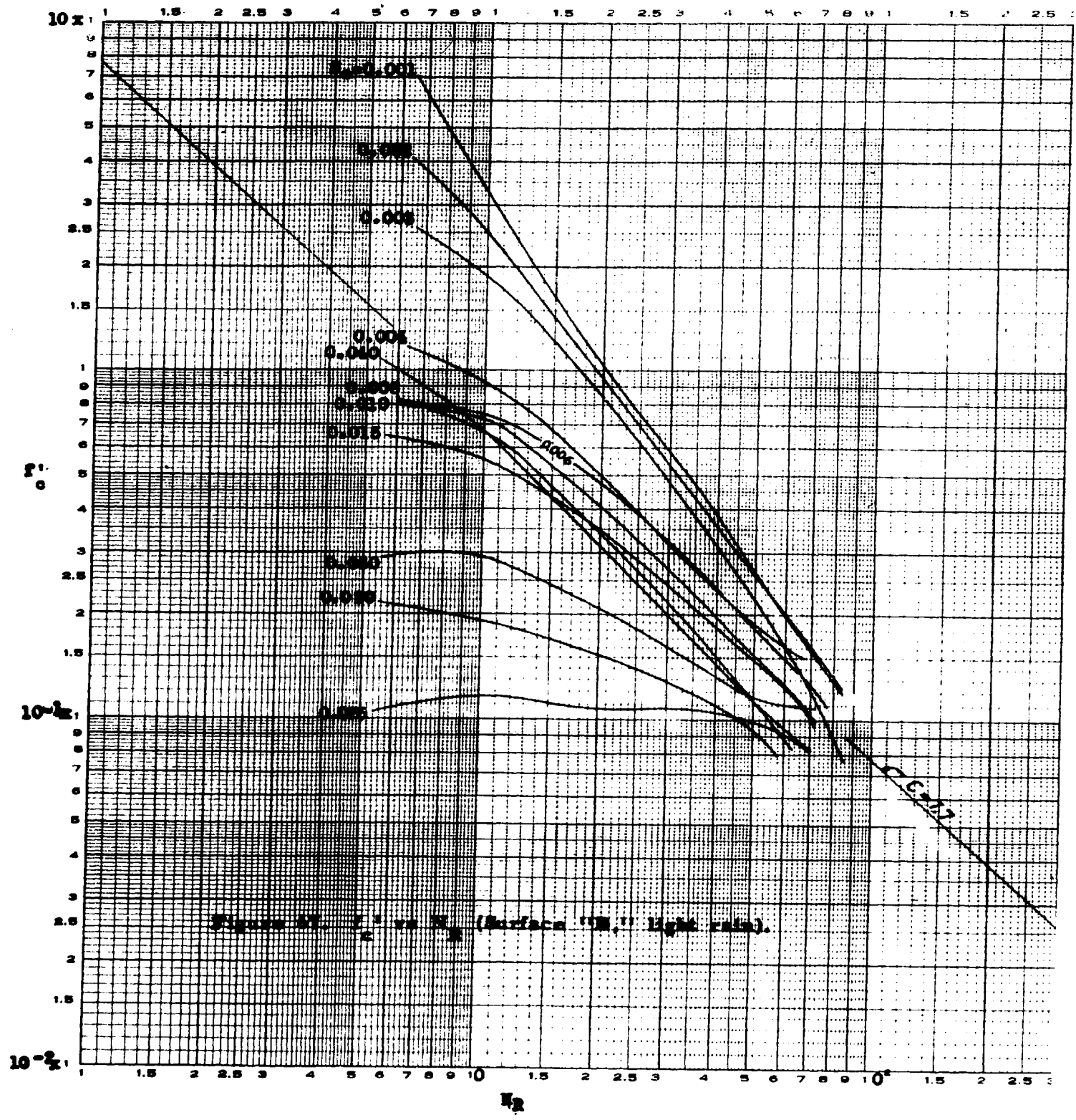


Figure 44. f'_c vs N_R (Surface "B", light rain).

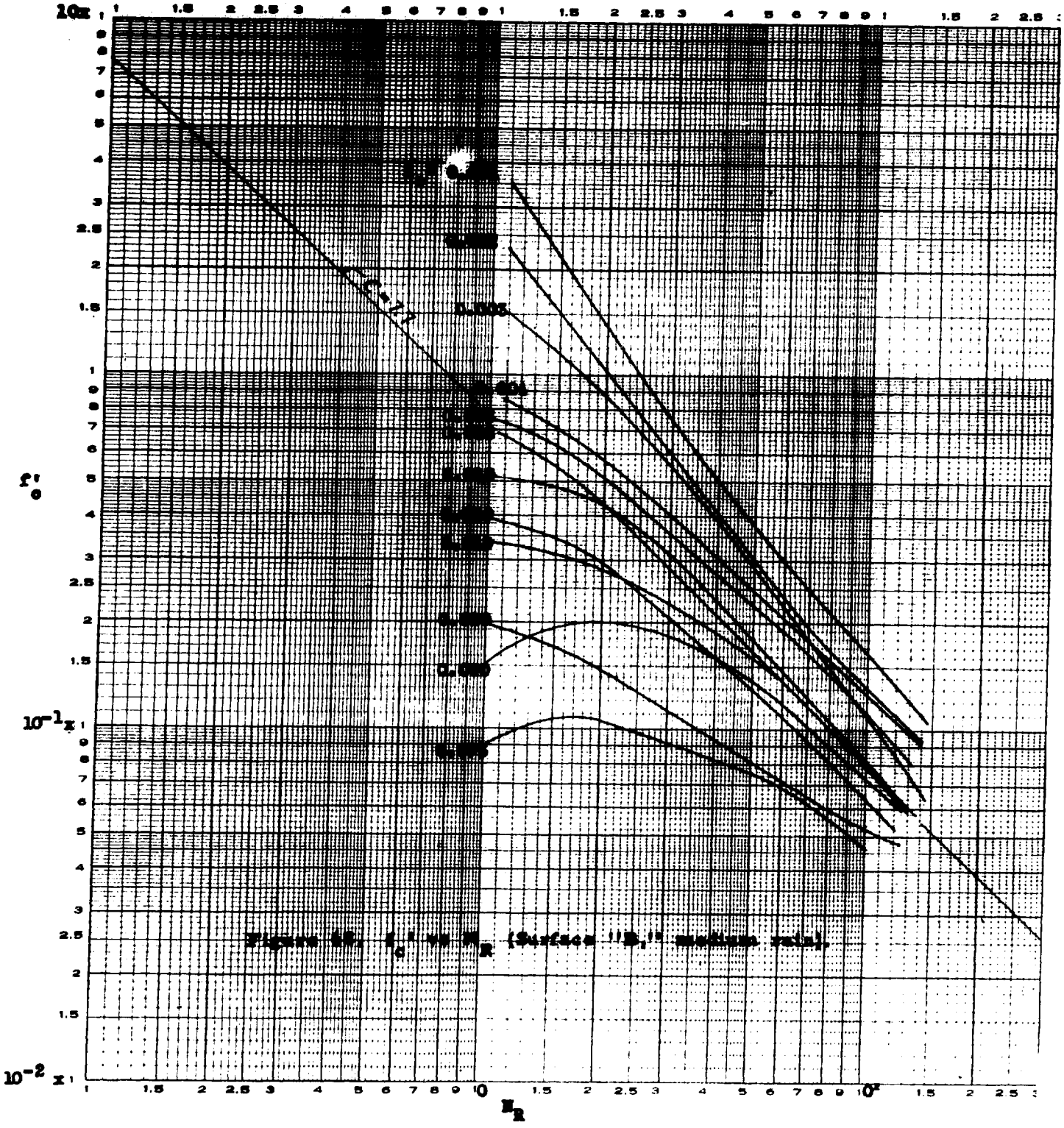


Figure 66. f'_c vs R_R (Surface "B_1" medium rate).

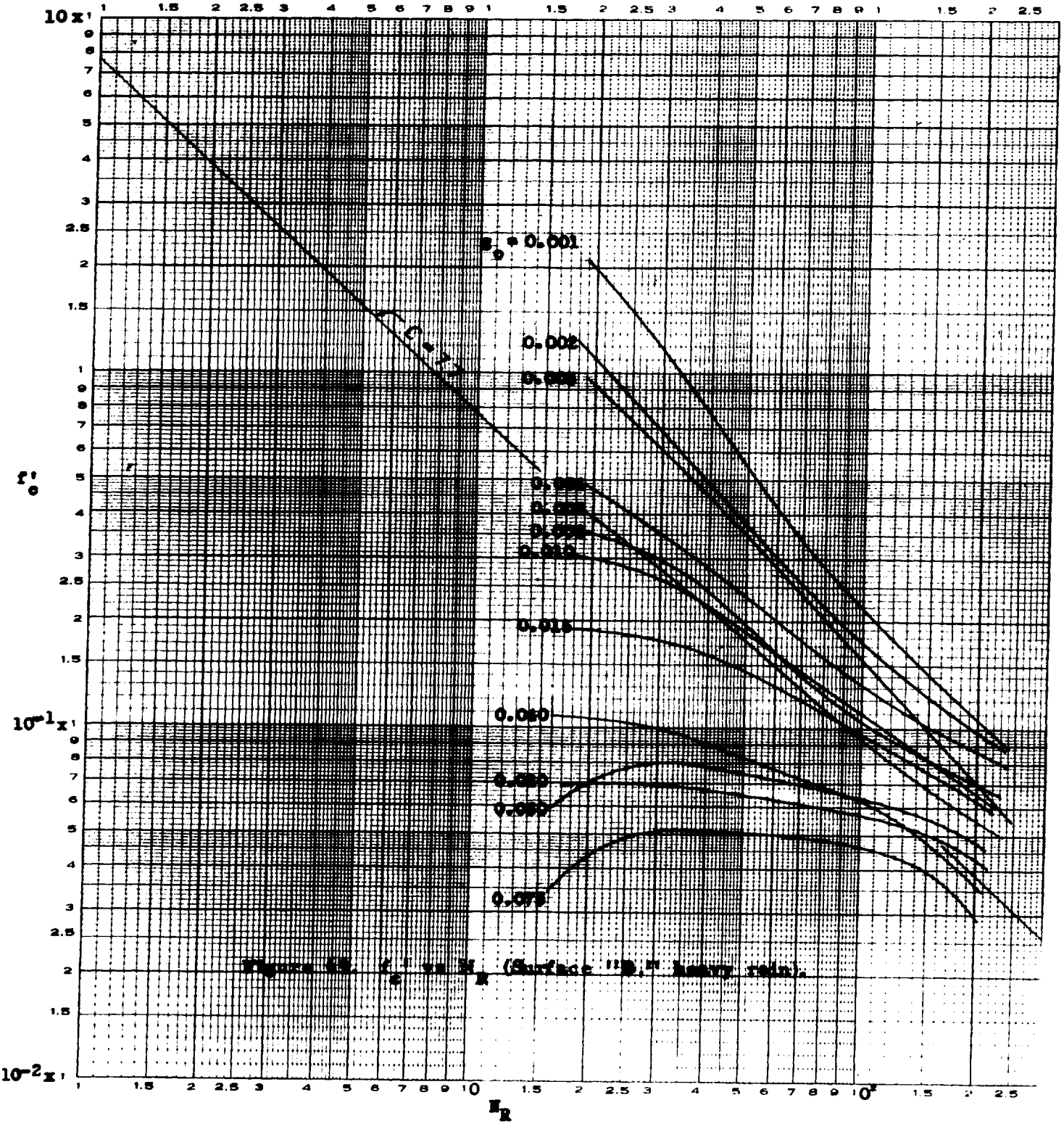
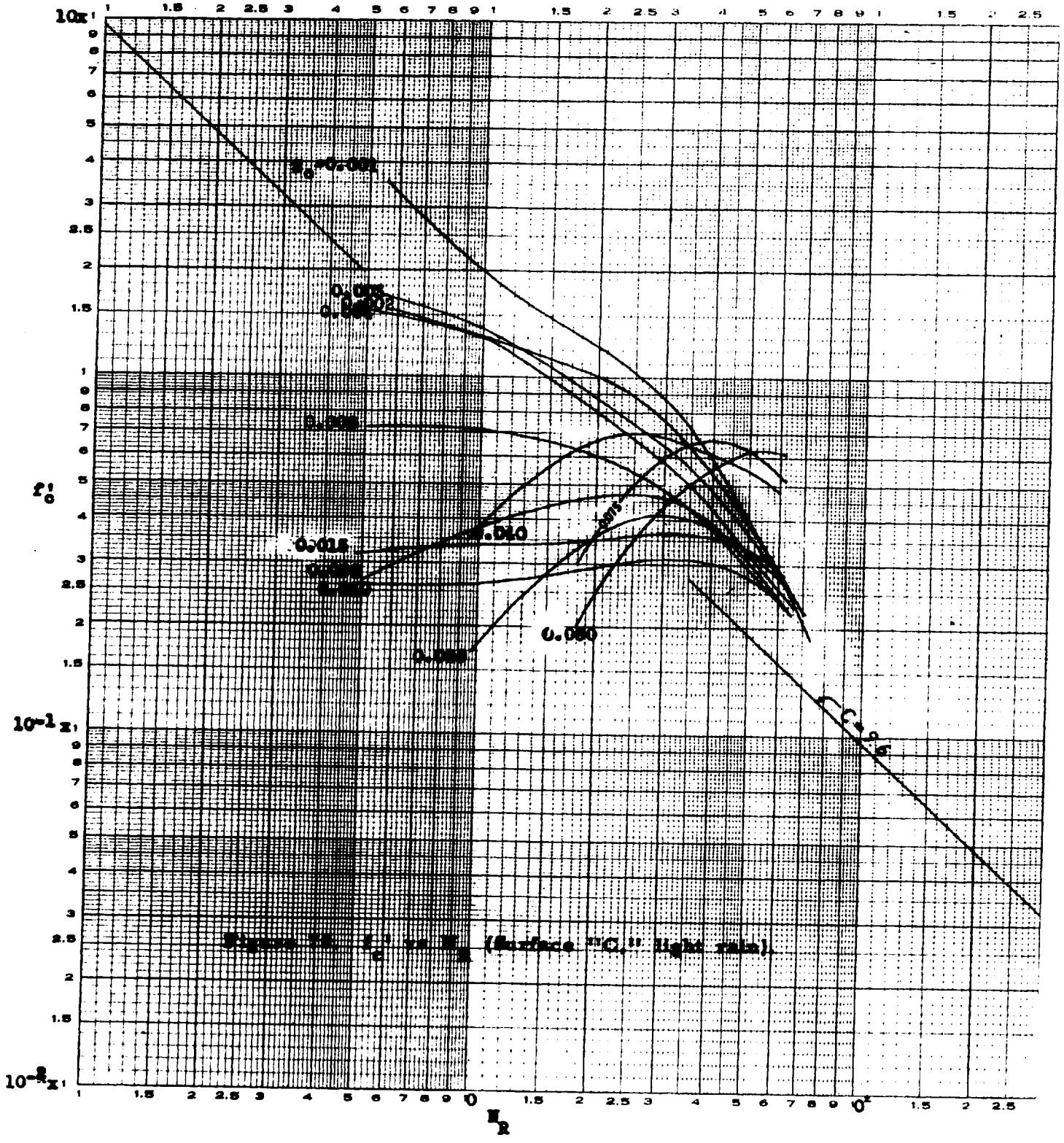


Figure 68. f'_c vs N_R (Surface III, 2" heavy rein).


$10x^1$
f'_c
$10^{-1}x_1$
$10^{-2}x_1$
N_R
C_f

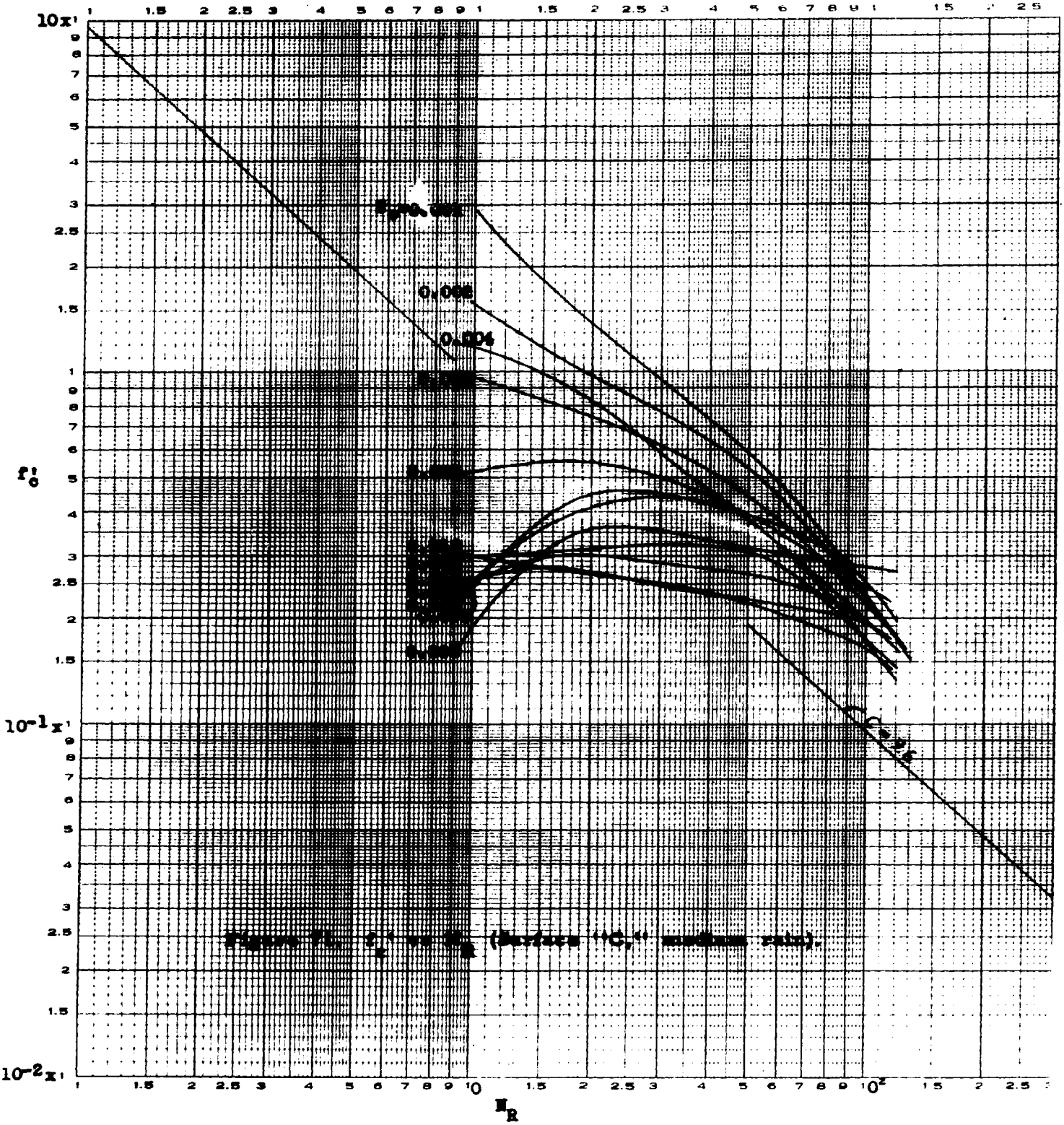
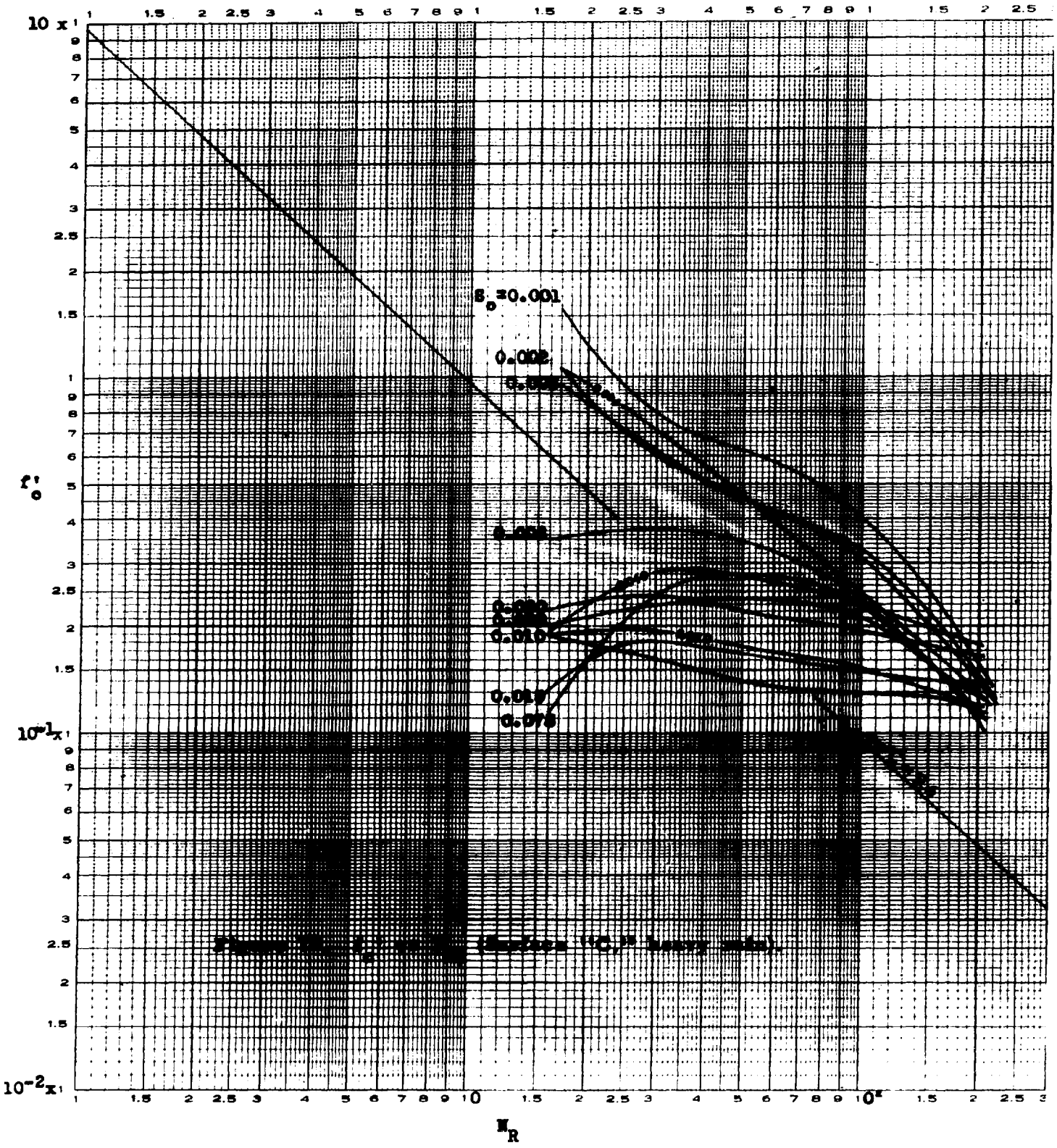


Figure 71. f_c' vs N_R (Surface "C," medium rate).


ε_0=0.001
0.002
0.004
0.008
0.010
0.012
0.016
f'_0
10^{-1} x
10^{-2} x
R_R

EFFECT OF RAINDROP IMPACT ON C AGAINST BOTTOM SURFACE

C'/C vs S_o

C_H'/C_L' (& C_M'/C_L') vs S_o

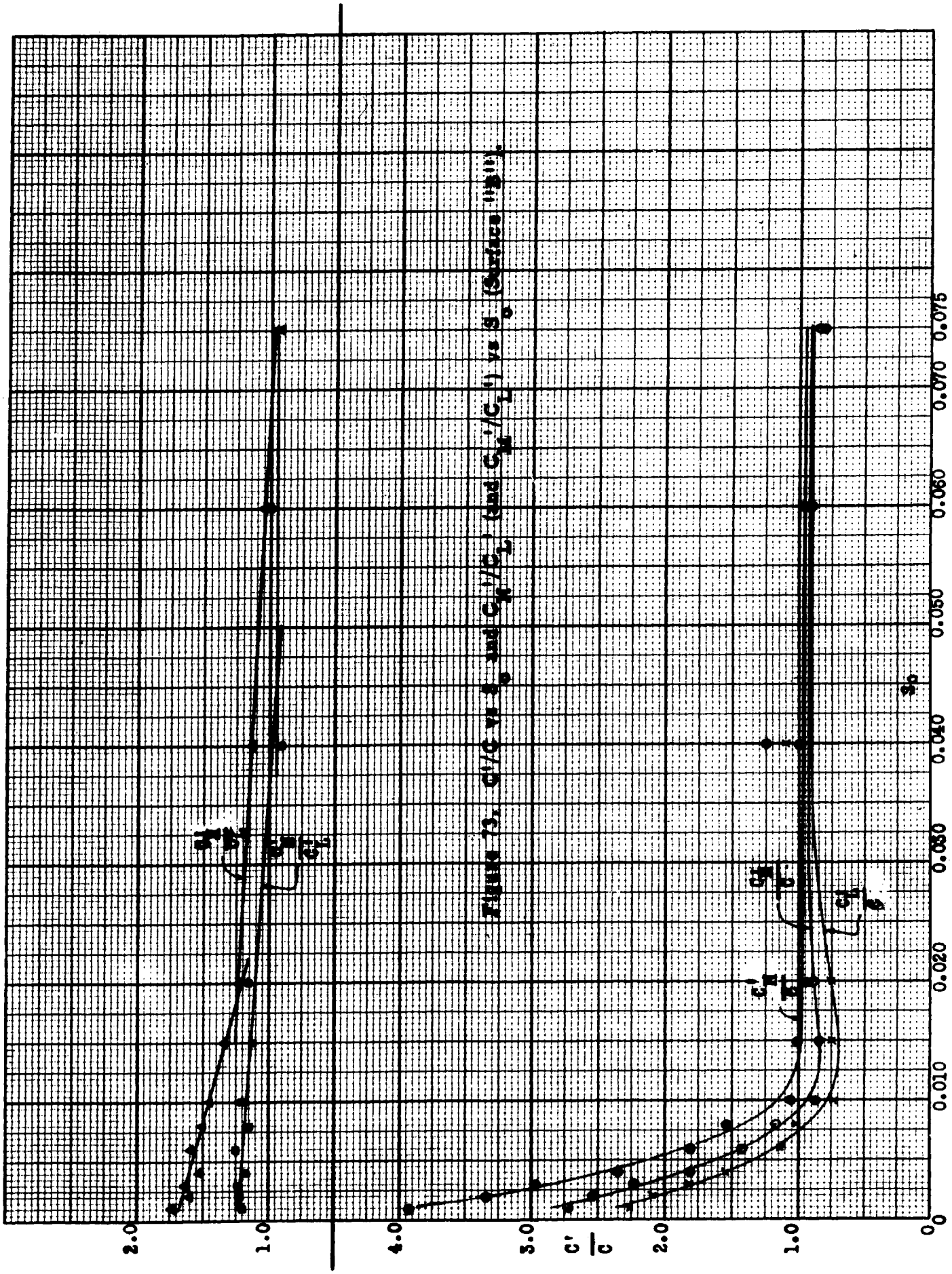
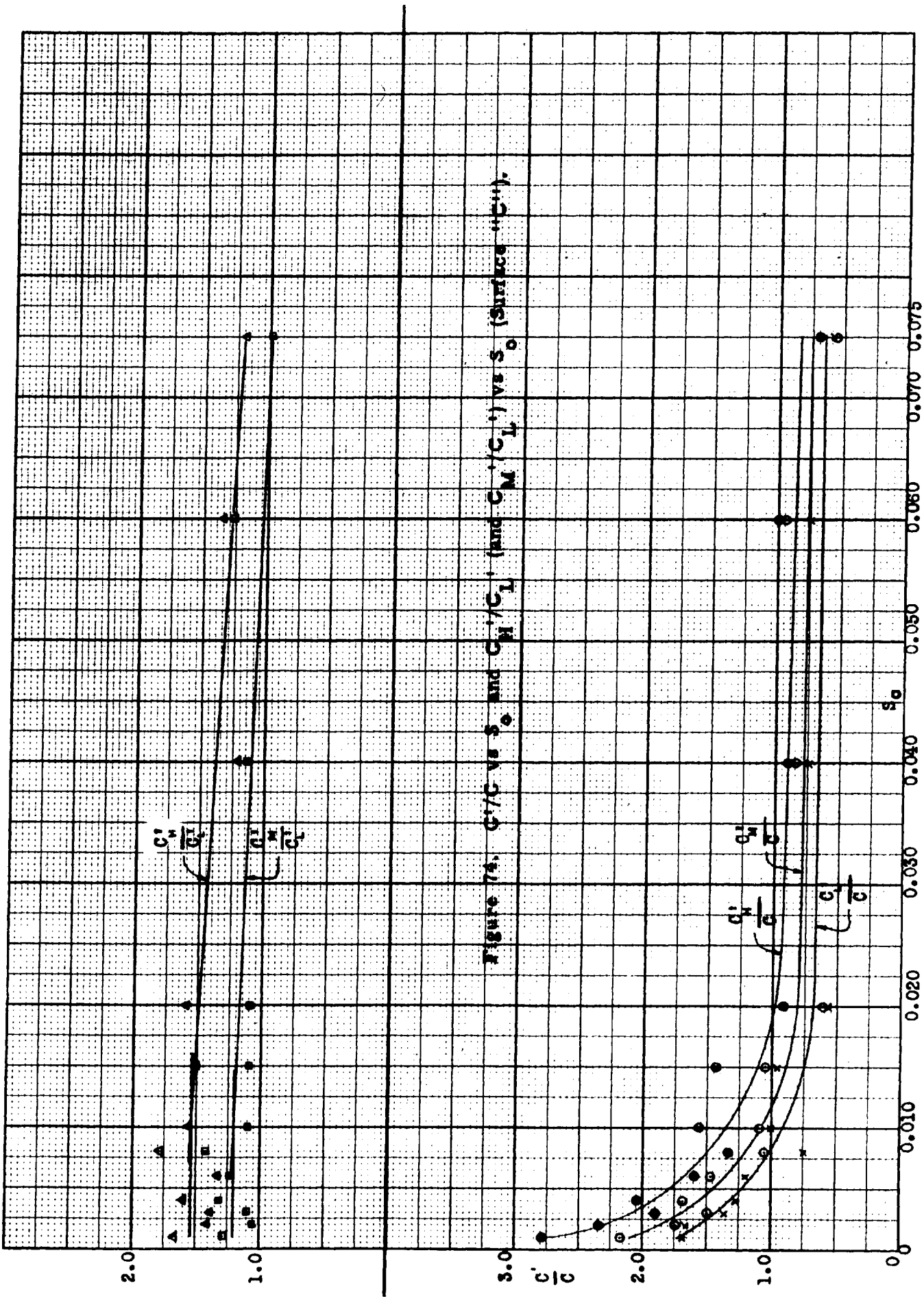


Figure 73. C'/C vs s_0 and C_H'/C_L' (and C_H'/C_L') vs s_0 (Surface Light)

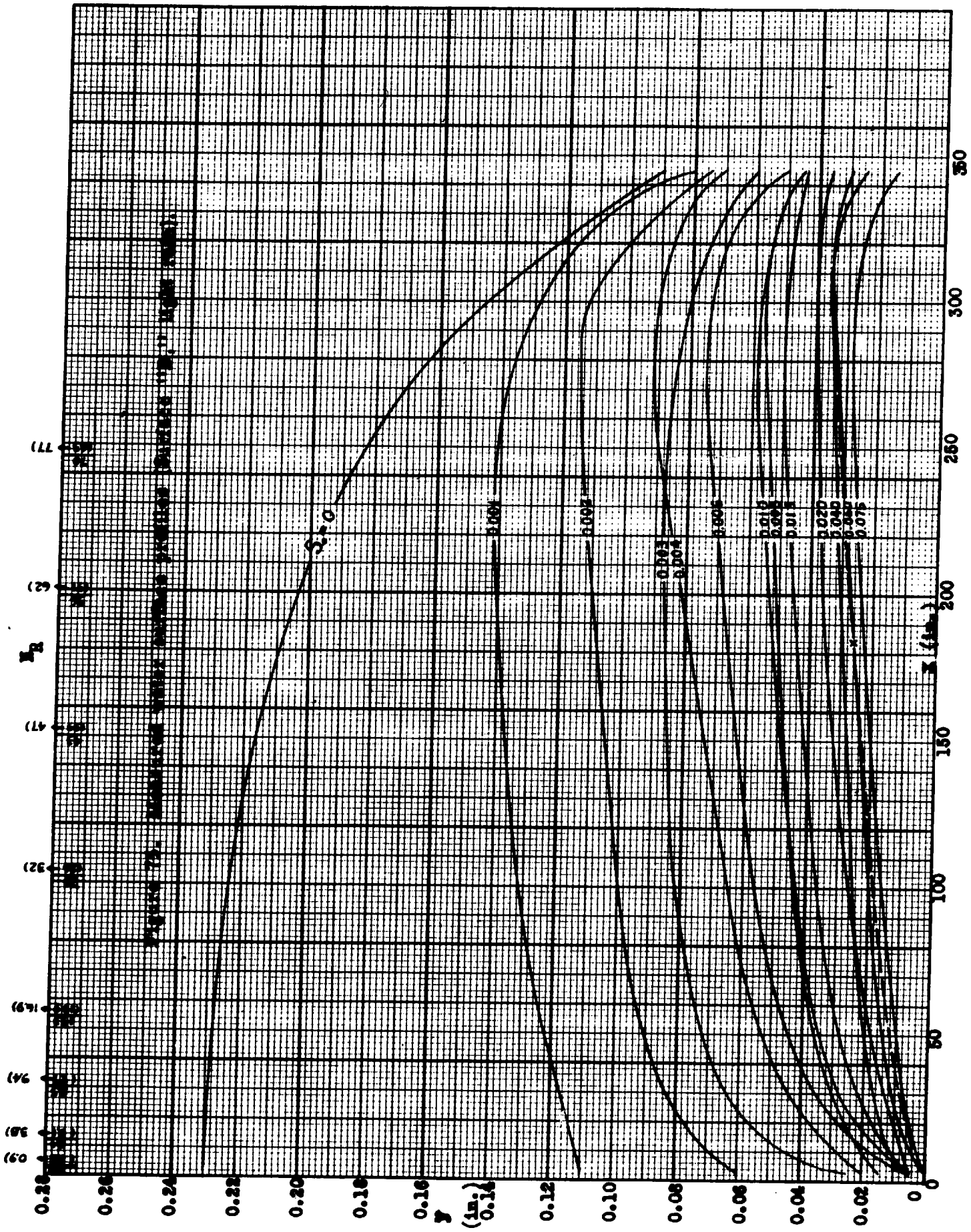

Figure 74. C'/C vs s_o and C_M'/C_L' (and C_M'/C_L') vs s_o (Surface "C'').
$\frac{C_M'}{C_L'}$
$\frac{C_M'}{C_L'}$
$\frac{C_M'}{C'}$
$\frac{C_L'}{C'}$
$\frac{C_M'}{C'}$
s_o
0
0.010
0.020
0.030
0.040
0.050
0.060
0.070
0.075
$\frac{C'}{C}$
3.0
2.0
1.0
2.0
1.0

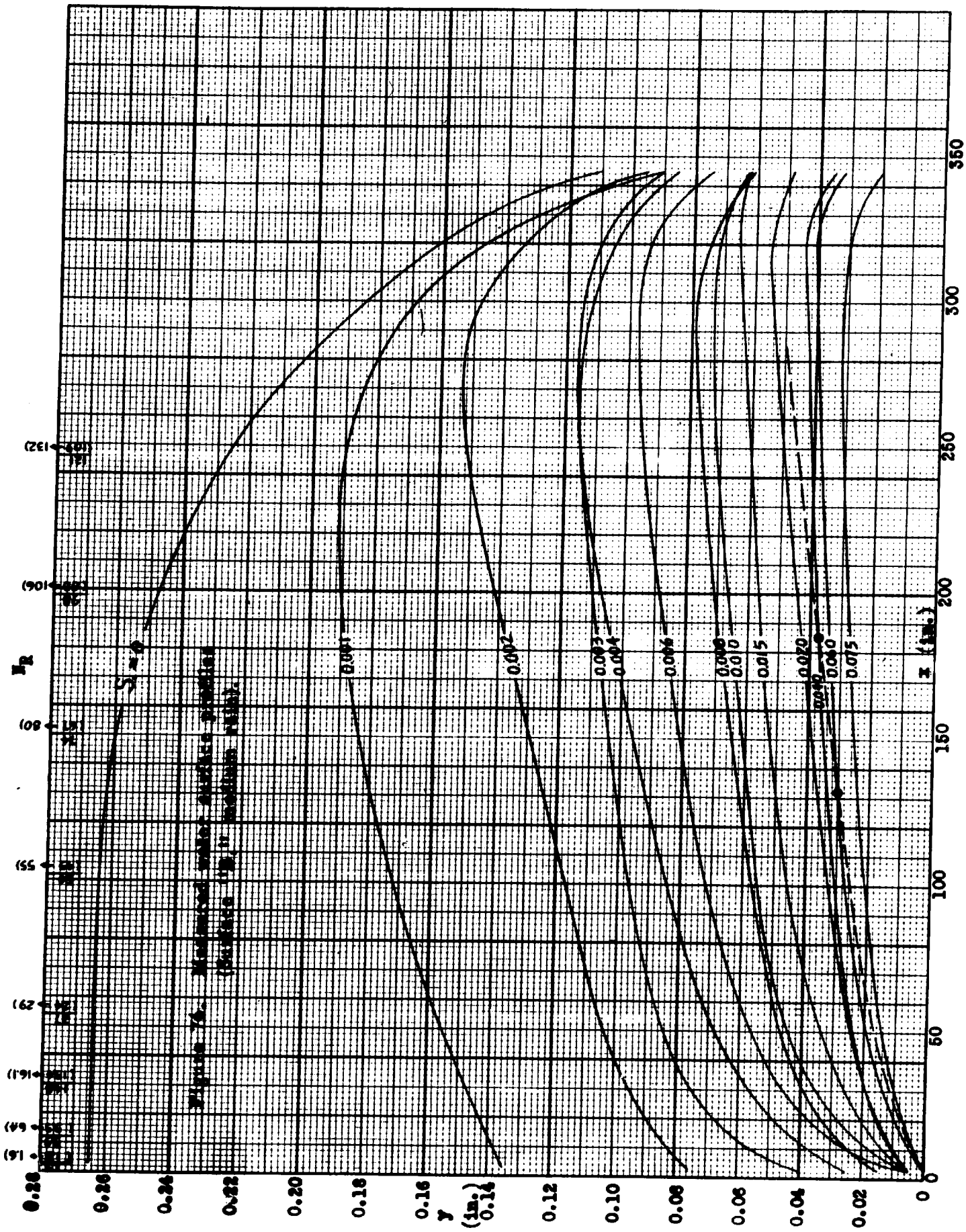
MEASURED WATER SURFACE PROFILES

(condensed)

Legend

---------- represents the position of critical depth; to its left side the velocity is subcritical and to the right side it is supercritical.


0.28
0.26
0.24
0.22
0.20
0.18
0.16
0.14
0.12
0.10
0.08
0.06
0.04
0.02
0
50
100
150
200
250
300
350
0.100
0.008
0.006
0.004
0.003
0.010
0.008
0.015
0.020
0.040
0.060
0.075


0.28
0.26
0.24
0.22
0.20
0.18
0.16
0.14
0.12
0.10
0.08
0.06
0.04
0.02
0
y (in.)
0
50
100
150
200
250
300
350
x (in.)
0.001
0.002
0.003
0.004
0.006
0.008
0.010
0.015
0.020
0.030
0.040
0.075
S = 0

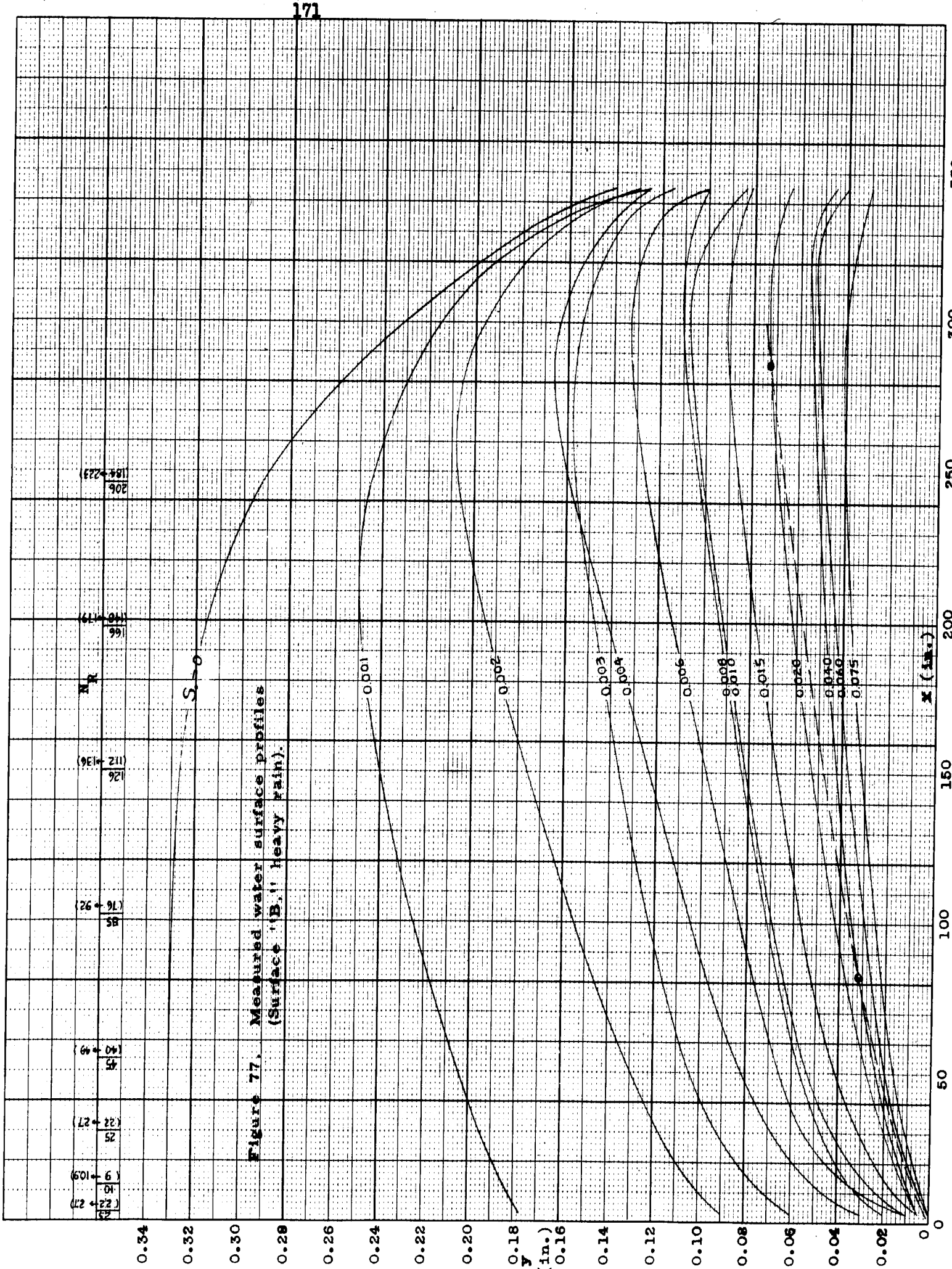
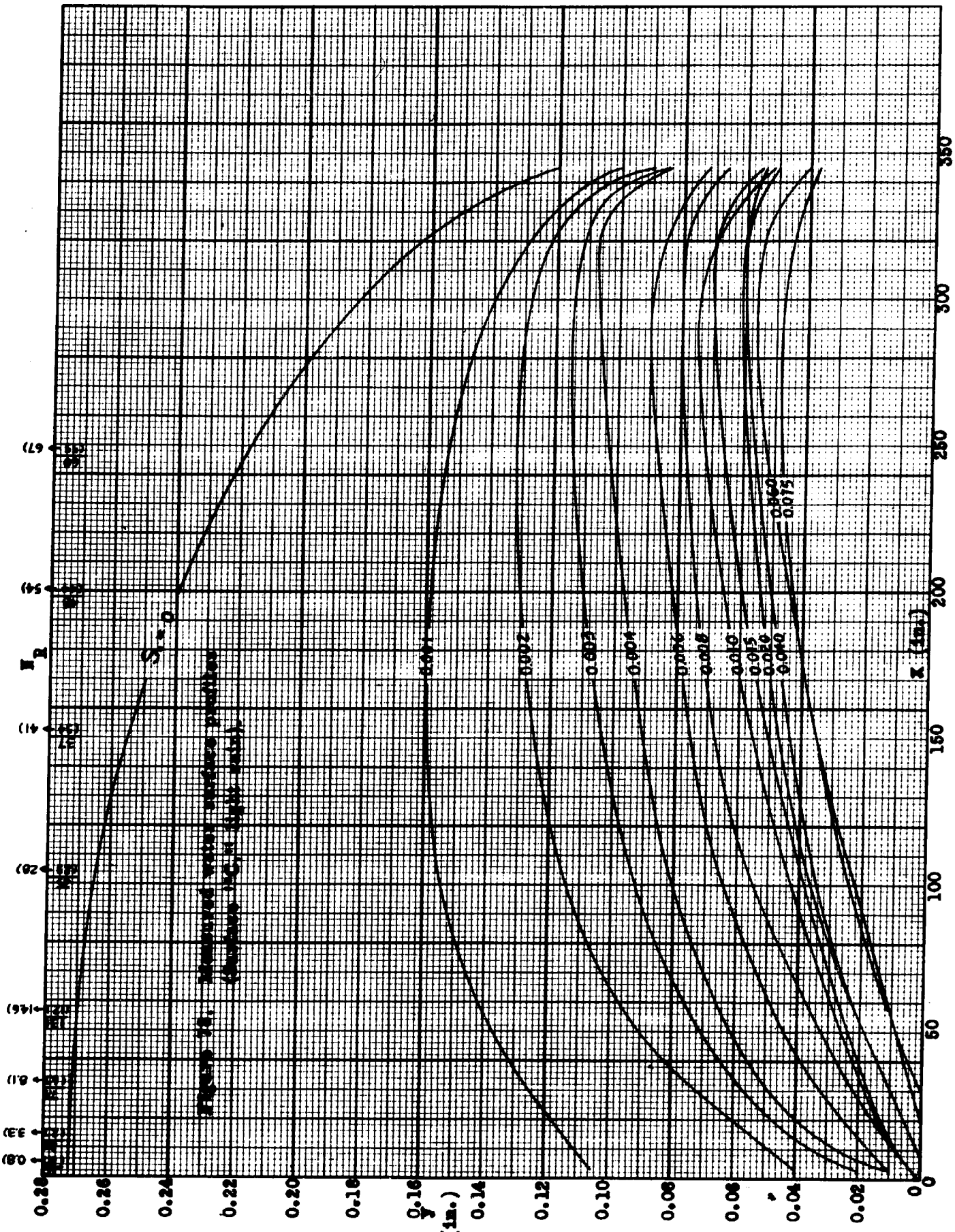


Figure 77. Measured water surface profiles (Surface 'B,' heavy rain).


Measured water surface profiles
(Reynolds No. = 3.0 x 10⁵)
$S_o = 0$
0.001
0.002
0.003
0.004
0.006
0.008
0.010
0.015
0.020
0.040
0.060
0.075
x (in.)
y (in.)
0
50
100
150
200
250
300
350
0.02
0.04
0.06
0.08
0.10
0.12
0.14
0.16
0.18
0.20
0.22
0.24
0.26
0.28

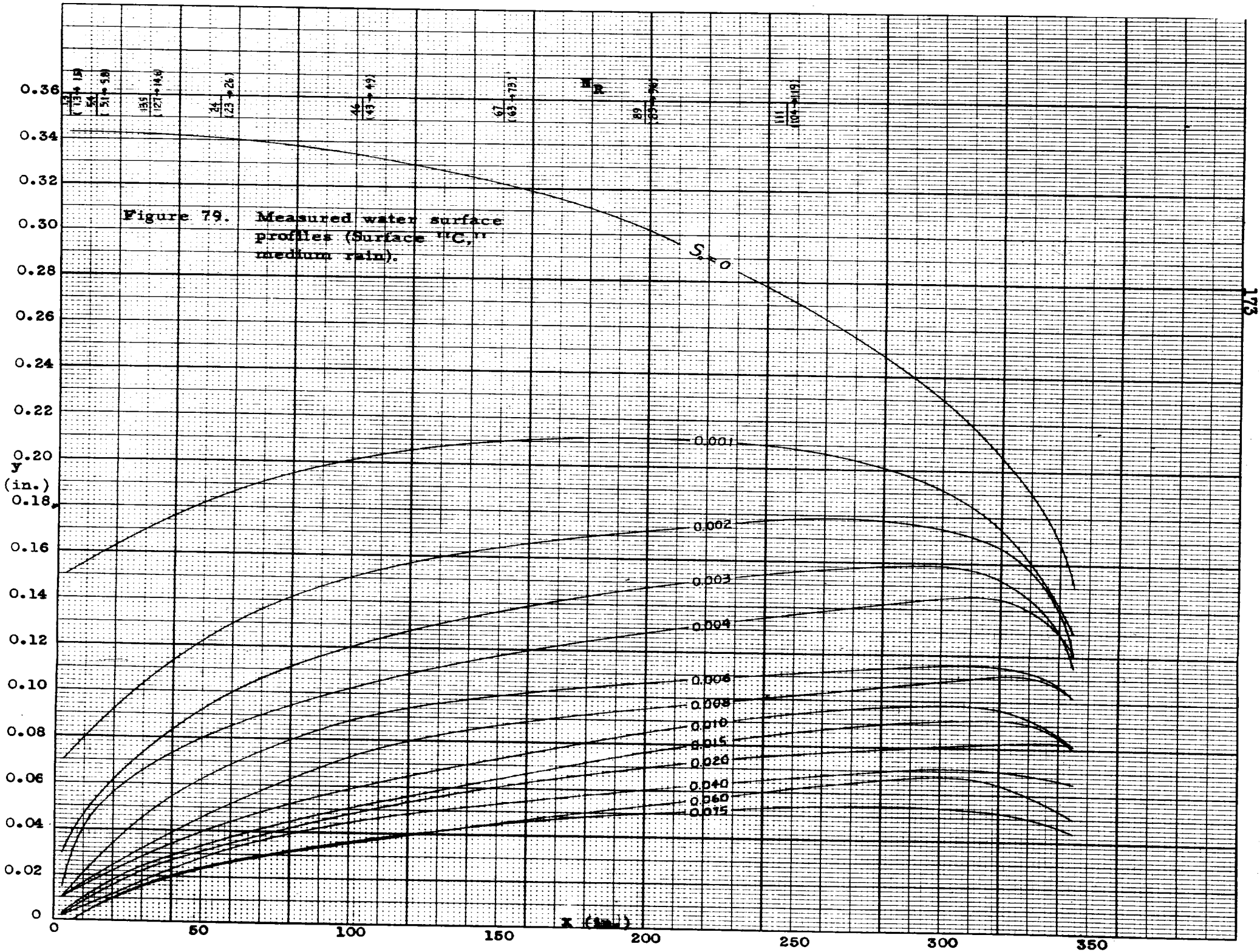


Figure 79. Measured water surface profiles (Surface "C," medium rain).

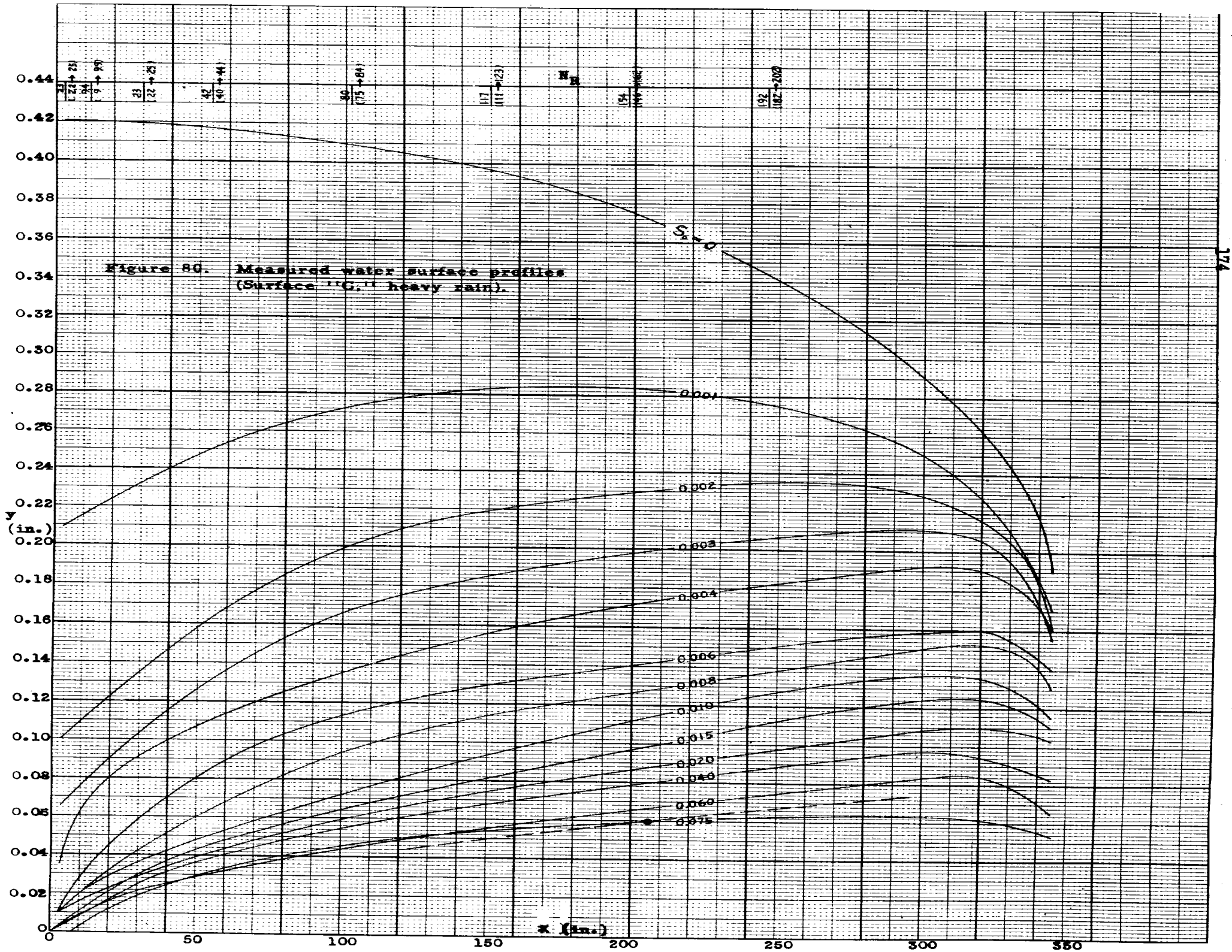
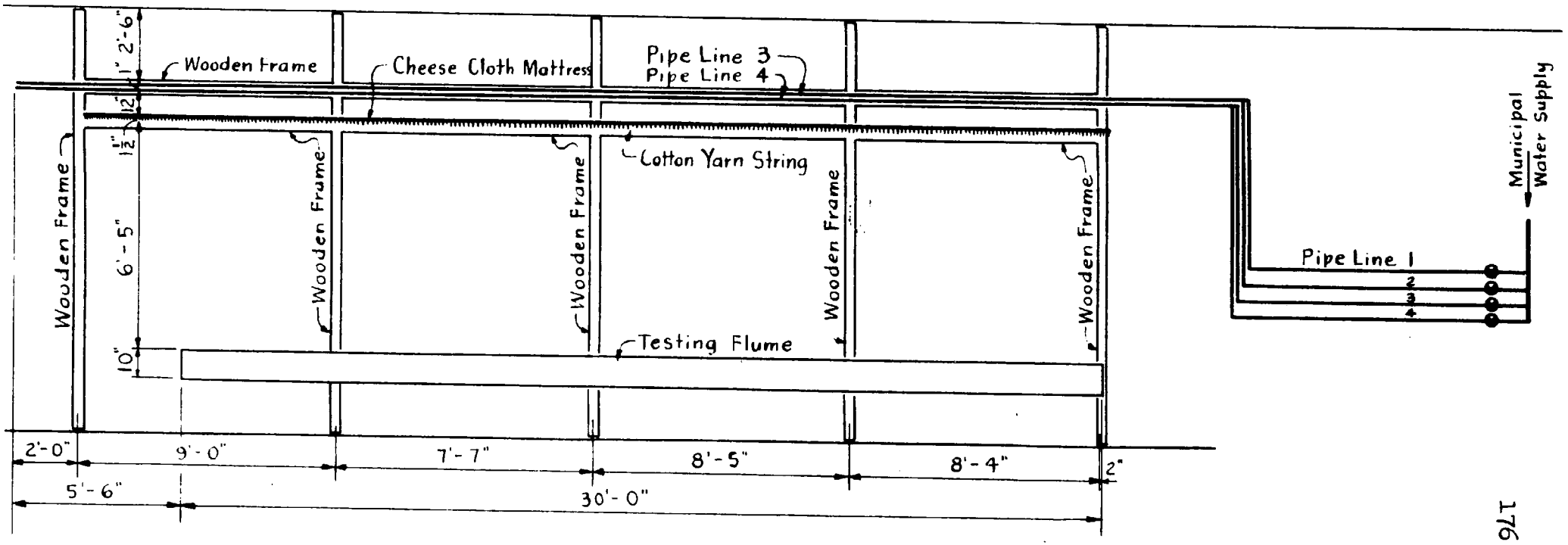
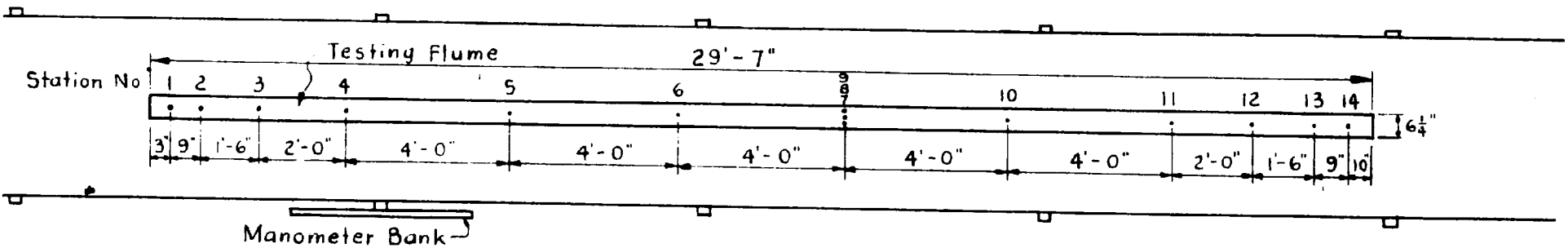


Figure 80. Measured water surface profiles (Surface "G," heavy rain).

DRAWINGS

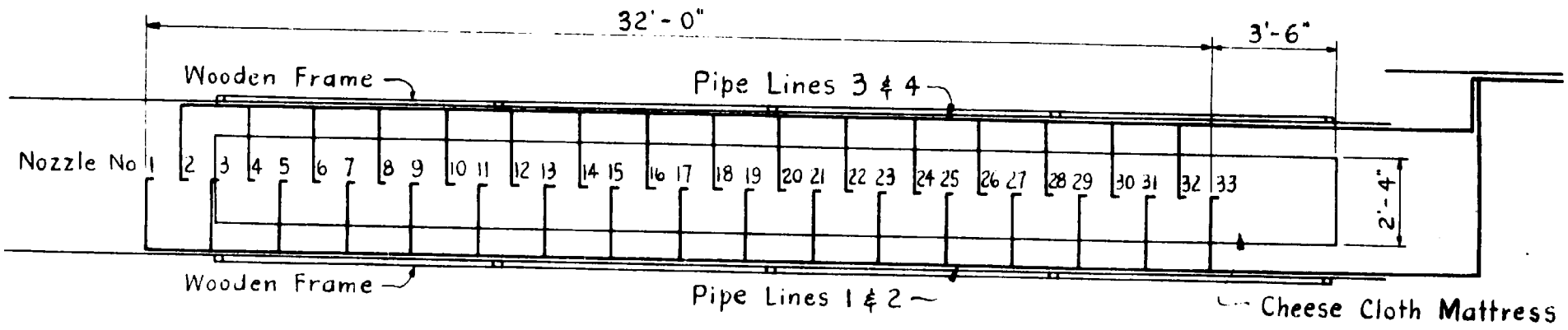


Sketch of General Arrangement through Center Line



Plan of Testing Flume with Stations Marked

DRAWING 1



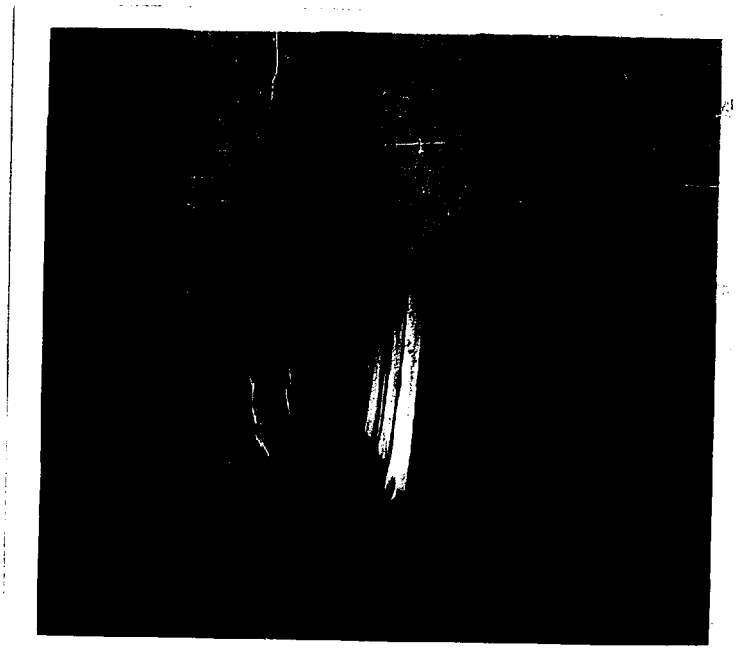
Plan of Nozzles

177

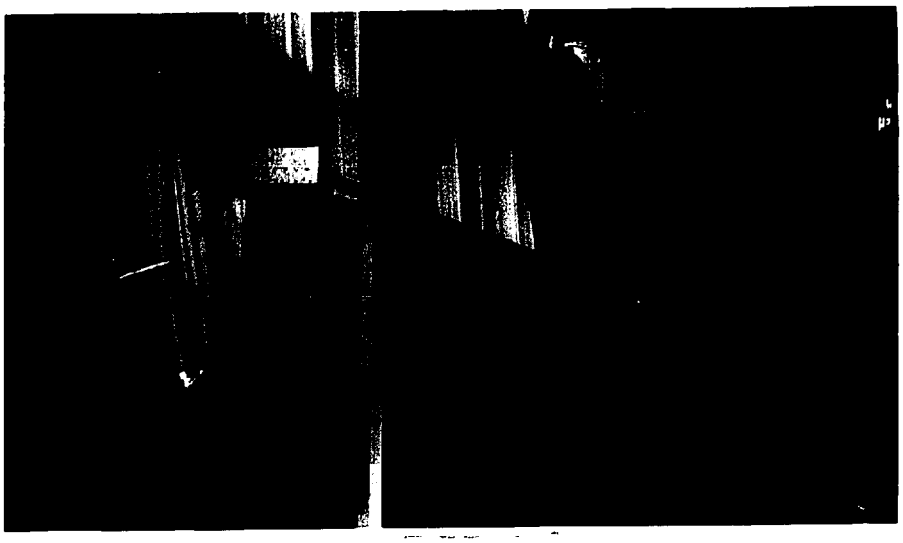
Pipe Line	Nozzles										Rain		
											Light	Medium	Heavy
1		3		7		11		15		19	23	27	31		x	x
2	1		5		9		13		17		21	25	29	33	x	x	x
3		2		6		10		14		18	22	26	30				x
4			4		8		12		16		20	24	28	32			x

DRAWING 2

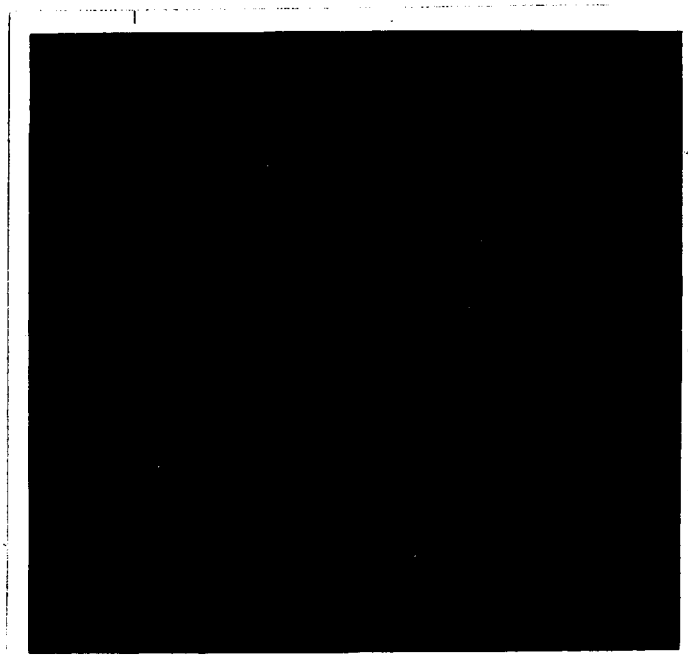
PHOTOGRAPHS



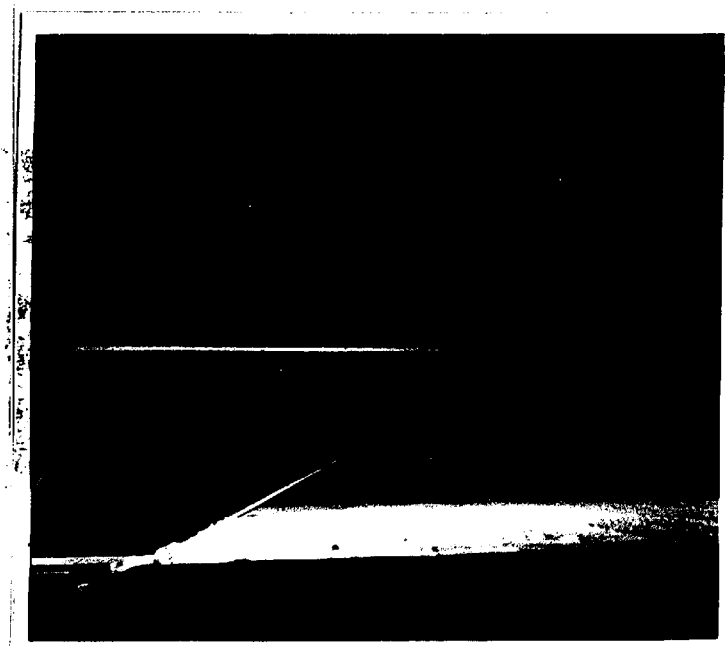
Photograph 1. Experimental arrangement (from lower end, looking upstream; $S_o = 0$).



Photograph 2. Testing flume (from upper end, looking downstream; $S_o = 0.075$).



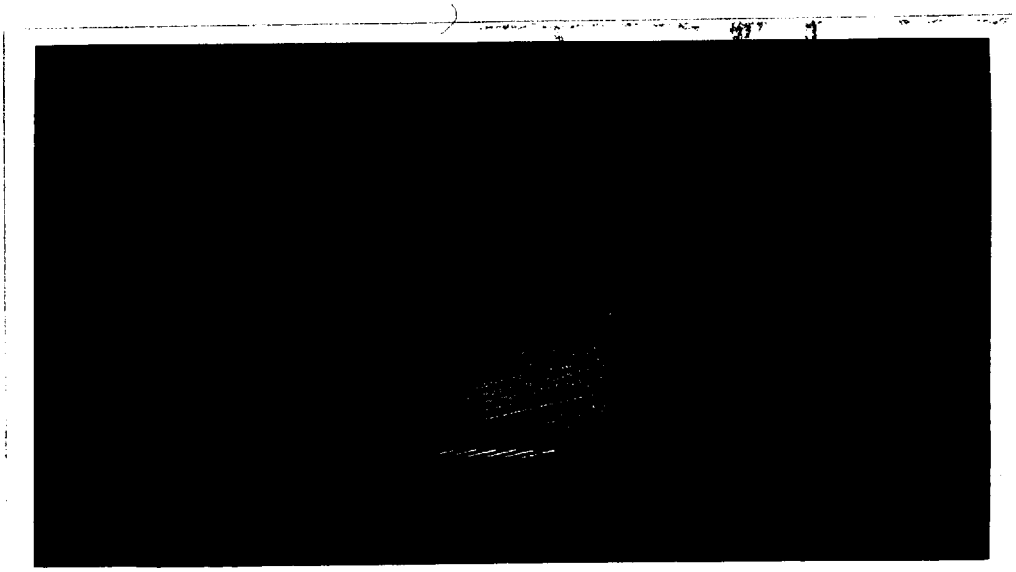
Photograph 3. Cheesecloth mattress with cotton yarn strings (looking up).



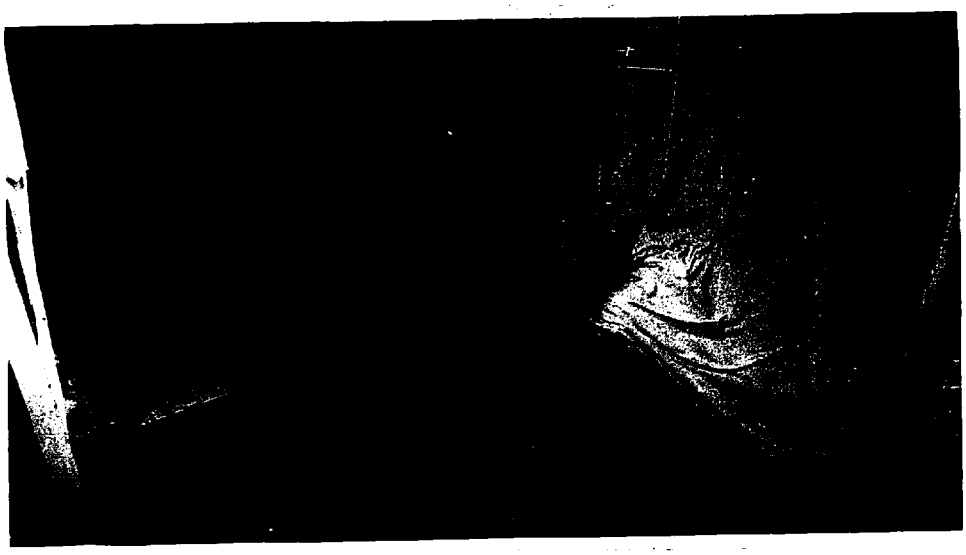
Photograph 4. Nozzles with drains (looking down on mattress.



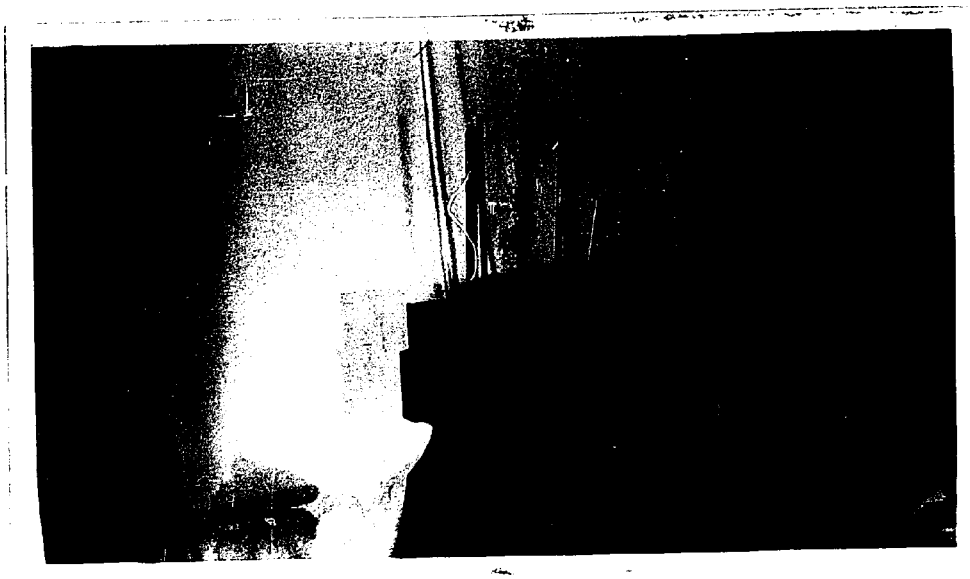
Photograph 5. Close-up of nozzle and drain (above the cheesecloth mattress).



Photograph 6. Manometer bank.



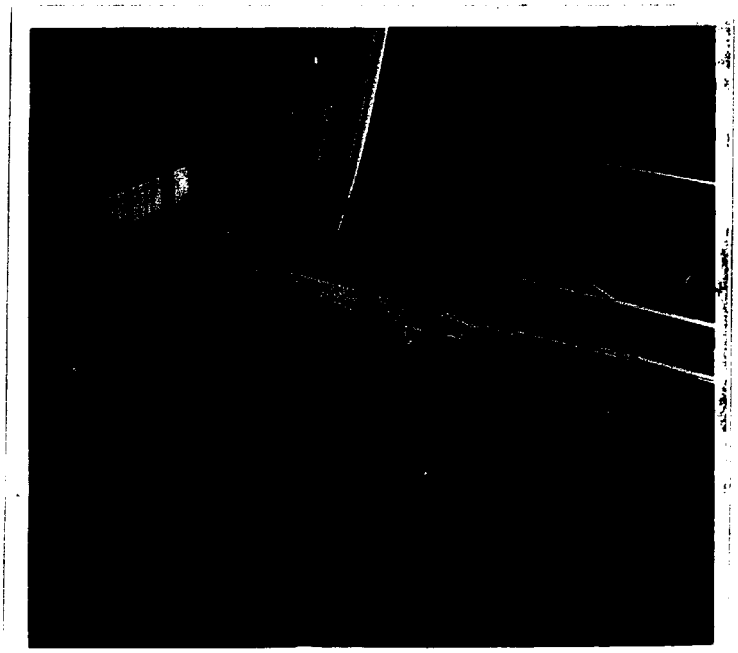
Photograph 7. Volumetric tank with portable point gage.



Photograph 8. Flume support and slope indicator.



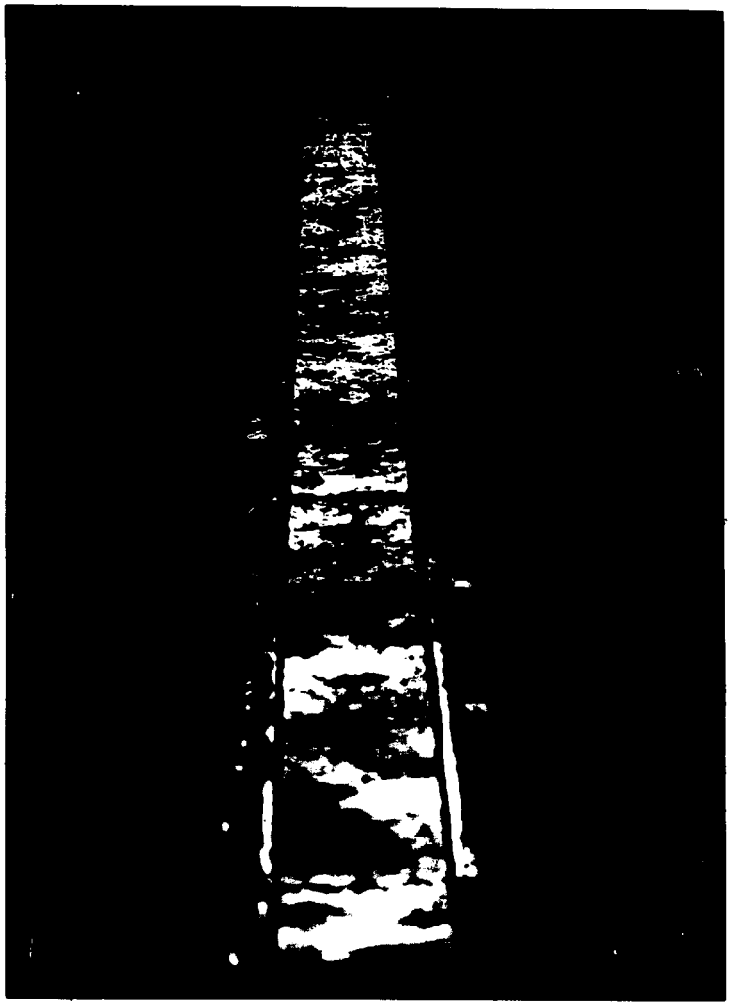
Photograph 9. Beakers to measure rainfall distribution.



Photograph 10. Part 1 roughness test (water supply to upper end; $S_o = 0$).



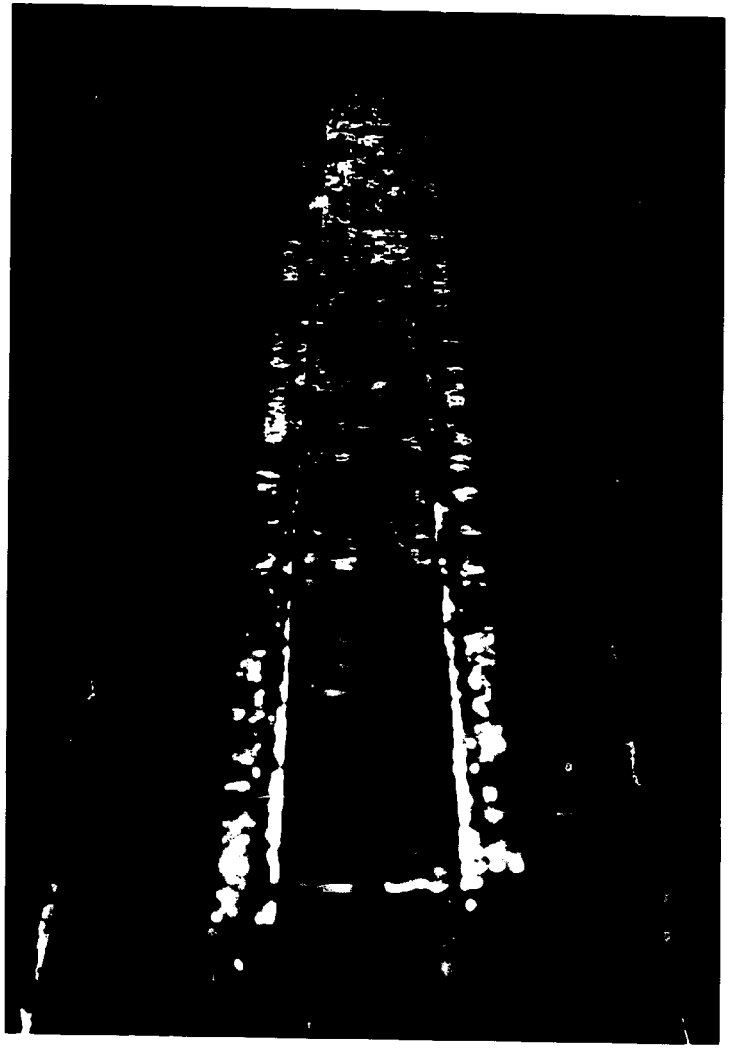
Photograph 11. Part 2 rainfall test (from upper end looking downstream; $S_o = 0.075$. Note fine spray above mattress. Raindrops can be seen impinging on water surface in flume.).



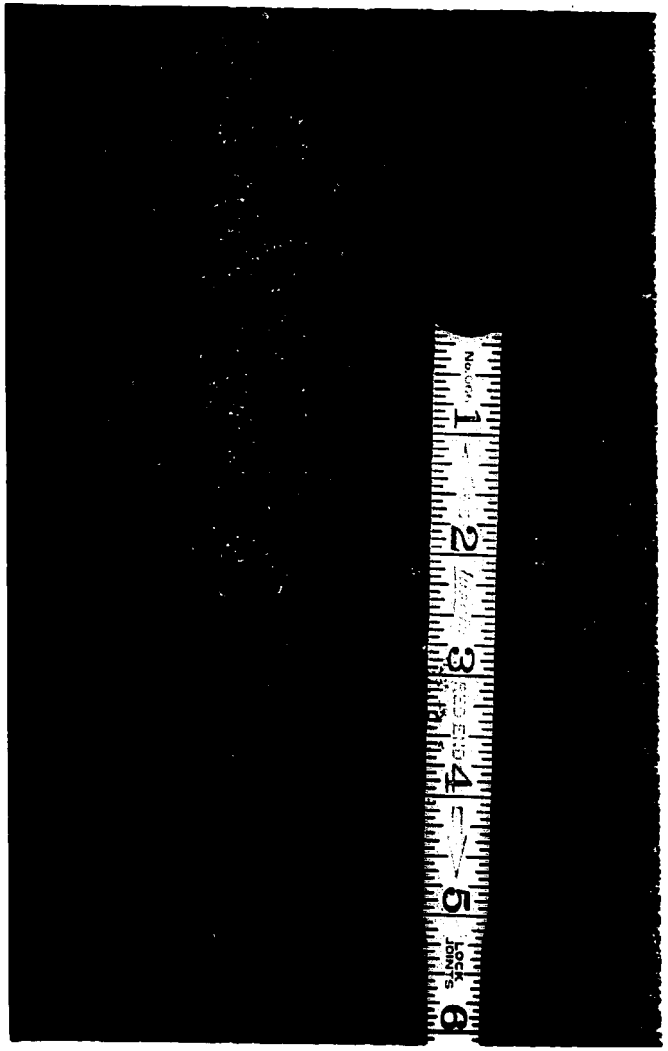
Photograph 12. Part 2 rainfall test (Surface "C," S_o = 0, light rain).



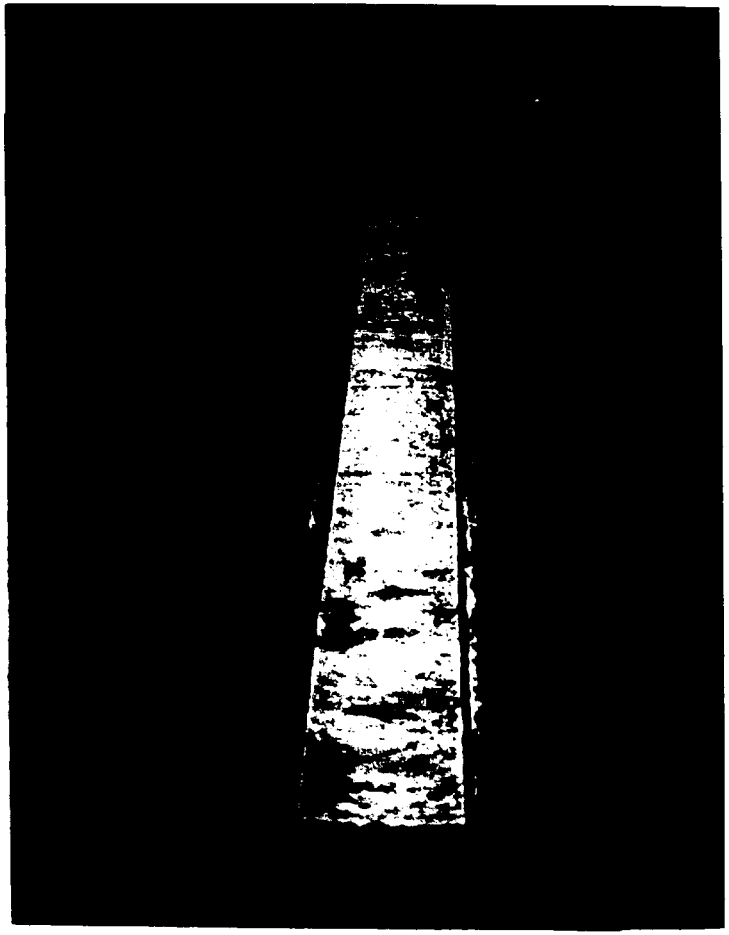
Photograph 13. Part 2 rainfall test (Surface "C," S_o = 0, medium rain).



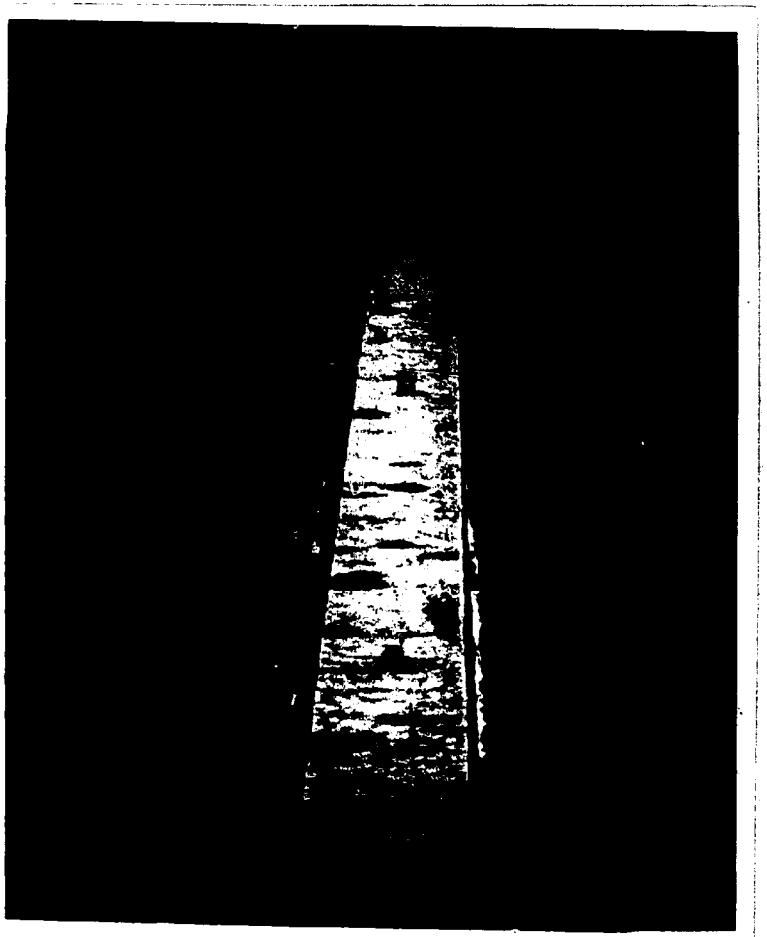
Photograph 14. Part 2 rainfall test (Surface "C," S_o = 0, heavy rain).



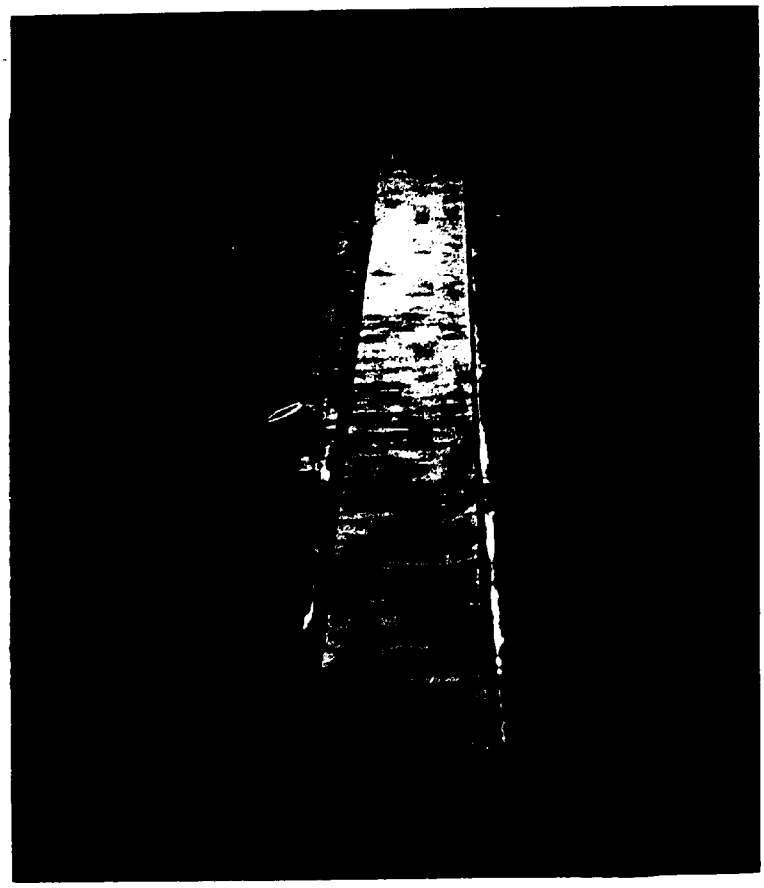
Photograph 15. Surface "C"--cemented sand surface and the water depth station.



Photograph 16. Part 2 rainfall test (Surface "C," S_o = 0.075, light rain).



Photograph 17. Part 2 rainfall test (Surface "C," S_o = 0.075, medium rain).



Photograph 18. Part 2 rainfall test (Surface "C," S_o = 0.075, heavy rain).

APPENDIXES

APPENDIX I

NOZZLE TEST AND THE FINAL DESIGN ADOPTED, ITS ARRANGEMENT AND SPRAY PATTERNS

Extensive research for a perfect nozzle to spray evenly was done before the final design was adopted.

Two-inch beakers were placed at 1-foot interval from the nozzle along its center line to measure the spray distribution. Close observations for the spray pattern were made. The different designs of nozzle tested are summarized in Table V on page 190. A detail drawing of the final design adopted with a sketch showing its arrangement is shown on page 192. The spray pattern of a single nozzle and the superimposed patterns of two nozzles spaced 4 feet apart are shown in Figure 81 on page 193.

The final design, which was originally used by the Ohio State University for soil erosion research in 1952, gave a fine mist of spray covering quite evenly for a width of 2 feet or so. When two nozzles of such design were set in the position described on page 192 at 4-foot spacing, they would produce an almost exactly constant longitudinal spray distribution provided that the water pressure in the pipe was maintained at 40 pounds per square inch.

TABLE V

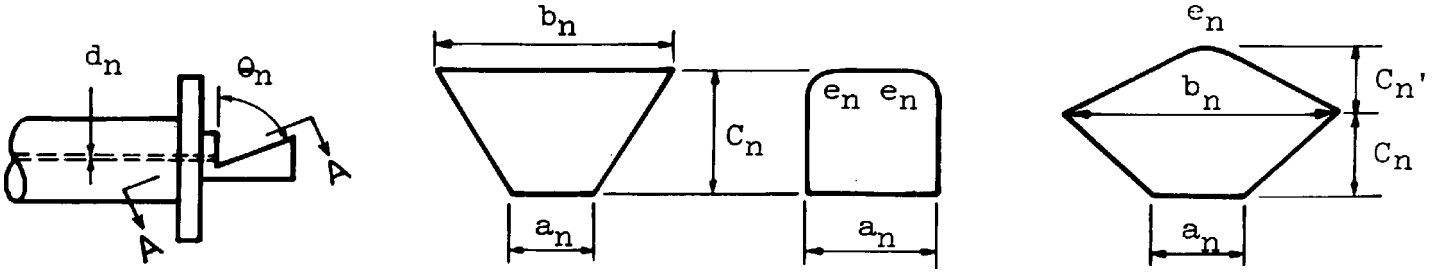
SUMMARY OF NOZZLE TESTS

Surface Shape	d_n	a_n	b_n	c_n	e_n	θ_n	ϕ_n
	in.	in.	in.	in.	in.	deg.	deg.
	1/32	0.15 to 0.40	0.20 to 1.20	0.18 to 0.50		-45 to +60	-60 to +60
	1/64 to 3.5/64	0.128 to 0.60		0.20 to 0.73	small to large	+45 to +60	0 to +45
	1/32	0.15	0.48	0.18 C_n' = 0.12	small	45	0

d_n -- diameter of discharging hole in nozzle
a_n, b_n, c_n, c_n' -- dimensions of nozzle surface
e_n -- curvature at upper corners of nozzle surface
θ_n -- angle of inclination of nozzle surface
ϕ_n -- angle of position of nozzle to the horizontal
Z_s -- highest point of spray above nozzle
Z_n -- height of nozzle from cheesecloth mattress
p -- water pressure

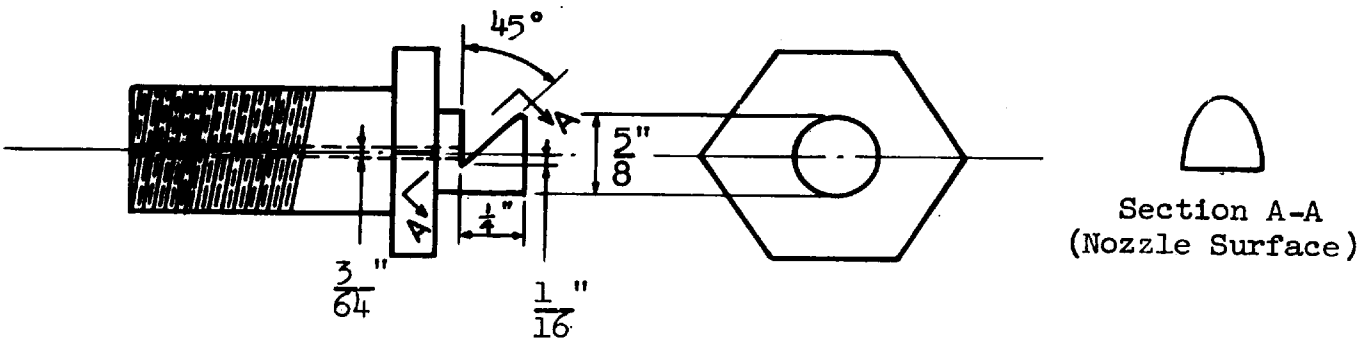
TABLE V--Continued

Z_s	Z_n	p	General Comments
ft.-in.	ft.-in.	p.s.i.	
1-0 to 4-0	1-8 to 4-10	15 to 43	1. The spray contained larger drops, not of mist form, and low in intensity. 2. When b_n was large and p was low, then the spray narrowed on a longitudinal strip. 3. When p was high, then the spray covered much too wide transversely, and not enough longitudinally. When b_n was reduced, then the spray concentrated on the central portion and along two sides, forming two jets at high pressures. 4. The +60° surface gave better results.
0 to 1-9	0 to 1-9	15 to 41	1. For d_n = 1/64 and 1/32 in., the spray was too small and concentrated on the central strip 6 inches wide. 2. At low pressures the spray contained larger drops and low in intensity. 3. For d_n = 1/28 in., the spray was small and did not give good distribution longitudinally.
		40	1. The spray concentrated on the central portion.

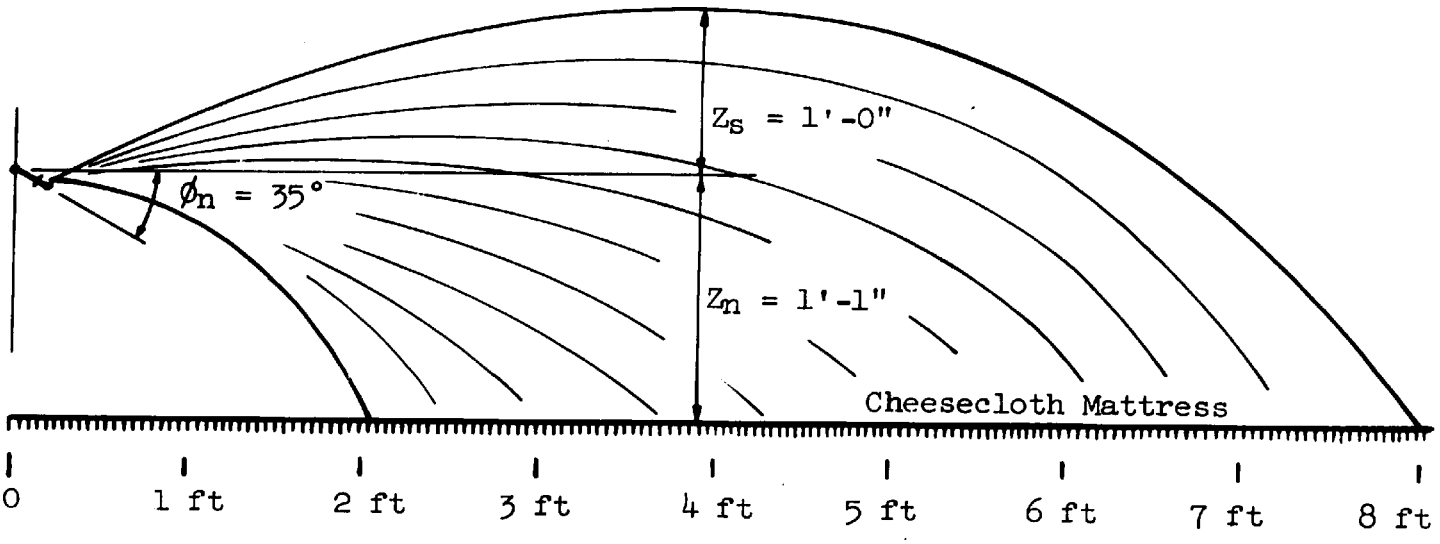


Section A-A (nozzle surface)

THE FINAL DESIGN OF NOZZLE ADOPTED
(from the one used by Ohio State University for soil erosion research, September, 1952)



The Arrangement to Produce Best Spray



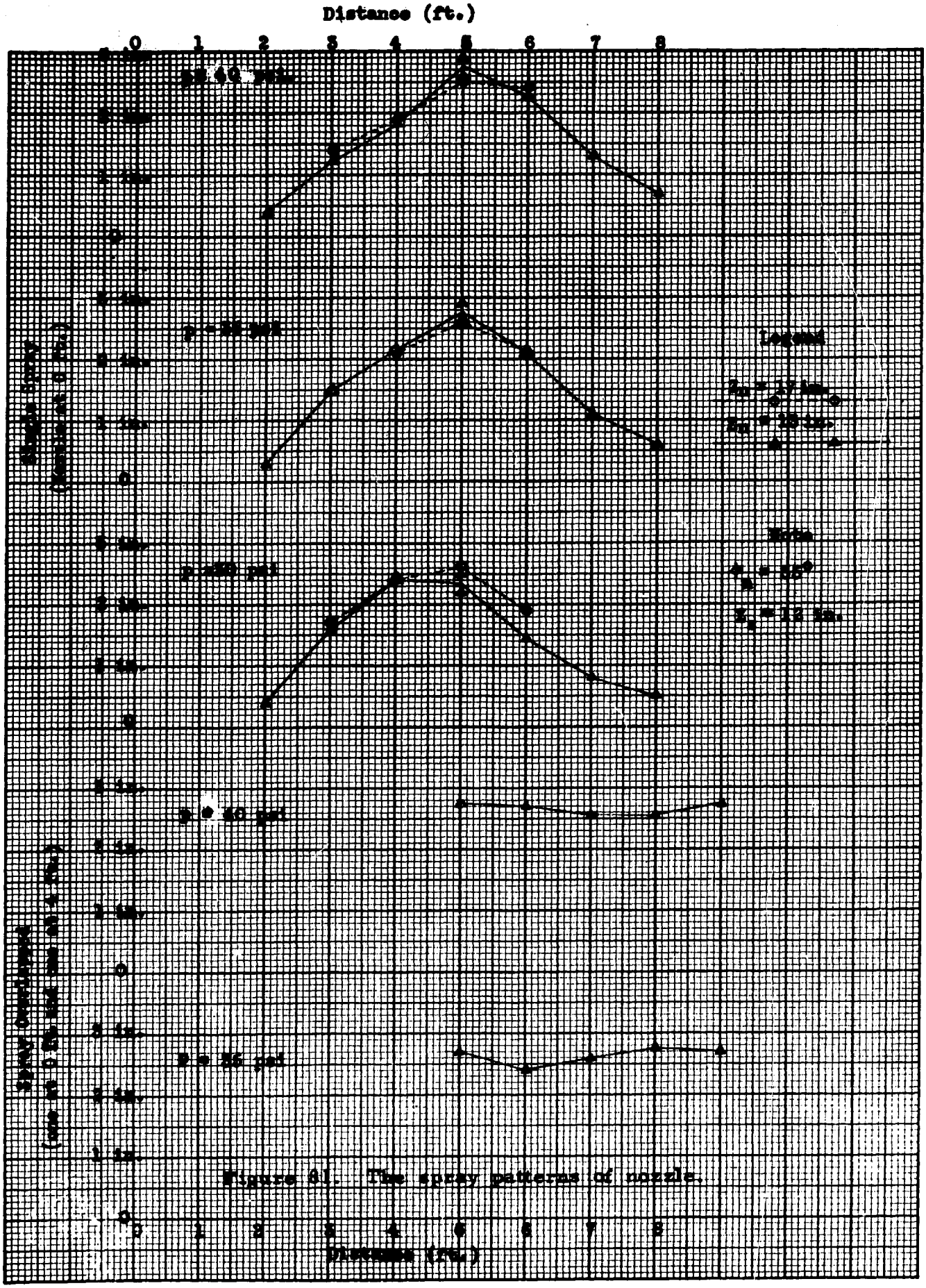
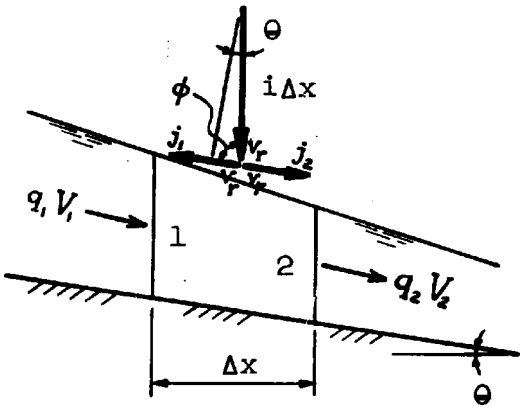


Figure 81. The spray patterns of nozzle.

APPENDIX II

THE CONSIDERATION OF ACTUAL CHANGE OF MOMENTUM DUE TO THE EFFECT OF RAINDROP IMPACT

By assuming that the falling rain on the flowing water acts the same as a continuous jet impinging on an ideal inclined plane, the derivation of equation (15), including the effect of raindrop impact on change of momentum, might be made as follows:



$$i\,\Delta x = j_1 + j_2$$

$$q_2 = q_1 + i\,\Delta x = q_1 + j_1 + j_2$$

$$j_1 = 1/2\; i\;\Delta x(1 - \text{Cos}\;\phi)$$

$$j_2 = 1/2\; i\;\Delta x(1 + \text{Cos}\;\phi)$$

where j_1 is the portion of precipitation which initially moves upstream, and j_2 is the portion of precipitation which initially moves downstream. The rate of change in momentum from section 1 to 2 is

$$\frac{\Delta M}{\Delta t} = \frac{q_1 w}{g}(V_2 - V_1) + \frac{j_1 w}{g}[V_2 - (-v_r)] + \frac{j_2 w}{g}(V_2 - v_r)$$

$$= \frac{q_1 w}{g}(V_2 - V_1) + \frac{i\,\Delta x\, w}{g}(V_2 - v_r \text{Cos}\;\phi)$$

Since $\phi = (90 - \theta)$ then $\text{Cos}\;\phi = \text{Sin}\;\theta$, thus

$$\frac{\Delta M}{\Delta t} = \frac{w}{g}[q_1 \Delta V + i\,\Delta x\,(V_2 - v_r \text{Sin}\;\theta)]$$

When this is combined with the external forces,

$$F = w\left(y_m \Delta Y - \frac{f_c\,\Delta x\, V_m^2}{2g}\right)$$

it gives

$$\Delta Y = \frac{1}{g\, y_m}\left[q_1\, \Delta V + i\, \Delta x\, (V_2 - v_r \operatorname{Sin} \theta) + \frac{f_c\, \Delta x\, V_m^2}{2} \right] \quad . \; . \; . \qquad (29)$$

The above equation shows clearly that this effect will be an important factor in determining the water surface profile on a very smooth surface of steep slope with a large difference of relative velocity ($V_2 - v_r$). However, the bottom surfaces in this study are rough, hence the friction term in equation (29) dominates the water surface profile. For example, for the case of heavy rain falling on a slope of 0.075, at the upper end of the flume, where V_2 is nearly zero, the term taking care of this effect has the following value

$$i\, \Delta x\, (V_2 - v_r \operatorname{Sin} \theta) = i\, \Delta x\, (0 - 4.8^{*} \times 3.2808 \times 12 \times 0.075)$$
$$= i\, \Delta x\, (-14.2) \qquad \text{in./sec.}$$

This is about 1/20 of the friction term $f_c\, \Delta x\, V_m^2/2$, and the effect on the water depth in the computed water surface profile, for this worst case, only amounts to less than 2 percent. For smaller slopes and increasing distances, this effect will soon be reduced to zero, and therefore, in this study, it is not important in comparison with the friction term. Moreover, the raindrop bounces out in all directions, not as assumed in the derivation; this tends to further reduce the effect of raindrop impact on the water surface profile.

---

* From Table IV on page 56.

APPENDIX III

MODIFYING THE DERIVATION OF EQUATION (15) TO INCLUDE THE COEFFICIENT OF MOMENTUM

In the derivation of the equation (15),

$$\Delta Y = \frac{1}{g\, y_m}\left(q_1\, \Delta V + i\, \Delta x\, V_2 + \frac{f_c\, \Delta x\, V_m^2}{2}\right) \ldots\ldots \quad (15)$$

The coefficient of momentum, C_m, is regarded as unity. The actual importance of this coefficient and the effect of raindrop impact to it can be understood from the following investigation.

By considering the coefficient C_m, the derivation would be (using the water depth perpendicular to the bottom surface) as follows. The equation numbers used correspond to those in the original derivations as shown on pages 7 to 9.

$$M_1 = C_m \frac{q_1\, w\, \Delta t}{g} V_1$$

$$M_2 = (C_m + dC_m) \frac{q_2\, w\, \Delta t}{g} V_2$$

Neglecting dC_m,

$$\Delta M = M_2 - M_1 = \frac{w\, \Delta t}{g}(C_m\, q_1\, \Delta V + C_m\, \Delta q\, V_2)$$

or

$$\frac{\Delta M}{\Delta t} = \frac{w}{g}(C_m\, q_1\, \Delta V + C_m\, \Delta q\, V_2) \ldots\ldots\ldots \quad (2a)$$

The external forces are

$$P_{s1} = \frac{w\, y_1^2}{2}$$

$$P_{s2} = \frac{w\, y_2^2}{2}$$

$$P_{s1} - P_{s2} = \frac{w}{2}(y_1^2 - y_2^2) \ldots\ldots\ldots\ldots\ldots\ldots \quad (4a)$$

$$P_g = w\left(\frac{y_1 + y_2}{2}\right) \Delta x\, S_o \ldots\ldots\ldots\ldots\ldots\ldots \quad (5a)$$

$$P_f = f_c \Delta x \, w \frac{V_m^2}{2g} \quad \ldots\ldots\ldots\ldots\ldots\ldots \quad (12a)$$

From equations (2a), (4a), (5a), and (12a), equation (15) should be

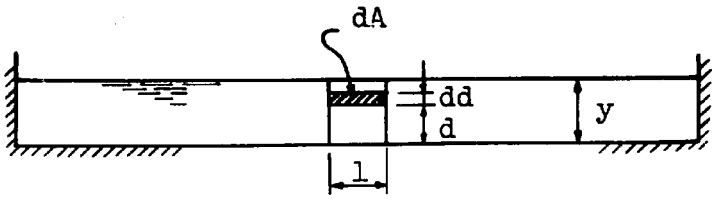
$$\Delta Y = \frac{1}{g \, y_m}\left(C_m \, q_1 \, \Delta V + C_m \, i \, \Delta x \, V_2 + \frac{f_c \, \Delta x \, V_m^2}{2}\right) \ldots \quad (15a)$$

The C_m value for uniform laminar flow in a wide channel is independent of the depth and can be calculated as 1.2 (Appendix IV). Values of C_m for fully turbulent flow vary with the condition of bottom surface roughness and its relative height to the depth of water. From Nikuradze's experimental results (22) (whose roughness was made by the same general way as this study) the C_m is computed and plotted on page 202 in Appendix IV. It has a value smaller than 1.175 for y/k_s (water depth/average size of sand particle) greater than 1, and is gradually approaching to 1 as limit. For most of time in this study y/k_s is greater than 1.

The C_m value for nonuniform flow is not yet known, but it may be safe to predict a maximum C_m value of 1.2. Moreover, the two terms involving C_m in equation (15a) play only a minor role compared with the friction term, hence the assumption of C_m as unity does not affect the result of the analysis.

APPENDIX IV

COEFFICIENT OF MOMENTUM, C_m, FOR UNIFORM LAMINAR AND TURBULENT FLOW



For unit width,

$$A = 1 \cdot y = y$$

$$dA = 1 \cdot dd = dd$$

In one second the differential weight of water that passes the cross section dA with a velocity u is w u dA, then the corresponding differential mass is dm = (w u dA)/g, the momentum M of the water that passes the cross section A of a channel in one second is

$$M = \int_o^y dm \cdot u = \int_o^y \frac{w\ u\ dA}{g}\ u = \frac{w}{g} \int_o^y u^2\ dA$$

Expressed in terms of mean velocity V and including the coefficient C_m, this same momentum is

$$M = C_m \frac{w}{g} V^2 A$$

Equating the above two values of M and reducing,

$$C_m = \frac{1}{A\ V^2} \int_o^y u^2\ dA = \frac{1}{y\ V^2} \int_o^y u^2\ dd \quad \ldots\ldots \quad (30)$$

C_m for Uniform Laminar Flow

For wide channel the vertical velocity distribution and its mean velocity can be expressed by the following equations (19):

$$u = \frac{w\ S}{\mu}\left(y\ d - \frac{d^2}{2}\right)$$

$$V = \frac{w\ S_o\ y^2}{3\ \mu}$$

Substituting these values into equation (30), then

$$C_m = \frac{1}{y\,V^2}\int_o^y u^2\,dd$$

$$= \frac{1}{y\left(\frac{w\,S_o\,y^2}{3\,\mu}\right)^2}\int_o^y \left[\frac{w\,S_o}{\mu}\left(y\,d - \frac{d^2}{2}\right)\right]^2 dd$$

$$= \frac{9}{y^5}\int_o^y \left(y\,d - \frac{d^2}{2}\right)^2 dd$$

$$= \frac{9}{y^5}\left(\frac{y^5}{3} - \frac{y^5}{4} + \frac{y^5}{20}\right)$$

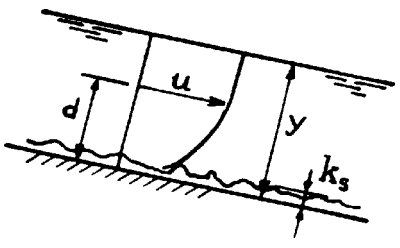
$$= 1.2$$

C_m for Uniform Turbulent Flow

For wide rough channel and high velocity of flow, Keulegan (23) proved that the vertical velocity distribution can be computed by using Prandtl and Kármán's law of velocity distribution for turbulent flow with Nikuradze's experimental result:

$$\frac{u}{\sqrt{\frac{\tau_u}{\rho}}} = 8.48 + 5.75 \log \frac{d}{k_s}$$

where k_s is the average size of the closely packed sand grains of the type used by Nikuradze in his experiments. From this equation the mean velocity can be computed



$$V = \frac{\int_o^y u\,dA}{A}$$

$$= \frac{1}{y}\int_o^y \left[\sqrt{\frac{\tau_u}{\rho}}\left(8.48 + 5.75 \log \frac{d}{k_s}\right)\right] dd$$

$$= \sqrt{\frac{\tau_u}{\rho}}\left(5.98 + 5.75 \log \frac{y}{k_s}\right)$$

Substituting these values into equation (30) and integrating,

$$C_m = \frac{1}{y\,V^2}\int_0^y u^2\,dd$$

$$= \frac{1}{y\left[\sqrt{\frac{\tau_u}{\rho}}\left(5.98 + 5.75\log\frac{y}{k_s}\right)\right]^2}\int_0^y\left[\sqrt{\frac{\tau_u}{\rho}}\left(8.48 + 5.75\log\frac{d}{k_s}\right)\right]^2 dd$$

$$\approx \frac{42 + 68.8\log\frac{y}{k_s} + 33.08\left(\log\frac{y}{k_s}\right)^2}{35.76 + 68.8\log\frac{y}{k_s} + 33.08\left(\log\frac{y}{k_s}\right)^2} \quad \cdots\cdots\cdots \quad (31)$$

From equation (31) values of C_m can be obtained if the ratio of y/k_s is known. Table VI on page 201 shows the variation of C_m with y/k_s changing from 0.1 to 1000 and a part of the result (for y/k_s from 0.3 to 10) is plotted in Figure 82 on page 202.

TABLE VI

VALUES OF COEFFICIENT OF MOMENTUM, C_m, FOR FULLY TURBULENT FLOW
(computed from equation 31)

y/k_s	$\log y/k_s$	$68.8 \log y/k_s$	$33.08 (\log y/k_s)^2$	C_m
0.1	-1	-68.8	33.08	157
0.2	-0.6986	-48.06	16.13	2.63
0.3	-0.5227	-35.97	9.04	1.707
0.4	-0.398	-27.4	5.24	1.46
0.5	-0.301	-20.72	3.00	1.346
0.6	-0.222	-15.27	1.63	1.281
0.7	-0.155	-10.66	0.79	1.24
0.8	-0.097	- 6.67	0.31	1.211
0.9	-0.046	- 3.16	0.07	1.191
1.0	0	0	0	1.174
1.25	0.097	6.67	0.31	1.146
1.5	0.176	12.1	1.02	1.127
1.75	0.2434	16.73	1.96	1.114
2	0.3014	20.73	3.01	1.104
3	0.4773	32.85	7.54	1.081
4	0.602	41.4	12.0	1.07
5	0.699	48.1	16.16	1.062
6	0.778	53.5	20.0	1.057
7	0.845	58.1	23.6	1.053
8	0.903	62.1	27.0	1.05
9	0.954	65.6	30.1	1.047
10	1	68.8	33.08	1.045
100	2	137.6	132.32	1.021
1000	3	206.4	297.72	1.011

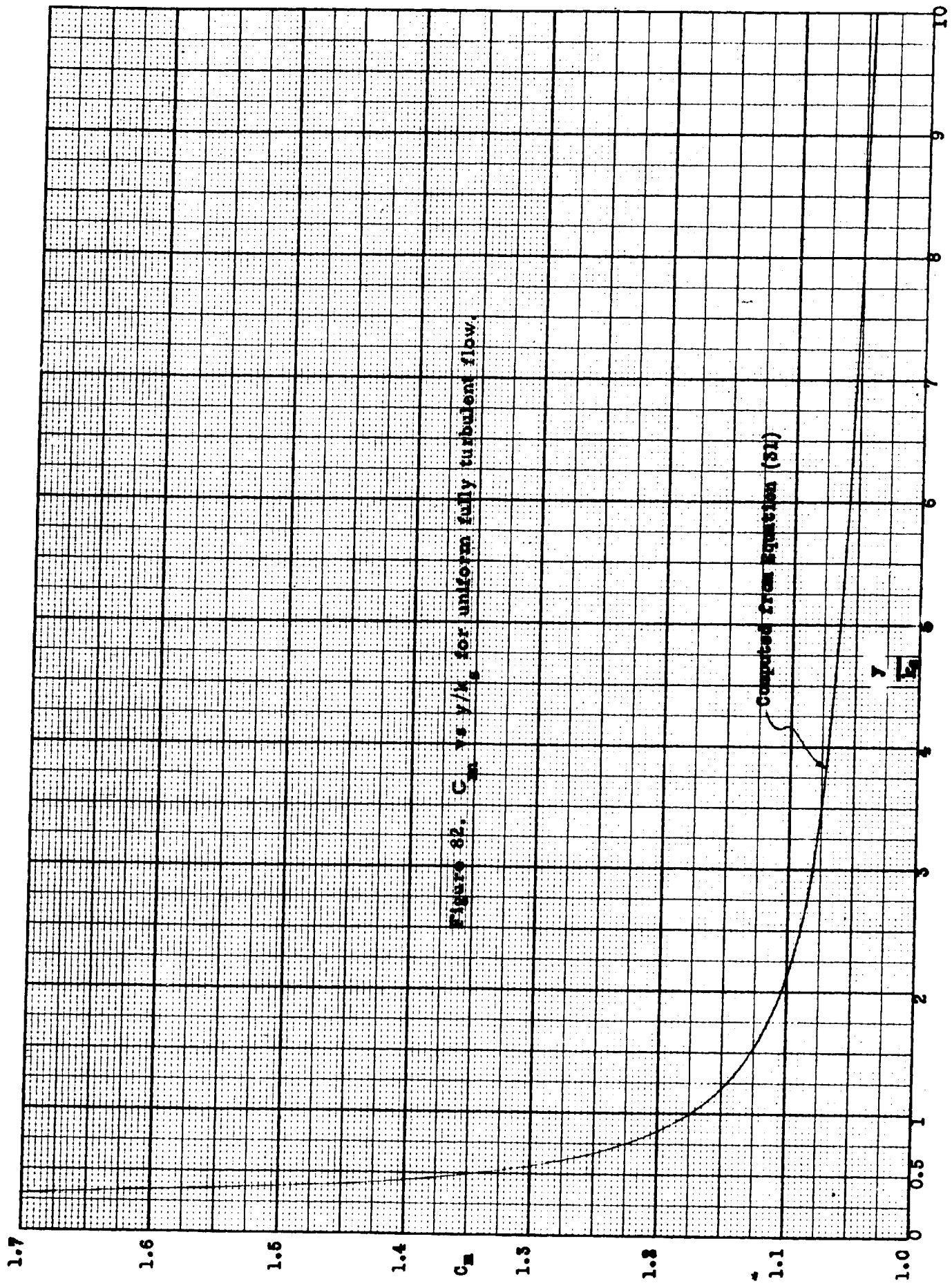


Figure 82. C_m Vs y/k_s for uniform fully turbulent flow.

NOMENCLATURE

A	cross-sectional area
b	channel width
C	$f_c = C/N_R$
C'	$f_c' = C'/N_R$
C_L'	C' for light rain
C_M'	C' for medium rain
C_H'	C' for heavy rain
C_m	coefficient of momentum
D	diameter of pipe
d	perpendicular distance from bottom surface
F	external force
f_ℓ	coefficient of friction for uniform laminar flow in pipe
f_t	coefficient of friction for uniform turbulent flow in pipe (Darcy-Weisbach)
f_p	coefficient of friction in pipe, in general
f_c	coefficient of friction in wide open channel
f_c'	effective coefficient of friction in wide open channel (includes effect of raindrop impact)
g	gravitational acceleration, 32.2 ft./sec.^{2} or 386.4 in./sec.^{2}
h_f	head lost by friction

i	rainfall intensity (in./hr. and in./sec.)
j_1	portion of precipitation which initially moves upstream
j_2	portion of precipitation which initially moves downstream
K	magnitude of surface roughness
K_s	shearing coefficient
k_s	average size of the sand particles used to create roughness on the bottom surface
L	length along bottom surface
M	momentum
N_R	Reynolds' number
n	coefficient of roughness (Manning)
P_s	static pressure force of water
P_g	component of gravitational force parallel to bottom surface
P_f	friction force
Q	total discharge
q	discharge, per unit width
q_m	discharge per unit width, mean in a reach = $1/2\ (q_1 + q_2)$
R	hydraulic radius
S	slope of energy gradient
S_o	slope of bottom surface
T_{H_2O}	Temperature of water (°C)
t	time
u	velocity component in the direction of flow

V	mean velocity for water depth perpendicular to bottom surface
V_m	mean velocity for water depth perpendicular to bottom surface, mean in a reach = $1/2\ (V_1 + V_2)$
$\mathcal{V}$	volume
$\mathcal{V}_s$	volume of one sand particle
$\mathcal{V}_w$	volume of void water
v_r	raindrop velocity
w	specific weight of water
x	horizontal distance
Y	vertical distance
y	water depth, perpendicular to bottom surface
y_c	critical water depth, perpendicular to bottom surface
y_m	water depth perpendicular to bottom surface, mean in a reach = $1/2\ (y_1 + y_2)$
y'	vertical water depth
μ	absolute viscosity
ν	kinematic viscosity ($in.^2/sec.$)
ρ	density, mass per unit volume = w/g
τ	shearing stress at bottom surface
τ_u	shearing stress at bottom surface for uniform flow
ϑ	inclination angle of bottom surface
ϕ	angle between the raindrop direction and the bottom surface
Surface "A"	smooth surface--redwood

Surface "B"	rough surface--Masonite board
Surface "C"	very rough surface--cemented sand of an average size of 1 mm. in diameter

BIBLIOGRAPHY

1. Hinds, J., "Side Channel Spillways: Hydraulic Theory, Erosion Factors, and Experimental Determination of Losses," Transactions A.S.C.E., Vol. 89, 1926, pp. 881-939.

2. Favre, H., "Contribution A I'Étude Des Courants Liquides," S. A. Rascher & Cie., Zurich, 1933.

3. Beij, K. H., "Flow in Roof Gutters," Journal of Research, Bureau of Standards, Vol. 12, Feb., 1934, pp. 193-213.

4. Horton, R. E., "The Interpretation and Application of Runoff Plat Experiments with Reference to Soil Erosion Problems," Proceedings Soil Science Society of America, 1938, pp. 340-349.

5. Jens, S. W., "Drainage of Airport Surfaces--Some Basic Design Considerations," Transactions A.S.C.E., Vol. 113, 1948, pp. 785-836 (E. F. Brater's Discussion, pp. 819-825).

6. Camp, T. R., "Lateral Spillway Channels," Transactions A.S.C.E., Vol. 105, 1940, pp. 606-637.

7. Keulegan, G. H., "Spatially Variable Discharge Over A Sloping Plane," Transactions A.G.U., Part VI, 1944, pp. 956-958.

8. Izzard, C. F., "The Surface-profile of Overland Flow," Transactions A.G.U., Part VI, 1944, pp. 959-968.

9. Laws, J. O., "Measurements of the Fall-velocity of Waterdrops and Raindrops," Transactions A.G.U., Part III, 1941, pp. 709-721.

10. Parsons, D. A., "Depths of Overland Flow," SCS-TP-82, July 1949, U. S. Department of Agriculture, pp. 1-33.

11. Brater, E. F., "Hydraulics," Civil Engineering Handbook by Urquhart, 3rd Edition, 1950, pp. 366-368.

12. Hicks, W. I., "Discussion of Paper 'Preliminary Report on Analysis of Runoff Resulting from Simulated Rainfall on a Paved Plot' by C. F. Izzard and M. T. Augustine," Transactions A.G.U., Part VI, 1944, pp. 1039-1041.

13. Izzard, C. F., and Augustine, M. T., "Preliminary Report on Analysis of Runoff Resulting from Simulated Rainfall on a Paved Plot," Transactions A.G.U., Part II, 1943, pp. 500-511.

14. Laws, J. O., and Parsons, D. A., "The Relation of Raindrop-size to Intensity," Transactions A.G.U., Part II, 1943, pp. 452-460.

15. Wilm, H. G., "The Application and Measurement of Artificial Rainfall on Type FA and F Infiltrometers," Transactions A.G.U., Part II, 1943, pp. 480-487. (D. A. Parsons' Discussion on "The History of the Development of the Rainfall Applicator.")

16. Kelly, L. L., "A Comparison of the Colorado and Type-F Artificial Rainfall Applicator," 1940, U. S. Soil Conservation Service (Mimeographed).

17. Goodman, L. J., "Erosion Control in Engineering Works," Agricultural Engineering, March 1952, Vol. 33, No. 3, pp. 155-157.

18. Ellison, W. D., and Pomerene, W. H., "A Rainfall Applicator," Agricultural Engineering, June 1944, p. 220.

19. Horton, R. E., Leach, H. R., and Van Vliet, R., "Laminar Sheet-flow," Transactions A.G.U., Part II, 1934, pp. 393-404.

20. O'Brien, M. P., "Analyzing Hydraulic Models for Effects of Distortion," Engineering News-Record, Sept. 15, 1932, pp. 313-315.

21. Rouse, H., "Discharge Characteristics of the Free Overfall, Use of Crest Section as a Control Provides Easy Means of Measuring Discharge," Civil Engineering, Vol. 6, 1936, pp. 257-260.

22. Nikuradze, J., "Stromungsgesetze in rauhen Rohren," VDI-Forschungsheft 361. Beilage zu "Forschung auf dem Gebiete des Ingenieurwesens," Ausgabe B Band 4, July/August 1933. (English translation, Technical Memorandum 1292, National Advisory Committee for Aeronautics, Washington, 1950).

23. Keulegan, G. H., "Laws of Turbulent Flow in Open Channel," Journal of Research, National Bureau of Standards, Vol. 21, No. 6, Dec. 1938, pp. 707-741.